

Molecular characterization and surface reactivity of cyanobacteria and their lysates

by

Logan Reed Swaren

A thesis submitted in partial fulfillment of the requirements for the degree of

Doctor of Philosophy

Department of Earth and Atmospheric Sciences

University of Alberta

© Logan Reed Swaren, 2022

## Abstract

Cyanobacteria are among the most abundant primary producers in the oceans and are present in nearly every environment on the planet. They were one of the first organisms to evolve nearly 3.8 billion years ago, making them excellent analogs for the investigation of ancient ocean chemistry. The high density of proton-active functional groups on their surfaces makes them important in binding marine trace metals. Moreover, they are important components of the marine food web, as both intact cells and secondary organic matter. The distribution of cyanobacteria has a profound influence on trace metal speciation in modern and ancient oceans. This dissertation explores the impact of pH and ionic strength on the surface reactivity of cyanobacteria and investigates the reactivity and composition of organic matter derived from cell lysis.

In Chapter 1, I review our understanding of cyanobacterial surface reactivity, trace metal cycling in the modern marine environment, and the roles of particulate and dissolved organic matter (POM and DOM, respectively).

Chapter 2 focuses on the influence of solution ionic strength (IS) on the surface reactivity of the freshwater cyanobacteria *Synechocystis*. As particulates, including planktonic cyanobacteria, move from more terrestrial freshwater environments to more saline marine environments, they hold the potential to transport and release trace metals. The surface reactivity is investigated using common surface chemistry approaches, namely: (i) acid-base titrations, (ii) zeta potential measurements, and (iii) Cd adsorption experiments under simulated freshwater IS (0.01 M NaCl) and marine IS (0.56 M NaCl). The acid-base titrations and Cd adsorption experiment results are paired to produce a surface complexation model (SCM) for the cyanobacterium. *Synechocystis* demonstrated a more negative surface charge and a higher affinity towards Cd across the entire pH range studied. This suggests that *Synechocystis*, due to their

ubiquitous distribution in aquatic environments, as well as other planktonic cyanobacteria could play an important part in trace metal cycling especially in environments with large salinity gradients such as estuarine and deltaic settings.

In Chapter 3, I measure the buffering capacity and reactivity of organic detritus produced from the mechanical lysis of the common marine cyanobacterium *Synechococcus* (referred to as cyPOM and cyDOM), through proton adsorption and release experiments using potentiometric acid-base titrations. The results are compared with existing literature on modern DOM samples from a variety of environments (e.g., terrestrial, marine, lab cultures). My results suggest that cyPOM is relatively unimportant in trace metal transport to the ocean floor even though it makes up an increasing portion of POM with depth relative to the intact cyanobacterial cells. When cyDOM is included in the system, even at much smaller amounts (e.g., 10:1 *Synechococcus*:cyDOM), the DOM dominates metal speciation as observed in nature.

In Chapter 4, I investigate the composition of cellular DOM derived from two extant cyanobacteria, the marine *Synechococcus* and euryhaline *Synechocystis*, using electrospray ionization (ESI) Fourier transform ion cyclotron resonance (FTICR) mass spectroscopy. *Synechococcus*- and *Synechocystis*-derived DOM contained 1548 and 1474 unique compounds, respectively, with >80% of assignments constituting nitrogen-containing molecules with a significant portion of sulfur- and phosphorous-containing ligands, ~35% and ~37%, respectively. When compared to terrestrially-derived DOM, the cyanobacterial-derived DOM also has lower oxygen/carbon and higher hydrogen/carbon ratios. Interestingly, despite cyanobacteria comprising the major producers of marine DOM today, their contribution to the marine DOM pool appears less significant than DOM derived from land. However, in the Precambrian oceans – before the evolution of land plants – cyanobacterial-derived DOM was likely the primary source of the

marine DOM pool. This means that the Precambrian DOM pool would consist chiefly of more reactive nutrient-rich (N, P, and S) molecules with a high affinity to bind trace metals

Chapter 5 summarizes our current understanding of marine dissolved organic matter and I propose future research directions.

## Preface

This manuscript is papers-based and consists of 3 original research articles that are the collective effort of several projects focused on cyanobacteria surface reactivity, cyanobacterial-derived particulate and dissolved organic matter (POM and DOM, respectively), and the molecular characterization of said cyanobacterial-derived DOM. All research conducted in this thesis was supervised by Drs. Kurt Konhauser and Daniel Alessi at the University of Alberta. In each chapter I was the project manager in charge of cultivating and maintaining euxinic cyanobacterial cultures, project design, data collection, analysis, interpretation, and manuscript drafting. My contribution to each chapter is outlined below.

**Chapter 2** has been published in *Chemical Geology* as: Swaren, L., Hao, W., Melnyk, S., Baker, D., Li, Y., Owtrim, G.W., Zeng, H., Gingras, M.K., Alessi, D.S., Konhauser, K.O. (2021). Surface reactivity of the cyanobacterium *Synechocystis* sp. PCC 6803 – Implications for trace metals transport to the oceans, *Chemical Geology*, 562, 120045. I was responsible for maintaining cyanobacterial cultures, designing experiments, collecting data, and protonation data modeling. S. Melnyk and D. Baker assisted me with metal adsorption experiments and W. Hao assisted with surface complexation modeling. The manuscript was written by me with contributions from all authors.

**Chapter 3** has been published in *Geochimica et Cosmochimica Acta* as: Swaren, L., Alessi, D.S., Owtrim, G.W., Konhauser, K.O. (2021). Acid-base properties of *Synechococcus*-derived organic matter, *Geochimica et Cosmochimica Acta*, 315, 89-100. I was responsible for conceptualizing the study, experimental design, data collection, data processing and interpretation, and surface complexation modeling. I prepared the initial manuscript, and it was improved prior to publication with input from all authors.

**Chapter 4** is currently in review with *Geochimica et Cosmochimica Acta* as: Swaren, L., Kitova, E.N., Klassen, J.S., Owtrim, G.W., Alessi, D.S., Konhauser, K.O. (2022). Contribution of cyanobacteria to marine dissolved organic matter, *Geochimica et Cosmochimica Acta*. I was responsible for maintaining cyanobacterial cultures, sample preparation, experimental design, data processing, and literature review in order to assign molecular formula to the resulting mass data. E. Kitova ran the Fourier transform ion cyclotron resonance (FTICR) mass spectrometer and assisted with raw data processing. The manuscript was written by me with contributions from all authors.

“This abstract, which I now publish, must necessarily be imperfect. I cannot here give references and authorities for my several statements; and I must trust to the reader reposing some confidence in my accuracy. No doubt errors will have crept in, though I hope I have always been cautious in trusting to good authorities alone. I can give here only the general conclusions at which I have arrived, with a few facts in illustration, but which, I hope, in most cases will suffice. No one can feel more sensible than I do of the necessity of hereafter publishing in detail all the facts, with references, on which my conclusions have been grounded; and I hope in a future work to do this.”

- *Charles Darwin, The Origin of Species (1859)*

## Acknowledgements

First and foremost, I would like to thank my supervisor Dr. Kurt Konhauser for welcoming me into his lab. It was my honour to work under such a well-respected scientist, great supervisor, and awesome human being. I would also like to thank my co-supervisor Dr. Daniel Alessi for taking me on as an undergraduate student, sparking my interest in aqueous chemistry and geochemical modelling. Additionally, I would like to thank Dr. Murray Gingras for his insightful discussions and support over the past 4 years, Dr. Sasha Wilson for her patience in teaching me X-ray diffraction, and Dr. Elena Kitova for countless hours of running and explaining Fourier transform ion cyclotron resonance mass spectrometry.

I would also like to thank Dr. Jamie Robbins for convincing me to upgrade to my PhD over a walk to grab some coffee, Brendan Bishop for teaching me how to talk to cyanobacteria, Drs. Samrat Alam and Weiduo Hao for teaching me how to conduct basic science when I first started out as both an undergrad and graduate student, not to mention FITEQL. I would also like to thank my friends in the lab, past and present: Tyler, Kaarel, Adam, Rong, Konstantin, Jason, Katherine, Kayode, Salman, Daniela, Kelly, Cody, Jenifer, Scott, and Dan for their ideas, encouragement, and willingness to have a pint after a long day.

I would also like to thank my parents who have cultivated my curiosity and supported me through the many years of academics. I will be forever grateful for their love and support, as well as the continued support of the rest of my family, especially my brothers, Sean and Mitchel. Most importantly I would like to thank my wife, Danielle, and son, Brooks, who deserve countless hours of my undivided attention. I will forever cherish her persistence in pushing me to become better in whichever venture I pursued.

# Table of Contents

Chapter 1: Introduction.....	1
1.1. Bacterial surface reactivity.....	1
1.2. Importance of dissolved organic matter on marine trace metals cycling.....	2
1.3. References.....	6
Chapter 2: The role of cyanobacteria in trace metal transport to the oceans.....	12
2.1. Introduction.....	12
2.2. Methods.....	14
2.2.1. Cyanobacteria growth and harvesting.....	15
2.2.2. Potentiometric titrations.....	15
2.2.3. Attenuated total reflectance fourier transform infrared (ATR-FTIR) spectroscopy.....	17
2.2.4. Zeta potential.....	17
2.2.5. Cadmium adsorption experiments.....	18
2.3. Results.....	19
2.3.1. Potentiometric titrations.....	19
2.3.2. ATR-FTIR.....	19
2.3.3. Zeta potential.....	20
2.3.4. Cadmium adsorption.....	21
2.4. Discussion.....	22
2.4.1. Surface reactivity of <i>Synechocystis</i> .....	22
2.4.2. Implications for trace metal cycling in transitional settings.....	23
2.5. Conclusions.....	26

2.6. References.....	27
Chapter 3: Acid-base properties of <i>Synechococcus</i> -derived organic matter.....	39
3.1. Introduction.....	39
3.2. Methods.....	41
3.2.1. <i>Synechococcus</i> sp. PCC 7002 growth.....	41
3.2.2. <i>Synechococcus</i> harvesting.....	42
3.2.3. Preparation of mechanically lysed cyPOM and cyDOM.....	43
3.2.4. ATR-FTIR.....	44
3.2.5. Zeta potential.....	44
3.2.6. Potentiometric titrations.....	45
3.2.7. Trace metal adsorption experiments to cyPOM.....	46
3.3. Results.....	46
3.3.1. ATR-FTIR.....	46
3.3.2. Zeta potential.....	47
3.3.3. Potentiometric titrations.....	48
3.3.4. Experimental trace metal adsorption to cyPOM.....	48
3.4. Discussion.....	50
3.4.1. Comparison of cyPOM and cyanobacterial cell surface reactivities.....	50
3.4.2. Differences in trace metal affinities between intact cells and cyPOM.....	51
3.4.3. Surface reactivity of seawater cyDOM.....	52
3.4.4. Trace metal interactions with marine DOM.....	53
3.5. Conclusions.....	56
3.6. References.....	57

Chapter 4: Contribution of cyanobacteria to marine dissolved organic matter.....	77
4.1. Introduction.....	77
4.2. Methods.....	80
4.2.1. Cyanobacteria growth and harvesting.....	80
4.2.2. Preparation of mechanically lysed dissolved organic matter.....	80
4.2.3. Electrospray ionization Fourier transform ion cyclotron resonance mass spectrometry (ESI-FTICR-MS).....	81
4.3. Results.....	82
4.4. Discussion.....	83
4.4.1. Comparison between <i>Synechococcus</i> and <i>Synechocystis</i> .....	83
4.4.2. Cyanobacterial DOM in comparison to modern marine DOM.....	83
4.4.3. Precambrian implications.....	85
4.5. Conclusions.....	88
4.6. References.....	90
Chapter 5: Conclusions.....	107
5.1. Predictive ligand modelling.....	109
5.2. Future research directions.....	110
5.3. References.....	115
Bibliography.....	130
Appendix 1. Supplementary information for Chapter 2.....	157
Appendix 2. Supplementary information for Chapter 3.....	175
Appendix 3. Supplementary information for Chapter 4.....	193
Appendix 4. Supplementary information for Chapter 5.....	204

## List of Tables

Table 2.1: Summary of protonation and surface complexation modeling results from duplicate titration data of <i>Synechocystis</i> sp. PCC 6803 in various electrolyte solutions modelled using FITEQL 4.0. Site concentration is in units of mol g <sup>-1</sup> .....	35
Table 3.1: Summary of protonation modeling of cyPOM in comparison with intact <i>Synechococcus</i> cells from Liu et al. (2015).....	70
Table 3.2: Best fit, 2- and 1-site protonation models for cyDOM in comparison with values compiled from literature. Site concentrations are in units of μmol g <sup>-1</sup> .....	71
Table 3.3: Best fit binding constants for trace metal-cyPOM complexes and previously studied trace metal- <i>Synechococcus</i> sp. PCC 7002 complexes. All experiments were conducted in 0.56 M NaCl.....	73
Table 5.1: Ligand values input into the modified thermo_minteq database for biotic modelling.....	119

## List of Figures

Figure 1.1: Typical nutrient-like depth profile in the marine environment.....	10
Figure 1.2: Generalized diagram of DOM and POM production in modern marine settings .....	11
Figure 2.1: Zeta potential measurements performed on 0.2 g L <sup>-1</sup> suspensions of <i>Synechocystis</i> sp. PCC 6803 in 0.01 and 0.56 M NaCl as a function of pH.....	36
Figure 2.2: Modeling (lines) and experimental (points) results of Cd adsorption onto 10 g L <sup>-1</sup> <i>Synechocystis</i> sp. PCC 6803 in 0.01 and 0.56 M NaCl.....	37
Figure 2.3: <i>Synechocystis</i> cell surface functional groups responsible for Cd adsorption as a function of varying pH.....	38
Figure 3.1: Attenuated total reflectance fourier transform infrared (ATR-FTIR) spectra of dried and ground <i>Synechococcus</i> sp. PCC 7002 cells overlain with dried and ground cyPOM.....	74
Figure 3.2: Zeta potential measurements performed on 0.2 g L <sup>-1</sup> suspensions of <i>Synechococcus</i> sp. PCC 7002 and cyPOM in 0.56 M NaCl as a function of pH.....	75
Figure 3.3: Modeling (red lines) and experimental (points) results of trace metal adsorption onto 10 g L <sup>-1</sup> <i>Synechococcus</i> sp. PCC 7002 derived cyPOM in 0.56 M NaCl. Error bars indicate 1-sigma standard deviation.....	76
Figure 4.1: Generalized Van Krevelen diagram with boxes corresponding to common organic compound classes (Adapted from Sleighter & Hatcher, 2008; Ma et al. 2018; Niu et al. 2018). Compounds associated with terrestrial origin are outlined in grey dashed lines. The plots are presented for reference and do not necessarily imply the presence of the indicated compounds.....	102
Figure 4.2: Negative ESI Fourier Transform Ion Cyclotron Resonance (FTICR) Mass Spectra (MS) of intracellular <i>Synechococcus</i> sp. PCC 7002 dissolved organic matter (7002) and	

intracellular <i>Synechocystis</i> sp, PCC 6803 dissolved organic matter (6803) mixed 1:1 (v:v) with methanol (MeOH).....	103
Figure 4.3: Distribution of molecular formulas assigned for <i>Synechococcus</i> sp. PCC 7002 DOM (7002) and <i>Synechocystis</i> sp. PCC 6803 DOM (6803).....	104
Figure 4.4: Distribution of (A) S-containing molecules (CHOS and CHONS) and (B) P-containing molecules (CHOP and CHONP) for <i>Synechococcus</i> sp. PCC 7002 DOM (7002) and <i>Synechocystis</i> sp. PCC 6803 DOM (6803) plotted on a van Krevelen diagram.....	105
Figure 4.5: Schematic diagram comparing the major naturally occurring inputs of DOM in modern versus Precambrian oceans.....	106
Figure 5.1: Modern Ni speciation (-3.5 log atm CO <sub>2</sub> , 10 nM Ni, 0.56 M Na and Cl).....	120
Figure 5.2: Modern Cu speciation (-3.5 log atm CO <sub>2</sub> , 10 nM Cu, 0.56 M Na and Cl). Note that Cu <sup>2+</sup> and CuCl <sup>+</sup> are present in both abiotic and ligand containing diagrams but only in the ligand containing legend to preserve space.....	121
Figure 5.3: Euxinic Ni (-2.2 log atm CO <sub>2</sub> , 10 nM Ni, 0.56 M Na and Cl, 400 uM H <sub>2</sub> S).....	122
Figure 5.4: Euxinic Cu (-2.2 log atm CO <sub>2</sub> , 10 nM Cu, 0.56 M Na and Cl, 400 uM H <sub>2</sub> S).....	123
Figure 5.5: Post-GOE Ni speciation (-2.2 log atm CO <sub>2</sub> , 10 nM Ni, 0.56 M Na and Cl, 50 uM Fe(II), and 5 uM H <sub>2</sub> S).....	124
Figure 5.6: Post-GOE Cu speciation (-2.2 log atm CO <sub>2</sub> , 10 nM Cu, 0.56 M Na and Cl, 50 uM Fe(II), and 5 uM H <sub>2</sub> S).....	125
Figure 5.7: Ferruginous Ni (-2.2 log atm CO <sub>2</sub> , 10 nM Ni and Cu, 0.56 M Na and Cl, 50 uM Fe(II)).....	126
Figure 5.8: Ferruginous Cu (-2.2 log atm CO <sub>2</sub> , 10 nM Cu and Cu, 0.56 M Na and Cl, 50 uM Fe(II)).....	127

Figure 5.9: Ni speciation through time in the presence of Ni-binding ligands.....128

Figure 5.10: Cu speciation through time in the presence of Cu-binding ligands.....129

## Chapter 1: Introduction

### 1.1. Bacterial surface reactivity

Cyanobacteria are among the most ubiquitous primary producers on Earth, and as such, their surface reactivity may significantly contribute to metals cycling and substratum colonization in soils, sediment and aqueous environments. Their ability to bind metal cations stems from the presence of proton-active carboxyl, phosphoryl, sulfhydryl, amine and hydroxyl surface functional groups located on cell walls, exopolysaccharides (EPS), and extracellular sheaths (Yee and Fein, 2001; Phoenix et al. 2002). The cell surface can behave either hydrophobically or hydrophilically depending on the surface functional groups expressed under different aqueous conditions (Liu et al. 2015). Hydrophobic cell surfaces are often composed of a neutral sheath which lowers the cyanobacterial surface charge to increase the adherence of benthic species to a substrate (Phoenix et al. 2002), whereas planktonic species in the marine water column lack these neutral sheaths, creating a hydrophilic surface that makes them efficient at adsorbing bioessential metal cations from solution (Liu et al. 2015; Bishop et al. 2019).

Their ability to adsorb bioessential trace metals is influenced by solution ionic strength (IS) and pH (Liu et al. 2015). Due to this change in trace metal affinity owing to variable environmental conditions, it is important to understand the surface reactivity of cyanobacteria under these varying conditions. Low IS, representative of freshwater conditions, and high IS, representative of marine conditions will inherently influence trace metal adsorption, and the transfer of cyanobacteria from one condition to another (e.g., in deltaic or estuary settings) will influence the adsorption or desorption of metals from their surfaces, and by extension, global biogeochemical cycles. Therefore, Chapter 2 investigates the difference in surface reactivity of the freshwater cyanobacteria *Synechocystis* at IS representative of both freshwater and marine settings. Our

results provide insight on the trace element distribution of cyanobacteria when transitioning from freshwater to marine settings. Moreover, the acidity constants and metal binding mass action constants (in this case, for  $\text{Cd}^{2+}$ ) can be applied in determining speciation in modern environmental and ancient geochemical systems.

## **1.2 Importance of dissolved organic matter on marine trace metals cycling**

The distribution of most trace metals (e.g., Cd, Co, Cu, Ni, and Zn) is closely related to marine primary productivity and biological cycling in the water column (Bruland, 1980; Bruland et al. 1991; Morel and Price, 2003; Saito et al. 2003). Some trace metals demonstrate little concentration variability with ocean depth, such as Mo, even though they are bioessential co-factors in various enzymatic processes (Bruland and Lohan, 2003). However, most trace metals demonstrate a nutrient-type concentration distribution in the oceans, characterized by a sharp decrease in concentration in surface waters due to assimilation by phytoplankton paired with increased concentration with depth due to remineralization as a result of respiration (Figure 1.1) (Bruland and Lohan, 2003). From a geochemical perspective, the uptake of bioessential trace metals from sunlit surface waters and their eventual transport to the seafloor is an important factor in the eventual sequestration of those metals into marine sediments.

There are numerous studies that have investigated the surface reactivity of cyanobacterial cells (described in Chapter 1.1) and there is an expanding understanding of the of the cyanobacteria-derived organic matter pool, namely dissolved organic matter (DOM) and particulate organic matter (POM) (e.g., Zhao et al. 2017, 2019; Ma et al. 2018; Zheng et al. 2019). There are two major processes by which cyanobacterial POM is produced: (1) lysis by viral pathogens and (2) zooplankton grazing (see Figure 1.2 for schematic diagram of marine DOM

production) (Kawasaki et al. 2011; Zheng et al. 2019). Viral lysis of microorganisms, namely cyanobacteria, occurs due to the infection of cells by cyanophages that disrupt and kill the cell (Suttle, 2007). Related to the latter process is “sloppy feeding”, a term attributed to the disaggregation of phytoplankton cells by zooplankton mouthparts resulting in the release of uningested particulates as well as DOM (Strom et al. 1997; Saba et al. 2011). Following cell breakage via sloppy feeding, there are changes to the surface functional group expression and structure of phytoplankton, as observed in copepod fecal pellets and marine snow (Volkman and Tanoue, 2002). In Chapter 3, the surface reactivity and metal binding capacity of intact cyanobacterial cells as well as their particulates following mechanical lysis were investigated. Moreover, differences in the reactivity of intact cyanobacterial cells, cyanobacterial-derived POM and DOM were determined using potentiometric titrations and compared with modern environmental investigations representing different sources (e.g., terrestrial versus marine).

In the modern oceans DOM is a complex mixture of macromolecules, mostly comprised of carboxyl-rich, alicyclic molecules (CRAM), humic and fulvic acids, and polysaccharides that represent a bulk pool of terrestrial and marine sources (Jiao et al. 2018). Most marine DOM is produced by phytoplankton in the photic zone as cellular exudates, a product of primary production. The degradation of POM and the viral lysis of marine cyanobacteria due to viral pathogens both contribute to the global marine DOM pool (Suttle, 2007; Hansell, 2013). Terrestrial-derived DOM is typically identified as lignin and tannin derived products that are dominated by CHO molecules (Hedges et al. 1997; Lechtenfeld et al. 2014). In Chapter 4, cyanobacterial-derived DOM was investigated via Fourier transform ion cyclotron resonance (FTICR) mass spectrometry and molecular composition compared with that of modern marine samples.

In addition to DOC, various organisms can produce metal-chelating ligands. Some ligands make metals bioavailable, such as siderophores. These are iron (Fe)-specific binding ligands that are excreted by numerous microbial cells to keep Fe(III) in soluble form and amenable for assimilation (Vraspir and Butler, 2009). Other ligands are produced and released extracellularly to immobilize toxic metals, such as copper (Cu) and cadmium (Cd) (Bruland et al. 1991). The production of these organic ligands is of global significance in terms of trace metal cycling, with estimates suggesting, for example, that 99.7% of Cu in the northeast Pacific is organically complexed (Coale and Bruland, 1988). Other metals are complexed to a lesser extent, with only 30-50% of nickel being associated with organic ligands (Boiteau et al. 2016). The generally high percentage of metals organically bound versus in ionic form (e.g.,  $\text{Cu}^{2+}$ ) means that marine plankton, and the organic ligands that they generate, directly control trace metals speciation and cycling in modern oceans. For instance, Bishop et al. (2019) investigated the binding properties of bioessential metals to the common marine cyanobacteria *Synechococcus*. After modelling experimental metal adsorption data with previously reported DOC ligand metal binding constants, they found that 99% of metals at marine conditions would be complexed with DOC ligands. The abundance and composition of metal-specific marine ligands is well documented (e.g., Fe, Co, Cu, Ni and Zn), but little attention has been paid to the role of specific DOM contributions of modern plankton to the overall organic ligand pool.

Understanding trace metal interactions with live marine cyanobacteria and their DOC derivatives is not only important for the modern oceans, but also for understanding the role of the ancient marine biosphere in controlling trace metal availability, and ultimately their burial in marine sediments. For instance, a number of previous studies have used the chemical composition of banded iron formations as proxies for interpreting redox evolution on Earth and the composition

of paleo-seawater (e.g., Konhauser et al. 2009 and 2018; Robbins et al. 2016). However, the role that DOM may have played as a vector for transferring trace metals into the sediment pile has largely been ignored. In this regard, my goal is to determine the efficiency of DOM as a possible exit channel for trace metals into ancient marine settings, and how this affected their expression in the rock record. By determining the metal binding behavior of trace metals to cyanobacterial-DOM, models containing multiple sorbents and metals can be developed (Bishop et al. 2019), allowing for better identification of trace metal biosignatures in the rock record. Chapter 5 is a revisit of trace metal speciation under various marine conditions throughout Earth's history that includes the implications of my new findings on cyanobacterial-DOM. Overall, my dissertation emphasizes the influence of cyanobacteria and cyanobacterial-derived organic matter on the distribution of bioessential trace elements.

### 1.3. References

- Bishop, B.A., Flynn, S.L., Warchola, T.J., Alam, M.D., Robbins, L.J., Liu, Y., Owtrim, G.W., Alessi, D.S., Konhauser, K.O. (2019). Adsorption of biologically critical trace elements to the marine cyanobacterium *Synechococcus* sp. PCC 7002: Implications for marine trace metal cycling. *Chemical Geology* **525**, 28-36.
- Boiteau, R. M., Till, C. P., Ruacho, A., Bundy, R. M., Hawco, N. J., McKenna, A. M., Barbeau, K. A., Bruland, K. W., Saito, M. A., Repeta, D. J. (2016). Structural Characterization of Natural Nickel and Copper Binding Ligands along the US GEOTRACES Eastern Pacific Zonal Transect. *Frontiers in Marine Science* **3**, 243.
- Bruland, K.W. (1980). Oceanographic distributions of cadmium, zinc, nickel, and copper in the North Pacific. *Earth and Planetary Science Letters* **47**, 176-198.
- Bruland, K.W., Donat, J.R., Hutchins, D.A. (1991). Interactive influences of bioactive trace metals on biological production in oceanic waters. *Limnology and Oceanography* **36**, 1555-1577.
- Bruland, K.W., Lohan M.C. (2003). Controls of trace metals in seawater. *Treatise on Geochemistry* **6**, 23-47.
- Coale, K. H., Bruland, K. W. (1988). Copper complexation in the Northeast Pacific. *Limnology and Oceanography* **33**, 1084-1101.
- Fein, J.B., Daughney, C.J., Yee, N., Davis, T.A. (1997). A chemical equilibrium model for metal adsorption onto bacterial surfaces. *Geochimica et Cosmochimica Acta* **61**, 3319-3328.
- Hansell, D. A. (2013). Recalcitrant dissolved organic carbon fractions. *Annual Review of Marine Sciences* **5**, 421-445.
- Hedges, J. I., Keil, R. G., Benner, R. (1997). What happens to terrestrial organic matter in the ocean? *Organic Geochemistry* **27**, 195-212.

- Jiao, N., Cai, R., Zheng, Q., Tang, K., Liu, J., Jiao, F., Wallace, D., Chen, F., Li, C., Amann, R., Benner, R., Azam, F. (2018). Unveiling the enigma of refractory carbon in the ocean. *National Science Review* **5**, 459-463.
- Kawasaki, N., Sohrin, R., Ogawa, H., Nagata, T., Benner, R. (2011). Bacterial carbon content and the living and detrital bacterial contributions to suspended particulate organic carbon in the North Pacific Ocean. *Aquatic Microbial Ecology* **62**, 165-176.
- Konhauser, K. O., Pecoits, E., Lalonde, S. V., Papineau, D., Nisbet, E. G., Barley, M. E., Arndt, N. T., Zahnle, K., Kamber, B. S. (2009). Oceanic nickel depletion and a methanogen famine before the Great Oxidation Event. *Nature* **458**, 750-753.
- Konhauser, K. O., Robbins, L. J., Alessi, D. S., Flynn, S. L., Gingras, M. K., Martinez, R. E., Kappler, A., Swanner, E. D., Li, Y.-L., Crowe, S. A., Planavsky, N.J., Reinhard, C. T., Lalonde, S. V. (2018) Phytoplankton contributions to the trace-element composition of Precambrian banded iron formations. *Geol. Soc. Am. Bull.* **130**, 941-951.
- Lechtenfeld, O. J., Kattner, G., Flerus, R., McCallister, S. L., Schmitt-Kopplin, P., Koch, B. P. (2014). Molecular transformation and degradation of refractory dissolved organic matter in the Atlantic and Southern Ocean. *Geochimica et Cosmochimica Acta* **126**, 321-337.
- Liu, Y., Alessi, D. S., Owttrim, G. W., Petrash, D. A., Mloszewska, A. M., Lalonde, S. V., Martinez, R. E., Zhou, Q., Konhauser, K. O. (2015) Cell surface reactivity of *Synechococcus* sp. PCC 7002: Implications for metal sorption from seawater. *Geochim. Cosmochim. Acta* **169**, 30-44.

- Ma, X., Coleman, M.L., Waldbauer, J.R. (2018). Distinct molecular signatures in dissolved organic matter produced by viral lysis of marine cyanobacteria. *Environmental Microbiology* **20**, 3001-3011.
- Morel, F.M.M., Price, N.M. (2003). The biogeochemical cycles of trace metals in the oceans. *Science* **300**, 944-947.
- Phoenix, V. R., Martinez, R. E., Konhauser, K. O., Ferris, F. G. (2002). Characterization and Implications of the Cell Surface Reactivity of *Calothrix* sp. Strain KC97. *Applied and Environmental Microbiology* **68**, 4827-4834.
- Robbins, L.J., Lalonde, S.V., Planavsky, N.J., Partin, C.A., Reinhard, C.T., Kendall, B., Scott, C., Hardisty, D.S., Gill, B.C., Alessi, D.S., Dupont, C.L., Saito, M.A., Crowe, S.A., Poulton, S.W., Bekker, A., Lyons, T.W., Konhauser, K.O. (2016). Trace elements at the intersection of marine biological and geochemical evolution. *Earth-Science Reviews*, **163**, 323-348.
- Saba, G.K., Steinberg, D.K., Bronk, D.A. (2011). The relative importance of sloppy feeding, excretion, and fecal pellet leaching in the release of dissolved carbon and nitrogen by *Acartia tonsa* copepods. *Journal of Experimental Marine Biology and Ecology* **404**, 47-56.
- Saito, M.A., Sigman, D.M., Morel, F.M.M. (2003). The bioinorganic chemistry of the ancient ocean: The coevolution of cyanobacterial metal requirements and biogeochemical cycles at the Archean-Proterozoic boundary? *Inorganica Chimica Acta* **356**, 308-318.
- Strom, S. L., Benner, R., Ziegler, S., Dagg, M. J. (1997). Planktonic grazers are a potentially important source of marine dissolved organic carbon. *Limnology and Oceanography* **42**, 1364-1374.
- Suttle, C. (2007). Marine viruses – major players in the global ecosystem. *Nature Reviews Microbiology* **5**, 801-812.

- Volkman, J. K., Tanoue, E. (2002). Chemical and biological studies of particulate organic matter in the ocean. *Journal of Oceanography* **58**, 265-279.
- Vraspir, J. M.; Butler, A. (2009). Chemistry of marine ligands and siderophores. *Annual Review of Marine Science* **1**, 43-63.
- Yee, N., Fein, J. (2001). Cd adsorption onto bacterial surfaces: A universal adsorption edge? *Geochimica et Cosmochimica Acta* **65**, 2037-2042.
- Zhao, Z., Gonsoir, M., Luek, J., Timko, S., Ianiri, H., Hertkorn, N., Schmitt-Kopplin, P., Fang, X., Zeng, Q., Jiao, N., Chen F. (2017). Picocyanobacteria and deep-ocean fluorescent dissolved organic matter share similar optical properties. *Nature Communications* **8**, 15284.
- Zhao, Z., Gonsoir, M., Schmitt-Kopplin, P., Zhan, Y., Zhang, J., Jiao, N., Chen F. (2019). Microbial transformation of virus-induced dissolved organic matter from picocyanobacteria: coupling of bacterial diversity and DOM chemodiversity. *The ISME Journal* **13**, 2551-2565.
- Zheng, Q., Chen, Q., Cai, R., He, C., Guo, W., Wang, Y., Shi, Q., Chen, C., Jiao, N. (2019). Molecular characteristics of microbially mediated transformation of *Synechococcus*-derived dissolved organic matter as revealed by incubation experiments. *Environmental Microbiology* **21**, 2533-2542.

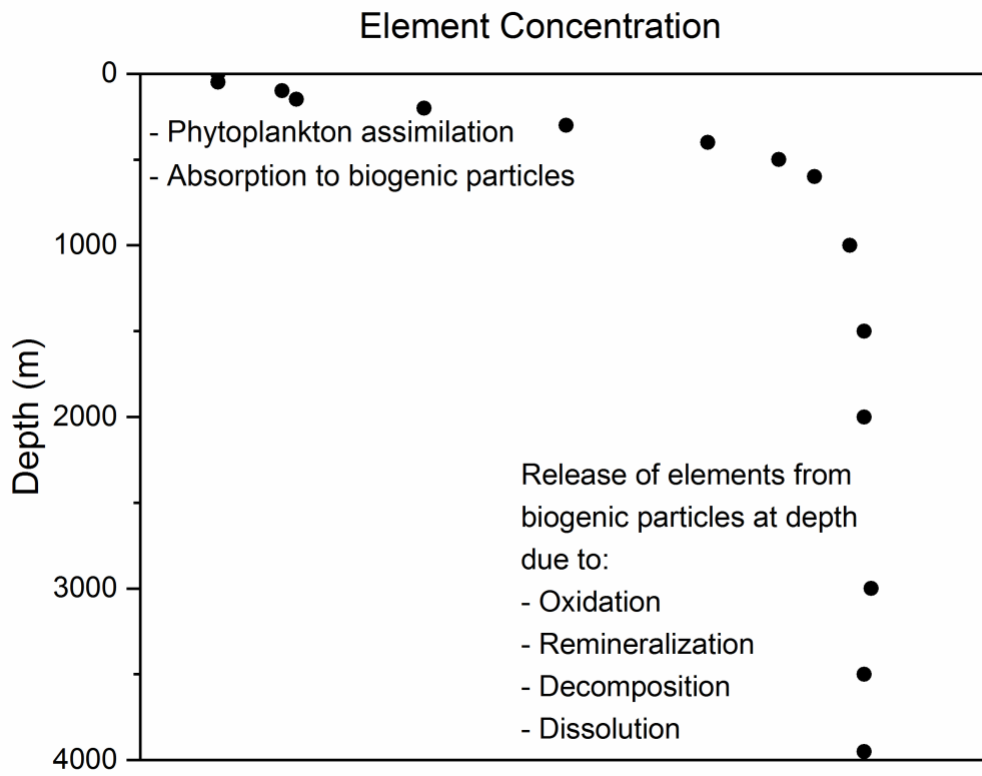


**Figure 1.1:** Typical nutrient-like depth profile in the marine environment.

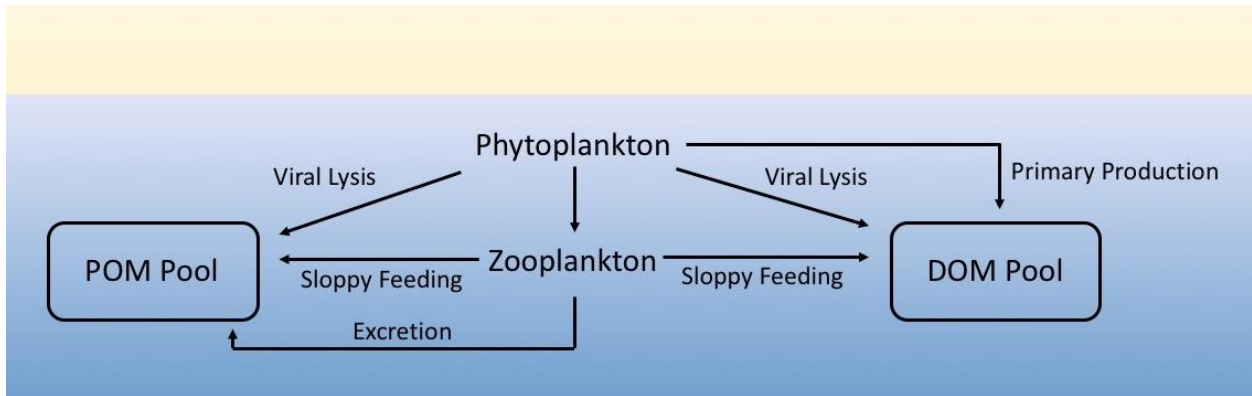


**Figure 1.2:** Generalized diagram of DOM and POM production in modern marine settings

## Chapter 2: The role of cyanobacteria in trace metal transport to the oceans<sup>1</sup>

### 2.1. Introduction

Cyanobacteria are amongst the most abundant primary producers on Earth, and as such, their surface reactivity may significantly contribute to metal cycling in soils, sediment and aqueous environments. Populations of cyanobacteria are highly variable across different species and typically range from  $10^4$  to  $10^5$  cells per mL in the marine photic zone (Flombaum et al. 2013). Their general ability to bind metal cations stems from the presence of proton-active surface carboxyl, phosphoryl, sulfhydryl, amine and hydroxyl functional groups located on the cell walls, exopolysaccharides (EPS), and extracellular sheaths (Phoenix et al., 2002; Benning et al., 2004; Yee et al., 2004; Lalonde et al., 2005; Baker et al., 2010; Yu et al., 2014; Liu et al. 2015; Bishop et al. 2019). The cell surface can behave either hydrophobically or hydrophilically depending on the surface functional groups expressed under different aqueous conditions (Liu et al., 2015; Liu et al., 2016). Hydrophobic cell surfaces are often composed of a neutral sheath which lowers the cyanobacterial surface charge to increase the adherence of benthic species to a submerged solid substrate (Phoenix et al. 2002), whereas planktonic species in the marine water column lack these neutral sheaths, creating a hydrophilic surface that makes them efficient at adsorbing metal cations from solution (Liu et al. 2015; Bishop et al. 2019).

*Synechocystis* is a genus of unicellular, planktonic cyanobacteria that performs oxygenic photosynthesis primarily in freshwater but has also been identified and isolated in various hydrothermal, brackish, and marine systems (Appendix 1 SI Table 1.1) (Stanier et al. 1971; Rippka et al. 1979; Zhang et al. 1999; Abed et al. 2002; Ozturk et al. 2009). Amongst these, *Synechocystis* sp. PCC 6803 (from here on *Synechocystis*), originally isolated from freshwater in California

---

<sup>1</sup>This chapter has been published in *Chemical Geology* as: Swaren, L., Hao, W., Melnyk, S., Baker, D., Li, Y., Owttrim, G.W., Zeng, H., Gingras, M.K., Alessi, D.S., Konhauser, K.O.

(Stanier et al. 1971; Rippka et al. 1979), has been extensively studied because it contains the required traits of model organisms; it reaches exponential growth relatively rapidly, and it is easy to manipulate for the purpose of genomic studies (Ikeucho and Tabata, 2001). *Synechocystis* was the first photosynthetic cyanobacterium to have its genome sequenced because of its common use in laboratories (Kaneko et al. 1996; Ikeucho and Tabata, 2001). Because of its ubiquity, it has been the subject of various metallomic studies for the purpose of understanding its adaptability to environmental changes and how it modifies the performance of photosystems and electron transport activity (e.g., Tiwari and Mohanty, 1996; Badarau and Dennison, 2011; Du et al. 2019). Additionally, *Synechocystis* has been demonstrated to possess euryhaline capabilities, meaning it can thrive in freshwater, brackish and saline conditions, such as coastal environments (Reed et al. 1985; Iijima et al. 2015).

Metallomic studies have revealed the ability of *Synechocystis* to sequester environmental pollutants. For instance, Khattar (2009) showed that a strain of *Synechocystis pevalekii* isolated from the industrially polluted Satluj River in India removed millimolar concentrations of Cd(II) from water above pH 6 but below the point of metal precipitation. Similarly, Ozturk et al. (2010) isolated two strains of *Synechocystis* from several lakes and a stream in Turkey and found that the majority (89% to 94%) of a 10 ppm Cd(II) solution was adsorbed within a few minutes of exposure to the cell walls, while intracellular accumulation only occurred after 7 days. Most of the recent literature on the adsorption of metals to *Synechocystis* uses empirical approaches such as isotherms (e.g., Langmuir and Freundlich) as well as linear distribution coefficients (Appendix 1 SI Table 1.2) to model metal adsorption data (e.g., Demirel et al. 2009; Ozturk et al. 2009; Zhang et al. 2011). Although these methods make suitable predictions within the range of the experimental conditions employed, they often cannot be applied to systems having different pH, ionic strength

(IS), competing ions, sorbate-to-sorbent ratios, and/or temperature (Koretsky, 2000; Alam et al. 2018). By contrast, the surface complexation model (SCM) approach, which is based on balanced reactions and equilibrium thermodynamics, can account for such fluctuations (Flynn et al. 2014; Fein, 2017; Alessi et al., 2019).

In this study, we analyzed the composition of the cell wall of *Synechocystis* and assessed its ability to adsorb dissolved Cd(II) over a range of pH. We chose Cd as our metal of interest because it has been used extensively in metal adsorption studies to microbial surfaces (e.g., Yee and Fein, 2001; Petrash et al. 2011; Liu et al. 2015; Konhauser et al., 2018; Bishop et al. 2019) making it ideal for comparison, and it is a common environmental pollutant released through various manufacturing processes (Ozturk et al. 2010). Most recently, Hao et al. (2019, 2020) investigated the effects of IS on the ability of clay minerals to adsorb Cd. In doing so, they found that Cd adsorption was greatest under freshwater conditions but upon exposure to marine conditions, Cd was desorbed. Given the ability of *Synechocystis* to tolerate salinity fluctuations and its widespread occurrence, it is an ideal microbial candidate to study if changes in aqueous chemistry impact cellular surface chemistry, and ultimately, the ability of microbial biomass to bind metals such as Cd. This determination is important since planktonic cells have been shown to be abundant and diverse in river systems – implying they could act as metal transport vectors to the oceans (Bolgovics et al. 2017; Descy et al. 2017) much like clay minerals (Hao et al. 2019, 2020). Understanding the fate of metals bound to river-transported microorganisms is a key missing parameter in understanding trace metal supply to the estuarine and coastal biosphere, and ultimately the trace metal concentrations and distributions found in the organic-rich shale record.

## **2.2. Methods**

### **2.2.1. Cyanobacterial growth & harvesting**

The axenic, glucose tolerant strain of *Synechocystis* sp. PCC 6803 was cultured aerobically on BG-11 mineral media (Allen, 1968; Rippka et al. 1979). During growth, cells were maintained at a light intensity of 50  $\mu\text{mol photons m}^{-2} \text{s}^{-1}$  and 30°C. When a visible colony developed, the cells were transferred via a sterile inoculation loop to a 150 mL Erlenmeyer flask containing 50 mL of BG-11. The 50 mL culture was aerated by shaking at 60 rpm at 30°C. After 3-5 days, the culture was transferred to a 1 L Erlenmeyer flask containing an additional 350 mL of BG-11. The 400 mL culture was aerated by shaking at 100 rpm at 30°C combined with continuous bubbling with filtered (Millipore, 0.20  $\mu\text{m}$ ), humidified air for a minimum of 5 days.

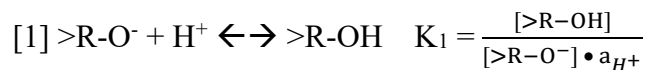
To harvest *Synechocystis* cells for re-suspension in 0.01 NaCl (low ionic strength), or 0.56 M NaCl (high ionic strength) solutions, the 400 mL culture was divided into 50 mL polypropylene tubes and centrifuged at 10,000 g for 5 minutes. The resulting supernatants were discarded, and the bacterial pellets re-suspended using a vortex in the appropriate electrolyte solution (0.01 M or 0.56 M NaCl). The cells were washed and re-suspended using the above procedure 4 additional times to ensure removal of growth media. Following the final wash cycle, the *Synechocystis* wet mass was weighed and the pellet re-suspended to 10 g L<sup>-1</sup> in the appropriate electrolyte solution. Following cell washing, the cells did not display the yellow-green coloration indicative of cell stress (Arunakumara and Xuecheng, 2009). Additionally, cell lysis has not been reported for cyanobacterial cell washing via centrifugation in electrolyte solutions similar or identical to the procedure outlined above (Liu et al. 2015; Bishop et al. 2019).

### **2.2.2. Potentiometric titrations**

Suspensions of *Synechocystis* cells were prepared for potentiometric acid-base titrations (Metrohm Titrando 905) by diluting 5 mL of the 10 g L<sup>-1</sup> *Synechocystis* stock suspension in 45 mL 0.01 M or 0.56 M NaCl to yield a 1 g L<sup>-1</sup> final solution: 1 g L<sup>-1</sup> is equivalent to 1.0-1.2×10<sup>6</sup> cells based on flow cytometry data (Appendix 1 SI Figure 1.1). The *Synechocystis* solution was sealed from the atmosphere and purged for 30 minutes prior to, and during, the titration with N<sub>2</sub> gas. Following the 30-minute N<sub>2</sub> purge, the titration was initiated by adding small aliquots of 0.1 M HNO<sub>3</sub> (diluted Fisher Scientific 70% solution weighed gravimetrically) to decrease the pH to 3 (referred to as the “down” titration). Once the cyanobacterial solution was acidified to pH 3, the titration continued with the addition of small volumes of 0.1 M NaOH (prepared gravimetrically from NaOH pellets in ultrapure water, Fisher Scientific) (referred to as the “up” titration). The “up” titration stopped at pH 10, and the second “down” titration began through the addition of 0.1 M HNO<sub>3</sub> until a pH of 3 was again achieved. The “down” titration was conducted in twice to confirm there was no hysteresis, and to test the reversibility of the titration (Hao et al. 2018) (Appendix 1 SI Figure 1.2). To ensure chemical equilibrium throughout the titration, an electrode stability of 0.1 mV s<sup>-1</sup> was required before the further addition of acid or base in both the up and down titrations. After completion, the *Synechocystis* solution was filtered onto pre-weighed 0.20 μm filters (Millipore Isopore Membrane Filters), rinsed 3× with ultrapure water, and air-dried for 48 h to determine the dry weight.

The pH and corresponding acid and base volumes added during the titrations were recorded automatically by the titration software (Tiamo 2.5 – Metrohm) and processed to determine the proton budget. *Synechocystis* cells were titrated in each electrolyte in triplicate. Blank titrations were, for comparison, conducted on 0.01 M NaCl solution without the addition of *Synechocystis*

to ensure that the proton reactivity was a property of the *Synechocystis* cells rather than a property of the electrolyte. The buffering capacity of the blank electrolyte solution was trivial in comparison to the cyanobacterial cell suspension. The protonation model was designed according to Reaction 1:



where  $>R-O^-$  is the deprotonated surface functional group and  $>R-OH$  is the corresponding protonated state; square brackets represent concentrations of surface sites, and  $a_{H^+}$  is the proton activity. The processed data were used to solve for the  $pK_a$  values and corresponding site concentrations of surface ligands, using the software FITEQL 4.0 (Herbelin and Westall, 1999). The resulting protonation model was subsequently used to develop a non-electrostatic surface complexation model (SCM) of Cd adsorption.

### **2.2.3. Attenuated total reflectance Fourier transform infrared (ATR-FTIR) spectroscopy**

Immediately following cell washing and harvesting, the  $10 \text{ g L}^{-1}$  stock *Synechocystis* suspension was filtered through  $0.20 \text{ }\mu\text{m}$  nylon membranes and rinsed with ultrapure water to minimize salt precipitation. Cells were removed from the  $0.20 \text{ }\mu\text{m}$  nylon membrane with ultrapure water and oven dried at  $50^\circ\text{C}$  for 24 h. Dried *Synechocystis* cells were then analyzed via ATR-FTIR spectroscopy (Bruker Platinum ATR). Samples were crushed using an agate mortar and pestle to produce a powder that could be loaded in the crystal. The spectra were recorded as 16 co-added interferograms at a resolution of  $4 \text{ cm}^{-1}$ .

### **2.2.4. Zeta potential**

Washed *Synechocystis* stock cells were re-suspended in either 0.01 M NaCl or 0.56 M NaCl to 10 g L<sup>-1</sup> in a sterile Erlenmeyer flask and diluted to 0.2 g L<sup>-1</sup> in sterile 50 mL polypropylene tubes. The pH of each tube was adjusted using 0.1 and 1 M HNO<sub>3</sub> and NaOH to cover a range of 3-9. Samples were placed on an end-over-end rotator at 25 rpm between adjustments. Samples were rotated for a minimum of 1 h between acid/base additions and left overnight following the final pH adjustment. Zeta potential measurements were conducted with a Zetasizer Nano Series instrument (Malvern Instruments, United Kingdom). Electrolyte solutions (0.01 and 0.56 M NaCl) without *Synechocystis* were used as controls. The average of 2 separate cultures are reported below, and each sample was measured in triplicate.

#### **2.2.5. Cadmium adsorption experiments**

After cell washing, *Synechocystis* cells were re-suspended in either 0.01 M NaCl or 0.56 M NaCl spiked with 1 ppm Cd (from a 1,000 ppm CdCl<sub>2</sub> stock solution) to 10 g L<sup>-1</sup> in an acid-washed 150 mL glass beaker. An identical experiment was conducted in 0.01 M NaNO<sub>3</sub> for direct comparison to the 0.01 M NaCl experiment to determine whether CdCl<sub>2</sub> complexes interfered with the experimental results. The mixture was stirred using a magnetic stir-bar for 10 min and 10 mL aliquots were transferred from the *Synechocystis* slurry to a set of seven 15 mL polypropylene test tubes. The pH was adjusted as above within a 24-hour time frame including a 12-hour equilibration time prior to measuring the final pH. Following the final pH reading, samples were filtered through 0.20 µm nylon membranes and diluted 10× with 2% HNO<sub>3</sub> and 0.5% HCl solution and analyzed via ICP-MS/MS (Agilent 8800 Triple Quadrupole). Experimental blanks were conducted at both IS without the addition of *Synechocystis* to identify any Cd loss to precipitation as CdCO<sub>3</sub> is

expected to precipitate at pH >8.5 in 0.56 M NaCl and pH >7.5 in 0.01 M NaCl (Appendix 1 SI Figures 1.3 and 1.4).

## **2.3. Results**

### **2.3.1. Potentiometric titrations**

Protonation model results are provided in Table 2.1 and duplicate data appear in Appendix 1 Table 1.3. Several models, including one-, two-, and three-site non-electrostatic protonation models were tested while fitting the titration data (Appendix 1 SI Figure 1.5). Both the two- and three-site models provide better fits to the titration data than the one-site model (Appendix 1 Figure 1.5). At both freshwater and marine IS, a two-site protonation models provided the best fits, based on the variance ( $V_y$ ) parameter in FITEQL being closest to 1.0 (Appendix 1 Table 1.3). At freshwater IS, the best-fitting non-electrostatic protonation model had two functional groups with  $pK_a$  values of 5.62 ( $\pm 0.17$ ), and 9.97 ( $\pm 0.06$ ), with corresponding site concentrations of  $4.37 \times 10^{-5}$  ( $\pm 6.55 \times 10^{-6}$ ) mol  $g^{-1}$  and  $6.95 \times 10^{-5}$  ( $\pm 1.29 \times 10^{-6}$ ) mol  $g^{-1}$ , respectively. Additionally, at marine IS, the best-fitting non-electrostatic protonation model had two functional groups with  $pK_a$  values of 5.37 ( $\pm 0.00$ ) and 9.65 ( $\pm 0.00$ ), with corresponding site concentrations of  $4.10 \times 10^{-5}$  ( $\pm 1.63 \times 10^{-6}$ ) mol  $g^{-1}$ , and  $4.49 \times 10^{-5}$  ( $\pm 1.32 \times 10^{-6}$ ) mol  $g^{-1}$ , respectively (replicate data can be found in Appendix 1 SI Table 1.3).

### **2.3.2. ATR-FTIR**

The ATR-FTIR spectra and respective functional group assignments for *Synechocystis* cells are summarized in Appendix 1 SI Figure 1.6 and SI Table 1.4, duplicate analyses can be found in Appendix 1 SI Figure 1.7. The broad peak spanning from 3500 – 3000  $cm^{-1}$  can be attributed to

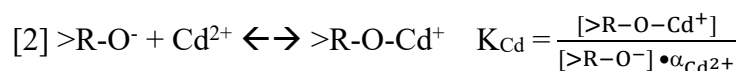
amino groups, likely overlapping with hydroxyl groups (Ozturk et al. 2010). The peak cluster focused around  $2924\text{ cm}^{-1}$  is indicative of alkanes, indicating the presence of methyl and methylene groups (Jiang et al. 2004). The distinctive peaks at  $1646$ ,  $1534$ , and  $1444\text{ cm}^{-1}$  indicate the presence of primary, secondary, and tertiary amide peaks, respectively, confirming the presence of proteins (Jiang et al. 2004; Delille et al. 2007; Minnes et al. 2017). The smaller peak at  $\sim 1736\text{ cm}^{-1}$ , likely obscured due to the intense primary amide, indicates the presence of ester ( $-\text{C}=\text{O}$ ) in lipids (Jiang et al. 2004). *Synechocystis* cells demonstrate characteristic carbohydrate spectra in the  $1200\text{-}950\text{ cm}^{-1}$  range (Bouhedja et al. 1997). Several distinct peaks in the carbohydrate range are likely cell wall components, such as amino sugars derived from peptidoglycan and phospholipids (Bouhedja et al. 1997). Interestingly, the distinct peak at  $1036\text{ cm}^{-1}$  suggests: (1) the potential presence of  $-\text{PO}$  groups likely associated with phospholipids (Minnes et al. 2017), and/or (2) the presence of  $\text{C}-\text{O}-\text{C}$  stretching due to carbohydrates on the cell wall after loss of EPS (Zhang et al. 2011). The strong peaks associated with EPS ( $1385$  and  $1342\text{ cm}^{-1}$ ) suggest that the  $1036\text{ cm}^{-1}$  peak represents phosphoryl groups of phospholipids.

### **2.3.3. Zeta potential**

*Synechocystis* cell surface charge was measured as a function of pH (Figure 2.1). The cells exhibit near neutral zeta potential from pH 3 to around pH 5 at both freshwater and marine IS (Figure 2.1). The cells remain negative and demonstrate a slight increase in electronegativity from pH 5 to 9 under marine IS,  $-0.9\text{ mV}$  to  $-5.7\text{ mV}$ , respectively. Under freshwater IS, *Synechocystis* cells demonstrate a slightly positive surface charge below pH 4 and show a sharp decrease from pH 6 to 7,  $-7.5\text{ mV}$  to  $-42.3\text{ mV}$ , respectively.

### 2.3.4. Cadmium adsorption

The results of cadmium pH adsorption edge experiments onto the cells of *Synechocystis* at marine (0.56 M NaCl) and freshwater (0.01 M NaCl) ionic strength (IS) are illustrated in Figure 2.2. Adsorption data from 0.01 M NaNO<sub>3</sub> experiments are shown in Figure S8, indicating that Cd-Cl complexation did not influence adsorption results. At freshwater IS, *Synechocystis* cells adsorb nearly ~80% of 1 ppm Cd at pH between 6 and 7.5. At marine IS and pH 7-9, Cd adsorption varies from ~20% at pH 7 up to ~68% at pH 9. The largest contrast in Cd adsorption occurs between pH 5-7.5, where 60% more of the total Cd is adsorbed at freshwater IS than at marine IS (Figure 2.2). The Cd adsorption data were modeled in FITEQL using the following reaction:



Aqueous complexation constants for the hydrolysis of Cd(II) and chloride complexation with Cd(II) were taken from Baes and Mesmer (1977). Experimental results are compared to SCM fits in Figure 2.2, the modeled Cd adsorption equilibrium constants (given as log  $K_{Cd}$ ) appear in Table 1, while a full list of reactions used in the SCM can be found in Appendix 1 SI Table 1.5. Various modeling methods were attempted, and the results can be found in Appendix 1 SI Table 1.6. The results showed that  $K_{Cd}$  values under freshwater conditions were in the same range for site 2 (10.2 versus 10.3, freshwater and marine, respectively) based on variance values close to 1 as those determined under marine conditions (Table 2.1), and within the range of ionic strength dependent variation reported by other authors (e.g., Borrok and Fein, 2005). The  $K_{Cd}$  values of site 1 had slightly more variation, 7.3 versus 6.2, in freshwater and marine, respectively. The distribution of Cd adsorption on each site as a function of pH can be found in Figure 2.3. At both IS site 1 has a higher affinity for Cd at more acidic pH values, whereas site 2 becomes dominant at pH 7 and 8 in freshwater and marine IS, respectively (Figure 2.3). Overall, *Synechocystis* cells

have a higher concentration of both site 1 and 2 to account for the larger concentration of Cd adsorbed (Figure 2.3). In addition, our models provide a good fit to experimental data across the tested pH range. Taken together, our SCMs provide a flexible tool to predicting Cd speciation with changes in ionic strength and pH typical of terrestrial-to-marine transitions in aqueous chemistry.

## **2.4. Discussion**

### **2.4.1. Surface reactivity of *Synechocystis***

The cyanobacterium *Synechocystis* sp. PCC 6803 has cell surface properties similar to previously studied bacteria. Between pH 3 and 9, a range encompassing most natural environments, both Gram-positive and Gram-negative bacteria typically exhibit three surface functional groups; carboxyl, phosphoryl, and either amine or hydroxyl (e.g., Yee and Fein, 2001). The functional groups identified with *Synechocystis* sp. likely correspond to a mixture of carboxyl, phosphoryl, hydroxyl, and amine. Both amine and hydroxyl sites have been found to have similar  $pK_a$  values, although hydroxyl sites typically have  $pK_a$  values  $>10$  associated with phenol groups (Fein et al. 1997; Cox et al. 1999). The second site, associated with  $pK_a$  9.65 and 9.97 in marine and freshwater, respectively, is likely representative of combination of amine, hydroxyl groups based on ATR-FTIR and titration data (Ngwenya et al. 2009; Ozturk et al. 2010). Additionally, Yu et al. (2014) determined that various bacterial species contain sulfhydryl functional groups with  $pK_a$  values ranging 9.2 to 9.4, similar to the second identified site on *Synechocystis*. Therefore, the cell surface of the cyanobacterium *Synechocystis* is likely composed of a combination of carboxyl, phosphoryl, hydroxyl, amine, and sulfhydryl, which we show can be modelled accurately using a 2-site protonation model.

As opposed to the potentiometric titration data, which measures the *Synechocystis* proton buffering capacity across a pH range (Alessi et al. 2019), zeta potential measures the slipping plane surface charge. Interestingly, both buffering capacity and zeta potential are influenced by variations in IS. Increasing solution IS, from freshwater to marine, caused the best-fit pK<sub>a</sub> values to decrease slightly (Table 2.1) and resulted in slightly different titration curves (Appendix 1 SI Figure 1.2). An increase in solution IS evidently influenced zeta potential much more than buffering capacity as witnessed in the drastic change in surface charge at freshwater versus marine IS (Figure 2.1). The zeta potential of *Synechocystis* at freshwater IS is more representative of true surface charge due to what is likely monovalent cation suppression of the bacterial surface charge occurring in marine IS (Alessi et al. 2010). With an abundance of Na<sup>+</sup> ions in solution, as in 0.56 M NaCl with respect to 0.01 M NaCl, the bulk solution is cation saturated compared to the slipping plane across the entire pH range, resulting in a relatively constant zeta potential measurement.

FTIR analyses indicated the presence of typical biomolecule bonding environments associated with cyanobacterial cell components – peptidoglycan, proteins, nucleic acids, cell membrane fatty acids, lipids, polysaccharides, and nucleic acid associated phospholipids (Filip and Hermann, 2001; Delille et al. 2007). Similarly, Ozturk et al. (2010) identified four shifts in FTIR spectra indicating four potential surface adsorption sites for Cd in two Turkish strains of *Synechocystis* sp. The identified shifts in spectra, inferred as surface adsorption sites, were prominent on O-H stretching groups, C=O stretching groups, as well as C-H and C-O groups (Ozturk et al. 2010).

#### **2.4.2. Implications for trace metal cycling in transitional settings**

There is an abundance of literature investigating the sorption of trace metals to cyanobacterial cell surfaces (e.g. Lalonde et al. 2007; Khattar, 2009; Ozturk et al. 2010; Zhang et al. 2011; Liu et al. 2015; Flynn et al., 2017; Konhauser et al., 2018). Here we demonstrate the influence of ionic strength (IS) on Cd sorption to *Synechocystis* cell walls. Cd sorption in the low IS solution (0.01 M NaCl), representative of freshwater, far exceeds that in higher IS solutions (0.56 M NaCl), representative of marine settings (Figure 2.2). The area of particular interest is from pH values 5 to 8 where the difference in Cd sorption is largest. Similarly, 1 ppm Cd adsorption by *Synechocystis* in 0.01 M NaNO<sub>3</sub> and 0.56 M NaNO<sub>3</sub> demonstrate trends where the greatest variation occurs at circumneutral pH (Liu et al. 2015). As a comparison, *Synechococcus* is capable of removing nearly 80% of a 1 ppm Cd from solution in 0.56 M NaCl at pH 8 (Liu et al. 2015), whereas *Synechocystis* reaches a maximum of ~50% removal under identical conditions. Liu et al. (2015) also determined that 1 ppm Cd adsorption onto *Synechococcus* was best fit by a 3-site protonation model rather than a 2-site. The Cd-binding surface ligands on *Synechococcus* had Cd-binding constants of 1.2, 1.8, and 2.7 in identical conditions, as compared to 6.2 and 10.3 for the two sites determined for *Synechocystis* in this study. Interestingly, the increase in negative surface charge exhibited between pH 5 to 6 in freshwater IS correlates well with the 60% increase in Cd adsorption. These results suggest that IS can be a primary control on Cd adsorption behavior with significant differences in the extent of adsorption between freshwater and marine/estuarine settings. These results imply that *Synechocystis* could be a major transporter of Cd from freshwater to marine environments.

Considering that *Synechocystis* cells have a stronger affinity for Cd at freshwater IS compared to marine IS suggests that such planktonic cyanobacteria could provide a means of Cd transport from rivers to coastal settings. Ozturk et al. (2010) discovered that Cd adsorption to

*Synechocystis* cell walls occurred within minutes of exposure, and that >89% was adsorbed to the cell wall and EPS where it could be desorbed given an increase in IS. At the conditions tested in our experiments that contain elevated Cd and *Synechocystis* concentrations, under freshwater IS and a pH of 8.0, *Synechocystis* is capable of near complete Cd removal of 1 ppm, whereas less removal is predicted at marine IS. This suggests that as *Synechocystis* cells are transported from freshwater to coastal systems, adsorbed Cd (and likely other divalent cations) will be released upon transitioning to higher IS environments.

As *Synechocystis* cells are found in abundance in brackish and transitional settings (Appendix 1 SI Table 1.1), they may act as a sink for trace metals prior to moving to the continental shelf. Some of these settings, such as estuaries, proffer an attenuated salinity gradient wherein Cd is desorbed gradationally along the length of the estuary. Other settings, such as deltas, display sharp salinity gradients and favor more rapid release of Cd. This suggests that Cd-bearing organic sediments are limited to areas characterized by fresh water, such as lakes, rivers and the inner parts of estuaries and that shallow-water mudstones associated with marine settings, such as prodelta sediments, will be measurably impoverished of Cd. Hao et al. (2020) demonstrated that clay minerals, namely kaolinite, illite, and montmorillonite, transport significant amounts of Cd (256.5 t of Cd annually) from river systems to estuaries, which subsequently desorbs from the clays at marine IS. Our results support a similar fate for Cd bound to planktonic cyanobacterial cells. Using concentrations of *Synechocystis* cells and kaolinite representative of natural conditions, we ran a predictive model to investigate the distribution of 1 ppm Cd in the presence of both 0.1 g/L cyanobacterial cells (Flombaum et al. 2014; Appendix 1 SI Figure 1.1) and kaolinite (Hao et al. 2020). The results indicate that 77.7% of Cd is adsorbed onto the cell surfaces as compared to 0.2% on the surface of kaolinite in freshwater IS and pH 6. Upon entering marine IS and pH 8, the

distribution shifts to 34.7% and 7.4% on the cell walls and kaolinite, respectively. Future studies will investigate the impact that the salinity gradient within estuarine systems has on: (1) trace metal adsorption in experimental systems containing multiple metals, (2) the impact of aggregation of planktonic cells with suspended clay minerals on metal adsorption, (3) the role of intracellular uptake on overall metal removal by planktonic microorganisms in estuary settings, and (4) the trace metal distribution along implied ancient salinity gradients.

## **2.5. Conclusion**

We studied the surface reactivity and Cd adsorption capacity of the model cyanobacteria, *Synechocystis*, at both freshwater (0.01 M NaCl) and marine (0.56 M NaCl) IS, to provide insights into trace metal transport mechanisms from riverine to marginal marine settings. At circumneutral pH (6-8), 10 g L<sup>-1</sup> *Synechocystis* adsorbs ~60% more Cd from a 1 ppm solution at freshwater IS than marine IS. Additionally, at typical riverine pH (7.5), *Synechocystis* is capable of nearly 100% Cd removal at freshwater IS as opposed to ~50% in marine IS at pH 8, typical of estuarine pH. The above results indicate that *Synechocystis*, and likely other widely distributed cyanobacteria, play an important role in trace metal cycling at the interfaces between freshwater and marine settings. This includes the ability to transport trace metals to coastal settings and their ultimate release to oceans. The mode of metals transport, adsorption to cell walls, and release due to increasing IS should be observable in sediments that are, at least partially, organic – a premise that needs to be tested in the rock record.

## 2.6. References

- Abed, R. M. M., Safi, N. M. D., Koster, J., de Beer, D., El-Nahhal, Y., Rullkotter, J., Garcia-Pichel, F. (2002) Microbial diversity of a heavily polluted microbial mat and its community changes following degradation of petroleum compounds. *Appl. Environ. Microbiol.* **68**, 1674-1683.
- Alam, M. D., Swaren, L., von Gunten, K., Cossio, M., Bishop, B., Robbins L. J., Hou, D., Flynn, S. L., Ok, Y. S., Konhauser, K. O., Alessi, D. S. (2018) Application of surface complexation modeling to trace metals uptake by biochar-amended agricultural soils. *Appl. Geochem.* **88**, 103-112.
- Alessi, D. S., Henderson, M., Fein, J. B. (2010) Experimental measurement of monovalent cation adsorption onto *Bacillus subtilis* cells. *Geomicrobiol. J.* **27**, 464-472.
- Alessi, D. S., Flynn, S. L., Alam, M. S., Robbins, L. J., Konhauser, K. O. (2019) *Potentiometric titrations to characterize the reactivity of geomicrobial surfaces*. In: Kenney, J. P. L., Veeramani, H., Alessi, D. S. (Eds.), *Analytical Geomicrobiology: A Handbook of Instrumental Techniques*, Cambridge University Press, Cambridge, United Kingdom, pp. 79-92.
- Allen, M. M. (1968) Simple conditions for growth of unicellular blue-green algae on plates. *J. Phycol.* **4**, 1-4.
- Arunakumara, K. K. I. U., Xuecheng, Z. (2009) Effects of heavy metals (Pb<sup>2+</sup> and Cd<sup>2+</sup>) on the ultrastructure, growth and pigment contents of the unicellular cyanobacterium *Synechocystis* sp. PCC 6803. *Chin. J. Oceanol. Limn.* **27**, 383-388.
- Badarau, A., Dennison, C. (2011) Thermodynamics of copper and zinc distribution in the cyanobacterium *Synechocystis* PCC 6803. *PNAS* **108**, 13007-13012.

- Baes, C. F., Mesmer, R. S. *The Hydrolysis of Cations*. John Wiley & Sons, New York, London, Sydney, Toronto 1976. 489 Seiten. *Berichte der Bunsengesellschaft für physikalische Chemie* 81, 245–246 (1977).
- Baker, M. G., Lalonde, S. V., Konhauser, K. O., and Foght, J. M. (2010) The role of extracellular substances in the surface chemical reactivity of *Hymenobacter aerophilus*, a psychotolerant bacterium. *Appl. Environ. Microbiol.* **76**, 102-109.
- Bolgovics, A., Varbiro, G., Acs, E., Trabert, Z., Kissm K. T., Pozderka, V., Gorgenyi, J., Boda, P., Lukacs, B. A., Nagy-Laszlo, Z., Abonyi, A., Borics, G. (2017) Phytoplankton of rhithral rivers: Its origin, diversity and possible use for quality-assessment. *Ecol. Indic.* **81**, 587-596.
- Borrok, D. M., Fein, J. B. (2005) The impact of ionic strength on the adsorption of protons, Pb, Cd, and Sr onto the surfaces of Gram negative bacteria: testing non-electrostatic, diffuse, and triple-layer models. *J. Colloid Interf. Sci.* **286**, 110-126.
- Bouhedja, W., Sockalingum, G. D., Pina, P., Bloy, C., Labia, R., Millot, J. M., Manfait, M. (1997) ATR-FTIR spectroscopic investigation of *E. coli* transconjugants beta-lactams-resistance phenotype. *FEBS Letters* **412**, 39-42.
- Bishop, B. A., Flynn, S. L., Warchola, T. J., Alam, M. S., Robbins, L. J., Liu, Y., Owttrim, G. W., Alessi, D. S., Konhauser, K. O. (2019) Adsorption of biologically critical trace elements to the marine cyanobacterium *Synechococcus* sp. PCC 7002: Implications for marine trace metal cycling. *Chem. Geol.* **525**, 28-36.
- Buslov, D. K., Nikonenko, N. A., Sushko, N. I., Zhibankov, R. G. (2002) Analysis of the structure of the bands in the IR spectrum of beta-D glucose by the regularized method of deconvolution. *J. Appl. Spectro.* **69**, 817-824.

- Caccamo, M. T., Gugliandolo, C., Zammuto, V., Magazu, S. (2020) Thermal properties of an exopolysaccharide produced by a marine thermotolerant *Bacillus licheniformis* by ATR-FTIR spectroscopy. *Int. J. Biol. Macromol.* **145**, 77-83.
- Cox, J. S., Smith, D. S., Warren, L. A., Ferris, F. G. (1999) Characterizing heterogeneous bacterial surface functional groups using discrete affinity spectra for proton binding. *Environ. Sci. Technol.* **33**, 4514-4521.
- Delille, A., Quiles, F., Humbert, F. (2007) In situ monitoring of the nascent *Pseudomonas fluorescens* biofilm response to variations in the dissolved organic carbon level in low-nutrient water by attenuated total reflectance-Fourier transform infrared spectroscopy. *Applied and Environmental Microbiology* **73**, 5782-5788.
- Demirel, S., Ustun, B., Aslim, B., Suludere, Z. (2009) Toxicity and uptake of Iron ions by *Synechocystis* sp. E35 isolated from Kucukcekmece Lagoon, Istanbul. *J. Hazard. Mat.* **171**, 710-716.
- Descy, J. P., Darchambeau, F., Lambert, T., Stoyneva-Gaertner, M. P., Bouillon, S., Borges, A. V. (2017) Phytoplankton dynamics in the Congo River. *Freshw. Biol.* **62**, 87-101.
- Du, J., Qiu, B., Gomes, M. P., Juneau, P., Dai, G. (2019) Influence of light intensity on cadmium uptake and toxicity in the cyanobacteria *Synechocystis* sp. PCC 6803. *Aquat. Toxicol.* **211**, 163-172.
- Fein, J. B., Daughney, C. J., Yee, N., Davis, T. A. (1997) A chemical equilibrium model for metal adsorption onto bacterial surfaces. *Geochim. Cosmochim. Acta* **61**, 3319-3328.
- Fein, J. B. (2017) Advanced biotic ligand models: Using surface complexation modeling to quantify metal bioavailability to bacteria in geologic systems. *Chem. Geol.* **464**, 127-136.

- Filip, Z., Hermann, S. (2001) An attempt to differentiate *Pseudomonas* spp. And other soil bacteria by FT-IR spectroscopy. *Eur. J. Soil Biol.* **37**, 137-143.
- Flombaum, P., Gallegos, J. L., Gordillo, R. A., Rincon, J., Zabala, L. L., Jiao, N., Karl, D. M., Li, W. K. W., Lomas, M. W., Veneziano, D., Vera, C. S., Vrugt, J. A., Martiny, A. C. (2013) Present and future global distributions of the marine cyanobacteria *Prochlorococcus* and *Synechococcus*. *PNAS*, **110**, 9824-9829.
- Flynn, S. L., Szymanowski, J. E. S., Fein, J. B. (2014) Modeling bacterial metal toxicity using a surface complexation approach. *Chem. Geol.* **375**, 110-116.
- Flynn, S. L., Gao, Q., Robbins, L. J., Warchola, T., Weston, J. N. J., Alam, S. M., Liu, Y., Konhauser, K. O., Alessi, D. S. (2017) Measurements of bacterial mat metal binding capacity in alkaline and carbonate-rich systems. *Chem. Geol.* **451**,17-24.
- Hao, W., Flynn, S. L., Alessi, D. S., Konhauser, K. O. (2018) Change of point of zero net proton charge (pHPZNPC) of clay minerals with ionic strength. *Chem. Geol.* **493**, 458-467.
- Hao, W., Flynn, S. L., Kashiwabara, T., Alam, M. S., Bandara, S., Swaren, L., Robbins, L. J., Konhauser, K. O. (2019) The impact of ionic strength on the proton reactivity of clay minerals. *Chem. Geol.* **529**, 119294.
- Hao, W., Kashiwabara, T., Jin, R., Takahashi, Y., Gingras, M. K., Alessi, D. S., Konhauser, K. O. (2020) Clay minerals as a source of cadmium to estuaries. *Sci. Rep.* **10**, 10417.
- Herbelin, A. L., Westall, J. C. (1999) FITEQL: a Computer Program for Determination of Equilibrium Constants from Experimental Data. Department of Chemistry, Oregon State University. Corvallis, OR. *Report 99-01*.

- Iijima, H., Nakaya, Y., Kuwahara, A., Hirai, M. Y., Osanai, T. (2015) Seawater cultivation of freshwater cyanobacterium *Synechocystis* sp. PCC 6803 drastically alters amino acid composition and glycogen metabolism. *Front.Microbiol.* **6**, 326.
- Ikeuchi, M., Tabata, S. (2001) *Synechocystis* sp. PCC 6803 – a useful tool in the study of genetics of cyanobacteria. *Photosynth. Res.* **70**, 73-83.
- Jiang, W., Saxena, A., Song, B., Ward, B. B., Beveridge, T. J., Myneni, S. C. B. (2004) Elucidation of functional groups on gram-positive and gram-negative bacterial surfaces using infrared spectroscopy. *Langmuir* **20**, 11433-11442.
- Kaneko, T., Sato, S., Kotani, H., Tanaka, A., Asamizu, E., Nakamura, Y., Miyajima, N., Hirose, M., Sugiura, M., Sasamoto, S., Kimura, T., Hosouchi, T., Matsuno, A., Muraki, A., Nakazaki, N., Naruo, K., Okumura, S., Shimpo, S., Takeuchi, C., Wada, T., Watanabe, A., Yamada, M., Tabata, S. (1996) Sequence analysis of the genome of the unicellular cyanobacterium *Synechocystis* sp. Strain PCC 6803. II. Sequence determination of the entire genome and assignment of potential protein-coding regions. *DNA Res.* **3**, 109-136.
- Khattar, S. J. I. S. (2009) Optimization of Cd<sup>2+</sup> removal by the cyanobacterium *Synechocystis pevalekii* using the response surface methodology. *Process Biochem.* **44**, 118-121.
- Konhauser, K. O., Robbins, L. J., Alessi, D. S., Flynn, S. L., Gingras, M. K., Martinez, R. E., Kappler, A., Swanner, E. D., Li, Y.-L., Crowe, S. A., Planavsky, N.J., Reinhard, C. T., Lalonde, S. V. (2018) Phytoplankton contributions to the trace-element composition of Precambrian banded iron formations. *Geol. Soc. Am. Bull.* **130**, 941-951.
- Koretsky, C. (2000) The significance of surface complexation reactions in hydrologic systems: a geochemist's perspective. *Journal of Hydrology* **230**, 127-171.

- Lalonde, S. V., Konhauser, K. O., Reysenbach, A. -L., and Ferris, F.G. (2005) The experimental silicification of Aquificales and their role in hot spring sinter formation. *Geobiology* **3**, 41-52.
- Lalonde, S., Amskold, L., Warren L. A., and Konhauser, K. O. (2007) Surface chemical reactivity and metal adsorptive properties of natural cyanobacterial mats from an alkaline hot spring, Yellowstone National Park. *Chem. Geol.* **243**, 36-52.
- Liu, Y., Alessi, D. S., Owtrim, G. W., Petrash, D. A., Mloszewska, A. M., Lalonde, S. V., Martinez, R. E., Zhou, Q., Konhauser, K. O. (2015) Cell surface reactivity of *Synechococcus* sp. PCC 7002: Implications for metal sorption from seawater. *Geochim. Cosmochim. Acta* **169**, 30-44.
- Liu, Y., Alessi, D., Owtrim, G.W., Kenney, J.P.L., Zhou, Q.X., Lalonde, S.V., and Konhauser, K.O. (2016) Cell surface acid-base properties of the cyanobacterium *Synechococcus*: Influences of nitrogen source, growth phase and N:P ratios. *Geochim. Cosmochim. Acta* **187**, 179-194.
- Minnes, R., Nissinmann, M., Maisels, Y., Gerlitz, G., Katzir, A., Yosef, R. (2017) Using Attenuated Total Reflection – Fourier Transform Infra-Red (ATR-FTIR) spectroscopy to distinguish between melanoma cells with a different metastatic potential. *Sci. Rep.* **7**, 4381.
- Ngwenya, B. T., Tournay, J., Magennis, M., Kapetas, L., Olive, V. (2009) A surface complexation framework for predicting water purification through metal biosorption. *Desalination* **248**, 344-351.
- Ozturk, S., Aslim, B., Turker, A. R. (2009) Removal of Cadmium Ions from Aqueous Samples by *Synechocystis* Sp. *Sep. Sci. Technol.* **44**, 1467-1483.

- Ozturk, S., Aslim, B., Suludere, Z. (2010) Cadmium(II) sequestration characteristics by two isolates of *Synechocystis* sp. In terms of exopolysaccharide (EPS) production and monomer composition. *Bioresour. Technol.* **101**, 9742-9748.
- Petrash, D. P., Raudsepp, M., Lalonde, S. V., and Konhauser, K.O. (2011) Assessing the importance of matrix materials in biofilm chemical reactivity: Insights from proton and cadmium adsorption onto the commercially-available biopolymer alginate. *Geomicrobiol. J.* **28**, 266-273.
- Phoenix, V. R., Martinez, R. E., Konhauser, K. O., Ferris, F. G. (2002) *Characterization and Implications of the Cell Surface Reactivity of Calothrix sp. Strain KC97.* *Appl. Environ. Microbiol.* **68**, 4827-4834.
- Reed, R. H., Warr, S. R. C., Richardson, D. L., Moore, D. J., Stewart, W. D. P. (1985) Multiphasic osmotic adjustment in a euryhaline cyanobacterium. *FEMS Microbiol. Letters* **28**, 225-229.
- Rippka, R., Deruelles, J., Waterbury, J. B., Herdman, M., Stainer, R. Y. (1979) Generic assignments, strain histories and properties of pure cultures of cyanobacteria. *J. Gen. Microbiol.* **111**, 1-61.
- Stanier, R. Y., Kunisawa, R., Mandel, M., Cohen-Bazire, G. (1971) Purification and Properties of Unicellular Blue-Green Algae (Order *Chroococcales*). *Bacteriol. Rev.* **35**, 171-205.
- Tiwari, S., Mohanty, P. (1996) Cobalt induced changes in photosystem activity in *Synechocystis* PCC 6803: Alterations in energy distribution and stoichiometry. *Photosynth. Res.* **50**, 243-256.
- Yee, N., Fein, J. (2001) Cd adsorption onto bacterial surfaces: A universal adsorption edge? *Geochim. Cosmochim. Acta* **65**, 2037-2042.

- Yu, Q., Szymanowski, J. Myneni, S. C. B., Fein, J. B. (2014) Characterization of sulfhydryl sites within bacterial cell envelopes using selective site-blocking and potentiometric titrations. *Chem. Geol.* **373**, 50-58.
- Zhang, K., Kurano, N., Miyachi, S. (1999) Outdoor culture of a cyanobacterium with a vertical flat-plate photobioreactor: effects on productivity of the reactor orientation, distance setting between the plates, and culture temperature. *Appl. Microbiol. Biotechnol.* **52**, 781-786.
- Zhang, D., Pan, X., Zhao, L., Mu, G. (2011). Biosorption of Antimony (Sb) by the cyanobacterium *Synechocystis* sp. *Pol. J. Environ.* **20**, 1353-1358.

**Table 2.1:** Summary of protonation and surface complexation modeling results from duplicate titration data of *Synechocystis* sp. PCC 6803 in various electrolyte solutions modelled using FITEQL 4.0. Site concentration is in units of mol g<sup>-1</sup>.

	0.01 M NaCl	0.56 M NaCl
logK <sub>ROH</sub>	5.62 (±0.17)	5.37 (±0.00)
site density	4.37×10 <sup>-5</sup> (±6.55×10 <sup>-6</sup> )	4.10×10 <sup>-5</sup> (±1.63×10 <sup>-6</sup> )
logK <sub>XOH</sub>	9.97 (±0.06)	9.65 (±0.00)
site density	6.95×10 <sup>-5</sup> (±1.29×10 <sup>-6</sup> )	4.49×10 <sup>-5</sup> (±1.32×10 <sup>-5</sup> )
logK <sub>ROcd</sub>	7.3	6.2
logK <sub>XOcd</sub>	10.2	10.3
V(y)	0.34	1.62

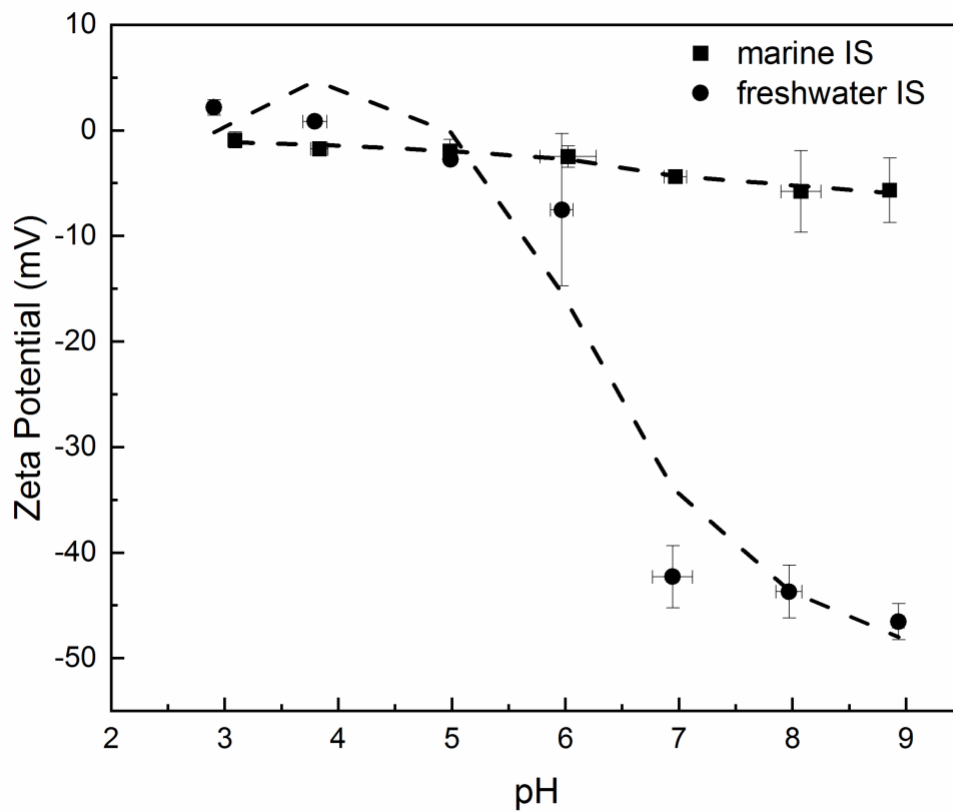


**Figure 2.1:** Zeta potential measurements performed on  $0.2 \text{ g L}^{-1}$  suspensions of *Synechocystis* sp. PCC 6803 in 0.01 and 0.56 M NaCl as a function of pH. Error bars represent 1-sigma standard deviation from duplicate analyses of separate cultures.

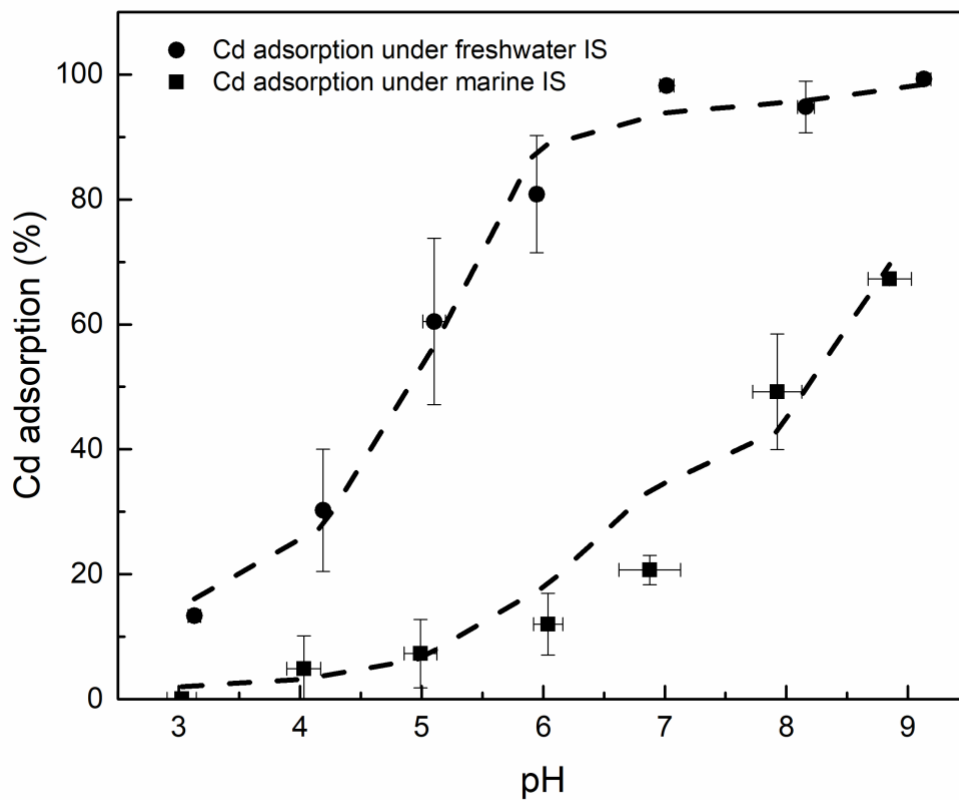


**Figure 2.2:** Modeling (lines) and experimental (points) results of Cd adsorption onto  $10 \text{ g L}^{-1}$  *Synechocystis* sp. PCC 6803 in 0.01 and 0.56 M NaCl. Error bars represent 1-sigma standard deviation from duplicate analyses of experiments performed on separate cultures.

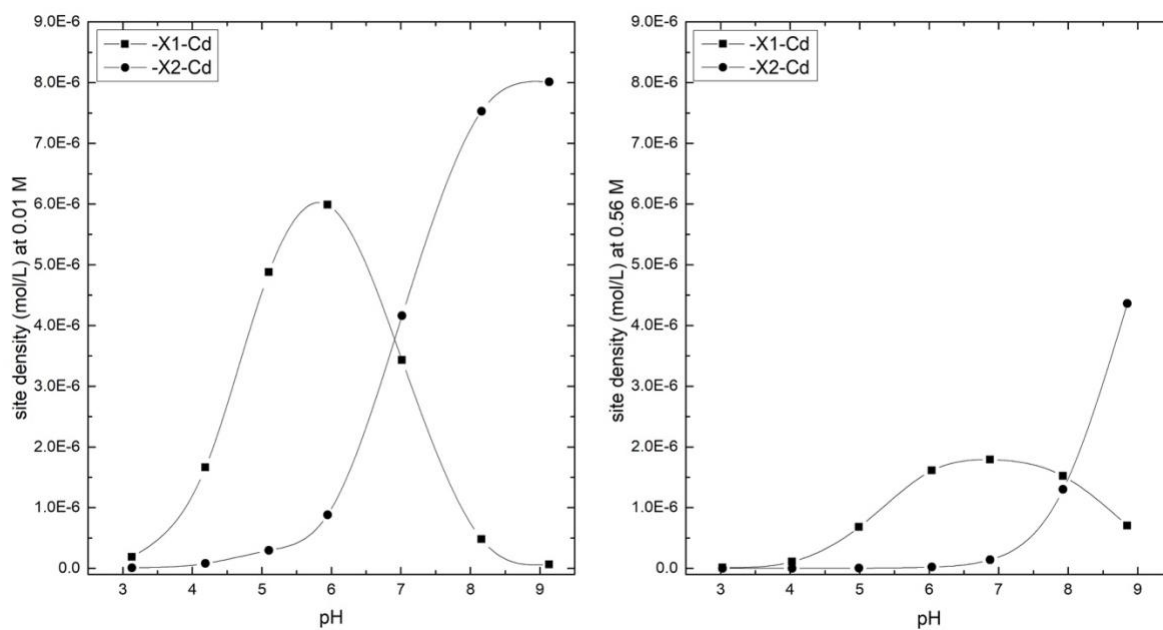


**Figure 2.3:** *Synechocystis* cell surface functional groups responsible for Cd adsorption as a function of varying pH.

## Chapter 3: Acid-base properties of *Synechococcus*-derived organic matter<sup>1</sup>

### 3.1. Introduction

The distributions of a number of trace metals (e.g., cadmium, cobalt, copper, nickel, and zinc) in seawater are closely correlated to marine primary productivity and biological cycling in the water column (Bruland, 1980; Bruland et al. 1991; Sunda and Hunstman, 1995; Morel and Price, 2003; Saito et al. 2003; Sunda, 2012; Bruland et al. 2013; Twinning and Baines, 2013). They demonstrate nutrient-type distributions in marine water columns, characterized by a sharp decrease in concentration in surface waters due to assimilation and adsorption by phytoplankton paired with an increase in concentration with depth due to remineralization as a result of respiration (Bruland and Lohan, 2003). The main primary producing phytoplankton in nutrient-rich regions of the oceans are marine cyanobacteria, namely *Prochlorococcus* and *Synechococcus* (Flombaum et al. 2013). *Synechococcus* populations vary from  $10^4$  to  $10^5$  cells mL<sup>-1</sup> within the photic zone in the relatively rich waters of the Arabian Sea and off the coast of Peru (Waterbury et al., 1979; Worden et al., 2004). Populations have been reported up to  $10^6$  cells mL<sup>-1</sup> in the Chesapeake Bay during warm summer months. During this time picoplankton primary productivity exceeds that of the heterotrophic bacteria community (Wang et al. 2011).

There are numerous studies that have investigated the ability of phytoplankton to assimilate trace metals (e.g., Ho et al. 2003; Twinning and Baines, 2013), but this is outside the focus of this work. Instead, we concentrate here on the adsorptive capacity of cyanobacteria and some of their lysates toward trace metals because past experimental work demonstrated that organic functional groups associated with their cell walls are reactive towards trace metals at seawater pH (e.g., Sañudo-Wilhelmy et al., 2004; Dittrich and Sibling, 2005; Hadjoudja et al., 2010; Liu et al., 2015;

---

<sup>1</sup>This chapter has been published in *Geochimica et Cosmochimica Acta* as: Swaren, L., Owttrim, G.W., Alessi, D.S., Konhauser, K.O.

Bishop et al., 2019; Swaren et al., 2021). Indeed, based on these studies, it has even been suggested that intact cells could conceivably adsorb nearly all the dissolved trace metals from seawater (Bishop et al., 2019). However, in nature the picture is more complicated because intact cells compete for dissolved metals with cell detritus, commonly particulate organic matter (POM) as well as the dissolved organic matter (DOM) pool.

Cyanobacterial cell-derived POM provides one mechanism by which trace metals can be transported to the sea floor (Beouf et al. 2019; Kharbush et al. 2020). POM is operationally defined as biomass, including phytoplankton, bacterial detritus (composed of dead cells and cell fragments), zooplankton fecal pellets, and various types of aggregates (Le Moigne, 2019; Kharbush et al. 2020). There are two major processes by which cyanobacterial cell detritus is produced: (1) lysis by viral pathogens and (2) zooplankton grazing (Pernthaler, 2005; Kawasaki et al. 2011; Zheng et al. 2019). Related to the latter process is “sloppy feeding”, a term attributed to the disaggregation of phytoplankton cells by zooplankton mouthparts resulting in the release of undigested particulates as well as DOM (Strom et al. 1997; Saba et al. 2011). Kawasaki et al. (2011) determined that approximately 15% of POM in the top 300 m of the open ocean in the North Pacific comprised of living cyanobacteria and that about 6% of the POM was composed of cyanobacteria and heterotrophic bacteria detritus. Interestingly, the ratio of cyanobacterial cell detritus to living cells increased with increasing depth, indicating that the lack of sunlight inhibits productivity and phytoplankton cells inevitably degrade as they sink (Kawasaki et al. 2011). For example, in the Southern Ocean, living cyanobacteria can make up 14 to 45% of surface water POM and decrease to as little as 2% at depths greater than 210 m (Tremblay et al. 2015). By contrast cyanobacteria and heterotrophic bacteria detritus made up to a maximum of 41% of deep (>210 m) POM in the same location (Laurenceau et al. 2014; Tremblay et al. 2015).

There is also a growing understanding of the molecular composition of the cyanobacteria-derived DOM pool (e.g., Zhao et al. 2017, 2019; Ma et al. 2018; Zheng et al. 2019). In the modern oceans DOM is a complex mixture of carboxyl-rich, alicyclic molecules (CRAM), humic and fulvic acids, and polysaccharides, representing a bulk pool of terrestrial and marine sources (Hansell & Carlson, 2001; Engel et al. 2004; Pedler-Sherwood et al. 2015; Walker et al. 2016; Fatayer et al. 2018; Jiao et al. 2018). Fulvic acids are the major constituent of organic matter found in rivers and streams (Celo et al. 2001), and lignin oxidation products are commonly employed as biomarkers to identify the influence of terrestrially-derived dissolved organic carbon (DOC) (Opsahl & Benner, 1997; Dilling & Kaiser, 2002; Dittmar et al. 2006). By contrast, marine-derived DOM comprises material from cell lysis but also organic ligands that are generated to either scavenge because of their nutritional requirements or to minimize their toxicity via organic chelation (Zhang et al. 2019).

In the present study we investigate the surface reactivity and trace metal binding behaviour of *Synechococcus* sp. PCC 7002 derived POM and DOM following mechanical lysis to assess how their surface reactivities compare to previous reports of intact cells. We chose *Synechococcus* because of the abundant extant literature on the composition of its cell wall, surface charge variations with pH and its ability to adsorb a number of trace metals from seawater. Therefore, we have a solid basis with which to compare our experimental results. Focusing on the acid-base surface properties and speciation of trace metals between *Synechococcus* and their derived cyanobacterial cell detritus also provides necessary insight to the distribution of trace metals being deposited on the seafloor via intact cells and their lysates.

### **3.2. Methods**

### **3.2.1. *Synechococcus* sp. PCC 7002 growth**

The unicellular cyanobacterium *Synechococcus* sp. PCC 7002 (*Synechococcus*) was cultured on A+ medium agar plates (Stevens & Van Baalen, 1973), aerobically, at 30°C under a light intensity of 50  $\mu\text{mol photons m}^{-2}\text{s}^{-1}$ . After a suitable colony was established, it was transferred to a 250 mL Erlenmeyer flask containing 50 mL of A+ medium using a sterile inoculation loop. The cyanobacterial solution was then gently agitated on an orbital shaker at 60 rpm for 3 days at 30°C to promote exponential growth and inhibit the settling of cells. The 50 mL solution was then transferred to a 1 L Erlenmeyer flask containing an additional 350 mL of A+ media. The 1 L flask was then agitated at 100 rpm for 10 days at 30°C until the *Synechococcus* achieved stationary growth phase (based on identical growing conditions and OD<sub>750</sub> measurements previously observed in our laboratory; see Liu et al. 2015). During the 10-day agitation period, the cyanobacterial solution was aerated with 0.2  $\mu\text{m}$  filtered, humidified air directly into the solution.

### **3.2.2. *Synechococcus* harvesting**

To harvest the *Synechococcus* cells, the bacterial solution was centrifuged (Sorvall Lynx 4000) five times at 10000 g for five-minute intervals with 0.56 M NaCl to simulate marine ionic strength, and to remove residual growth media as well as potential competing metals from the cell wall. After each centrifugation, the resulting supernatant was discarded, and the cells were resuspended in 0.56 M NaCl for each wash interval. Following the final wash interval, the wet mass of the resulting *Synechococcus* cell pellet was measured, and then resuspended in 0.56 M NaCl to give a final cell concentration of 10 g L<sup>-1</sup> as wet weight. No significant cell lysis has previously been recorded using this washing procedure (Fein et al. 1997; Fowle and Fein, 2000; Liu et al. 2015).

### 3.2.3. Preparation of mechanically lysed cyPOM and cyDOM

Mechanical lysis, achieved through high pressure homogenization, is commonly used to represent intracellular DOM resulting from cell breaking during sloppy feeding of phytoplankton by grazers such as copepods (Ma et al. 2018). Zheng et al. (2019) used high-pressure and freeze-thaw treatments to produce *Synechococcus*-derived DOM to investigate molecular characteristics of microbial recalcitrant DOM (RDOM) during incubation experiments. Outside the scope of these previous studies is the influence of mechanical lysis, or sloppy feeding, on remnant cell detritus surface reactivity. In this study, mechanical lysis of cyanobacterial cells was accomplished via sonication as it does not introduce chemicals that have the potential to adsorb to the lysed cells (Braun-Sonic 2000). To do so, 10 mL aliquots of the washed  $10 \text{ g L}^{-1}$  bacterial cell solution were separated into 15 mL polypropylene tubes prior to sonication. Each tube was sonicated at 160 MHz and 50 W for a duration of 30 seconds and then immediately inserted into an ice-water bath. Samples were cooled between cycles to minimize protein denaturing as a result of the heat produced during sonication. Each aliquot underwent eight cycles of sonication, with breaks after the third and sixth cycle to mix all tubes together into a sterile 250 mL Erlenmeyer flask, after which the suspension was re-distributed into 10 mL aliquots to ensure homogeneity of the resulting *Synechococcus* lysate solution. Cyanobacteria lysis was confirmed by autofluorescence using a Zeiss Axioskop 2 epifluorescence light microscope. The cultured *Synechococcus* displayed near complete autofluorescence (>99%) upon visual inspection whereas lysed cells displayed <5%. The lysed samples were centrifuged for five minutes at 10000 g to separate the dissolved and particulate fractions. The resulting supernatant was filtered through  $0.2 \text{ }\mu\text{m}$  nylon membranes. Hereafter we refer to the filtered lysate as cyDOM. The resulting wet pellet was weighed and re-suspended to

10 g L<sup>-1</sup> in 0.56 M NaCl. The resulting lysed solution was considered an analog for marine particulate organic matter, herein referred to as cyPOM.

#### **3.2.4. Attenuated total reflectance Fourier transform infrared (ATR-FTIR) spectroscopy**

After cyPOM resuspension in 0.56 M NaCl, the 10 g L<sup>-1</sup> solution was filtered through 0.2 µm nylon membranes. The filter was then rinsed with ultrapure water to minimize salt precipitation. The cyPOM was then removed from the nylon membrane using ultrapure water and then oven dried for 24 h at 50°C. Once dried, samples were crushed using an agate mortar and pestle to produce a powder. Intact *Synechococcus* cells were prepared in the same manner to compare the effect of mechanical lysis. The dried cyPOM was then analyzed by attenuated total reflectance Fourier transform infrared (ATR-FTIR) spectroscopy (Bruker Platinum ATR). The spectra were recorded as 16 co-added interferograms at a resolution of 4 cm<sup>-1</sup>. Baseline correction of the spectra was done using the OPUS software interface (Version 7.2).

#### **3.2.5. Zeta potential**

Following cell washing and lysis, the 10 g L<sup>-1</sup> cyPOM suspension was diluted to 0.2 g L<sup>-1</sup> in sterile 15 mL polypropylene tubes. The pH of each tube was adjusted to cover a range of 3-9 using small aliquots of 0.1 and 1 M HNO<sub>3</sub> and NaOH. Samples were placed on an end-over-end rotator at 30 rpm between pH adjustments. Samples were rotated for a minimum of 1 hr in between additions of acid or base and then left overnight to ensure equilibrium had been achieved prior to measuring the final solution pH values. Zeta potential measurements were conducted with a Zetasizer Nano Series instrument (Malvern Instruments, United Kingdom). The average of 3 separate cyPOM

batches are reported. Each sample was measured 3 times with a minimum of 10 readings per measurement.

### 3.2.6. Potentiometric titrations

Acid-base titrations were performed on 50 mL of the cyPOM suspension diluted 1:9 (v:v) with 0.56 M NaCl to yield a concentration of 0.14 g L<sup>-1</sup> (dry mass – 7:50 [dry:wet]) and 50 mL of the cyDOM diluted 1:1 (v:v) with 0.56 M NaCl, using a Metrohm Titrando 905 auto-titrator. Prior to titration, the pH probe was calibrated using commercially available pH buffers (Fischer Scientific; pH 4.0, 7.0, and 10.0). The lysate was isolated from the atmosphere and purged 30 minutes before and during the titration with N<sub>2</sub> gas. Following the 30-minute N<sub>2</sub> purge, the initial “down” titration was begun by adding 0.1 M HNO<sub>3</sub> to lower the pH to 3. Once the lysate pH reached 3, an “up” titration ensued by the addition of small volumes of 0.1 M NaOH. At pH 10.5, the “up” titration stopped and the subsequent “down” titration commenced through the addition of 0.1 M HNO<sub>3</sub> until a pH of 3 was achieved again. The second “down” titration was conducted to ensure that the cyPOM was not damaged during the process, as indicated by the presence of hysteresis between the forward and reverse proton buffering curves (Hao et al. 2018). An electrode stability of 0.1 mV s<sup>-1</sup> was achieved before further additions of acid or base to ensure chemical equilibrium throughout the titration procedure. The titration pH and corresponding volumes of acid and base added were recorded autonomously by the titration software (tiamo 2.5) and processed to find the proton budget. Titration data were modelled by invoking one, two, and three monoprotic reactions using the following reaction stoichiometry:



where  $>X^-$  is the general deprotonated surface functional group and  $>XH$  is the corresponding protonated state. The corresponding mass action constant (K) can be defined from equation (1) as:

$$K = \frac{[>XH]}{[>X^-] \cdot a_{H^+}} \quad (2)$$

where square brackets represent molar concentrations of surface sites and  $a_{H^+}$  is the solution proton activity. The processed data were used to develop a protonation model and solve for site concentrations and corresponding  $pK_a$  values using the software FITEQL 4.0 (Herbelin & Westall, 1999). Following the titration, the solution was vacuum filtered onto pre-weighted 0.2  $\mu\text{m}$  nylon membranes to determine the dry mass for normalization of modeled surface functional group site densities and to calculate the dry mass in  $\text{g L}^{-1}$  reported above.

### **3.2.7. Trace metal adsorption experiments to cyPOM**

Following lysis, cyPOM was re-suspended to  $10 \text{ g L}^{-1}$  in 0.56 M NaCl spiked with 1 ppm cadmium (Cd), cobalt (Co), copper (Cu), nickel (Ni), or zinc (Zn) in an acid-washed 150 mL beaker. The cyPOM-metal solution was then stirred using a magnetic stir-bar for 10 min to ensure homogeneity. After 10 min, while still being stirred, 10 mL aliquots were pipetted from the cyPOM slurry and transferred to a set of seven 15 mL polypropylene test tubes. The pH of each tube was adjusted as described above. Following the final pH reading, samples were filtered through 0.2  $\mu\text{m}$  nylon membranes, diluted 10 $\times$  with 2%  $\text{HNO}_3$  and 0.5% HCl solutions and the aqueous trace metal concentrations analyzed via ICP-MS/MS (Agilent 8800 Triple Quadrupole).

## **3.3. Results**

### **3.3.1. Attenuated total reflectance fourier transform infrared (ATR-FTIR) spectroscopy**

The ATR-FTIR spectra and functional group assignments for *Synechococcus* sp. PCC 7002 cells and derived cyPOM cells are summarized in Figure 3.1. Differences in the spectra of intact *Synechococcus* cells compared to those of cyPOM were minor and within the analytical error of the technique. The peak spanning broadly from 3500 – 3000  $\text{cm}^{-1}$  can be assigned to amino groups overlapping with hydroxyl groups in water (Ozturk et al. 2010; Liu et al. 2015). The peak cluster ranging 3000 – 2800  $\text{cm}^{-1}$  is characteristic of alkanes, indicating the presence of methyl and methylene groups typically found in fatty acid components of phospholipids in membrane components (Jiang et al. 2004; Benning et al., 2004; Yee et al. 2004). The distinct peaks at 1645, and 1535  $\text{cm}^{-1}$  indicate the presence of primary and secondary amides, respectively, characteristic of proteins and lipopolysaccharides on the cyanobacterial outer membrane (Jiang et al. 2004; Liu et al. 2015). Both *Synechococcus* cells and cyPOM demonstrate a peak cluster in the 1200-950  $\text{cm}^{-1}$  range characteristic of carbohydrates (Bouhedja et al. 1997; Jiang et al. 2004; Liu et al. 2015). Several peaks in the carbohydrate range can be attributed to cyanobacterial cell wall components – such as amino sugars likely derived from phospholipids and peptidoglycan (Bouhedja et al. 1997).

### **3.3.2. Zeta potential**

The cell surface charge was measured as a function of pH for both *Synechococcus* cells and cyPOM (Figure 3.2). Both intact *Synechococcus* and cyPOM exhibit a negative surface charge across the entire tested pH range (3-9). Intact *Synechococcus* remains around -15.0 mV from pH 3 to 9, whereas cyPOM becomes more negatively charged with increasing pH. At pH 3, cyPOM has cell surface charge of -4.0 mV and increases to -12.0 mV at pH 5 after which it remains consistent.

### 3.3.3. Potentiometric titrations

Best-fit protonation model results obtained from FITEQL 4.0 (Herbelin and Westall, 1999) and the triplicate titrations data for cyPOM and cyDOM can be found in Appendix 2 SI Tables 2.1 and 2.2, respectively. Negligible hysteresis was observed when comparing forward and reverse titrations data, indicating no damage to organic components or precipitation of inorganic phases (Appendix SI Figure 2.1). Several models, including one-, two-, and three-site non-electrostatic protonation models were tested while fitting the titration data (Appendix 2 SI Figure 2.2). By visual observation, both the two- and three-site models better fit the titration data than the one-site model. Results for cyPOM were determined to be best simulated by a two-site protonation model, based on the variance ( $V_y$ ) parameter in FITEQL being closest to 1.0 (Herbelin and Westall, 1999; Appendix 2 SI Table 2.1). Although the 3-site model  $V_y$  values are similar to those of the 2-site models, the 3-site models had higher variability in site concentration values than the 2-site models (Appendix 2 SI Table 2.1). Thus, the best-fitting non-electrostatic protonation model had two functional groups with  $pK_a$  values of 5.78 ( $\pm 0.07$ ) and 9.01 ( $\pm 0.29$ ), with corresponding site concentrations of 41.8 ( $\pm 8.15$ )  $\mu\text{mol g}^{-1}$  and 41.2 ( $\pm 5.28$ )  $\mu\text{mol g}^{-1}$ , respectively (Table 3.1).

Both 1- and 2-site non-electrostatic protonation models fit the cyDOM titration data well, with the 2-site model having slightly better  $V_y$  values (see modelling results in Table 3.2 and triplicate data in Appendix 2 SI Table 2.2). The 2-site non-electrostatic protonation model had functional groups with  $pK_a$  values of 4.89 ( $\pm 0.22$ ) and 6.80 ( $\pm 0.22$ ), and corresponding site concentrations of 42.8 ( $\pm 14.6$ )  $\mu\text{mol g}^{-1}$  and 37.3 ( $\pm 16.5$ )  $\mu\text{mol g}^{-1}$ , respectively (Table 3.2).

### 3.3.4 Experimental trace metal adsorption to cyPOM

Using the  $pK_a$  values and site concentrations determined from the potentiometric titration results, a non-electrostatic (NEM) surface complexation model (SCM) approach was utilized to model the trace metal adsorption data and calculate the trace metal adsorption equilibrium constants to cyPOM (K values). This was achieved by allowing the trace metal of interest ( $M^{m+}$ ) to sorb to the two proton-active functional groups, using reactions 2 and 3:



where  $>L-O^-$  is the generalized deprotonated surface functional group and  $>L-M^{(m-1)+}$  is the corresponding adsorbed trace metal-ligand complex. Aqueous complexation constants for the trace metals under investigation that were used in FITEQL 4.0 (Herbelin and Westall, 1999) are given in Table S3. The corresponding mass action constants (K) can be defined from equations (3) and (4) as:

$$K_1 = \frac{[>L_1-M^{(m-1)+}]}{[>L_1^-] \cdot a_{M^{m+}}} \quad (5)$$

$$K_2 = \frac{[>L_2-M^{(m-1)+}]}{[>L_2^-] \cdot a_{M^{m+}}} \quad (6)$$

Square brackets represent surface site molar concentrations and  $a_{M^{m+}}$  is the solution activity of the metal (M) of interest. Aqueous SCM fit results are shown with modelled experimental data in Figure 3.3, and the corresponding metal adsorption equilibrium constants are given in Table 3.3. The two chemical systems tested in FITEQL 4.0 and their resulting adsorption equilibrium constants can be found in Appendix 2 SI Table 2.3. The results provided in Appendix 2 SI Table 2.4 are based on the FITEQL 4.0 variance parameter,  $V(y)$ , the accepted values are between  $0.1 < V(y) < 20$  with the best fit being closest to 1.0 (Herbelin and Westall, 1999).

For all 5 trace metals tested (Cd, Co, Cu, Ni, and Zn) metal adsorption to cyPOM increased with increasing pH, a well-documented result consistent with the increasingly negative charge of

the cyPOM surface as its functional groups deprotonate at higher pH. All trace metals demonstrate minimal adsorption at acidic pH values (<4) with the exception of Cu that has nearly 40% adsorption at pH 3. Following Cu, Zn and Ni are the most readily adsorbed, followed by Co and Cd in the order  $Cd < Co < Ni < Zn < Cu$ . Best-fit metal binding constants for the two proton-active functional groups on cyPOM appear in Table 3.3.

### **3.4. Discussion**

#### **3.4.1. Comparison of cyPOM and cyanobacterial cell surface reactivities**

Previous investigations of *Synechococcus* sp. PCC 7002 using potentiometric titrations found that live cells were best modeled using a non-electrostatic 3-site protonation model (Liu et al. 2015), with  $pK_a$  values of 5.07, 6.71, and 8.54, inferred to correspond to carboxyl, phosphoryl, and amino surface functional groups, respectively. Following mechanical lysis via sonication, cyPOM investigated in this study was better fit using a 2-site protonation model with  $pK_a$  values of 5.78 and 9.01. The  $pK_a$  value 5.78 likely corresponds to a mixture of carboxyl and phosphoryl groups. The  $pK_a$  value of 9.01 is more likely a combination of various groups such as amino and hydroxyl. Small thiol-bearing molecules also have  $pK_a$  values that range from 8-10, as well as recently identified sulfhydryl groups (9.2-9.4) (Yu et al. 2014).

As the relative abundance of cyanobacteria and heterotrophic bacteria detritus increases with water column depth, the portion of POM released or exposed during sloppy feeding becomes more refractory as the labile portions are remineralized (Kawasaki et al. 2011). This relatively fresh portion of phytoplankton intracellular components demonstrate a lower overall site density ( $11.8 \text{ mmol g}^{-1}$ ) compared to that of intact cells ( $24.3 \text{ mmol g}^{-1}$ ; Liu et al. 2015). The ATR-FTIR spectra of both intact cells and cyPOM were nearly identical, indicating that there were not

measurable bonding environment differences between dried cells and bacterial detritus caused by mechanical lysis (Figure 3.1). Interestingly, the zeta potential of intact *Synechococcus* cells was more negative than cyPOM at more acidic pH,  $\text{pH} < 6$  (Figure 3.2), indicating that mechanical lysis influenced the cell surface charge, but not the bonding environments. This is likely due to changes in cell surface physiology following cell breakage resulting in surface charge changes, as well as the interaction of surface functional groups carrying a more positive charge with solution that were not in contact with solution prior to cell lysis. This change in surface functional group distribution is exhibited by the expression of surface functional group  $\text{pK}_a$  values in our protonation model. This alteration is likely not detected by ATR-FTIR as the method probes the cell as a whole and not simply the cell surface (Kenney and Gorzsas, 2019).

#### **3.4.2. Differences in trace metal affinities between intact cells and cyPOM**

The metal-binding constants for Cd identified for cyPOM were similar to values identified by Liu et al. (2015) for *Synechococcus* cells (1.6 and 1.1 versus 1.2, 1.8, and 2.7 for *Synechococcus*). Bishop et al. (2019) found that the metal-binding constants for *Synechococcus* were approximately 4× greater for site 1 and a minimum of 2× greater for site 2 than cyPOM (Table 3.3), the exception being the  $\log K_{\text{Cu}}$  value for the second site (6.3 for cyPOM versus 7.4 for intact *Synechococcus* cells). Our study and modern oceanographic investigations show that cyanobacteria and heterotrophic bacteria detritus is likely more representative of organic matter deposited in deep ocean sediments, meaning that previous estimates of trace metal sequestration based on the surface reactivity of intact phytoplankton are likely overestimated given the higher trace metal affinities to living cells.

Using the calculated pK<sub>a</sub> values, corresponding site concentrations, and metal binding constants from our thermodynamic modelling, combined with complimentary published *Synechococcus* cell data from our lab (Bishop et al. 2019), we ran predictive models using FITEQL 4.0 (Herbelin and Westall, 1999) to investigate the speciation of the trace metals in the presence of both intact *Synechococcus* and cyPOM. In the presence of both 1 g L<sup>-1</sup> *Synechococcus* and cyPOM, nearly all metal adsorption (>99.9%) is to *Synechococcus* at pH values above 7. Additionally, to account for the changing proportions of bacterial detritus versus intact cyanobacterial cells in the deep ocean, we modelled a system containing 0.1 g L<sup>-1</sup> *Synechococcus* and 1 g L<sup>-1</sup> cyPOM and found the same distribution; that trace metals demonstrated a profoundly higher propensity to adsorb to the surface of the cyanobacterial cells than to cyPOM.

### **3.4.3. Surface reactivity of seawater cyDOM**

Previous investigations of natural DOM yielded a large array of pK<sub>a</sub> values, hinting to the complexity of ligands occurring naturally in seawater (Table 3.2). In this study, the *Synechococcus*-derived cyDOM potentiometric titration data were fit with a 2-site model (Table 3.2). The cyDOM has pK<sub>a</sub> values of 4.89 and 6.80 when modelled with a 2-site approach, indicating the presence of carboxyl functional groups with pK<sub>a</sub> values commonly ranging from 3-6. As observed in Table 3.2, carboxyl groups are the most common proton active functional groups found in the environment. A large portion of the global DOM pool is composed of carboxyl-rich alicyclic molecules (CRAM) that can be of both terrestrial, with which they are commonly grouped, or marine microbial communities (Hansell, 2013; Lechtenfeld et al. 2014). The second site in the 2-site model has a pK<sub>a</sub> value of 6.80, inferred to correspond to a combination of amine and phosphoryl functional groups (Table 3.2). Site 2 and the site identified in the 1-site model

with a value of 6.48 likely correspond to the more complex N, P, and S containing biomolecules released from the cyanobacteria, such as amino and nucleic acids, proteins, nucleotides, and vitamins (Moran et al. 2016).

Previous studies have identified the presence of proton active functional groups in natural DOM from aqueous environments with pK<sub>a</sub> values closely resembling those found in cyDOM, 4.89 and 6.80 (Paxeus & Wedborg, 1985; Cai et al. 1998; Garnier et al. 2004). For instance, Cai et al. (1998) investigated the acid-base properties of DOM collected from the Satilla River estuary in Georgia, USA. They identified 4 possible proton active sites in the estuary, with pK<sub>a</sub> values of 4.46, 6.64, 8.94, and 10. The higher pK<sub>a</sub> values, greater than 10, are indicative of phenolic hydroxyl groups that represent the presence of terrestrial DOM with a high degree of aromaticity (Koch et al. 2005). Similar measurements were made by Garnier et al. (2004) who identified pK<sub>a</sub> values of ~10 in both Laurentian River fulvic and humic acids. Ritchie & Perdue (2003) found that various humic and fulvic acids of terrestrial origin were best modelled by 2-sites with pK<sub>a</sub> values of <4.5 and >8.7 hinting to the presence of CRAM and aromatic molecules. Moreover, Huizenga & Kester (1979) analyzed multiple oceanic and estuarine DOM and found only one site with a pK<sub>a</sub> of <3.8. However, their titration procedure did not include pH values above 7. Future oceanographic investigations of open ocean marine DOM should incorporate acid-base titrations to aid in the comparison with microbial-derived DOM. Current literature is commonly focused on riverine and estuarine DOM that has a large terrestrial input.

#### **3.4.4. Trace metal interactions with marine DOM**

Various marine organisms, including *Synechococcus* (Boiteau and Repeta, 2015), produce metal-chelating ligands. Some ligands make metals bioavailable, such as siderophores. These are iron

(Fe)-specific binding ligands that are excreted by numerous microbial cells to dramatically increase the solubility of Fe(III) and make it amenable to assimilation (Vraspir and Butler, 2009). Other ligands are produced and released extracellularly to immobilize toxic metals, such as Cu and Cd (Bruland et al. 1991). The production of these organic ligands is of global significance in terms of trace metal cycling, with estimates suggesting, for example, that 99.0% of marine Fe(III) is associated with siderophores, while 99.7% of Cu in the northeast Pacific is organically complexed (Coale and Bruland, 1988). Other metals are complexed to a lesser extent, with only 30-50% of Ni being associated with organic ligands (Boiteau et al. 2016). The generally high percentage of metals organically bound versus in ionic form (e.g.,  $\text{Cu}^{2+}$ ) means that marine plankton, and the organic ligands that they generate, directly control trace metals speciation and cycling in modern oceans.

Although the abundance and composition of metal-specific marine ligands is well documented (e.g., Fe, Co, Cu, Ni and Zn), little attention has been paid to the role of specific DOM contributions of modern plankton to the overall organic ligand pool. Quantifying the organic complexation of trace metals with *Synechococcus*-derived DOM is analytically difficult given the size range of DOM as well as the unique optimization required for each individual trace metal. For instance, the hydrated radius of the trace metals used commonly overlap with that of DOM inhibiting analysis in the same way as cyPOM (e.g., filtration and quantification via ICP-MS) unreliable (Nightingale Jr., 1959). Moreover, Zn has been identified using both differential pulse anodic stripping voltammetry (DPASV) (Muller et al. 2001) and competitive ligand exchange cathodic stripping voltammetry (CLE-CSV) (Lohan et al. 2005), whereas Ni is commonly only quantified using CLE-CSV (Van den Berg and Nimmo, 1987; Boiteau et al. 2016). The voltammetry procedure is sensitive to the properties of the DOM and requires careful selection

and optimization of the electrode, solution ionic strength, voltage range, metal concentrations, and the competitive ligand (Padan et al. 2020).

Building on our predictive model above, we created models consisting of equal site concentrations of *Synechococcus*, cyPOM, and cyDOM site densities using FITEQL 4.0 (Herbelin and Westall, 1999). Because of the difficulties in determining metal binding constants for DOM, we used the average of compiled modern oceanographic studies (Appendix 2 SI Table 2.5) for cyDOM, values from this study for cyPOM (Tables 3.1 and 3.3), and values previously identified from our lab for *Synechococcus* cells (Liu et al. 2015; Bishop et al. 2019). When previous studies identified only one metal binding constant (e.g., Cd, Co, Ni, and Zn – See Appendix 2 SI Table 2.5), the 1-site non-electrostatic protonation model  $pK_a$  value was used. The predictive models indicate that in systems containing equal amounts of all three components (intact cells, cyPOM, and cyDOM) metal speciation is almost entirely cyDOM bound (>99.9%). This is in agreement with similar Cu predictive modelling done by Bishop et al. (2019) including *Synechococcus* cells and published DOM values. The same holds true for a site concentrations ratio of 1:10:100 (cyDOM:*Synechococcus*:cyPOM) demonstrating the high affinity of trace metals to bind to cyDOM.

Although previous studies have predicted that intact cells can be important sorbents for trace metals (e.g., Konhauser et al. 2018; Bishop et al. 2019), the DOM – although yet to be tested experimentally – appears to be the most important fraction controlling metal speciation. Further studies analyzing trace metal availability in seawater should determine the source of metal-binding ligands, whether that be marine or terrestrial. Progression in high resolution mass spectroscopy (e.g., Fourier transform ion cyclotron resonance mass spectroscopy; FTICR-MS) is beginning to unravel the distinct molecular characteristics and chemical signatures of DOM from various

sources (e.g., Ma et al. 2018; Niu et al. 2018). Moreover, researchers are beginning to identify individual metal-binding ligands from DOM samples (e.g., Boiteau et al. 2016; Chen et al. 2017) which will be the motivation of future studies in our lab.

### **3.5. Conclusions**

In modern oceans, the majority of phytoplankton biomass deposited in deep ocean sediments is in the form of bacterial detritus rather than living cells. We present here an experimental study coupled to thermodynamic proton and metal binding modelling that indicates that almost all (>99.9%) of the trace metals Cd, Co, Cu, Ni, and Zn would be sorbed to cyanobacterial cells over cyPOM. Although only a small portion of modern POM that reaches the seafloor consists of intact cyanobacterial cells compared to bacterial detritus, that portion would be responsible for the deposition and eventual burial of the trace metals present. Moreover, even in the presence of 1:100 (cyDOM:cyPOM), our predictive models indicate that the metal speciation is almost entirely in the dissolved fraction (>99.9%), comparable to that of many modern marine speciation investigations. These findings further the notion that there is a clear need to better integrate DOM into trace metal speciation in both modern and ancient oceans.

### 3.6. References

- Algeo, T.J., Maynard, J.B. (2004). Trace-element behavior and redox facies in core shales of Upper Pennsylvanian Kansas-type cyclothems. *Chemical Geology*, **206**, 289-318.
- Benning, L.G., Phoenix, V., Yee, N., and Konhauser, K.O. (2004). The dynamics of cyanobacterial silicification: An infrared micro-spectroscopic investigation. *Geochimica et Cosmochimica Acta*, **68**, 743-757.
- Boeuf, D., Edwards, B.R., Eppley, J.M., Hu, S.K., Poff, K.E., Romano, A.E., Caron, D.A., Karl, D.M., DeLong, E.F. (2019). Biological composition and microbial dynamics of sinking particulate organic matter at abyssal depths in the oligotrophic open ocean. *Proceeding of the National Academy of Sciences*, **116**, 11824-11832.
- Boiteau, R.M., Repeta, D.J. (2015). An extended siderophore suite from *Synechococcus* sp. PCC 7002 revealed by LC-ICPMS-ESIMS. *Metallomics*, **7**, 877.
- Boiteau, R. M., Till, C. P., Ruacho, A., Bundy, R. M., Hawco, N. J., McKenna, A. M., Barbeau, K. A., Bruland, K. W., Saito, M. A., Repeta, D. J. (2016). Structural Characterization of Natural Nickel and Copper Binding Ligands along the US GEOTRACES Eastern Pacific Zonal Transect. *Frontiers in Marine Science* **3**, 243.
- Boning, P., Shaw, T., Pahnke, K., Brumsack, H.J. (2015). Nickel as indicator of fresh organic matter in upwelling sediments. *Geochimica et Cosmochimica Acta*, **162**, 99-108.
- Bouhedja, W., Sockalingum, G. D., Pina, P., Bloy, C., Labia, R., Millot, J. M., Manfait, M. (1997). ATR-FTIR spectroscopic investigation of *E. coli* transconjugants beta-lactams-resistance phenotype. *FEBS Letters*, **412**, 39-42.
- Boyd, P.W., Claustre, H., Levy, M., Siegel, D.A., Weber, T. (2019). Multi-faceted particle pumps drive carbon sequestration in the ocean. *Nature*, **568**, 327-335.

- Bruland, K.W. (1980). Oceanographic distributions of cadmium, zinc, nickel, and copper in the North Pacific. *Earth and Planetary Science Letters*, **47**, 176-198.
- Bruland, K.W., Donat, J.R., Hutchins, D.A. (1991). Interactive influences of bioactive trace metals on biological production in oceanic waters. *Limnology and Oceanography*, **36**, 1555-1577.
- Bruland, K.W., Lohan M.C. (2003). Controls of trace metals in seawater. *Treatise on Geochemistry*, **6**, 23-47.
- Bruland, K.W., Middag, R., Lohan, M.C. (2013). Controls of Trace Metals in Seawater. In: *Treatise on Geochemistry*, Second edition. 19–51.
- Cai, W., Wang, Y., Hodson, R.E. (1998). Acid-base properties of dissolved organic matter in the estuarine waters of Georgia, USA. *Geochimica et Cosmochimica Acta*, **62**, 473-483.
- Calvert, S.E., Pederson, T.F. (1993). Geochemistry of recent oxic and anoxic marine sediments: implications for the geological record. *Marine Geology*, **113**, 67-88.
- Celo, V., Murimboh, J., Salam, M. S. A., Chakrabarti, C. L. (2001). A kinetic Study of Nickel Complexation in Model Systems by Adsorptive Cathodic Stripping Voltammetry. *Environmental Science and Technology* **35**, 1084-1089.
- Cullen, J.T., Chase, Z., Coale, K.H., Fitzwater, S., Sherrell, R.M. (2003). Effect of iron limitation on the cadmium to phosphorus ratios of natural phytoplankton assemblages from the Southern Ocean. *Limnology and Oceanography*, **48**, 1079-1087.
- Cullen, J.T. (2006). On the nonlinear relationship between dissolved cadmium and phosphate in the modern global ocean: Could chronic iron limitation of phytoplankton cause the kink? *Limnology and Oceanography*, **51**, 1361-1380.
- Dilling, J., Kaiser, K. (2002). Estimation of the hydrophobic fraction of dissolved organic matter in water samples using UV photometry. *Water Research* **36**, 5037-5044.

- Dittmar, T., Hertkorn, N., Kattner, G., Lara, R. J. (2006). Mangroves, a major source of dissolved organic carbon to the oceans. *Global Biogeochemical Cycles* **20**, GB1012. 7 p.
- Dutkiewicz, A., O'Callaghan, S., Muller, R.D. (2016). Controls on the distribution of deep-sea sediments. *Geochemistry, Geophysics, Geosystems*, **17**, 3075-3098.
- Dvorak, P., Casamatta, D.A., Poulickova, A., Hasler, P., Ondrej, V., Sanges, R. (2014). *Synechococcus*: 3 billion years of global dominance. *Molecular Ecology*, **23**, 5538-5551.
- Egleston, E.S., Morel, F.M.M. (2008). Nickel limitation and zinc toxicity in a urea-grown diatom. *Limnology and Oceanography*, **53**, 2462-2471.
- Elderfield, H., Rickaby, R.E.M. (2000). Oceanic Cd/P ratio and nutrient utilization in the glacial Southern Ocean. *Nature*, **405**, 305-310.
- Engel, A., Thoms, S., Riebesell, U., Rochelle-Newall, E., Zondervan, I. (2004). Polysaccharide aggregation as a potential sink of marine dissolved organic carbon. *Letters to Nature* **428**, 929-932.
- Fatayer, S., Coppola, A. I., Schulz, F., Walker, B. D., Broek, T. A., Meyer, G., Druffel, E. R. M., McCarthy, M., Gross, L. (2018). Direct Visualization of Individual Aromatic Compound Structures in Low Molecular Weight Marine Dissolved Organic Carbon. *Geophysical Research Letters* **45**, 5590-5598.
- Fein, J.B., Daughney, C.J., Yee, N., Davis, T.A. (1997). A chemical equilibrium model for metal adsorption onto bacterial surfaces. *Geochimica et Cosmochimica Acta*, **61**, 3319-3328.
- Fischer, K., Dymond, J., Lyle, M., Soutar, A., Rau, S. (1986). The benthic cycle of copper: Evidence from sediment trap experiments in the eastern tropical North Pacific. *Geochimica et Cosmochimica Acta*, **50**, 1535-1543.

- Flombaum, P., Gallegos, J.L., Gordillo, R. A., Rincon, J., Zabala, L.L., Jiao, N., Karl, D.M., Li, W.K.W., Lomas, M.W., Veneziano, D., Vera, C.S., Vrugt, J.A., Martiny, A.C. (2013). Present and future global distributions of the marine Cyanobacteria *Prochlorococcus* and *Synechococcus*. *Proceedings of the National Academy of Sciences*, **24**, 9824-9829.
- Fowle, D., Fein, J.B. (2000). Experimental measurements of the reversibility of metal-bacteria adsorption reactions. *Chemical Geology*, **168**, 27-36.
- Glass, J.B., Dupont, C.L. (2017). *Chapter 2: Oceanic nickel biogeochemistry and the evolution of nickel use*. In: Zamlbe, D., Rowinska-Zyrek, M., Kozlowski, H. The biological chemistry of nickel. *Royal Society of Chemistry*. pp. 12-27.
- Hansell, D. A., Carlson, C. A. (2001). Marine Dissolved Organic Matter and the Carbon Cycle. *Oceanography* **14**, 41-49.
- Hansell, D. A. (2013). Recalcitrant Dissolved Organic Carbon Fractions. *Annual Review of Marine Science*, **5**, 421-445.
- Hao, W., Flynn, S.L., Alessi, D.S., Konhauser, K.O. (2018). Change of point of zero net proton charge (pHPZNPC) of clay minerals with ionic strength. *Chemical Geology*, **493**, 458-467.
- Herbelin, A.L., Westall, J.C. (1999). FITEQL: a Computer Program for Determination of Equilibrium Constants from Experimental Data. Department of Chemistry, Oregon State University. Corvallis, OR. *Report 99-01*.
- Ho, T.-Y., Quigg, A., Finkel, Z.V., Milligan, A.J., Wyman, K., Falkowski, P.G., Morel, F.M.M. (2003). The elemental composition of some marine phytoplankton. *Journal of Phycology*, **39**, 1145-1159.
- Huizenga, D.L., Kester, D.R. (1979). Protonation equilibria of marine dissolved organic matter. *Limnology and Oceanography*, **24**, 145-150.

- Jiang, W., Saxena, A., Song, B., Ward, B. B., Beveridge, T. J., Myneni, S. C. B. (2004). Elucidation of functional groups on gram-positive and gram-negative bacterial surfaces using infrared spectroscopy. *Langmuir* **20**, 11433-11442.
- Jiao, N., Cai, R., Zheng, Q., Tang, K., Liu, J., Jiao, F., Wallace, D., Chen, F., Li, C., Amann, R., Benner, R., Azam, F. (2018). Unveiling the enigma of refractory carbon in the ocean. *National Science Review* **5**, 459-463.
- Kawasaki, N., Sohrin, R., Ogawa, H., Nagata, T., Benner, R. (2011). Bacterial carbon content and the living and detrital bacterial contributions to suspended particulate organic carbon in the North Pacific Ocean. *Aquatic Microbial Ecology*, **62**, 165-176.
- Kenney, J.P.L., Gorzsas, A. (2019) Applications of Fourier-transform Infrared Spectroscopy in Geomicrobiology. In: Kenney, J.P.L., Veeramani, H., Alessi, D.S. (Eds.), *Analytical Geomicrobiology: A Handbook of Instrumental Techniques*, Cambridge University Press, Cambridge, United Kingdom, pp. 79-92.
- Kharbush, J.J., Close, H.G., Van Mooy, B.A.S., Arnosti, C., Smittenberg, R.H., Le Moigne, F.A.C., Mollenhauer, G., Scholz-Bottcher, B., Obreht, I., Koch, B.P., Becker, K.W., Iverson, M.H., Mohr, W. (2020). Particulate organic carbon deconstructed: Molecular and chemical composition of particulate organic carbon in the ocean. *Frontiers in Marine Science*, **7**, 518.
- Koch, B.P., Witt, M., Engbrodt, R., Dittmar, T., Kattner, G. (2005). Molecular formulae of marine and terrigenous dissolved organic matter detected by electrospray ionization Fourier transform ion cyclotron resonance mass spectrometry. *Geochemica et Cosmochimica Acta*, **69**, 3299-3308.

- Konhauser, K.O., Pecoits, E., Lalonde, S.V., Papineau, D., Nisbet, E.G., Barley, M.E., Arndt, N.T., Zahnle, K., Kamber, B.S. (2009). Oceanic nickel depletion and a methanogen famine before the Great Oxidation Event. *Nature*, **458**, 750-754.
- Konhauser, K.O., Robbins, L.J., Pecoits, E., Peacock, C., Kappler, A., Lalonde, S.V. (2015). The Archean nickel famine revisited. *Astrobiology*, **15**, 804-815.
- Konhauser, K.O., Robbins, L.J., Alessi, D.S., Flynn, S.L., Gingras, M.K., Martinez, R.E., Kappler, A., Swanner, E.D., Li, Y.L., Crowe, S.A., Planavsky, N.J., Reinhard, C.T., Lalonde, S.V. (2018). Phytoplankton contributions to the trace-element composition of Precambrian banded iron formations. *GSA Bulletin*, **130**, 941-951.
- Lane, E.S., Jang, K., Cullen, J.T., Maldonado, M.T. (2008). The interaction between inorganic iron and cadmium uptake in the marine diatom *Thalassiosira oceanica*. *Limnology and Oceanography*, **53**, 1784-1789.
- Laurenceau, E.C., Trull, T.W., Davies, D.M., Bray, S.G., Doran, J., Planchon, F., Carlotti, F., Jouandet, M.P., Cavagna, A.J., Waite, A.M., Blain, S. (2014). The relative importance of phytoplankton aggregates and zooplankton fecal pellets to carbon export: insights from free-drifting sediment trap deployments in naturally iron-fertilised waters near the Kerguelen plateau. *Biogeosciences*, **11**, 13623-13673.
- Lechtenfeld, O.J., Kattner, G., Flerus, R., McCallister, S.L., Schmitt-Kopplin, P., Koch, B.P. (2014). Molecular transformation and degradation of refractory dissolved organic matter in the Atlantic and Southern Ocean. *Geochimica et Cosmochimica Acta*, **126**, 321-337.
- Le Moigne, F.A.C. (2019). Pathways of organic carbon downward transport by the oceanic biological carbon pump. *Frontiers in Marine Science*, **6**, 634.

- Liu, Y., Alessi, D.S., Owttrim, G.W., Petrash, D.A., Mloszewska, A.M., Lalonde, S.V., Martinez, R.E., Zhou, Q., Konhauser, K.O. (2015). Cell surface reactivity of *Synechococcus* sp. PCC 7002: Implications for metal sorption from seawater. *Geochimica et Cosmochimica Acta*, **169**, 30-44.
- Lodeiro, P., Rey-Castro, C., David, C., Achterberg, E.P., Puy, J., Gledhill, M. (2020). Acid-base properties of dissolved organic matter extracted from the marine environment. *Science of the Total Environment*, **729**, 138437.
- Lohan, M. C., Crawford, D. W., Purdie, D. A., Statham, P. J. (2005). Iron and zinc enrichments in the northeastern subarctic Pacific: Ligand production and zinc availability in response to phytoplankton growth. *Limnology and Oceanography*, **50**, 1427-1437.
- Ma, X., Coleman, M.L., Waldbauer, J.R. (2018). Distinct molecular signatures in dissolved organic matter produced by viral lysis of marine cyanobacteria. *Environmental Microbiology*, **20**, 3001-3011.
- Moran, M. A., Kujawinski, E. B., Stubbins, A., Fatland, R., Aluwihare, L. I., Buchan, A., Crump, B. C., Dorrestein, P. C., Dyhrman, S. T., Hess, N. J., Howe, B., Longnecker, K., Medeiros, P. M., Niggemann, J., Obernosterer, I., Repeta, D. J., Waldbauer, J. R. (2016). Deciphering ocean carbon in a changing world. *Proceedings of the National Academy of Sciences*, **113**, 3143-3151.
- Morel, F.M.M., Price, N.M. (2003). The biogeochemical cycles of trace metals in the oceans. *Science*, **300**, 944-947.
- Muller, F. L. L., Batchelli, S. (2013). Copper binding by terrestrial versus marine organic ligands in the coastal plume of River Thurso, North Scotland. *Estuarine, Coastal and Shelf Science*, **133**, 137-146.

- Nightingale Jr., E.R. (1959). Phenomenological theory of ion solvation. Effective radii of hydrated ions. *Journal of Physical Chemistry*, **63**, 1381-1387.
- Niu, X.-Z., Harir, M., Schmitt-Kopplin, P., Croue, J.-P. (2018). Characterisation of dissolved organic matter using Fourier-transform ion cyclotron resonance mass spectrometry: Type-specific unique signatures and implications for reactivity. *Science of the Total Environment* **644**, 68-76.
- Opsahl, S., Benner, R. (1997). Distribution and cycling of terrigenous dissolved organic matter in the ocean. *Nature* **386**, 480-482.
- Ozturk, S., Aslim, B., Suludere, Z. (2010). Cadmium(II) sequestration characteristics by two isolates of *Synechocystis* sp. In terms of exopolysaccharide (EPS) production and monomer composition. *Bioresource Technology*, **101**, 9742-9748.
- Padan, J., Marcinek, S., Cindric, A.M., Santinelli, C., Broji, S.R., Radakovitch, O., Garnier, C., Omanovic, D. (2021). Organic copper speciation by anodic stripping voltammetry in estuarine waters with high dissolved organic matter. *Frontiers in Chemistry*, **8**, 628749.
- Paxeus, N., Wedborg, M. (1985). Acid-base properties of aquatic fulvic acid. *Analytica Chimica Acta*, **169**, 87-98.
- Pedler-Sherwood, B., Shaffer, E. A., Reyes, K., Longnecker, K., Aluwihare, L. I., Azam, F. (2015). Metabolic characterization of a model heterotrophic bacterium capable of significant chemical alteration of marine dissolved organic matter. *Marine Chemistry* **177**, 357-365.
- Pernthaler, J. (2005). Predation on prokaryotes in the water column and its ecological implications. *Nature Reviews Microbiology*, **3**, 537-546.
- Playter, T., Konhauser, K.O., Owttrim, G.W., Hodgson, C., Warchola, T., Mloszewska, A.M., Sutherland, B., Bekker, A., Zonneveld, J.P., Pemberton, S.G., Gingras, M.K. (2017).

- Microbe-clay interactions as a mechanisms for the preservation of organic matter and trace metal biosignatures in black shales. *Chemical Geology*, **459**, 75-90.
- Raven, J.A., and Falkowski, P.G. (1999). Oceanic sinks for atmospheric CO<sub>2</sub>. *Plant, Cell & Environment*, **22**, 741–755.
- Ritchie, J.D., Perdue, E.M. (2008). Analytical constraints on acidic functional groups in humic substances. *Organic Geochemistry*, **39**, 783-799.
- Robbins, L.J., Lalonde, S.V., Planavsky, N.J., Partin, C.A., Reinhard, C.T., Kendall, B., Scott, C., Hardisty, D.S., Gill, B.C., Alessi, D.S., Dupont, C.L., Saito, M.A., Crowe, S.A., Poulton, S.W., Bekker, A., Lyons, T.W., Konhauser, K.O. (2016). Trace elements at the intersection of marine biological and geochemical evolution. *Earth-Science Reviews*, **163**, 323-348.
- Saba, G.K., Steinberg, D.K., Bronk, D.A. (2011). The relative importance of sloppy feeding, excretion, and fecal pellet leaching in the release of dissolved carbon and nitrogen by *Acartia tonsa* copepods. *Journal of Experimental Marine Biology and Ecology*, **404**, 47-56.
- Saito, M.A., Sigman, D.M., Morel, F.M.M. (2003). The bioinorganic chemistry of the ancient ocean: The coevolution of cyanobacterial metal requirements and biogeochemical cycles at the Archean-Proterozoic boundary? *Inorganica Chimica Acta*, **356**, 308-318.
- Saito, M.A., Goepfert, T.J., Noble, A.E., Bertrand, E.M., Sedwick, P.N. (2010). A seasonal study of dissolved cobalt in the Ross Sea, Antarctica: Micronutrient behavior, absence of scavenging, and relationships with Zn, Cd, and P. *Biogeosciences*, **7**, 4059-4082.
- Scott, C., Planavsky, N.J., Dupont, C.L., Kendall, B., Gill, B.C., Robbins, L.J., Husband, K.F., Arnold, G.L., Wing, B.A., Poulton, S.W., Bekker, A., Anbar, A.D., Konhauser, K.O., Lyons, T.W. (2013). Bioavailability of zinc in marine sediments through time. *Nature Geoscience*, **6**, 125-128.

- Stevens, S., Van Baalen, C. (1973). Characteristics of nitrate reductions in a mutant of the blue-green alga *Agmenellum quadruplicatum*. *Plant Physiology*, **51**, 350-356.
- Strom, S. L.; Benner, R.; Ziegler, S.; Dagg, M. J. (1997). Planktonic grazers are a potentially important source of marine dissolved organic carbon. *Limnology and Oceanography*, **42**, 1364-1374.
- Stukel, M.R., Decima, M., Selph, K.E., Taniguchi, D.A.A., Landry, M.R. (2013). The role of *Synechococcus* in vertical flux in the Costa Rica upwelling dome. *Progress in Oceanography*, **112-113**, 49-59.
- Sunda, W.G., Huntsman, S.A. (1995). Cobalt and zinc interreplacement in marine phytoplankton: biological and geochemical implications. *Limnology and Oceanography*, **40**, 1404-1417.
- Sunda, W.G. (2012). Feedback interactions between trace metal nutrients and phytoplankton in the ocean. *Frontiers in Microbiology*, **3**, 1–22.
- Suttle, C.A. (2007). Marine viruses – major players in the global ecosystem. *Nature Reviews: Microbiology*, **5**, 801-812.
- Swaren, L., Hao, W., Melnyk, S., Baker, D., Li, Y., Owttrim, G.W., Zeng, H., Gingras, M.K., Alessi, D.S., Konhauser, K.O. (2021). Surface reactivity of the cyanobacterium *Synechocystis* sp. PCC 6803 – Implications for trace metal transport to the ocean. *Chemical Geology*, **562**, 120045.
- Tremblay, L., Caparros, J., Leblanc, K., Obernosterer, I. (2015). Origin and fate of particulate and dissolved organic matter in a naturally iron-fertilized region of the Southern Ocean. *Biogeosciences*, **12**, 607-621.
- Twining, B.S., Baines, S.B. (2013). The trace metal composition of marine phytoplankton.

- Annual Reviews in Marine Science*, **5**, 191–215.
- Van den Berg, C.M.G., Nimmo, M. (1987). Determination of interactions of nickel with dissolved organic material in seawater using cathodic stripping voltammetry. *Science of the Total Environment*, **60**, 185-195.
- Volkman, J. K., Tanoue, E. (2002). Chemical and biological studies of particulate organic matter in the ocean. *Journal of Oceanography*, **58**, 265-279.
- Vraspir, J. M., Butler, A. (2009). Chemistry of marine ligands and siderophores. *Annual Review of Marine Science* **1**, 43-63.
- Walker, B. D., Primeau, F. W., Beaupre, S. R., Guilderson, T. P., Druffel, E. R. M., McCarthy, M. D. (2016). Linked changes in marine dissolved organic carbon molecular size and radiocarbon age. *Geophysical Research Letters* **43**, 385-393.
- Wang, K., Wommack, E., Chen, F. (2011). Abundance and distribution of *Synechococcus* spp. And cyanophages in the Chesapeake Bay. *Applied and Environmental Microbiology*, **77**, 7459-7468.
- Waterbury, J.B., Watson, S.W., Guillard, R.R.L., Brand, L.E. (1979). Widespread occurrence of a unicellular, marine, planktonic, cyanobacterium. *Nature*, **277**, 293-294.
- Worden, A.Z., Nolan, J.K., Palenik, B. (2004). Assessing the dynamics and ecology of marine picoplankton: the importance of the eukaryotic component. *Limnology and Oceanography*, **49**, 168-179.
- Yee, N., Benning, L.G., Phoenix, V.R., Ferris, F.G. (2004). Characterization of metal-cyanobacteria sorption reactions; a combined macroscopic and infrared spectroscopic investigation. *Environmental Science and Technology*, **38**, 775-782.

- Yu, Q., Szymanowski, J., Myneni, S.C.B., Fein, J.B. (2014). Characterization of sulfhydryl sites within bacterial cell envelopes using selective site-blocking a potentiometric titrations. *Chemical Geology*, **373**, 50-58.
- Yu, Q., Fein, J.B. (2016). Sulfhydryl binding sites within bacterial extracellular polymeric substances. *Environmental Science and Technology*, **50**, 5498-5505.
- Zhang, Y., Green, N.W., Perdue, E.M. (2013). Acid-base properties of dissolved organic matter from pristine oil-impacted marshes of Barataria Bay, Louisiana. *Marine Chemistry*, **155**, 42-49.
- Zhang, J., Kattner, G., Koch, B.P. (2019). Interactions of trace elements and organic ligands in seawater and implications for quantifying biogeochemical dynamics: A review. *Earth Science Reviews*, **192**, 631-649.
- Zhao, Z., Gonsoir, M., Luek, J., Timko, S., Ianiri, H., Hertkorn, N., Schmitt-Kopplin, P., Fang, X., Zeng, Q., Jiao, N., Chen F. (2017). Picocyanobacteria and deep-ocean fluorescent dissolved organic matter share similar optical properties. *Nature Communications*, **8**, 15284.
- Zhao, Z., Gonsoir, M., Schmitt-Kopplin, P., Zhan, Y., Zhang, J., Jiao, N., Chen F. (2019). Microbial transformation of virus-induced dissolved organic matter from picocyanobacteria: coupling of bacterial diversity and DOM chemodiversity. *The ISME Journal*, **13**, 2551-2565.
- Zheng, Q., Chen, Q., Cai, R., He, C., Guo, W., Wang, Y., Shi, Q., Chen, C., Jiao, N. (2019). Molecular characteristics of microbially mediated transformation of *Synechococcus*-derived dissolved organic matter as revealed by incubation experiments. *Environmental Microbiology*, **21**, 2533-2542.

Zhou, Q., Liu, Y., Li, T., Zhao, H., Alessi, D.S., Liu, W., Konhauser, K.O. (2021). Cadmium adsorption to clay-microbe aggregates: Implications for marine heavy metals cycling. *Geochimica et Cosmochimica Acta*, **290**, 124-136.

**Table 3.1:** Summary of protonation modeling of cyPOM in comparison with intact *Synechococcus* cells from Liu et al. (2015).

Site	pKa	Site Density (mmol g <sup>-1</sup> )	Material	Reference
1	5.78(±0.07)	5.97(±1.16)	cyPOM	this study
	5.07(±0.03)	11.70(±0.62)	<i>Synechococcus</i> cells	Liu et al. (2015)
2	9.01(±0.29)	5.89(±0.75)	cyPOM	this study
	6.71(±0.07)	5.72(±0.22)	<i>Synechococcus</i> cells	Liu et al. (2015)
3	8.54(±0.15)	6.96(±0.76)	<i>Synechococcus</i> cells	Liu et al. (2015)

**Table 3.2:** Best fit, 2- and 1-site protonation models for cyDOM in comparison with values compiled from literature. Siteconcentrations are in units of  $\mu\text{mol g}^{-1}$ .

<b>pKa 1</b>	<b>Site Conc.</b>	<b>pKa 2</b>	<b>Site Conc.</b>	<b>Material/Sample Location</b>	<b>Reference</b>
4.89( $\pm 0.22$ )	42.8( $\pm 14.6$ )	6.80( $\pm 0.22$ )	37.3( $\pm 16.5$ )	cyDOM	This study
3.42( $\pm 0.03$ )	13.7( $\pm 0.27$ ) <sup>a</sup>	-	-	Narragansett Bay DOM	Huizenga & Kester, 1979
3.67( $\pm 0.02$ )	10.3( $\pm 0.13$ ) <sup>a</sup>	-	-	Mixed river water DOM	
3.56( $\pm 0.02$ )	10.0( $\pm 0.16$ ) <sup>a</sup>	-	-	Block Island Sound DOM (surface)	
3.56( $\pm 0.03$ )	11.6( $\pm 0.28$ ) <sup>a</sup>	-	-	Sargasso Sea DOM	
3.75( $\pm 0.03$ )	9.6( $\pm 0.25$ ) <sup>a</sup>	-	-	Equatorial Atlantic DOM	
3.61( $\pm 0.03$ )	9.7( $\pm 0.21$ ) <sup>a</sup>	-	-	Coastal Equatorial Atlantic DOM (surface)	
3.57( $\pm 0.04$ )	10.9( $\pm 0.31$ ) <sup>a</sup>	-	-	Equatorial Atlantic DOM (surface)	
3.67( $\pm 0.02$ )	9.0( $\pm 0.12$ ) <sup>a</sup>	-	-	Coastal Peru (low productivity)	Paxeus & Wedborg, 1985 <sup>c</sup> Cai et al. (1998) <sup>e</sup> Zhang et al. (2013)  Ritchie & Perdue, 2003
2.66( $\pm 0.10$ )	2.49( $\pm 0.07$ ) <sup>b</sup>	4.21( $\pm 0.08$ )	1.70( $\pm 0.05$ ) <sup>b</sup>	Aquatic Fulvic Acid	
4.46	80.0 <sup>d</sup>	6.64	105.0 <sup>d</sup>	Satilla River estuarine DOM	
4.07( $\pm 0.12$ )	-	-	-	Pristine Barataria Bay DOM	
4.57( $\pm 0.03$ )	-	-	-	Pristine Barataria Bay DOM	
4.64( $\pm 0.05$ )	-	-	-	Oil-impacted Barataria Bay DOM	
4.31( $\pm 0.03$ )	-	-	-	Oil-impacted Barataria Bay DOM	
4.13( $\pm 0.02$ )	-	-	-	Oil-impacted Barataria Bay DOM	
4.00	-	8.76	-	Simple Organic Acids	
3.91	-	10.09	-	Suwannee River Fulvic Acids	
4.28	-	9.90	-	Suwannee River Humic Acids	
3.82	-	10.28	-	Nordic Fulvic Acids	
4.25	-	10.19	-	Nordic Humic Acids	
3.61	-	9.87	-	Soil Fulvic Acids	
3.97	-	9.71	-	Peat Fulvic Acids	
4.18	-	5.33	-	Laurentian River Fulvic Acids	Garnier et al. (2004) <sup>f</sup>
4.71	-	5.90	-	Laurentian River Humic Acids	
3.26	-	8.60	-	Baltic fjord seawater (NW Germany)	Lodeiro et al. 2020

<sup>a</sup>Values reported in  $\mu\text{mol mg}^{-1}$  org C

<sup>b</sup>Values reported in mmol g<sup>-1</sup>

<sup>c</sup>Paxeus & Wedborg, 1985 reported 4 additional pKa values of 5.85, 6.65, 8.11, and 9.54.

<sup>d</sup>Values reported in μmol L<sup>-1</sup>

<sup>e</sup>Cai et al. (1998) reported the presence of 2 additional pKa values at 8.94 and ~10.

<sup>f</sup>Garnier et al. (2004) reported the presence of 4 additional pKa values for Laurentian River Fulvic Acids (6.58, 7.61, 8.93, and 9.99) and Laurentian River Humic Acids (6.67, 7.74, 9.2, and 10.08).

**Table 3.3:** Best fit binding constants for trace metal-cyPOM complexes and previously studied trace metal-*Synechococcus* sp. PCC 7002 complexes. All experiments were conducted in 0.56 M NaCl.

<b>Trace Metal</b>	<b>Site 1 logK</b>	<b>Site 2 logK</b>	<b>Site 3 logK</b>	<b>Material</b>	<b>Reference</b>
Cd	1.6	1.1	-	cyPOM	This study
	1.15	1.78	2.74	<i>Synechococcus</i> cells	Liu et al. (2015)
Co	1.2	2.8	-	cyPOM	This study
	4.6	6.3	-	<i>Synechococcus</i> cells	Bishop et al. (2019)
Cu	0.7	6.3	-	cyPOM	This study
	3.7	7.4	-	<i>Synechococcus</i> cells	Bishop et al. (2019)
Ni	0.8	3.7	-	cyPOM	This study
	4.7	6.1	-	<i>Synechococcus</i> cells	Bishop et al. (2019)
Zn	1.1	2.7	-	cyPOM	This study
	4.4	7.9	-	<i>Synechococcus</i> cells	Bishop et al. (2019)

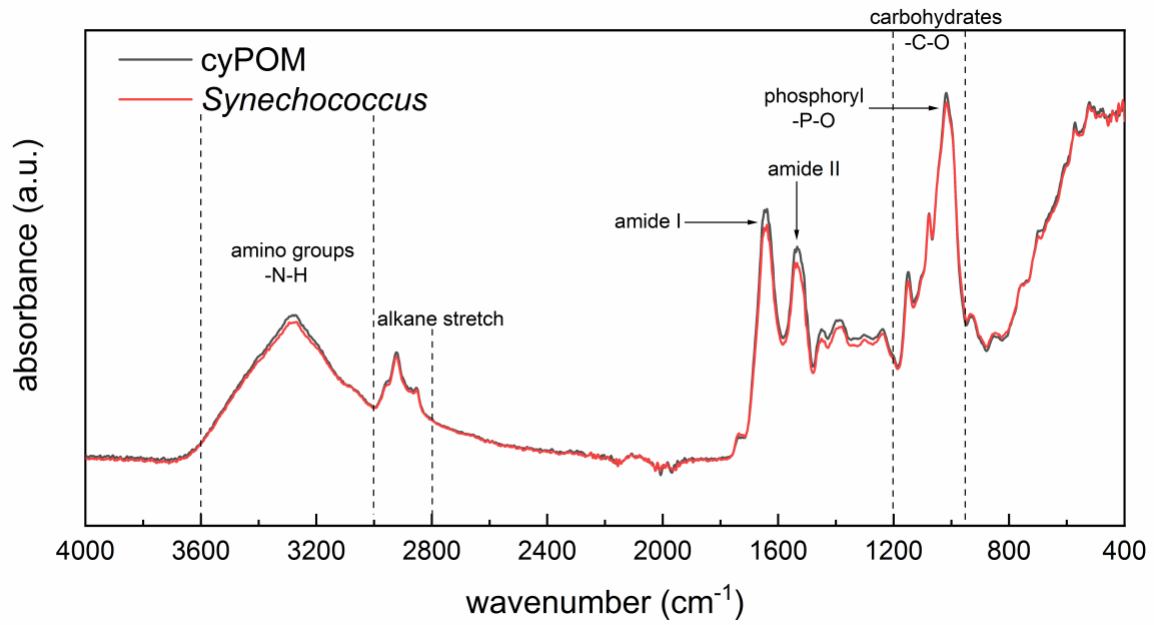


**Figure 3.1:** Attenuated total reflectance fourier transform infrared (ATR-FTIR) spectra of dried and ground *Synechococcus* sp. PCC 7002 cells overlain with dried and ground cyPOM.

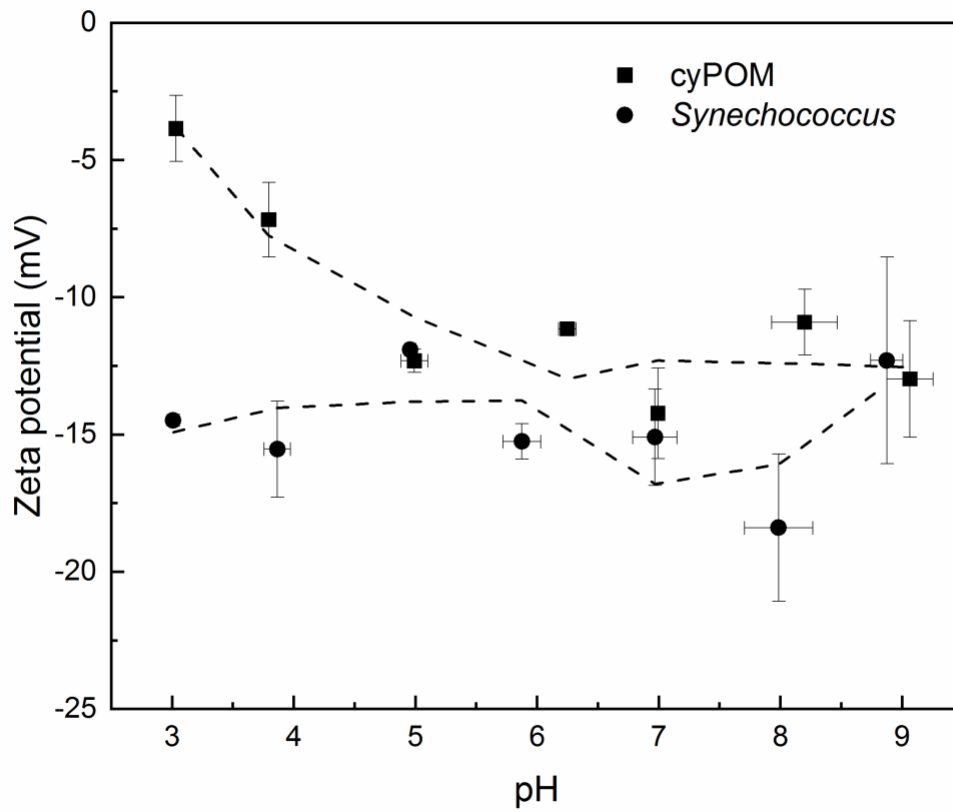


**Figure 3.2:** Zeta potential measurements performed on 0.2 g L<sup>-1</sup> suspensions of *Synechococcus* sp. PCC 7002 and cyPOM in 0.56 M NaCl as a function of pH.

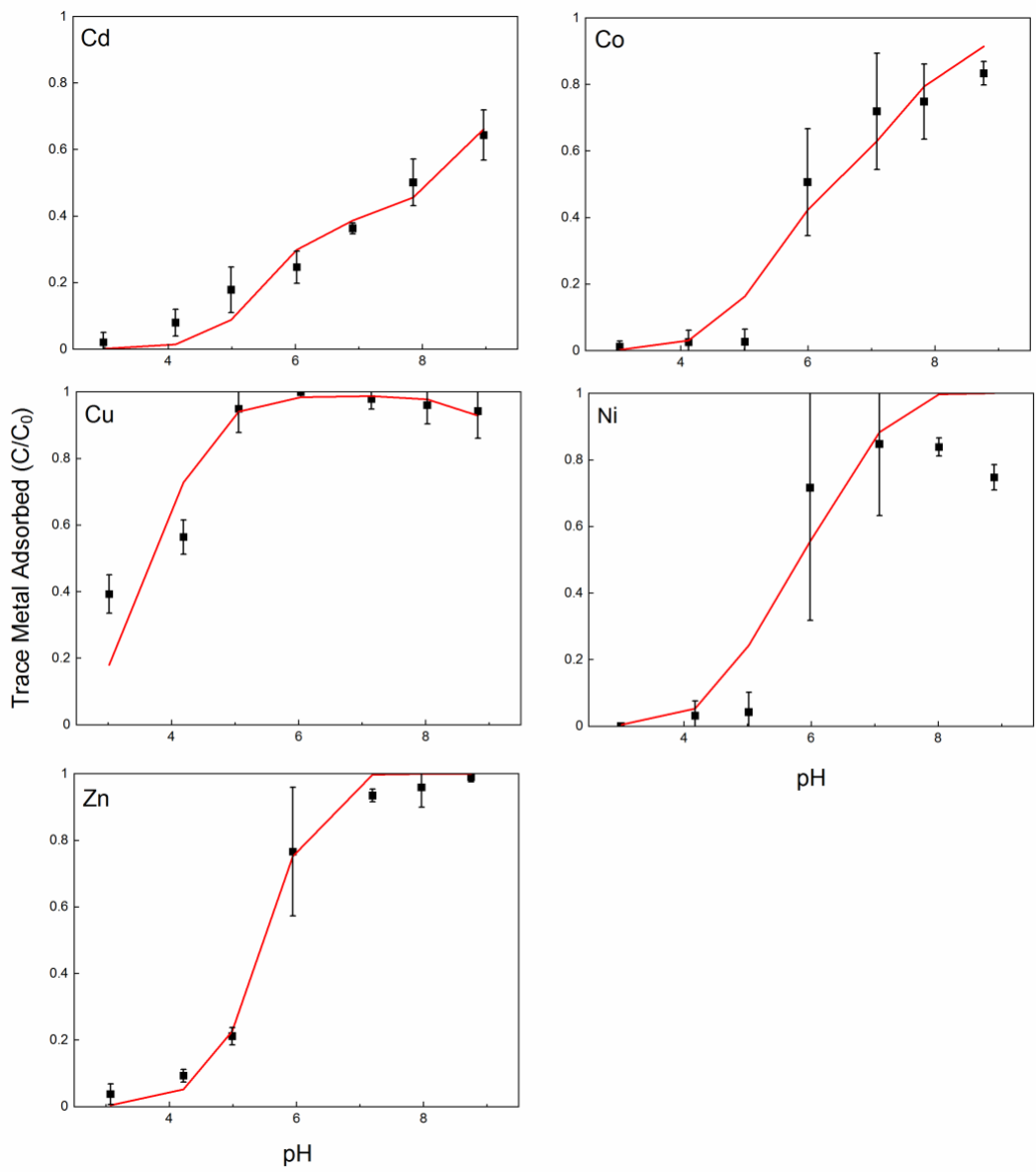


**Figure 3.3:** Modeling (red lines) and experimental (points) results of trace metal adsorption onto  $10 \text{ g L}^{-1}$  *Synechococcus* sp. PCC 7002 derived cyPOM in  $0.56 \text{ M NaCl}$ . Error bars indicate 1-sigma standard deviation.

## Chapter 4: Contribution of cyanobacteria to marine dissolved organic matter<sup>1</sup>

### 4.1. Introduction

The marine dissolved organic carbon (DOC) pool - defined as aqueous organic carbon that is <0.2 µm in size (Benner et al. 1992; Jiao et al. 2014) - constitutes a large carbon reservoir comparable in size to that of atmospheric CO<sub>2</sub> (Fry et al. 1998; Koch et al. 2005; Moran et al. 2016). DOC is, therefore, an important intermediate of the biological pump in which atmospheric CO<sub>2</sub> is fixed into biomass, and upon cell lysis, some of the DOC is converted to refractory dissolved organic carbon (RDOC) that is considered biochemically inert and sequestered in deep ocean sediments for millennia (Jiao et al. 2010; Ridgwell and Arndt, 2015). In addition to the sequestration of carbon to ocean depths, DOC occupies a key role in the marine food web via the microbial loop and viral shunt (Jiao et al. 2010; Wang et al. 2011).

Dissolved organic matter (DOM) is a complex mixture comprised primarily of DOC, dissolved organic nitrogen (DON), phosphorus (DOP), and lower concentrations of oxygen-, hydrogen-, and sulfur-containing compounds whose importance has not yet been extensively researched (Stedmon and Nelson, 2015; Li et al. 2017). Various studies have been conducted in an effort to extract and isolate DOC and DOM from seawater (Dittmar et al. 2008; Flerus et al. 2011; Li et al. 2017). The commonly used methods include filtering seawater through cartridges containing various sorbents, such as XAD resins and modified styrene divinyl benzene polymers (Dittmar et al. 2008; Green et al. 2014). Although solid-phase extraction techniques propose to isolate and recover a significant fraction of marine DOM (~30-65% but closer to 100% when

---

<sup>1</sup>This chapter is currently in review with *Geochimica et Cosmochimica Acta* as: Swaren, L., Kitova, E.N., Klassen, J.S., Owtrim, G.W., Alessi, D.S., Konhauser, K.O.

coupled with reverse osmosis/electrodialysis) these extractions necessarily operate on the bulk marine DOM pool, including terrestrial components (Green et al. 2014).

Significant advances at unraveling the complex molecular composition of marine DOM have been made with the implementation of Fourier transform ion cyclotron resonance mass spectrometry (FTICR-MS) (Woods et al. 2011; Zark et al. 2017; Jiao et al. 2018; Zark and Dittmar, 2018). From these ultrahigh resolution mass spectroscopy studies, a plethora of carboxyl-rich alicyclic molecules (CRAM), dissolved polysaccharides, transparent exopolymer particles (TEP), fulvic and humic substances, and lignin degradation products have been identified (Opsahl & Benner, 1997; Strom et al. 1997; Hansell & Carlson, 2001; Dilling & Kaiser, 2002; Engel et al. 2004; Hertkorn et al. 2006; Jiao et al. 2014; Lechtenfeld et al. 2014; Fatayer et al. 2018). The latter terrestrially derived components of the DOM pool, principally lignin and tannins, consist of molecules with H/C and O/C ratios inhabiting distinct areas on van Krevelen plots (Figure 4.1) (Hedges et al. 1997; Hansell, 2013; Lechtenfeld et al. 2014). In these plots, terrestrial-derived DOM dominates modern marine samples, evidencing the persistence and recalcitrant nature of terrestrial DOM in the marine environment.

More recently, Zhao et al. (2017) investigated the optical properties of marine chromophoric DOM (CDOM) with that of DOM isolated from solid-phase extraction (SPE-DOM). They used SPE-DOM collected from cultures of common marine cyanobacteria *Synechococcus* and *Prochlorococcus* to ensure that the source was solely marine and biological. The authors found that *Synechococcus*-derived DOM is composed largely of nitrogen (N)-containing molecules (1137) rather than carbon-hydrogen-oxygen (CHO) molecules (284). Ma et al. (2018) mechanically lysed *Synechococcus* cells to investigate the intracellular DOM, simulating the kind of DOM production witnessed in nature due to zooplankton grazing. The intracellular

DOM had H/C and O/C ratios indicative of biomolecules such as lipids, proteins, pigments (Ma et al. 2018).

Understanding the source and composition of cyanobacterial DOM is important for elucidating the role of the ancient marine biosphere in controlling trace metal availability, and ultimately bio-deposition of metals in marine sediments. For instance, previous studies have used the chemical composition of banded iron formations as proxies for interpreting redox evolution on Earth and the composition of paleo-seawater (Konhauser et al. 2009; 2011). However, the role that DOM may have played as a vector for transferring trace metals into marine sediments has only been investigated recently (Swaren et al. 2021). What is less understood is the DOM pool composition prior to the diversification of terrestrial plants and how cyanobacteria influenced Precambrian ocean composition. The shift to land took place near the Silurian-Devonian boundary, although fossil records may have pushed the plant transition further back into the Ordovician (Kenrick & Crane, 1997; Bateman et al. 1998). Cyanobacteria may have evolved as early as 3.5 billion years ago (Garcia-Pichel et al., 2019; Boden et al., 2021; Fournier et al., 2021; Sánchez-Baracaldo et al., 2021), so for nearly 3 billion years cyanobacterial DOM dominated seawater without a terrestrial component. Therefore, it is important to study and appreciate the differing contributions of freshwater and marine DOM had on the food web and trace metal cycling in oceans predating the evolution of terrestrial plants.

In an effort to investigate DOM produced solely from cyanobacteria that is representative of DOM in ancient oceans, we investigated the properties of the clarified supernatants produced from two species of cyanobacteria, and then mechanically lysed and filtered the material through 0.2 µm filters to obtain the ‘dissolved’ component. We chose *Synechococcus* because the genus is one of the most important primary producers in the modern oceans and it is one of the most

evolutionary successful lineages of cyanobacteria dating back to the Archean (Flombaum et al. 2013; Dvorak et al. 2014). To further constrain the compositional characteristics of the broader cyanobacterial DOM pool, we investigated *Synechocystis* because it is one of the most widely distributed cyanobacteria in a wide range of aqueous environments, including freshwater, brackish settings and seawater (Rippka et al. 1979).

#### **4.2.0. Methods**

##### **4.2.1. Cyanobacteria growth and harvesting**

Cyanobacterial strains used in this study were maintained axenically under aerobic conditions. *Synechococcus* sp. PCC 7002 (from herein *Synechococcus*) and *Synechocystis* sp. PCC 6803 (from herein *Synechocystis*) were cultured on A+ without EDTA and BG-11 agar plates, respectively, at 30°C and a light intensity of 50  $\mu\text{mol photons m}^{-2}\text{s}^{-1}$  (Owtrim, 2012). Liquid cyanobacterial cultures were grown from individual colonies inoculated into the appropriate growth media (50 mL) for 3 days with aeration provided by shaking at 60 rpm. These cultures were used to inoculate 300 mL cultures that were aerated with filtered, humidified air and grown until stationary growth phase was achieved ( $\text{OD}_{750} > 0.5$ ) (Li et al. 2021).

Cyanobacterial cells were harvested by centrifugation (Sorvall Lynx 4000) at 10,000 g for five-minutes followed by washing the cell pellet with 18.2 M $\Omega\bullet\text{cm}$  ultrapure water to remove residual growth media as well as potential competing metals from the cell wall. The washings were repeated four times and the final pellet resuspended in ultrapure water at a final concentration of 10 g/L.

##### **4.2.2. Preparation of mechanically lysed dissolved organic matter**

Cyanobacterial cell lysis was accomplished via sonication (Braun-Sonic 2000) as described previously by Bishop (2018) and Swaren et al. (2021). Sonication was preferred, as it does not introduce any chemicals that could potentially adsorb to the lysed cells. 10 mL aliquots of the washed bacterial cell solution were separated into 15 mL polypropylene falcon tubes prior to sonication. Each tube was sonicated at 160 MHz for a duration of 30 seconds and then immediately inserted into an ice-water bath. Each aliquot underwent 10 cycles of sonication, with breaks after the third and sixth cycle to mix together all tubes into a sterile 250 mL Erlenmeyer flask and redistribute the 10 mL aliquots. To achieve uniform lysis, aliquots were mixed and redistributed after the third and sixth sonication cycle. The lysed samples were centrifuged for five minutes at 10,000 *g* to separate the dissolved fraction. The resulting supernatant was then filtered through 0.2  $\mu\text{m}$  nylon membranes. The resulting filtered solution was considered an analog for intracellular cyanobacterial dissolved organic matter (cyDOM).

#### **4.2.3. Electrospray ionization Fourier transform ion cyclotron resonance mass spectrometry (ESI-FTICR-MS)**

Mass spectra were obtained using a 15T FTICR-MS (Solarix XR, Bruker Daltonics, Bremen, Germany) equipped with a nanoflow ESI (nanoESI) source. NanoESI tips were prepared from borosilicate capillaries (1.0 mm o.d., 0.68 mm i.d.) pulled at one end to  $\sim 5 \mu\text{m}$  using a P-1000 micropipette puller (Sutter Instruments, Novato, CA). To perform nanoESI, a voltage of +0.9 kV (positive ion mode) or -0.9 kV (negative ion mode) was applied to a platinum wire inserted into solution in the nanoESI tip. No pH adjustments were made before analysis. The cyDOM suspensions were mixed 1:1 (v:v%) with methanol (HPLC Grade, Fisher Chemical, Massachusetts, United States). Arginine was added prior to analysis and served as an internal

calibrant. Data acquisition was performed using the Bruker FtmControl software (version 2.2). Peaks were identified with Bruker Data Analysis software (version 5.0). Peaks with a signal/noise (S/N) ratio greater than 4 were transferred to a spreadsheet for further chemical formula determination. Molecular formulas were identified using the browser based UltraMassExplorer (UME) application (Leefman et al. 2019). Within the UME, the “All CHONSP” library was used to assign molecular formulas (See Appendix 3 SI Table 1 for UME input parameters). From the assigned formulas, they were filtered based on the possible molecular formula composition  $C_{0-100}H_{0-100}O_{0-100}N_{0-30}P_{0-2}S_{0-2}$  (Koch et al. 2007). Ultrapure water blanks with Arginine were also ran as described above and molecular formulas identified in the blank were removed from the dataset (Appendix 3 SI Figures 1–6). For a schematic of the pipeline from cyDOM production to data interpretation see Appendix 3 SI Figure 7.

### 4.3. Results

Fourier transform ion cyclotron resonance (FTICR) mass spectrometry of *Synechococcus*- and *Synechocystis*-derived DOM yielded >4000 and >3100 distinct mass peaks, respectively, with a  $S/N > 4$  in negative ionization mode in duplicate analysis across two separate cultures (Figure 4.2). Following molecular formula assignment in the browser based UltraMassExplorer (UME) and further refinement based on the composition criterion  $C_{0-100}H_{0-100}O_{0-100}N_{0-30}P_{0-2}S_{0-2}$  (Koch et al. 2007) there are 1548 and 1474 unique molecular formulas assigned to mass peaks for *Synechococcus*- and *Synechocystis*-derived DOM, respectively (Figure 4.3). There is an overlap of 222 formulas that are identified in both cyanobacteria. In addition to CHO backbones, much of the cyanobacterial-derived DOM (>80%) contains N (Figure 4.3). Additionally, both cyanobacteria contained large proportions of sulfur (S)- and phosphorous (P)-containing

molecules, ~35% and ~37% respectively, as CHONS and CHONP molecules with lesser amounts of CHOS and CHOP (Figure 4.3).

#### **4.4. Discussion**

##### **4.4.1. Comparison between *Synechococcus* and *Synechocystis***

There are abundant nutrient (N, P, and S) containing molecules identified in the cyanobacteria-derived DOM (Figure 4.4). The abundance of N-containing molecules is likely due to both *Synechococcus* and *Synechocystis* possessing phycobilisome complexes (Rakhimberdieva et al. 2007; Zhao et al. 2017; Zhao et al. 2019). These are light-harvesting pigments that can make up 30%–40% of the cellular dry mass of cyanobacteria (Bennett and Bogorad, 1973). In addition, the phycobilisoms have an O/C ratio < 0.4, the same as that found in cyanobacterial-derived DOM, suggesting that a large fraction of the DOM may actually be pigments (Figure 4.1) (Gantt, 1980). Moreover, *Synechococcus* and *Synechocystis* are both Gram-negative bacteria, contain abundant membrane lipids such as sulfolipids and glycolipids which accounts for their high S-content (Van Mooy et al. 2006). The abundant P-containing molecules are associated with a suite of biochemicals including DNA, RNA, phospholipids, and phosphorylated proteins (Van Mooy et al. 2006). Although there are only ~200 identically assigned interspecies molecules, the general distribution of CHO as well as N-, P-, and S-containing molecules is similar between *Synechococcus* and *Synechocystis* (Figure 4.3).

##### **4.4.2. Cyanobacterial DOM in comparison to modern marine DOM**

The molecular characterization of DOM gradually changes from terrestrial settings (e.g., rivers) through estuaries and deltas to deeper marine setting such as the outer shelf and continental slope

(Schmidt et al. 2009). As one might expect, marine samples farther from shore contain a larger component of more recalcitrant molecules identified as by-products of microbial metabolism (e.g., lipids, proteins, and amino sugars) compared to river samples dominated by CHO compounds (Schmidt et al. 2009). For instance, in a transect starting with river waters draining into the Iberian coast in Spain, and extending oceanward to the outer shelf, clusters of low O/C ( $<0.2$ ) and low H/C ( $<0.8$ ) molecules commonly associated with pyrogenic carbon were observed in all samples and other terrestrial-derived molecules (e.g., lignin and tannin) decreased oceanward (Schmidt et al., 2009). By comparison, our data from cyanobacterial lysates identified higher O/C ratios, with a diverse range of H/C ratios. In another study of riverine DOM from around the globe, Niu et al. (2018) identified a dominance of CHO and CHON molecules with H/C and O/C ratios similar to those of terrestrially derived DOM (Figure 4.1). There are, however, predictable exceptions. As an example, DOM collected off Ross Island, Antarctica had the largest variability in molecular complexity with the highest proportion of CHOS and CHONS molecules (Figure 4.3). Niu et al. (2018) speculated that this pattern likely reflected the lack of higher plants, a source of lignin and tannins that dominates the continental riverine composition in most settings. Isolated from such sources, the Ross Island DOM was similar to microbial-derived DOM that closely resembles the more nutrient-dense composition of the cyanobacterial-derived DOM investigated here (Figure 4.4). Similarly, Bhatia et al. (2010) identified a dominant microbial influence on the composition of DOM from the Greenland ice sheet. The highest concentration of lipids and proteins are found in supraglacial samples that also demonstrate the lowest terrestrial input. Shifts to a higher relative proportion of terrestrial-derived molecules is paired with decreasing microbial DOM contributions with migration from the supraglacial environment to the subglacial and eventually tarm (Bhatia et al. 2010). By contrast, Lechtenfeld et al. (2014) found that aged Southern Ocean ultra-refractory

molecules plot similarly to terrestrial-derived products (Figures 4.1 and 4.4). Given the low annual primary production and H/C and O/C ratios matching that of terrestrial-derived DOM, it is proposed that terrestrial CHO molecules comprise the majority of those that are sequestered to the ocean interior (Lechtenfeld et al. 2014).

Recent investigations of cyanobacterial-derived DOM show that trends in their chemical formulas differ in comparison to most marine samples. Ma et al. (2018) investigated the DOM from *Synechococcus* WH7803 derived from controlled culture experiments. They produced intracellular DOM via mechanical lysis and the introduction of a viral pathogen, as well as DOM exuded directly from the living cells via primary production. All three distinct DOM samples produced thousands of molecules that have atomic H/C and O/C ratios commonly associated with lipids, proteins, and pigments (Figure 4.1). Both the *Synechococcus*- and *Synechocystis*-derived DOM produced in the present study and Ma et al. (2018) primarily contained molecules with high H/C (>1.0) and low O/C (<0.6) ratios that do not reflect terrestrial-derived molecules such as lignin and tannin (Figure 4.1). CRAM overlaps almost entirely with the H/C and O/C ratios of terrestrial-derived molecules, lignin specifically (Figure 4.1). In addition to various terrestrial sources, CRAM are also known to originate degradation products of more complex biomolecules previously identified from marine phytoplankton, namely cell wall and membrane components, resulting in slight overlap on van Krevelen diagrams (Hertkorn et al. 2006). Although the exact source of CRAM molecules identified in marine DOM is has not been elucidated, nuclear magnetic resonance (NMR) studies have proposed terpenoids as the source in marine DOM (Hertkorn et al. 2006).

#### **4.4.3. Precambrian Implications**

The majority of modern seawater DOM is composed of terrestrial-derived CHO molecules fed to the oceanic pool via riverine runoff (Figure 4.5) (Hedges, 1997; Stedmon et al. 2003; Koch et al. 2005; Hansell, 2013; Jorgensen et al. 2014; Koch et al. 2014; Lechtenfeld et al. 2014). DOM that originates from terrestrial plants can be differentiated from marine DOM by lignin content because microbial-derived DOM lacks lignin (Hedges et al. 2000). Other terrestrial sources of DOM originate from aeolian deposition of terrestrial POM to the ocean surface (Opsahl & Benner, 1997), tropical mangroves (Dittmar et al. 2006; Shank et al. 2010), and submarine groundwater discharge (Swarzenski et al. 2006; Linkhorst et al. 2017). In addition to naturally derived terrestrial DOM, there are many anthropogenic sources. A significant amount of DOM is deposited to the oceans in the form of black carbon due to fossil fuel burning (Dittmar, 2008; Hansell, 2013; Lechtenfeld et al. 2014). Furthermore, black carbon is produced through biomass burning such as slash and burn agriculture and natural wildfires (Dittmar, 2008; Dittmar and Paeng, 2009; Hansell, 2013; Jaffe et al. 2013). Pyrogenic carbon can be identified based on the dominant polycyclic aromatic structure and has been identified as contributing 10% of the global riverine DOM flux to the oceans (Dittmar, 2008; Dittmar and Paeng, 2009; Jaffe et al. 2013).

Primary production by phytoplankton accounts for a majority of marine DOM production in the global oceans on a daily basis. Primary production yields approximately  $50 \text{ Pg C yr}^{-1}$  although most of this DOM is recycled within the photic zone (Martin et al. 1987; Hedges et al. 1997). Only approximately 4% of DOM created through primary production evades microbial degradation and gets sequestered to the ocean interior (Lonborg et al. 2018). DOM that is sequestered to ocean depths is transported through the “microbial carbon pump” (MCP; Jiao et al. 2010; Hansell, 2013; Ridgwell and Arndt, 2015). Lysis, due to viral infection, is a significant source of DOM that accounts for approximately  $3 \text{ Pg C yr}^{-1}$  (Aluwihare & Repeta, 1999; Suttle,

2007; Brussard et al. 2008; Jiao et al. 2010; Durham et al. 2015; Moran et al. 2016; Walker et al. 2016; Zhao et al. 2017). It is estimated that 5 to 14% of *Synechococcus* are lysed globally over a one-day cycle due to cyanophages (Wang et al. 2011). More broadly, 20-40% of marine prokaryotes are estimated to be removed each day due to viral lysis (Suttle, 2007).

Cyanobacteria-derived DOM is a more chemically complex mixture with a higher portion of nutrient containing molecules than modern marine DOM (Figure 4.5). Although N, P, and S containing molecules comprise a relatively small fraction of the total DOM pool in modern oceans, they play an important role in the carbon cycle considering the rapid nutrient recycling in the photic zone. Even if only 4% of DOM resists uptake and degradation in the photic zone (Lonborg et al. 2018), the remaining deep marine DOM pool of the modern CHO dominated oceans will be vastly different than that of the Precambrian oceans where no terrestrial or pyrogenic DOM input existed (Figure 4.5).

Prior to the evolution of land plants, the DOM pool would be largely controlled by marine plankton, such as cyanobacteria. This signifies a DOM pool that is largely governed by nutrient-rich, cyanobacterial-derived DOM (Figure 4.5). Following the Great Oxidation Event (GOE) at ca. 2.5 Ga (Warke et al., 2020), and during periods of higher nutrient supply to the oceans, such as the 2.22 to 2.06 Ga Lomagundi-Jatuli Event (Bekker and Holland, 2012), there was increased nutrient supply to the coastal biosphere that would significantly increase primary productivity and DOM associated with the phytoplankton community (Konhauser et al., 2011; Mand et al. 2020). Moreover, periods following 'snowball Earth' glaciations (Planavsky et al., 2010) or periods of intense chemical weathering associated with a warmer planet (e.g., Paleocene-Eocene Thermal Maximim; Hao et al., 2021), with similar spikes in nutrient transport to the oceans, would increase coastal marine primary productivity and drive the development of a nutrient-rich DOM reservoir

sourced from cyanobacteria. This would have significant implications for trace metal cycling in Precambrian oceans as trace metals have a much higher affinity for N-, S-, and P-containing ligands (Zhang et al. 2019). Indeed, this is confirmed by modelling the amount of dissolved cadmium ( $\text{Cd}^{2+}$ ) that can be bound to various organic ligands comprising microbial biomass. Using the published binding constant for  $\text{Cd}^{2+}$  to bacterial sulfhydryl sites ( $\log K_{\text{Cd}} = 8.3$ ; Yu and Fein, 2015), which are consistent with model thiol ligands such as cysteine (Walsh and Ahner, 2013), and combined with the *Synechococcus* carboxyl ligand constant for  $\text{Cd}^{2+}$  ( $\log K_{\text{Cd}} = 1.1$ ; Liu et al. 2015), we ran predictive models using FITEQL 4.0 (Herbelin and Westall, 1999) to examine the speciation of the trace metals in the presence of both model ligands (thermodynamic and metal binding constants can be found in Appendix 3 SI Tables 2 and 3). At pH 7 and ratios of 1:1000 (thiol:carboxyl) – an exaggeration of modern ligand distribution - the speciation of Cd(II) is almost entirely (>99%) thiol. Similarly, using phosphate groups associated with cell wall material (e.g., phospholipids), we show that at a 1:1 (phosphate:carboxyl), >77% is bound to phosphoryl, while using N-containing ligands (e.g., amino) we show that at a 1:1 (amino:carboxyl), >53% is bound to amino. What these calculations collectively imply is that in an ocean where N-, S-, and P-containing ligands comprise the DOM pool, that they would be more effective sorbents of divalent metals than modern CHO-dominated DOM.

#### **4.5. Conclusions**

In modern oceans the DOM pool is impacted by terrestrial degradation products, largely CHO molecules that make up a significant portion of the environmental DOM pool. In Precambrian oceans the DOM pool would primarily, if not solely, be contributed by planktonic marine organisms. Cyanobacteria-derived DOM contains molecules that are compositionally similar to

those of microbe dominated environmental samples with little to no terrestrial influence, such as supraglacial lakes. This leads us to hypothesize that Precambrian marine DOM was chiefly composed of N, P, and S-containing molecules rather than CHO molecules of today (Figure 4.5). An ocean containing a large amount of N, P, and S ligands would have major implications for trace metal bioavailability.

#### 4.6. References

- Aluwihare, L. I., Repeta, D. J. (1999). A comparison of the chemical characteristics of oceanic DOM and extracellular DOM produced by marine algae. *Marine Ecology Progress Series* **186**, 105-117.
- Bateman, R. M., Crane, P. R., DiMichele, W. A., Kenrick, P. R., Rowe, N. P., Speck, T., Stein, W. E. (1998). Early Evolution of Land Plants: Phylogeny, Physiology, and Ecology of the Primary Terrestrial Radiation. *Annual Reviews of Ecological Systems* **29**, 263-292.
- Bekker, A., Holland, H.D. (2012). Oxygen overshoot and recovery during the early Paleoproterozoic. *Earth and Planetary Science Letters* **317**, 295-304.
- Benner, R., Pakulsi, J. D., McCarthy, M., Hedges, J. I., Hatcher, P. G. (1992). Bulk chemical characteristics of dissolved organic matter in the ocean. *Science* **255**, 1561-1564.
- Bennett, A., Bogorad, L. (1973). Complementary chromatic adaptation in a filamentous blue-green alga. *Journal of Cell Biology* **58**, 419-435.
- Bhatia, M.P., Das, S.B., Longnecker, K., Charette, M.A., Kujawinski, E.B. (2010). Molecular characterization of dissolved organic matter associated with the Greenland ice sheet. *Geochimica et Cosmochimica Acta* **74**, 3768-3784.
- Bishop, B.A. (2018). The effects of cyanobacteria and dissolved organic carbon on marine trace metal cycling. Thesis – Master of Science, University of Alberta.
- Boden, J.S., Konhauser, K.O., Robbins, L.J., Sanchez-Baracaldo, P. (2021). Timing the evolution of antioxidant enzymes in cyanobacteria. *Nature Communications* **12**, 4742.  
<https://doi.org/10.1038/s41467-021-24396-y>
- Brussard, C. P. D., Wilhelm, S. W., Thingstad, F., Weinbauer, M. G., Bratbak, G., Heldal, M., Kimmance, S. A., Middelboe, M., Nagasaki, K., Paul, J. H., Schroeder, D. C., Suttle, C. A.,

- Vaque, D., Wommack, K. E. (2008). Global-scale processes with a nanoscale drive: the role of marine viruses. *International Society for Microbial Ecology* **2**, 575-578.
- Dilling, J., Kaiser, K. (2002). Estimation of the hydrophobic fraction of dissolved organic matter in water samples using UV photometry. *Water Research* **36**, 5037-5044.
- Dittmar, T., Hertkorn, N., Kattner, G., Lara, R. J. (2006). Mangroves, a major source of dissolved organic carbon to the oceans. *Global Biogeochemical Cycles* **20**, GB1012. 7 p.
- Dittmar, T., Koch, B., Hertkorn, N., Kattner, G. (2008). A simple and efficient method for the solid-phase extraction of dissolved organic matter (SPE-DOM) from seawater. *Limnology and Oceanography: Methods* **6**, 230-235.
- Dittmar, T., Paeng, J. (2009). A heat-induced molecular signature in marine dissolved organic matter. *Nature Geoscience* **2**, 175-179.
- Durham, B. P., Sharma, S., Luo, H., Smith, C. B., Amin, S. A., Bender, S. J., Dearth, S. P., Van Mooy, B. A. S., Campagna, S. R., Kujawinski, E. B., Armbrust, E. V., Moran, M. A. (2015). Cryptic carbon and sulfur cycling between surface ocean plankton. *Proceedings of the National Academy of Sciences* **112**, 453-457.
- Dvorak, P., Casamatta, D.A., Poulickova, A., Hasler, P., Ondrej, V., Sanges, R. (2014). *Synechococcus*: 3 billion years of global dominance. *Molecular Ecology* **23**, 5538-5551.
- Engel, A., Thoms, S., Riebesell, U., Rochelle-Newall, E., Zondervan, I. (2004). Polysaccharide aggregation as a potential sink of marine dissolved organic carbon. *Letters to Nature* **428**, 929-932.
- Fatayer, S., Coppola, A. I., Schulz, F., Walker, B. D., Broek, T. A., Meyer, G., Druffel, E. R. M., McCarthy, M., Gross, L. (2018). Direct Visualization of Individual Aromatic Compound

- Structures in Low Molecular Weight Marine Dissolved Organic Carbon. *Geophysical Research Letters* **45**, 5590-5598.
- Flerus, R., Koch, B. P., Schmitt-Kopplin, P., Witt, M., Kattner, G. (2011). Molecular level investigation of reactions between dissolved organic matter and extraction solvents using FT-ICR MS. *Marine Chemistry* **124**, 100-107.
- Flombaum, P., Gallegos, J. L., Gordillo, R. A., Rincon, J., Zabala, L. L., Jiao, N., Karl, D. M., Li, W. K. W., Lomas, M. W., Veneziano, D., Vera, C. S., Vrugt, J. A., Martiny, A. C. (2013). Present and future global distributions of the marine Cyanobacteria *Prochlorococcus* and *Synechococcus*. *Proceedings of the National Academy of Sciences* **24**, 9824-9829.
- Fournier, G.P., Moore, K.R., Rangel, L.T., Payette, J.G., Momper, L., Bosak, T. (2021). The Archean origin of oxygenic photosynthesis and extant cyanobacterial lineages. *Proceedings of the Royal Society B* **288**, 20210675. <https://doi.org/10.1098/rspb.2021.0675>
- Fry, B., Hopkinson Jr, C. S., Nolin, A., Wainwright, S. C. (1998).  $^{13}\text{C}/^{12}\text{C}$  composition of marine dissolved organic carbon. *Chemical Geology* **152**, 113-118.
- Gantt, E. (1980). Structure and function of phycobilisomes: light harvesting pigment complexes in red and blue-green algae. *International Review of Cytology* **66**, 45-80.
- Garcia-Pichel, F., Lombard, J., Soule, T., Dunaj, S., Wu, S.H., Wojciechowski, M.F. (2019). Timing the evolutionary advent of cyanobacteria and the later Great Oxidation Event using gene phylogenies of a sunscreen. *mBio* **10**, e00561-19.
- Green, N. W., Perdue, E. M., Aiken, G. R., Butler, K. D., Chen, H., Dittmar, T. (2014). An intercomparison of three methods for large-scale isolating of oceanic dissolved organic matter. *Marine Chemistry* **161**, 14-19.

- Hansell, D. A., Carlson, C. A. (2001). Marine Dissolved Organic Matter and the Carbon Cycle. *Oceanography* **14**, 41-49.
- Hansell, D. A. (2013). Recalcitrant dissolved organic carbon fractions. *Annual Review of Marine Sciences* **5**, 421-445.
- Hedges, J. I., Keil, R. G., Benner, R. (1997). What happens to terrestrial organic matter in the ocean? *Organic Geochemistry* **27**, 195-212.
- Hedges, J.I., Eglinton, G., Hatcher, P.G, Kirchman, D.L., Arnosti, C., Derenne, S., Evershed, R.P., Kogel-Knabner, I., de Leeuw, J.W., Littke, R., Michaelis, W., Rullkotter, J. (2000). The molecularly-uncharacterized component of nonliving organic matter in natural environments. *Organic Geochemistry* **31**, 945-958.
- Herbelin, A.L., Westall, J.C. (1999). FITEQL: a Computer Program for Determination of Equilibrium Constants from Experimental Data. Department of Chemistry, Oregon State University. Corvallis, OR. *Report 99-01*.
- Hertkorn, N., Benner, R., Frommberger, M., Schmitt-Kopplin, P., Witt, M., Kaiser, K., Kettrup, A., Hedges, J. I. (2006). Characterization of a major refractory component of marine dissolved organic matter. *Geochimica et Cosmochimica Acta* **70**, 2990-3010.
- Jaffe, R., Ding, Y., Niggemann, J., Vahatalo, A.V., Stubbins, A., Spencer, R.G.M., Campbell, J., Dittmar, T. (2013). Global charcoal mobilization from soils via dissolution and riverine transport to the oceans. *Science* **340**, 345-347.
- Jiao, N., Herndl, G. J., Hansell, D. A., Benner, R., Kattner, G., Wilhelm, S. W., Kirchman, D. L., Weinbauer, M. G., Luo, T., Chen, F., Azam, F. (2010). Microbial production of recalcitrant dissolved organic matter: long-term carbon storage in the global ocean. *Nature Reviews Microbiology* **8**, 593-599.

- Jiao, N., Robinson, C., Azam, F., Thomas, H., Baltar, F., Dang, H., Hardman-Mountford, N. J., Johnson, M., Kirchman, D. L., Koch, B. P., Legendre, L., Li, C., Liu, J., Luo, T., Luo, Y. W., Mitra, A., Romanou, A., Tang, K., Wang, X., Zhang, C., Zhang, R. (2014). Mechanisms of microbial carbon sequestration in the ocean – future research directions. *Biogeosciences* **11**, 5285-5306.
- Jiao, N., Cai, R., Zheng, Q., Tang, K., Liu, J., Jiao, F., Wallace, D., Chen, F., Li, C., Amann, R., Benner, R., Azam, F. (2018). Unveiling the enigma of refractory carbon in the ocean. *National Science Review* **5**, 459-463.
- Jorgensen, L., Stedmon, C.A., Granskog, M.A., Middelboe, M. (2014). Tracing the long-term microbial production of recalcitrant fluorescent dissolved organic matter in seawater. *Geophysical Research Letters* **41**, 2481-2488.
- Kenrick, P., Crane, P. R. (1997). The origin and early evolution of plants on land. *Nature* **389**, 33-39.
- Koch, B. P., Witt, M., Engbrodt, R., Dittmar, T., Kattner, G. (2005). Molecular formulae of marine and terrigenous dissolved organic matter detected by electrospray ionization Fourier transform ion cyclotron resonance mass spectrometry. *Geochimica et Cosmochimica Acta* **69**, 3299-3308.
- Koch, B.P., Dittmar, T., Witt, M., Kattner, G. (2007). Fundamentals of molecular formula assignment to ultrahigh resolution mass data of natural organic matter. *Analytical Chemistry* **79**, 1758-1763.
- Koch, B.P., Kattner, G., Witt, M., Passow, U. (2014). Molecular insights into the microbial formation of marine dissolved organic matter: recalcitrant or labile? *Biogeosciences* **11**, 4173-4190.

- Konhauser, K.O., Pecoits, E., Lalonde, S.V., Papineau, D., Nisbet, E.G., Barley, M.E., Arndt, N.T., Zahnle, K., Kamber, B.S. (2009). Oceanic nickel depletion and a methanogen famine before the Great Oxidation Event. *Nature* **458**, 750-753.
- Konhauser, K.O., Lalonde, S.V., Planavsky, N.J., Pecoits, E., Lyons, T.W., Mojzsis, S.J., Rouxel, O. J., Barley, M.E., Rostere, C., Fralick, P.W., Kump, L.R., Bekker, A. (2011). Aerobic bacterial pyrite oxidation and acid rock drainage during the Great Oxidation Event. *Nature* **478**, 369-373.
- Kvenvolden, K.A., Lorenson, T.D., Reeburgh, W.S. (2001). Attention turs to naturally occurring methane seepage. *EOS* **82**, 457-458.
- Lang, S.Q., Butterfield, D.A., Lilley, M.D., Johnson, H.P., Hedges, J.I. (2006). Dissolved organic carbon in ridge-axis and ridge-flank hydrothermal systems. *Geochimica et Cosmochimica Acta* **70**, 3830-3842.
- Lechtenfeld, O. J., Kattner, G., Flerus, R., McCallister, S. L., Schmitt-Kopplin, P., Koch, B. P. (2014). Molecular transformation and degradation of refractory dissolved organic matter in the Atlantic and Southern Ocean. *Geochemica et Cosmochimica Acta* **126**, 321-337.
- Leefman, T., Frickenhaus, S., Koch, B. P. (2019). UltraMassExplorer: a browser-based application for the evaluation of high-resolution mass spectrometric data. *Rapid Communications in Mass Spectrometry* **33**, 193-202.
- Li, Y., Harir, M., Uhl, J., Kanawati, B., Lucio, M., Smirnov, K. S., Koch, B. P., Schmitt-Kopplin, P., Hertkorn, N. (2017). How representative are dissolved organic matter (DOM) extracts? A comprehensive study of sorbent selectivity for DOM isolation. *Water Research* **116**, 316-323.

- Li, Y., Sutherland, B.R., Gingras, M.K., Owttrim, G.W., Konhauser, K.O. (2021). A novel approach to investigate the deposition of (bio) chemical sediments: The sedimentation velocity of cyanobacteria-ferrihydrite aggregates. *Journal of Sedimentary Research* **91**, 390-398.
- Lin, Y.-S., Koch, B.P., Feseker, T., Ziervogel, K., Goldhammer, T., Schmidt, F., Witt, M., Kellermann, M.Y., Zabel, M., Teske, A., Hinrichs, K.-U. (2017). Near-surface heating of young rift sediment causes mass production and discharge of reactive dissolved organic matter. *Scientific Reports* **7**, 44864.
- Linkhorst, L., Dittmar, T., Waska, H. (2017). Molecular fractionation of dissolved organic matter in a shallow subterranean estuary: the role of the iron curtain. *Environmental Science and Technology* **51**, 1312-1320.
- Liu, Y., Alessi, D.S., Owttrim, G.W., Petrash, D.A., Mloszewska, A.M., Lalonde, S.V., Martinez, R.E., Zhou, Q., Konhauser, K.O. (2015). Cell surface reactivity of *Synechococcus* sp. PCC 7002: Implications for metal sorption from seawater. *Geochimica et Cosmochimica Acta*, **169**, 30-44.
- Lonborg, C., Alvarez-Salgado, X.A., Letscher, R.T., Hansell, D.A. (2018). Large stimulation of recalcitrant dissolved organic carbon degradation by increasing ocean temperatures. *Frontiers in Marine Science* **4**, 436.
- Ma, X., Coleman, M. L., Waldbauer, J. R. (2018). Distinct molecular signatures in dissolved organic matter produced by viral lysis of marine cyanobacteria. *Environmental Microbiology* **20**, 3001-3011.
- Mand, K., Lalonde, S.V., Robbins, L.J., Thoby, M., Paiste, K., Kreitsmann, T., Paiste, P., Reinhard, C.T., Romashkin, A.E., Planavsky, N.J., Kirsimae, K., Lepland, A., Konhauser, K.O. (2020).

- Palaeoproterozoic oxygenated oceans following the Lomagundi-Jatuli Event. *Nature Geoscience* **13**, 302-306.
- Martin, J. H., Knauer, G. A., Karl, D. M., Broenkow, W. W. (1987). VERTEX: carbon cycling in the northeast Pacific. *Deep-Sea Research* **34**, 267-285.
- Moran, M. A., Kujawinski, E. B., Stubbins, A., Fatland, R., Aluwihare, L. I., Buchan, A., Crump, B. C., Dorrestein, P. C., Dyhrman, S. T., Hess, N. J., Howe, B., Longnecker, K., Medeiros, P. M., Niggemann, J., Obernosterer, I., Repeta, D. J., Waldbauer, J. R. (2016). Deciphering ocean carbon in a changing world. *Proceedings of the National Academy of Sciences* **113**, 3143-3151.
- Niu, X.-Z., Harir, M., Schmitt-Kopplin, P., Croue, J.-P. (2018). Characterisation of dissolved organic matter using Fourier-transform ion cyclotron resonance mass spectrometry: Type-specific unique signatures and implications for reactivity. *Science of the Total Environment* **644**, 68-76.
- Opsahl, S., Benner, R. (1997). Distribution and cycling of terrigenous dissolved organic matter in the ocean. *Nature* **386**, 480-482.
- Owtrim, G.W. (2012). RNA Helicases in Cyanobacteria: Biochemical and Molecular Approaches. *Methods in Enzymology* **511**, 385-403.
- Planavsky, N.J., Rouxel, O.J., Bekker, A., Lalonde, S.V., Konhauser, K.O., Reinhard, C.T., Lyons, T.W. (2010). The evolution of the marine phosphate reservoir. *Nature Letters* **467**, 1088-1090.
- Pohlman, J.W., Bauer, J.E., Waite, W.F., Osburn, C.L., Chapman, N.R. (2010). Methane hydrate-bearing seeps as a source of aged dissolved organic carbon to the oceans. *Nature Geoscience* **4**, 37-41.

- Rakhimberdieva, M.G., Vavilin, D.V., Vermaas, W.F.J., Elanskaya, I.V., Karapetyan, N.V. (2007). Phycobilin/chlorophyll excitation equilibration upon carotenoid-induced non-photochemical fluorescence quenching in phycobilisomes of the cyanobacterium *Synechocystis* sp. PCC 6803. *Biochimica et Biophysica Acta – Bioenergetics* **1767**, 757-765.
- Ridgwell, A., Arndt, S. (2015). Chapter 1: Why Dissolved Organics Matter: DOC in Ancient Oceans and Past Climate Change. In: Hansell, D. A., Carlson, C. A. *Biogeochemistry of Marine Dissolved Organic Matter*. Elsevier, Cambridge, Massachusetts, pp. 1-20.
- Rippka, R., Deruelles, J., Waterbury, J.B., Herdman, M., Stainer, R.Y. (1979). Generic assignments, strain histories and properties of pure cultures of cyanobacteria. *Journal of General Microbiology* **111**, 1-61.
- Sanchez-Baracaldo, P., Bianchini, G., Wilson, J.D., Knoll, A.H. (2021 in press). Cyanobacteria and biogeochemical cycles through Earth history. *Trends in Microbiology*.  
<https://doi.org/10.1016/j.tim.2021.05.008>
- Schmidt, F., Elvert, M., Koch, B.P., Witt, M., Hinrichs, K., U. (2009). Molecular characterization of dissolved organic matter in pore water of continental shelf sediments. *Geochimica et Cosmochimica Acta* **73**, 3337-3358.
- Shank, G.C., Lee, R., Vahatalo, A., Zepp, R.G., Bartels, E. (2010). Production of chromophoric dissolved organic matter from mangrove leaf litter and floating *Sargassum* colonies. *Marine Chemistry* **119**, 172-181.
- Sleighter, R. L., Hatcher, P. G. (2008). Molecular characterization of dissolved organic matter (DOM) along a river to ocean transect of the lower Chesapeake Bay by ultrahigh resolution electrospray ionization Fourier transform ion cyclotron resonance mass spectrometry. *Marine Chemistry* **110**, 140-152.

- Stedmon, C.A., Markager, S., Bro, R. (2003). Tracing dissolved organic matter in aquatic environments using a new approach to fluorescence spectroscopy. *Marine Chemistry* **82**, 239-254.
- Stedmon, C. A., Nelson, N. B. (2015). Chapter 10: The Optical Properties of DOM in the Ocean. In: Hansell, D. A., Carlson, C. A. *Biogeochemistry of Marine Dissolved Organic Matter*. Elsevier, Cambridge, Massachusetts, pp. 481-508.
- Strom, S. L., Benner, R., Ziegler, S., Dagg, M. J. (1997). Planktonic grazers are a potentially important source of marine dissolved organic carbon. *Limnology and Oceanography* **42**, 1364-1474.
- Suttle, C. (2007). Marine viruses – major players in the global ecosystem. *Nature Reviews Microbiology* **5**, 801-812.
- Swaren, L., Alessi, D.S., Owttrim, G.W., Konhauser, K.O. (2021). Acid-base properties of *Synechococcus*-derived organic matter. *Geochimica et Cosmochimica Acta* **315**, 89-100.  
<https://doi.org/10.1016/j.gca.2021.10.003>
- Swarzenski, P.W., Orem, W.H., McPherson, B.F., Baskaran, M., Wan, Y. (2006). Biogeochemical transport in the Loxahatchee River estuary, Florida: The role of submarine groundwater discharge. *Marine Chemistry* **101**, 248-265.
- Van Mooy, B.A.S., Rocap, G., Fredricks, H.F., Evans, C.T., Devol, A.H. (2006). Sulfolipids dramatically decrease phosphorus demand by picocyanobacteria in oligotrophic marine environments. *Proceedings of the National Academy of Sciences* **103**, 8607-8612.
- Walker, B. D., Primeau, F. W., Beaupre, S. R., Guilderson, T. P., Druffel, E. R. M., McCarthy, M. D. (2016). Linked changes in marine dissolved organic carbon molecular size and radiocarbon age. *Geophysical Research Letters* **43**, 385-393.

- Walsh, M.J., Ahner, B.A. (2013). Determination of stability constants of Cu(I), Cd(II), and Zn(II) complexes with thiols using fluorescent probes. *Journal of Inorganic Biochemistry* **128**, 112-123.
- Wang, K., Wommack, K. E., Chen, F. (2011). Abundance and Distribution of *Synechococcus* spp. And Cyanophages in the Chesapeake Bay. *Applied and Environmental Microbiology* **77**, 7459-7468.
- Warke, M.R., Di Rocco, T., Zerkle, A. L., Lepland, A., Prave, A.R., Martin, A.P., Ueno, Y., Condon, D.J., Claire, M.W. (2020). The Great Oxidation Event preceded a Paleoproterozoic “snowball Earth”. *PNAS* **117**, 13314-13320.
- Woods, G. C., Simpson, M. J., Koerner, P. J., Napoli, A., Simpson, A. J. (2011). HILIC-NMR; Toward the Identification of Individual Molecular Components in Dissolved Organic Matter. *Environmental Science and Technology* **45**, 3880-3886.
- Yu, Q., Fein, J.B. (2015). The effect of metal loading on Cd adsorption onto *Shewanella oneidensis* bacterial cell envelopes: The role of sulfhydryl sites. *Geochimica et Cosmochimica Acta* **167**, 1-10.
- Zark, M., Christoffers, J., Dittmar, T. (2017). Molecular properties of deep-sea dissolved organic matter are predictable by the central limit theorem: Evidence from tandem FT-ICR-MS. *Marine Chemistry* **191**, 9-15.
- Zark, M., Dittmar, T. (2018). Universal molecular structures in natural dissolved organic matter. *Nature Communications* **9**, 3178.
- Zhang, J., Kattner, G., Koch, B.P. (2019). Interactions of trace elements and organic ligands in seawater and implications for quantifying biogeochemical dynamics: A review. *Earth-Science Reviews* **192**, 631-649.

- Zhao, Z., Gonsoir, M., Luek, J., Timko, S., Ianiri, H., Hertkorn, N., Schmitt-Kopplin, P., Fang, X., Zeng, Q., Jiao, N., Chen, F. (2017). Picocyanobacteria and deep-ocean fluorescent dissolved organic matter share similar optical properties. *Nature Communications* **8**, 15284. 10 p.
- Zhao, Z., Gonsoir, M., Schmitt-Kopplin, P., Zhan, Y., Zhang, R., Jiao, N., Chen, F. (2019). Microbial transformation of visur-induced dissolved organic matter from picocyanobacteria: coupling of bacterial diversity and DOM chemodiversity. *The ISME Journal* **13**, 2551-2565.
- Zheng, Q., Chen, Q., Cai, R., He, C., Guo, W., Wang, Y., Shi, Q., Chen, C., Jiao, N. (2019). Molecular characteristics of microbially mediated transformations of *Synechococcus*-derived dissolved organic matter as revealed by incubation experiments. *Environmental Microbiology*, **21**, 2533-2543.

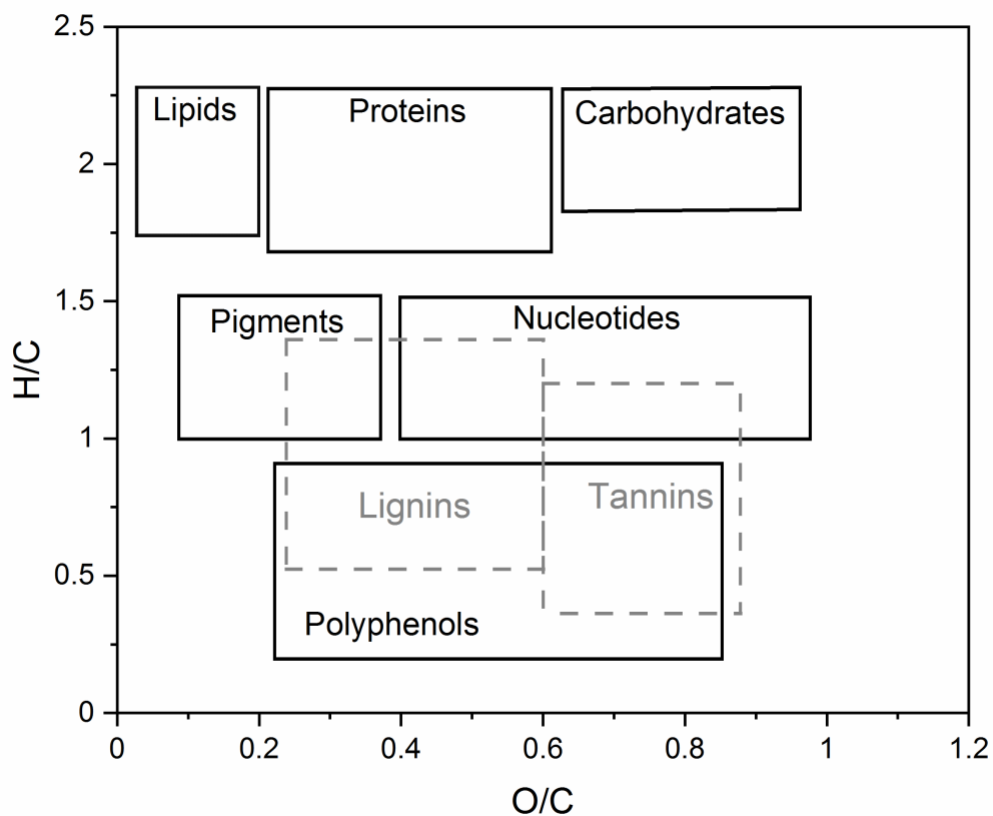


**Figure 4.1:** Generalized Van Krevelen diagram with boxes corresponding to common organic compound classes (Adapted from Sleighter & Hatcher, 2008; Ma et al. 2018; Niu et al. 2018). Compounds associated with terrestrial origin are outlined in grey dashed lines. The plots are presented for reference and do not necessarily imply the presence of the indicated compounds.

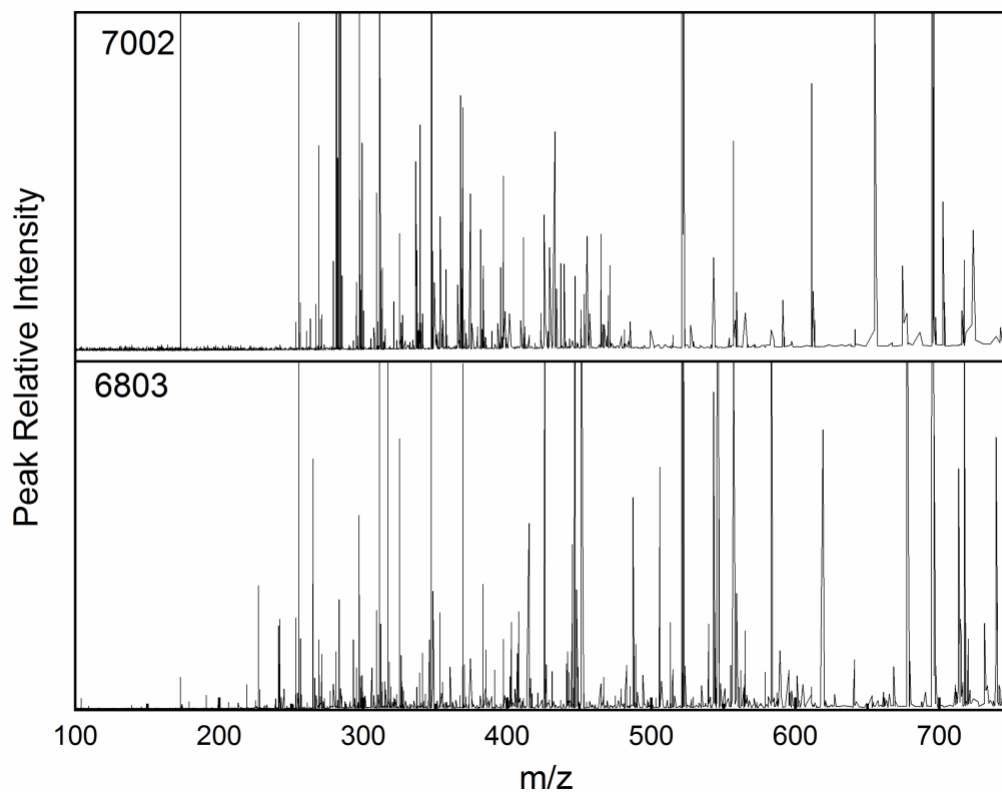


**Figure 4.2:** Negative ESI Fourier Transform Ion Cyclotron Resonance (FTICR) Mass Spectra (MS) of intracellular *Synechococcus* sp. PCC 7002 dissolved organic matter (7002) and intracellular *Synechocystis* sp, PCC 6803 dissolved organic matter (6803) mixed 1:1 (v:v) with methanol (MeOH).

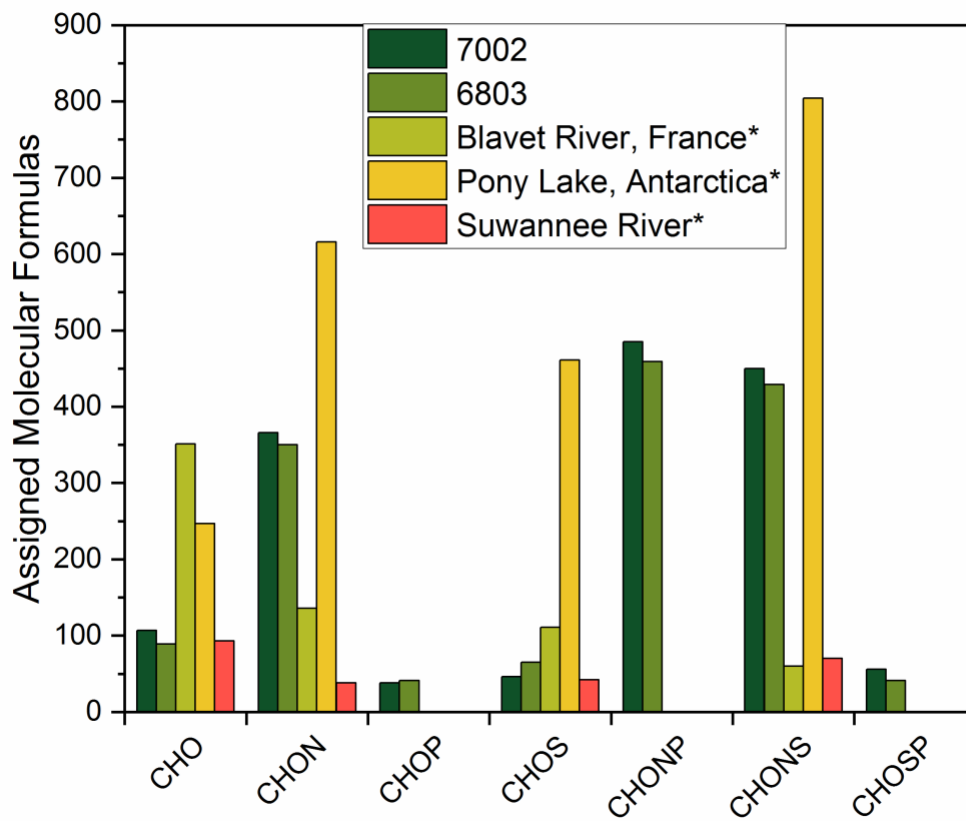


**Figure 4.3:** Distribution of molecular formulas assigned for *Synechococcus* sp. PCC 7002 DOM (7002) and *Synechocystis* sp. PCC 6803 DOM (6803).

\*Blavet River, France; Suwannee River, Georgia, US; and Pony Lake, Antarctica CHO, CHOS, CHON, and CHONS distribution from Niu et al. (2018).

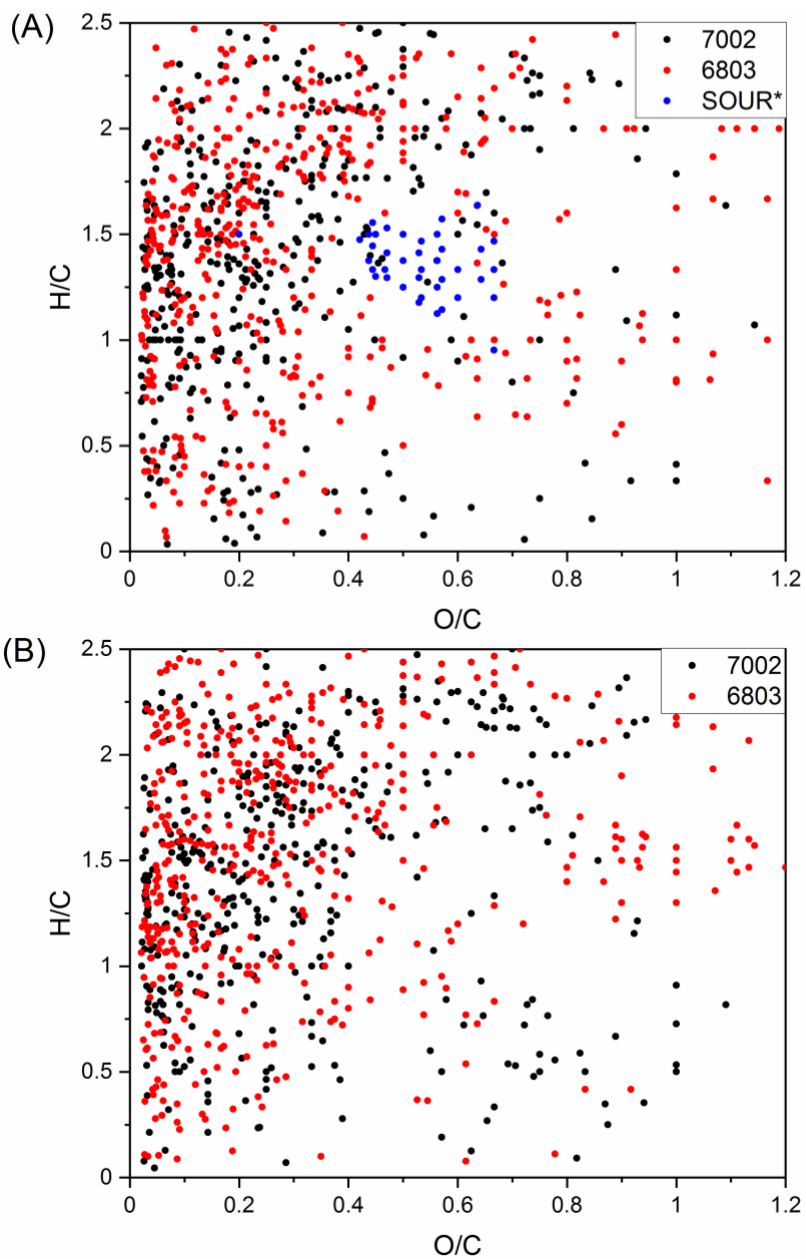


**Figure 4.4:** Distribution of (A) S-containing molecules (CHOS and CHONS) and (B) P-containing molecules (CHOP and CHONP) for *Synechococcus* sp. PCC 7002 DOM (7002) and *Synechocystis* sp. PCC 6803 DOM (6803) plotted on a van Krevelen diagram.

\*S-containing Southern Ocean Ultra-Refractory (SOUR) molecules (Lechtenfeld et al. 2014).

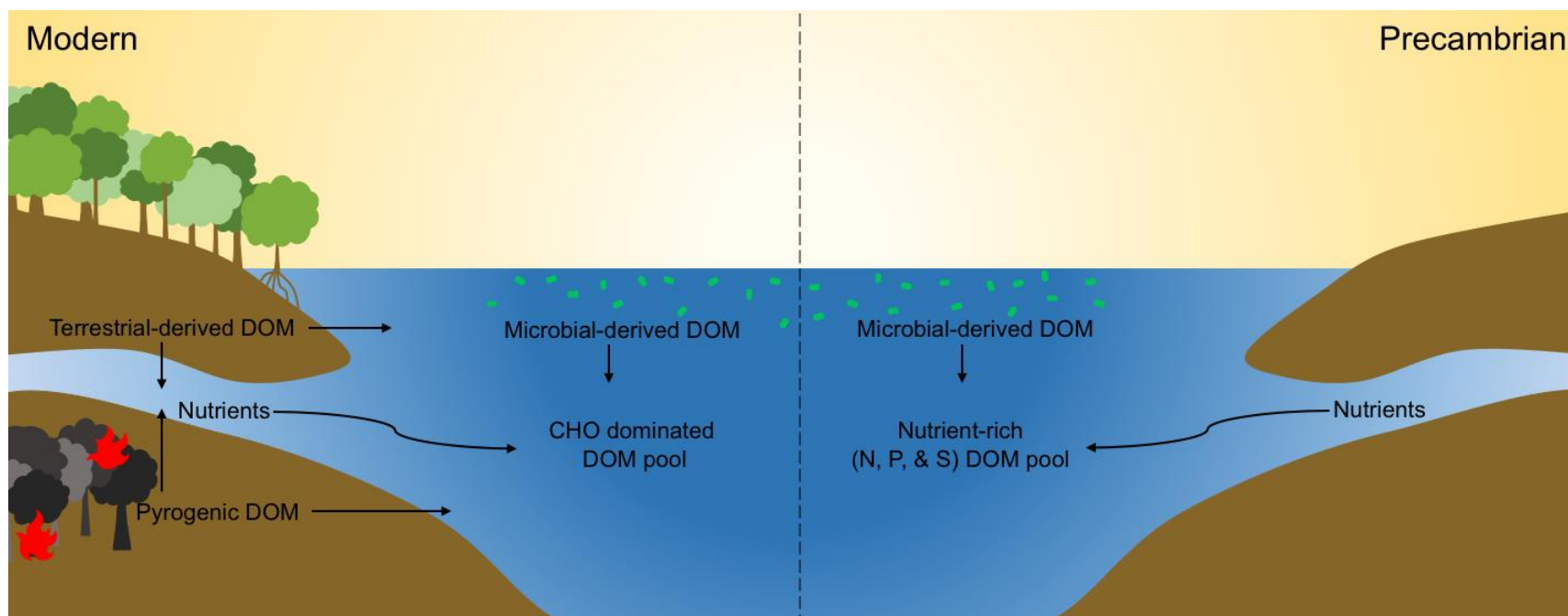


**Figure 4.5:** Schematic diagram comparing the major naturally occurring inputs of DOM in modern versus Precambrian oceans.

## Chapter 5: Conclusions

Trace element signatures are preserved in organic rich sediments such as black shales and biogenic rocks such as banded iron formations (BIF), leading past researchers to speculate that phytoplankton played a role in trace metals sequestration to the rock record (Playter et al. 2017; Konhauser et al. 2018; Bishop et al. 2019). These previous investigations identified three plausible routes for trace element signatures in the rock record. First, trace elements could adsorb to detrital clay minerals transported to the marine realm via terrestrial weathering and aeolian deposition (Hao et al. 2019 and 2020). Secondly, through incorporation with sulfide minerals such as pyrite under reducing conditions following organic matter degradation in marine sediment. Lastly, trace element signatures could be derived from organic matter and the ancient marine biosphere, including cyanobacteria and their derivatives, the focus of this thesis.

The work conducted in this thesis provides fundamental information about the surface chemistry of cyanobacterial cells at varying pH and ionic strengths (IS). Chapter 2 investigated the surface reactivity and cadmium binding capacity of the common euryhaline cyanobacterium *Synechocystis* sp. PCC 6803 at both freshwater and marine IS and across a range of environmentally relevant pH values (3-9). From this thorough investigation, I confirmed that the surface charge, identified through zeta potential, is indeed less negative at higher IS. This finding correlated well with the cation ( $\text{Cd}^{2+}$ ) binding capacity, where the higher IS led to lower amounts of Cd sorption. Both freshwater and marine IS demonstrate increasing Cd sorption with increasing pH due to the deprotonation of surface functional groups. From these results, we can hypothesize that cyanobacteria migrating from freshwater settings to marine settings, such as transport from rivers to estuaries, will result in cation transport and subsequent release in the higher IS and higher pH marine environment.

Decades of investigations into the acid-base properties of dissolved organic matter overlooked the important connection between the source of the organic matter and pKa characteristics. The research in Chapter 3 determined the acid-base properties of cyanobacterial-derived dissolved in comparison to modern environmental samples, where cyanobacterial DOM demonstrates distinct pKa values compared to terrestrial-derived DOM. Moreover, the surface reactivity studies of Chapter 3 found that cyanobacterial-derived particulate matter (cyPOM) is relatively unimportant in the transport of trace elements from surface waters to marine sediments. This is due to the much higher affinity of trace elements (Cd, Co, Cu, Ni, and Zn investigated here) to the dissolved portion (cyDOM).

The compositional characteristics of dissolved organic matter (DOM) derived solely from cyanobacteria was investigated through Fourier transform ion cyclotron resonance (FTICR) mass spectrometry for ultrahigh resolution molecular data. Chapter 4 built on the findings of Chapter 3, providing detailed insights on the molecular differences between cyDOM and terrestrial-derived DOM. As in previous studies, the molecular composition of cyDOM had far higher concentrations of nutrients (N, P, and S) in comparison to the simpler CHO-dominated terrestrial pool.

The discoveries of this research have laid the foundation for two separate lines of ongoing work. The first, is a collaboration with Drs. Rene Boiteau and Christian Dewey at Oregon State University. The cyDOM investigated in Chapters 3 and 4 has been shipped to our collaborators and is under further investigation via ultrahigh resolution mass spectrometry (i.e., FTICR-MS and liquid chromatography (LC) mass spectrometry). The purpose of this continuation of research is to identify the specific metal binding ligands that come to light when the cyDOM is spiked with trace amounts of Ni and Cu. This work is being carried out in collaboration with Drs. Boiteau and

Dewey due to their experience in identifying metal-binding ligands in modern seawater samples (Boiteau et al. 2016).

The second work that is in the pipeline following the research outlined in this dissertation is the predictive modelling of ancient oceans under varying redox conditions. Through Earth's history, the atmosphere and oceans have undergone drastic changes in redox states which have an influence on trace metal speciation (Anbar and Knoll, 2002; Saito et al. 2003). What I preliminarily propose in Section 5.1 is the influence of metal-binding ligands identified in the modern oceans on Ni and Cu speciation through Earth's history.

### **5.1. Predictive ligand modelling**

The generalization of Earth's ancient oceans as being anoxic versus oxic ignores the fact that in the modern oceans, bioactive trace elements are complexed by organic compounds (e.g., Vraspir and Butler, 2009). For biologically critical metals in ocean surface waters, such as Cu, >99% is complexed by organic ligands (e.g., Bruland and Lohan, 2003; Moffett and Dupont, 2007), while Ni is complexed to a lesser extent, 30-50% in marine settings (Boiteau et al. 2016) and up to 99% in freshwater (Glass and Dupont, 2017).

Preliminary geochemical modelling was performed to assess the speciation and distribution of Cu and Ni in the presence of cyanobacterial-derived DOM over a realistic pH range. Speciation modeling was performed using SpecE8 in Geochemist's Workbench (Community Edition 2020), using a modified version of the thermo\_minteq database which includes both Ni and Cu chloride, hydroxide, carbonate, and sulfide aqueous complexes. For models which included ligand speciation, the database was modified to incorporate ligand specific values as presented in Table 5.1 from an average of the extensive literature compilation in Appendix 4 SI Table 1. Model

scenarios were conducted at 25°C with 0.56 M NaCl, standard ionic strength used extensively in our lab that approximates the contribution of Na and Cl ions in seawater.

The CO<sub>2</sub>, reduced Fe<sup>2+</sup>, and HS<sup>-</sup> concentrations represent model scenarios for their respective timeframes, rasterizing these parameters should be the focus of future studies. For this investigation, I have limited CO<sub>2</sub> to 20x the modern value at -2.2 log atm for all scenarios besides the modern (-3.5 log atm). Reduced Fe is set at 50 uM for both ferruginous and the brief post-GOE models. Sulfur concentrations ranged from low, 5 uM immediately following the GOE, to high, 400 uM for intermittently euxinic environments.

Modern Ni and Cu speciation follow trends observed in modern marine environments and act as a ground truth for the ligand values (Figures 5.1 and 5.2). Nickel speciation is nearly 50% free Ni<sup>2+</sup> and 50% organically complexed with a single, high affinity ligand (Figure 5.1). Whereas Cu speciation is dominated almost 50:50 by both a low concentration, high affinity ligand (L2) and a high concentration, low affinity ligand (L1) resulting in >99% organically complexed. This trend of ligand-dominated speciation can be observed in all models containing the metal-binding ligands found in modern oceans (Figures 5.1-5.8). This starkly contrasts the free ion (e.g., Ni<sup>2+</sup>), chloride, sulfide, or carbonate dominated speciation observed in solely abiotic models (Figures 5.1-5.8). Nickel presents a unique speciation throughout time because the speciation is dependent on the concentration of the high affinity Ni-binding ligand (Figure 5.9), whereas the remainder Ni in solution is determined by environmental conditions (e.g., NiHS<sup>+</sup> during periods of euxinia). This ligand masking effect is most demonstrated throughout every geochemical environment modelled for Cu (Figure 5.10).

## **5.2. Future research directions**

Trace metal deposition through Earth's history is controlled by environmental events such as anoxia, euxinia, and increased sedimentation rates (Playter et al. 2017). Those authors investigated the preservation potential of *Synechococcus* sp. PCC 7002 in the presence of the clay minerals kaolinite and montmorillonite. Through SEM imaging, they found that clay minerals encrusted cyanobacterial cells, leading them to hypothesize that the aggregation of cells by clay minerals was a way for organic matter to contribute to marine sediments by inhibiting its remineralization at depth. This leads me to suggest the following future research directions with respect to clay mineral and cyanobacterial cell interactions:

- i) Associations between clay minerals and cyanobacterial cells can be studied experimentally in laboratory setting (e.g., one type of cell and one type of clay), but it is unclear if encrustation of cells by clay minerals occurs in real-world settings such as deltas and estuaries. Therefore, I suggest that more sampling needs to be conducted in estuaries and deltas to assess the relative magnitude of clay-cyanobacterial interactions. Furthermore, it is unknown if these associations are observed at ocean depths beyond the continental shelf. Deep ocean sampling via submersibles could provide sample collection and insight on the particulates that settle in the deep ocean.
- ii) To what degree does encrustation and/or aggregation between cells and clay minerals influence the surface reactivity of the aggregate? Hao et al. (in review) investigated the acid-base and Cd reactivity of *Synechococcus* and *Synechocystis* in the presence of clay minerals (kaolinite, illite, and montmorillonite). Based on preliminary findings, the Cd-binding capacity of the cell-clay aggregates demonstrates a site-blocking effect, rather than an additive effect. This preliminary work needs to be followed up on by a more

thorough investigation of these binary systems using spectroscopic techniques to identify which sorbent is doing the binding.

Recent studies on the metal binding of bacterial cells and EPS have begun to identify the importance of sulfhydryl sites (Yu and Fein, 2016; Nell and Fein, 2017; Yu and Fein, 2017; Yu et al. 2018). Using ultrahigh resolution mass spectrometry a few researchers have now identified unique metal complexing molecules found in nature (e.g., Boiteau et al. 2016; Chen et al. 2017). Boiteau et al. (2016) isolated marine DOM from the Eastern Pacific Ocean, identifying two and three molecules responsible for the chelating of Ni and Cu, respectively. Chen et al. (2017) conducted FTICR-MS analysis on isolated DOM from a creek in Oak Ridge, Tennessee and Suwanee River natural organic matter to identify Hg-complexing molecules. Interestingly, of all the metal chelating molecules identified from natural organic matter, reduced sulfur ligands are common among metal binding sites (Boiteau et al. 2016; Chen et al. 2017). Mercury's strong affinity for sulfur containing thiol ligands is well documented (e.g., Skyllberg and Drott, 2010; Gu et al. 2011) and now confirmed by recent FTICR-MS analysis. This differs from functional group reactivity made at high metal:cell ratios where high abundance, low affinity sites, such as carboxyl, dominate metal binding (Fein et al. 1997). Studies investigating high metal concentration (e.g., >1 ppm) identified an abundance of carboxyl groups and a general three-site trend - carboxyl, hydroxyl, and phosphoryl. Moving forward, with higher resolution techniques available, there needs to be more consideration given to the sorbate:sorbent ratios with the new findings about low concentration, high affinity sites (e.g., sulfhydryl) (Yu and Fein, 2016 and 2017; Yu et al. 2018).

- iii) Although there is a plethora of surface functional group and associated pKa values published in literature, future studies should aim to understand the proton and metal binding behavior, as well as identity. Furthermore, investigations on ligand reactivity

should include mass spectrometry data, such as FTICR-MS or liquid chromatography (LC-MS), to better understand the composition of the ligands in question.

The trace metals, the focus of this thesis, are considered bioessential as they are required by living organisms in small amounts and present in nature at trace amounts (typically pM to nM concentrations). This leads to their depletion in surface waters where there is considerable biological activity and concurrent release at depths, resulting in a “nutrient-like” depth profile (illustrated in Figure 1.1).

- iv) Future investigations should focus on those trace elements that do not display nutrient-like depth profiles, such as molybdenum. For instance, Mo displays a conservative distribution in modern oceans even though it is a critical enzyme in a variety of biological pathways. In the presence of reduced sulfur, Mo is effectively removed, which would have geochemical implications for Proterozoic oceans with sulfidic seawater.
- v) Additionally, elements that are redox-sensitive, such as chromium and uranium could prove interesting to investigate under varying conditions as their isotope abundances have been linked to variations in atmospheric oxygenation. Laboratory studies should be conducted to investigate the partitioning of these redox-sensitive elements onto cyanobacterial cell surfaces versus DOM.

Life began on Earth approximately 3.5 billion years ago. This research utilized the modern, evolutionarily successful cyanobacteria, *Synechococcus*, whose lineage has been traced back over 3 billion years (Flombaum et al. 2013; Dvorak et al. 2014). Although *Synechococcus* is one of the main primary producers in modern oceans and dates back 3 billion years, there are alternative

photoferrotrophs that have been suggested to be responsible for BIF precipitation (Konhauser et al. 2002).

- vi) Future investigations utilizing ultrahigh resolution mass spectrometry approaches should investigate anoxygenic photosynthetic bacteria (photoferrotrophs), including both marine species (*Rhodovulum iodense*, *Rhodovulum robiginosum*) and freshwater species (*Rhodobacter ferrooxidans*, *Rhodomicrobium vannielii*, *Chlorobium ferrooxidans*, *Thiodictium* sp.) to determine whether different species demonstrate varying levels of metal binding molecules, or if there are common molecules that transcend species.

## 5.2. References

- Anbar, A.D., Knoll, A.H. (2002). Proterozoic ocean chemistry and evolution: a bioinorganic bridge? *Science*, **297**, 1137-1142.
- Bishop, B.A., Flynn, S.L., Warchola, T.J., Alam, M.D., Robbins, L.J., Liu, Y., Owttrim, G.W., Alessi, D.S., Konhauser, K.O. (2019). Adsorption of biologically critical trace elements to the marine cyanobacterium *Synechococcus* sp. PCC 7002: Implications for marine trace metal cycling. *Chemical Geology*, **525**, 28-36.
- Boiteau, R. M., Till, C. P., Ruacho, A., Bundy, R. M., Hawco, N. J., McKenna, A. M., Barbeau, K. A., Bruland, K. W., Saito, M. A., Repeta, D. J. (2016). Structural Characterization of Natural Nickel and Copper Binding Ligands along the US GEOTRACES Eastern Pacific Zonal Transect. *Frontiers in Marine Science* **3**, 243.
- Bruland, K.W., Lohan M.C. (2003). Controls of trace metals in seawater. *Treatise on Geochemistry* **6**, 23-47.
- Chen, H., Johnston, R. C., Mann, B. F., Chu, R. K., Tolic, N., Parks, J. M., Gu, B. (2017). Identification of Mercury and Dissolved Organic Matter Complexes Using Ultrahigh Resolution Mass Spectrometry. *Environmental Science and Technology Letter* **4**, 59-65.
- Dvorak, P., Casamatta, D.A., Poulickova, A., Hasler, P., Ondrej, V., Sanges, R. (2014). *Synechococcus*: 3 billion years of global dominance. *Molecular Ecology*, **23**, 5538-5551.
- Fein, J.B., Daughney, C.J., Yee, N., Davis, T.A. (1997). A chemical equilibrium model for metal adsorption onto bacterial surfaces. *Geochimica et Cosmochimica Acta* **61**, 3319-3328.
- Flombaum, P., Gallegos, J. L., Gordillo, R. A., Rincon, J., Zabala, L. L., Jiao, N., Karl, D. M., Li, W. K. W., Lomas, M. W., Veneziano, D., Vera, C. S., Vrugt, J. A., Martiny, A. C. (2013)

Present and future global distributions of the marine cyanobacteria *Prochlorococcus* and *Synechococcus*. *PNAS*, **110**, 9824-9829.

Glass, J.B., Dupont, C.L. (2017). *Chapter 2: Oceanic nickel biogeochemistry and the evolution of nickel use*. In: Zamlbe, D., Rowinska-Zyrek, M., Kozlowski, H. The biological chemistry of nickel. *Royal Society of Chemistry*. pp. 12-27.

Gu, B., Bian, Y., Miller, C. L., Dong, W., Jiang, X., Liang, L. (2011). Mercury reduction and complexation by natural organic matter in anoxic environments. *Proceedings of the National Academy of Sciences*, **108**, 1479-1483.

Hao, W., Pudasainee, D., Gupta, R., Kashiwabara, T., Alessi, D.S., Konhauser, K.O. (2019). Effect of acidic conditions on surface properties and metal binding capacity of clay minerals. *ACS Earth and Space Chemistry*, **11**, 2421-2429.

Hao, W., Kashiwabara, T., Jin, R., Takahashi, Y., Gingras, M.K., Alessi, D.S., Konhauser, K.O. (2020). Clay minerals as a source of cadmium to estuaries. *Scientific Reports*, **10**, 1-11.

Hao, W., Swaren, L., Baker, D., Melnyk, S., Li, Y., Liu, Y., Owttrim, G.W., Zeng, H., Gingras, M.K., Alessi, D.S., Konhauser, K.O. (in review – WR65357). The impact of aggregation between clay and planktonic cyanobacteria on trace elemental cycling in estuaries. *Water Research*.

Konhauser, K.O., Hamade, T., Raiswell, R., Morris, R.C., Ferris, F.G., Southam, G., Canfield, D.E. (2002). Could bacteria have formed the Precambrian banded iron formations? *Geology*, **30**, 1079-1082.

Konhauser, K.O., Robbins, L.J., Alessi, D.S., Flynn, S.L., Gingras, M.K., Martinez, R.E., Kappler, A., Swanner, E.D., Li, Y.L., Crowe, S.A., Planavsky, N.J., Reinhard, C.T., Lalonde, S.V.

- (2018). Phytoplankton contributions to the trace-element composition of Precambrian banded iron formations. *GSA Bulletin*, **130**, 941-951.
- Moffett, J. W., Dupont, C. (2007) Cu complexation by organic ligands in the sub-arctic NW Pacific and Bering Sea. *Deep Sea Research Part I: Oceanographic Research Papers* 54(4): 586-595.
- Nell, R. M., Fein, J. B. (2017). Influence of sulfhydryl sites on metal binding by bacteria. *Geochimica et Cosmochimica Acta* **199**, 210-221.
- Playter, T., Konhauser, K.O., Owttrim, G.W., Hodgson, C., Warchola, T., Mloszewska, A.M., Sutherland, B., Bekker, A., Zonneveld, J.P., Pemberton, S.G., Gingras, M.K. (2017). Microbe-clay interactions as a mechanisms for the preservation of organic matter and trace metal biosignatures in black shales. *Chemical Geology*, **459**, 75-90.
- Saito, M.A., Sigman, D.M., Morel, F.M.M. (2003). The bioinorganic chemistry of the ancient ocean: The coevolution of cyanobacterial metal requirements and biogeochemical cycles at the Archean-Proterozoic boundary? *Inorganica Chimica Acta* **356**, 308-318.
- Skyllberg, U., Drott, A. (2010). Competition between disordered iron sulfide and natural organic matter associated thiols for mercury(II)- an EXAFS study. *Environmental Science and Technology* **44**, 1254-1259.
- Vraspir, J. M.; Butler, A. (2009). Chemistry of marine ligands and siderophores. *Annual Review of Marine Science* **1**, 43-63.
- Yu, Q., Fein, J. B. (2016). Sulfhydryl Binding Sites within Bacterial Extracellular Polymeric Substances. *Environmental Science and Technology* **50**, 5498-5505.

Yu, Q., Fein, J. B. (2017) Enhanced Removal of Dissolved Hg(II), Cd (II), and Au (III) from Water by *Bacillus subtilis* Bacterial Biomass Containing an Elevated Concentration of Sulfhydryl Sites. *Environmental Science and Technology* **51**, 14360-14367.

Yu, Q., Boyanov, M. I., Liu, J., Kemmer, K. M., Fein, J. B. (2018) Adsorption of Selenite onto *Bacillus subtilis*: The Overlooked Role of Cell Envelope Sulfhydryl Sites in the Microbial Conversion of Se(IV). *Environmental Science and Technology* **52**, 10400-10407.

**Table 5.1:** Ligand values input into the modified thermo minteq database for biotic modelling.

Ligand	Concentration	pKa	Log KCu	Log KNi
L1	50 uM	6	8	-
L2	5 nM	9	13	18

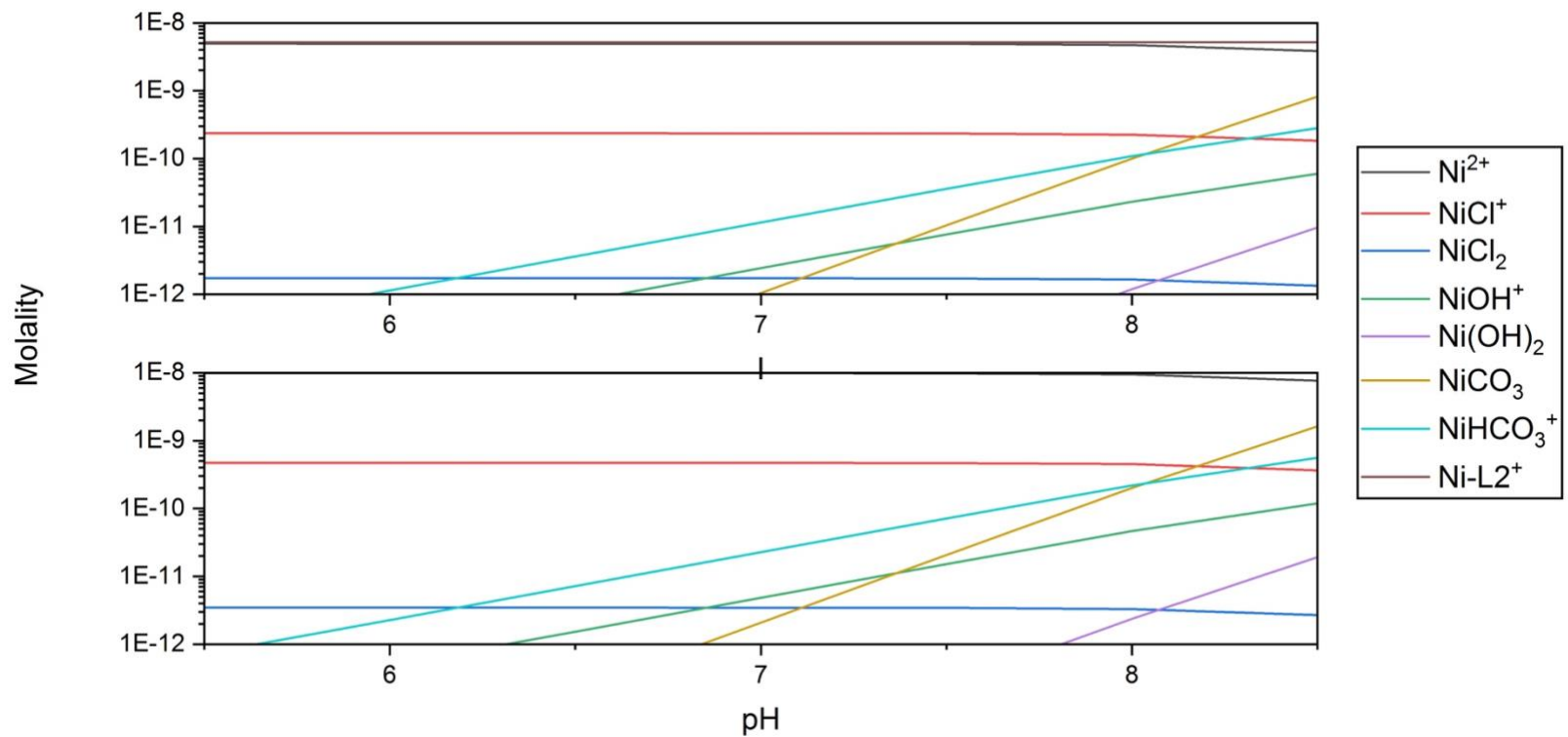


**Figure 5.1:** Modern Ni speciation (-3.5 log atm CO<sub>2</sub>, 10 nM Ni, 0.56 M Na and Cl)

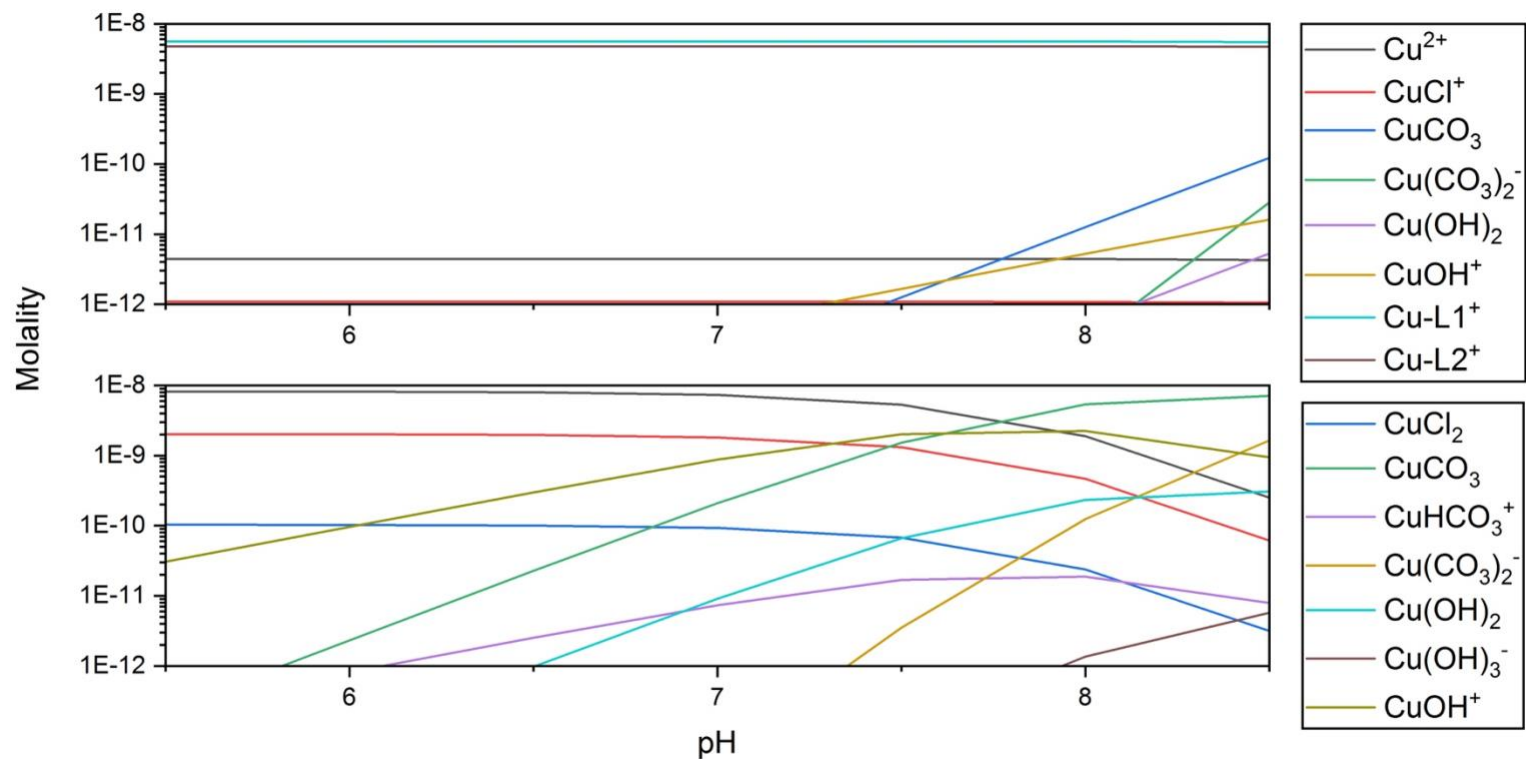


**Figure 5.2:** Modern Cu speciation ( $-3.5 \log \text{atm CO}_2$ , 10 nM Cu, 0.56 M Na and Cl). Note that  $\text{Cu}^{2+}$  and  $\text{CuCl}^+$  are present in both abiotic and ligand containing diagrams but only in the ligand containing legend to preserve space.

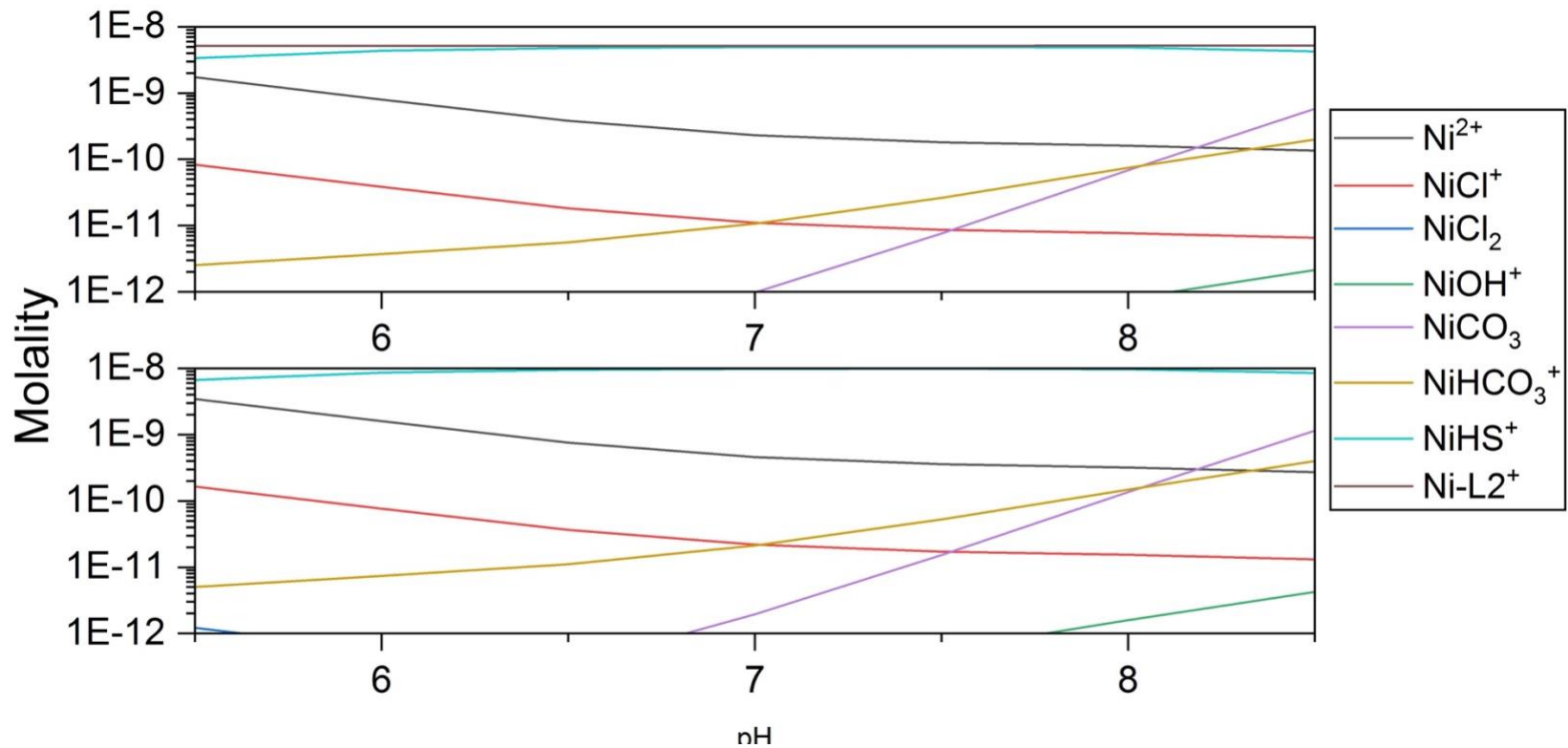
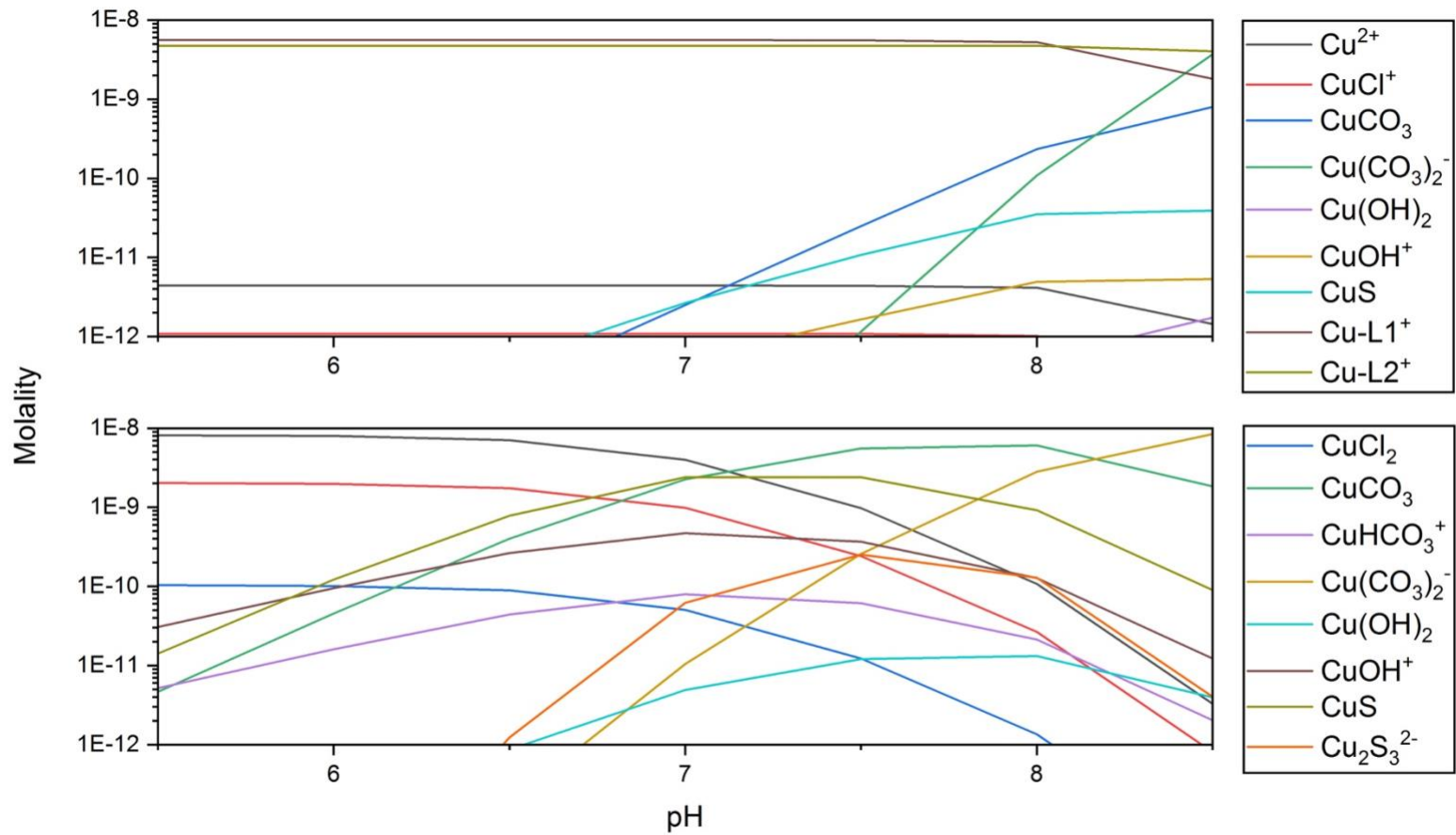
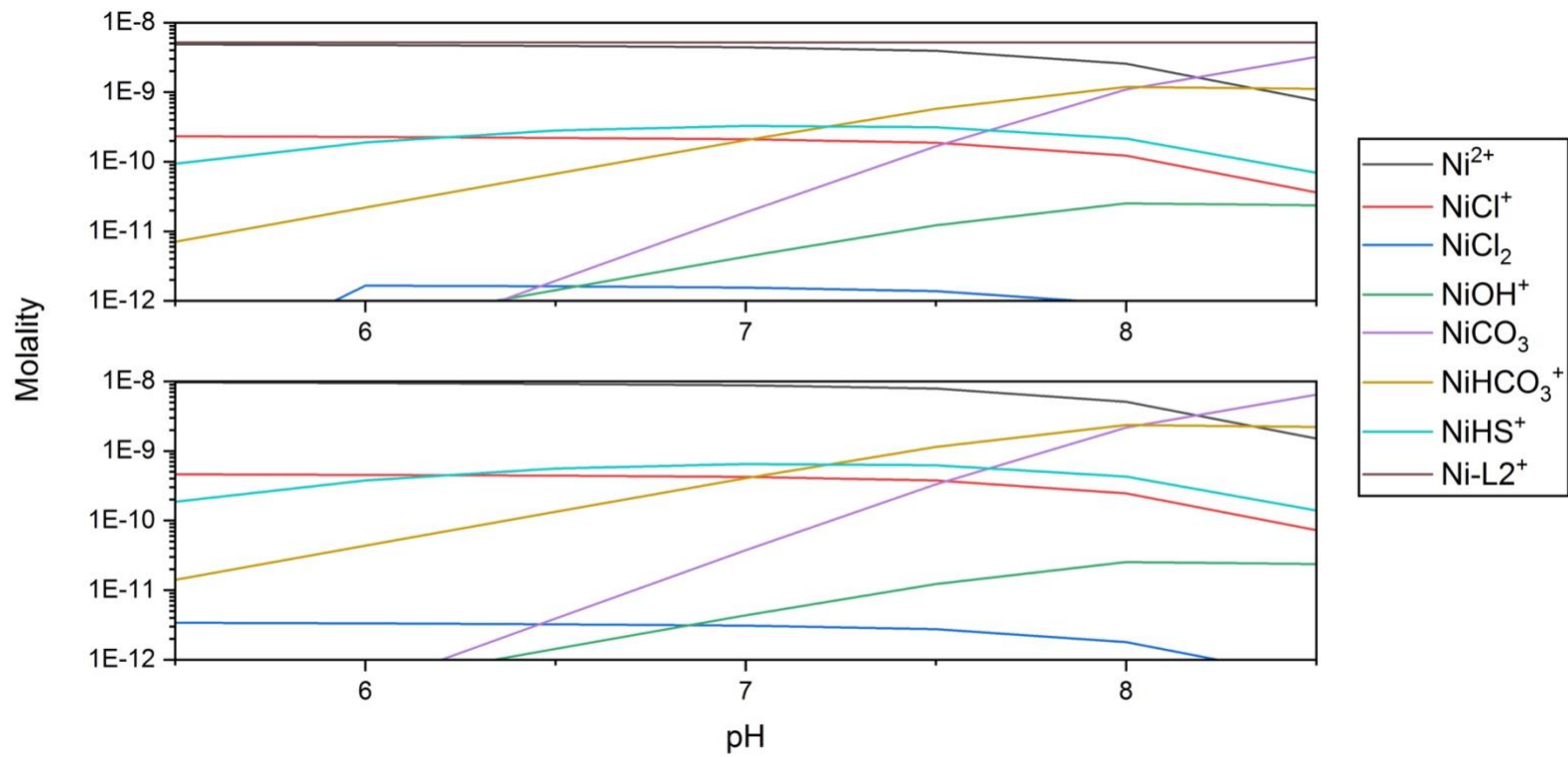


Figure 5.3: Euxinic Ni (-2.2 log atm CO<sub>2</sub>, 10 nM Ni, 0.56 M Na and Cl, 400 uM H<sub>2</sub>S)



**Figure 5.4:** Euxinic Cu (-2.2 log atm CO<sub>2</sub>, 10 nM Cu, 0.56 M Na and Cl, 400 uM H<sub>2</sub>S)



**Figure 5.5:** Post-GOE Ni speciation (-2.2 log atm CO<sub>2</sub>, 10 nM Ni, 0.56 M Na and Cl, 50 uM Fe(II), and 5 uM H<sub>2</sub>S)

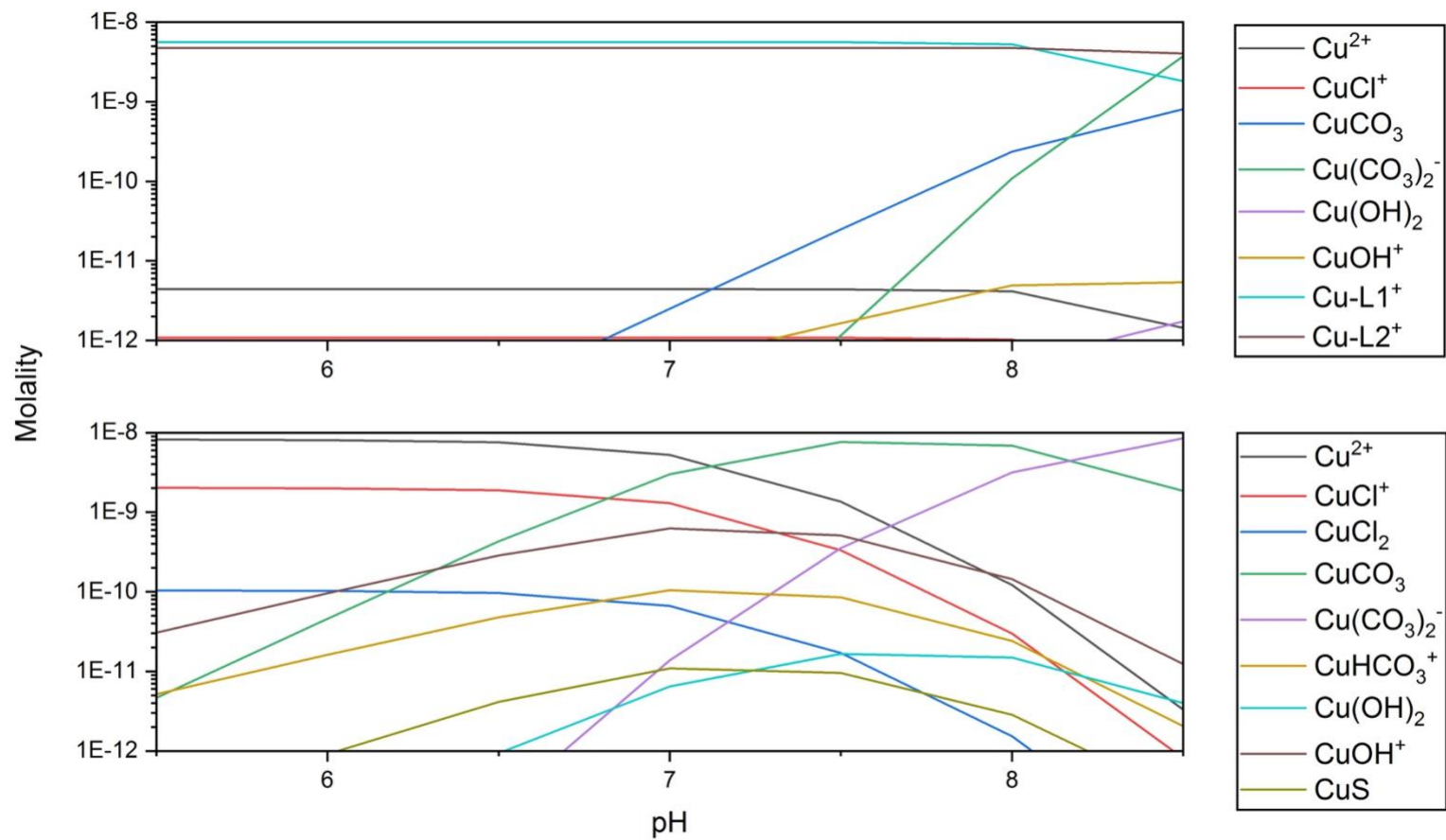


**Figure 5.6:** Post-GOE Cu speciation (-2.2 log atm CO<sub>2</sub>, 10 nM Cu, 0.56 M Na and Cl, 50 uM Fe(II), and 5 uM H<sub>2</sub>S).

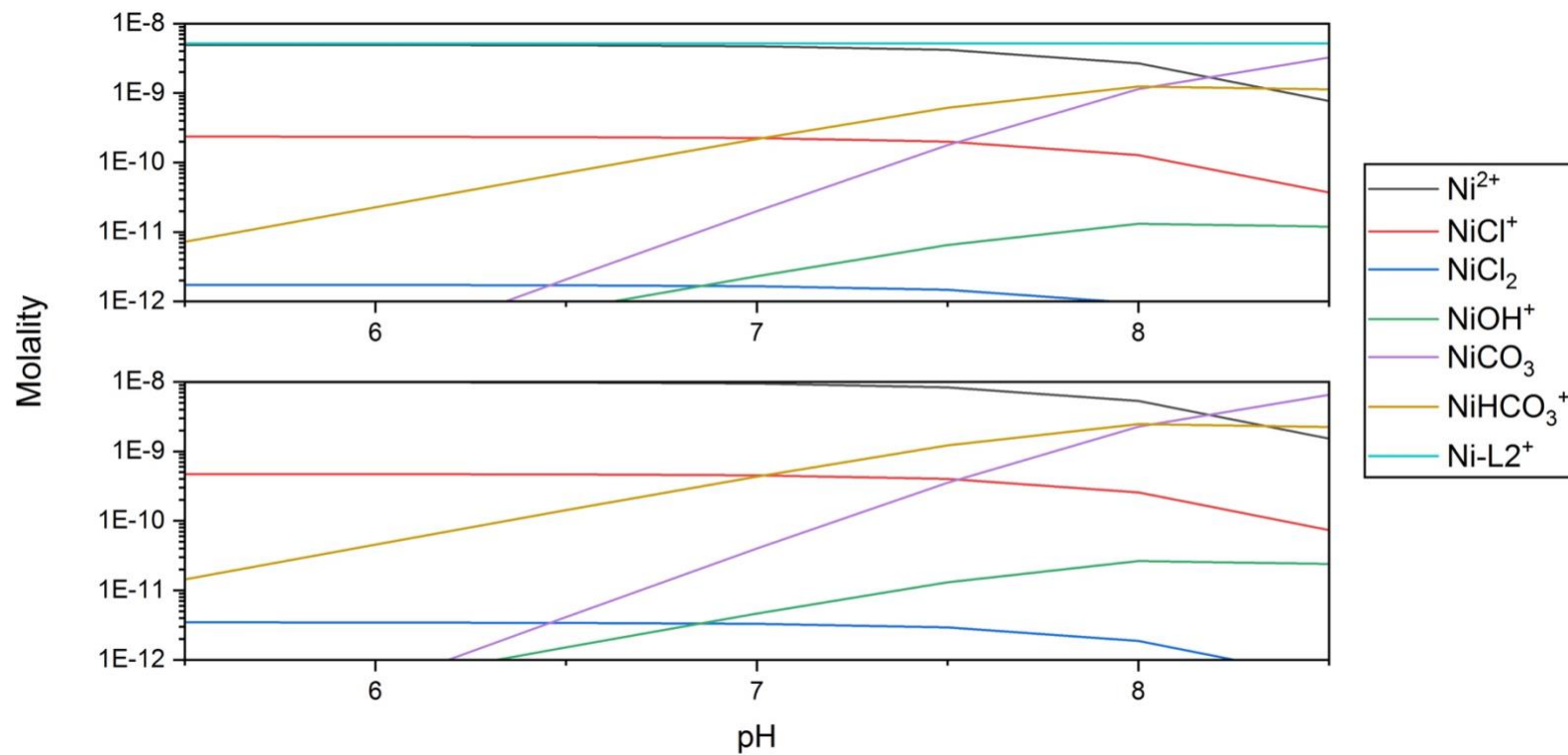


**Figure 5.7:** Ferruginous Ni (-2.2 log atm CO<sub>2</sub>, 10 nM Ni and Cu, 0.56 M Na and Cl, 50 uM Fe(II)).

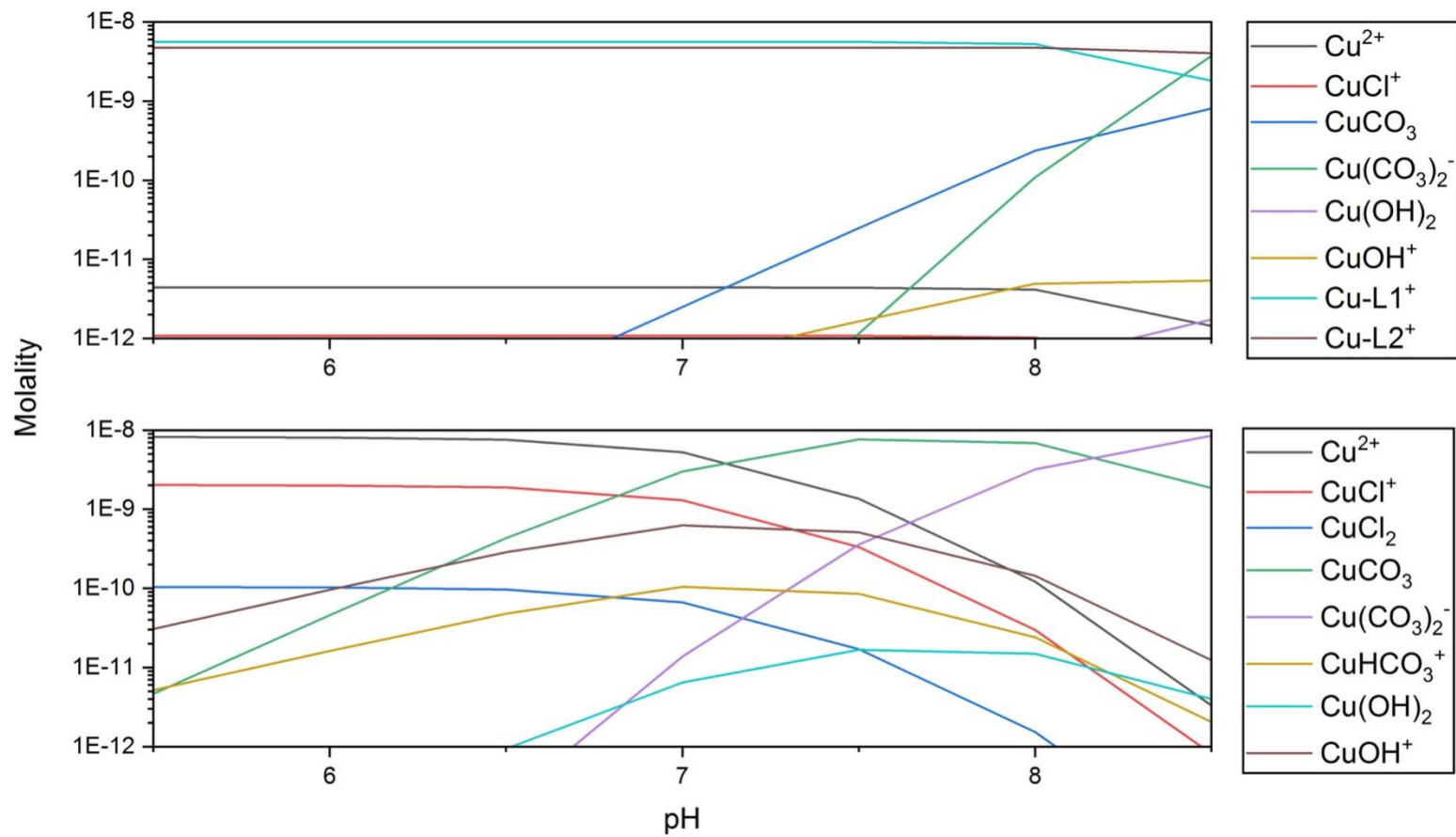


**Figure 5.8:** Ferruginous Cu (-2.2 log atm CO<sub>2</sub>, 10 nM Cu and Cu, 0.56 M Na and Cl, 50 uM Fe(II)).

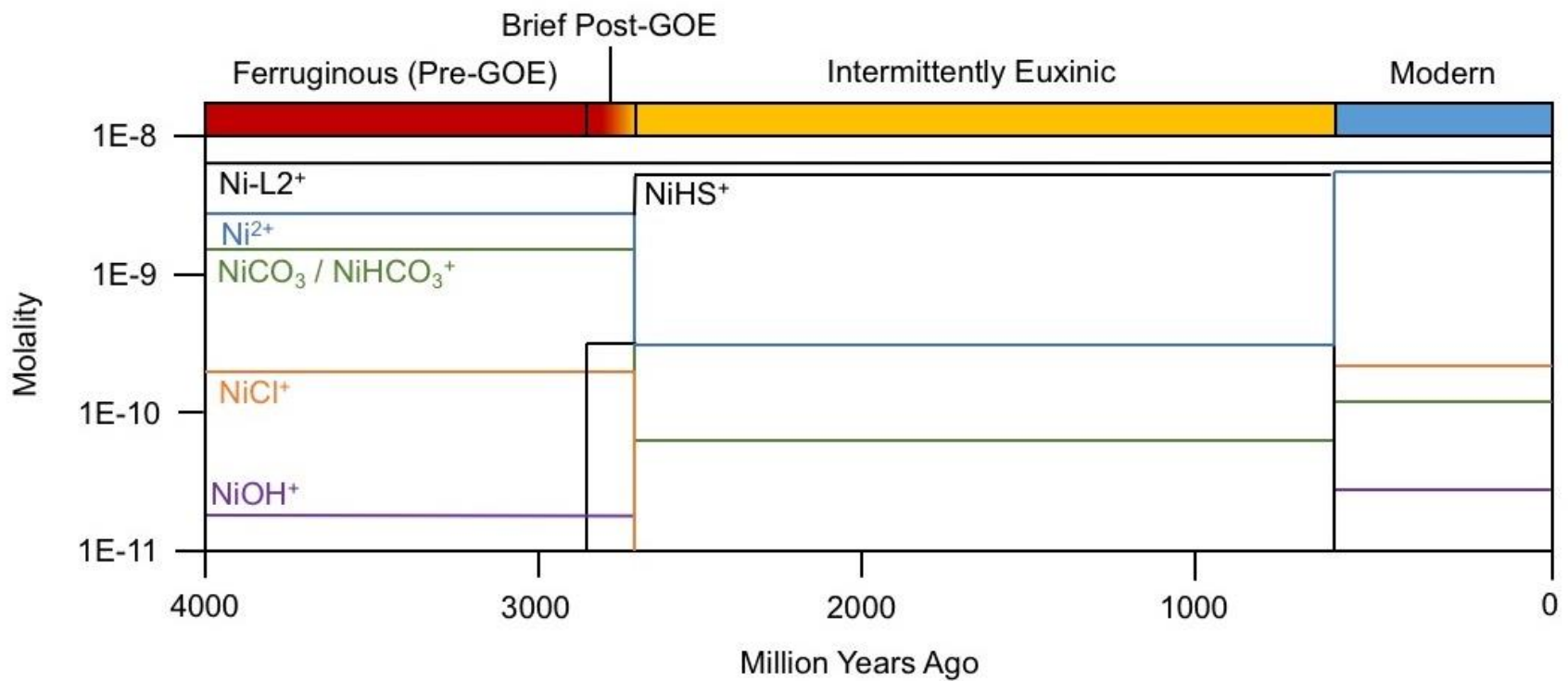


**Figure 5.9:** Ni speciation through time in the presence of Ni-binding ligands.

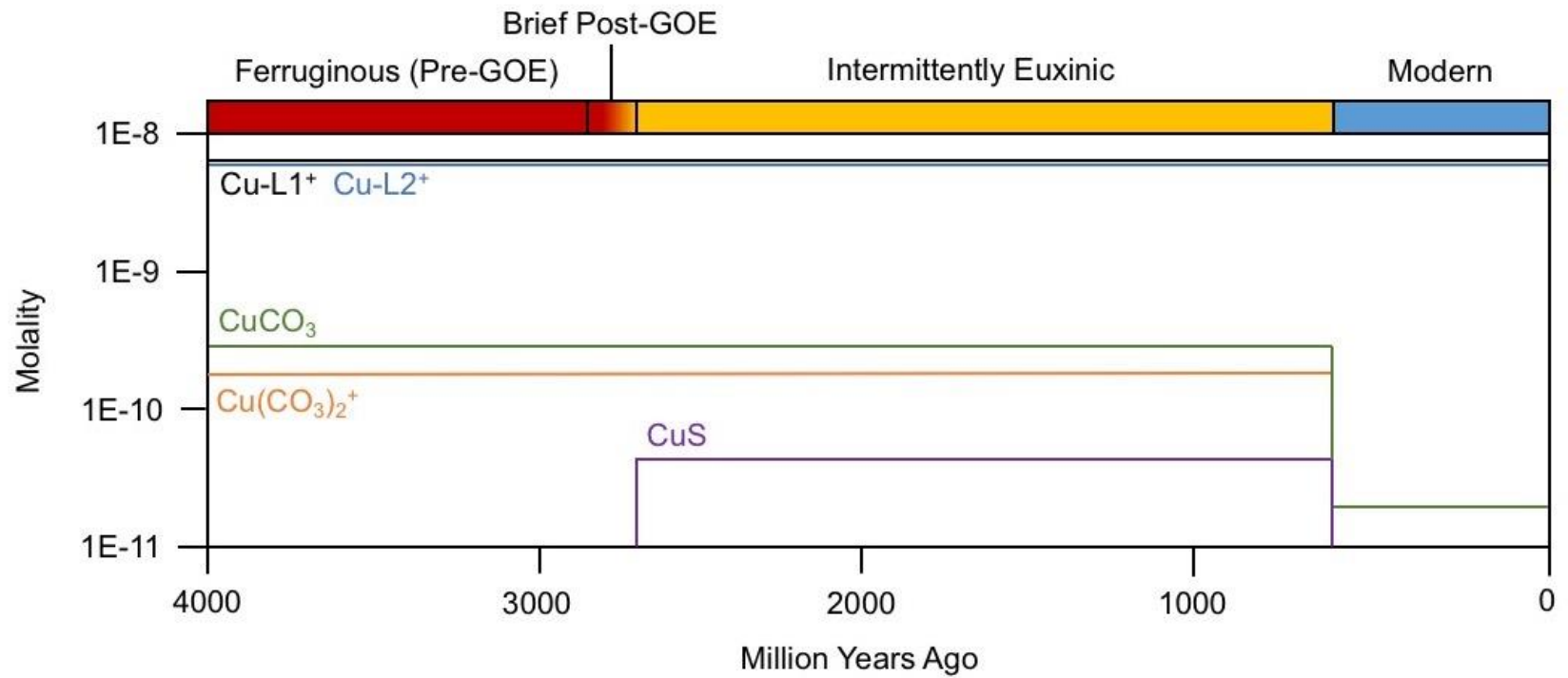


**Figure 5.10:** Cu speciation through time in the presence of Cu-binding ligands.

## Bibliography

- Abed, R. M. M., Safi, N. M. D., Koster, J., de Beer, D., El-Nahhal, Y., Rullkotter, J., Garcia-Pichel, F. (2002) Microbial diversity of a heavily polluted microbial mat and its community changes following degradation of petroleum compounds. *Appl. Environ. Microbiol.* **68**, 1674-1683.
- Alam, M. D., Swaren, L., von Gunten, K., Cossio, M., Bishop, B., Robbins L. J., Hou, D., Flynn, S. L., Ok, Y. S., Konhauser, K. O., Alessi, D. S. (2018) Application of surface complexation modeling to trace metals uptake by biochar-amended agricultural soils. *Appl. Geochem.* **88**, 103-112.
- Alessi, D. S., Henderson, M., Fein, J. B. (2010) Experimental measurement of monovalent cation adsorption onto *Bacillus subtilis* cells. *Geomicrobiol. J.* **27**, 464-472.
- Alessi, D. S., Flynn, S. L., Alam, M. S., Robbins, L. J., Konhauser, K. O. (2019) *Potentiometric titrations to characterize the reactivity of geomicrobial surfaces*. In: Kenney, J. P. L., Veeramani, H., Alessi, D. S. (Eds.), *Analytical Geomicrobiology: A Handbook of Instrumental Techniques*, Cambridge University Press, Cambridge, United Kingdom, pp. 79-92.
- Algeo, T.J., Maynard, J.B. (2004). Trace-element behavior and redox facies in core shales of Upper Pennsylvanian Kansas-type cyclothems. *Chemical Geology*, **206**, 289-318.
- Allen, M. M. (1968) Simple conditions for growth of unicellular blue-green algae on plates. *J. Phycol.* **4**, 1-4.
- Aluwihare, L. I., Repeta, D. J. (1999). A comparison of the chemical characteristics of oceanic DOM and extracellular DOM produced by marine algae. *Marine Ecology Progress Series* **186**, 105-117.

- Arunakumara, K. K. I. U., Xuecheng, Z. (2009) Effects of heavy metals (Pb<sup>2+</sup> and Cd<sup>2+</sup>) on the ultrastructure, growth and pigment contents of the unicellular cyanobacterium *Synechocystis* sp. PCC 6803. *Chin. J. Oceanol. Limn.* **27**, 383-388.
- Badarau, A., Dennison, C. (2011) Thermodynamics of copper and zinc distribution in the cyanobacterium *Synechocystis* PCC 6803. *PNAS* **108**, 13007-13012.
- Baes, C. F., Mesmer, R. S. Te Hydrolysis of Cations. John Wiley & Sons, New York, London, Sydney, Toronto 1976. 489 Seiten. Berichte der Bunsengesellschaft für physikalische Chemie 81, 245–246 (1977).
- Baker, M. G., Lalonde, S. V., Konhauser, K. O., and Foght, J. M. (2010) The role of extracellular substances in the surface chemical reactivity of *Hymenobacter aerophilus*, a psychotolerant bacterium. *Appl. Environ. Microbiol.* **76**, 102-109.
- Bateman, R. M., Crane, P. R., DiMichele, W. A., Kenrick, P. R., Rowe, N. P., Speck, T., Stein, W. E. (1998). Early Evolution of Land Plants: Phylogeny, Physiology, and Ecology of the Primary Terrestrial Radiation. *Annual Reviews of Ecological Systems* **29**, 263-292.
- Bekker, A., Holland, H.D. (2012). Oxygen overshoot and recovery during the early Paleoproterozoic. *Earth and Planetary Science Letters* **317**, 295-304.
- Benner, R., Pakulsi, J. D., McCarthy, M., Hedges, J. I., Hatcher, P. G. (1992). Bulk chemical characteristics of dissolved organic matter in the ocean. *Science* **255**, 1561-1564.
- Bennett, A., Bogorad, L. (1973). Complementary chromatic adaptation in a filamentous blue-green alga. *Journal of Cell Biology* **58**, 419-435.
- Benning, L.G., Phoenix, V., Yee, N., and Konhauser, K.O. (2004). The dynamics of cyanobacterial silicification: An infrared micro-spectroscopic investigation. *Geochimica et Cosmochimica Acta*, **68**, 743-757.

- Bhatia, M.P., Das, S.B., Longnecker, K., Charette, M.A., Kujawinski, E.B. (2010). Molecular characterization of dissolved organic matter associated with the Greenland ice sheet. *Geochimica et Cosmochimica Acta* **74**, 3768-3784.
- Bishop, B. A., Flynn, S. L., Warchola, T. J., Alam, M. S., Robbins, L. J., Liu, Y., Owttrim, G. W., Alessi, D. S., Konhauser, K. O. (2019) Adsorption of biologically critical trace elements to the marine cyanobacterium *Synechococcus* sp. PCC 7002: Implications for marine trace metal cycling. *Chem. Geol.* **525**, 28-36.
- Boden, J.S., Konhauser, K.O., Robbins, L.J., Sanchez-Baracaldo, P. (2021). Timing the evolution of antioxidant enzymes in cyanobacteria. *Nature Communications* **12**, 4742.
- Boeuf, D., Edwards, B.R., Eppley, J.M., Hu, S.K., Poff, K.E., Romano, A.E., Caron, D.A., Karl, D.M., DeLong, E.F. (2019). Biological composition and microbial dynamics of sinking particulate organic matter at abyssal depths in the oligotrophic open ocean. *Proceeding of the National Academy of Sciences*, **116**, 11824-11832.
- Boiteau, R.M., Repeta, D.J. (2015). An extended siderophore suite from *Synechococcus* sp. PCC 7002 revealed by LC-ICPMS-ESIMS. *Metallomics*, **7**, 877.
- Boiteau, R. M., Till, C. P., Ruacho, A., Bundy, R. M., Hawco, N. J., McKenna, A. M., Barbeau, K. A., Bruland, K. W., Saito, M. A., Repeta, D. J. (2016). Structural Characterization of Natural Nickel and Copper Binding Ligands along the US GEOTRACES Eastern Pacific Zonal Transect. *Frontiers in Marine Science* **3**, 243.
- Bolgovics, A., Varbiro, G., Acs, E., Trabert, Z., Kissm K. T., Pozderka, V., Gorgenyi, J., Boda, P., Lukacs, B. A., Nagy-Laszlo, Z., Abonyi, A., Borics, G. (2017) Phytoplankton of rhithral rivers: Its origin, diversity and possible use for quality-assessment. *Ecol. Indic.* **81**, 587-596.

- Boning, P., Shaw, T., Pahnke, K., Brumsack, H.J. (2015). Nickel as indicator of fresh organic matter in upwelling sediments. *Geochimica et Cosmochimica Acta*, **162**, 99-108.
- Borrok, D. M., Fein, J. B. (2005) The impact of ionic strength on the adsorption of protons, Pb, Cd, and Sr onto the surfaces of Gram negative bacteria: testing non-electrostatic, diffuse, and triple-layer models. *J. Colloid Interf. Sci.* **286**, 110-126.
- Bouhedja, W., Sockalingum, G. D., Pina, P., Bloy, C., Labia, R., Millot, J. M., Manfait, M. (1997) ATR-FTIR spectroscopic investigation of *E. coli* transconjugants beta-lactams-resistance phenotype. *FEBS Letters* **412**, 39-42.
- Boyd, P.W., Claustre, H., Levy, M., Siegel, D.A., Weber, T. (2019). Multi-faceted particle pumps drive carbon sequestration in the ocean. *Nature*, **568**, 327-335.
- Bruland, K.W. (1980). Oceanographic distributions of cadmium, zinc, nickel, and copper in the North Pacific. *Earth and Planetary Science Letters* **47**, 176-198.
- Bruland, K.W., Donat, J.R., Hutchins, D.A. (1991). Interactive influences of bioactive trace metals on biological production in oceanic waters. *Limnology and Oceanography* **36**, 1555-1577.
- Bruland, K.W., Lohan M.C. (2003). Controls of trace metals in seawater. *Treatise on Geochemistry* **6**, 23-47.
- Bruland, K.W., Middag, R., Lohan, M.C. (2013). Controls of Trace Metals in Seawater. In: *Treatise on Geochemistry*, Second edition. 19–51.
- Buslov, D. K., Nikonenko, N. A., Sushko, N. I., Zhabankov, R. G. (2002) Analysis of the structure of the bands in the IR spectrum of beta-D glucose by the regularized method of deconvolution. *J. Appl. Spectro.* **69**, 817-824.
- Brussard, C. P. D., Wilhelm, S. W., Thingstad, F., Weinbauer, M. G., Bratbak, G., Heldal, M., Kimmance, S. A., Middelboe, M., Nagasaki, K., Paul, J. H., Schroeder, D. C., Suttle, C. A.,

- Vaque, D., Wommack, K. E. (2008). Global-scale processes with a nanoscale drive: the role of marine viruses. *International Society for Microbial Ecology* **2**, 575-578.
- Caccamo, M. T., Gugliandolo, C., Zammuto, V., Magazu, S. (2020) Thermal properties of an exopolysaccharide produced by a marine thermotolerant *Bacillus licheniformis* by ATR-FTIR spectroscopy. *Int. J. Biol. Macromol.* **145**, 77-83.
- Cai, W., Wang, Y., Hodson, R.E. (1998). Acid-base properties of dissolved organic matter in the estuarine waters of Georgia, USA. *Geochimica et Cosmochimica Acta*, **62**, 473-483.
- Calvert, S.E., Pederson, T.F. (1993). Geochemistry of recent oxic and anoxic marine sediments: implications for the geological record. *Marine Geology*, **113**, 67-88.
- Celo, V., Murimboh, J., Salam, M. S. A., Chakrabarti, C. L. (2001). A kinetic Study of Nickel Complexation in Model Systems by Adsorptive Cathodic Stripping Voltammetry. *Environmental Science and Technology* **35**, 1084-1089.
- Chen, H., Johnston, R. C., Mann, B. F., Chu, R. K., Tolic, N., Parks, J. M., Gu, B. (2017). Identification of Mercury and Dissolved Organic Matter Complexes Using Ultrahigh Resolution Mass Spectrometry. *Environmental Science and Technology Letter* **4**, 59-65.
- Coale, K. H., Bruland, K. W. (1988). Copper complexation in the Northeast Pacific. *Limnology and Oceanography* **33**, 1084-1101.
- Cox, J. S., Smith, D. S., Warren, L. A., Ferris, F. G. (1999) Characterizing heterogeneous bacterial surface functional groups using discrete affinity spectra for proton binding. *Environ. Sci. Technol.* **33**, 4514-4521.
- Cullen, J.T., Chase, Z., Coale, K.H., Fitzwater, S., Sherrell, R.M. (2003). Effect of iron limitation on the cadmium to phosphorus ratios of natural phytoplankton assemblages from the Southern Ocean. *Limnology and Oceanography*, **48**, 1079-1087.

- Cullen, J.T. (2006). On the nonlinear relationship between dissolved cadmium and phosphate in the modern global ocean: Could chronic iron limitation of phytoplankton cause the kink? *Limnology and Oceanography*, **51**, 1361-1380.
- Delille, A., Quiles, F., Humbert, F. (2007) In situ monitoring of the nascent *Pseudomonas fluorescens* biofilm response to variations in the dissolved organic carbon level in low-nutrient water by attenuated total reflectance-Fourier transform infrared spectroscopy. *Applied and Environmental Microbiology* **73**, 5782-5788.
- Demirel, S., Ustun, B., Aslim, B., Suludere, Z. (2009) Toxicity and uptake of Iron ions by *Synechocystis* sp. E35 isolated from Kucukcekmece Lagoon, Istanbul. *J. Hazard. Mat.* **171**, 710-716.
- Descy, J. P., Darchambeau, F., Lambert, T., Stoyneva-Gaertner, M. P., Bouillon, S., Borges, A. V. (2017) Phytoplankton dynamics in the Congo River. *Freshw. Biol.* **62**, 87-101.
- Dilling, J., Kaiser, K. (2002). Estimation of the hydrophobic fraction of dissolved organic matter in water samples using UV photometry. *Water Research* **36**, 5037-5044.
- Dittmar, T., Hertkorn, N., Kattner, G., Lara, R. J. (2006). Mangroves, a major source of dissolved organic carbon to the oceans. *Global Biogeochemical Cycles* **20**, GB1012. 7 p.
- Dittmar, T., Koch, B., Hertkorn, N., Kattner, G. (2008). A simple and efficient method for the solid-phase extraction of dissolved organic matter (SPE-DOM) from seawater. *Limnology and Oceanography: Methods* **6**, 230-235.
- Dittmar, T., Paeng, J. (2009). A heat-induced molecular signature in marine dissolved organic matter. *Nature Geoscience* **2**, 175-179.

- Du, J., Qiu, B., Gomes, M. P., Juneau, P., Dai, G. (2019) Influence of light intensity on cadmium uptake and toxicity in the cyanobacteria *Synechocystis* sp. PCC 6803. *Aquat. Toxicol.* **211**, 163-172.
- Durham, B. P., Sharma, S., Luo, H., Smith, C. B., Amin, S. A., Bender, S. J., Dearth, S. P., Van Mooy, B. A. S., Campagna, S. R., Kujawinski, E. B., Armbrust, E. V., Moran, M. A. (2015). Cryptic carbon and sulfur cycling between surface ocean plankton. *Proceedings of the National Academy of Sciences* **112**, 453-457.
- Dutkiewicz, A., O'Callaghan, S., Muller, R.D. (2016). Controls on the distribution of deep-sea sediments. *Geochemistry, Geophysics, Geosystems*, **17**, 3075-3098.
- Dvorak, P., Casamatta, D.A., Poulickova, A., Hasler, P., Ondrej, V., Sanges, R. (2014). *Synechococcus*: 3 billion years of global dominance. *Molecular Ecology*, **23**, 5538-5551.
- Egleston, E.S., Morel, F.M.M. (2008). Nickel limitation and zinc toxicity in a urea-grown diatom. *Limnology and Oceanography*, **53**, 2462-2471.
- Elderfield, H., Rickaby, R.E.M. (2000). Oceanic Cd/P ratio and nutrient utilization in the glacial Southern Ocean. *Nature*, **405**, 305-310.
- Engel, A., Thoms, S., Riebesell, U., Rochelle-Newall, E., Zondervan, I. (2004). Polysaccharide aggregation as a potential sink of marine dissolved organic carbon. *Letters to Nature* **428**, 929-932.
- Fatayer, S., Coppola, A. I., Schulz, F., Walker, B. D., Broek, T. A., Meyer, G., Druffel, E. R. M., McCarthy, M., Gross, L. (2018). Direct Visualization of Individual Aromatic Compound Structures in Low Molecular Weight Marine Dissolved Organic Carbon. *Geophysical Research Letters* **45**, 5590-5598.

- Fein, J. B., Daughney, C. J., Yee, N., Davis, T. A. (1997) A chemical equilibrium model for metal adsorption onto bacterial surfaces. *Geochim. Cosmochim. Acta* **61**, 3319-3328.
- Fein, J. B. (2017) Advanced biotic ligand models: Using surface complexation modeling to quantify metal bioavailability to bacteria in geologic systems. *Chem. Geol.* **464**, 127-136.
- Filip, Z., Hermann, S. (2001) An attempt to differentiate *Pseudomonas* spp. And other soil bacteria by FT-IR spectroscopy. *Eur. J. Soil Biol.* **37**, 137-143.
- Fischer, K., Dymond, J., Lyle, M., Soutar, A., Rau, S. (1986). The benthic cycle of copper: Evidence from sediment trap experiments in the eastern tropical North Pacific. *Geochimica et Cosmochimica Acta*, **50**, 1535-1543.
- Flerus, R., Koch, B. P., Schmitt-Kopplin, P., Witt, M., Kattner, G. (2011). Molecular level investigation of reactions between dissolved organic matter and extraction solvents using FT-ICR MS. *Marine Chemistry* **124**, 100-107.
- Flombaum, P., Gallegos, J. L., Gordillo, R. A., Rincon, J., Zabala, L. L., Jiao, N., Karl, D. M., Li, W. K. W., Lomas, M. W., Veneziano, D., Vera, C. S., Vrugt, J. A., Martiny, A. C. (2013) Present and future global distributions of the marine cyanobacteria *Prochlorococcus* and *Synechococcus*. *PNAS*, **110**, 9824-9829.
- Flynn, S. L., Szymanowski, J. E. S., Fein, J. B. (2014) Modeling bacterial metal toxicity using a surface complexation approach. *Chem. Geol.* **375**, 110-116.
- Flynn, S. L., Gao, Q., Robbins, L. J., Warchola, T., Weston, J. N. J., Alam, S. M., Liu, Y., Konhauser, K. O., Alessi, D. S. (2017) Measurements of bacterial mat metal binding capacity in alkaline and carbonate-rich systems. *Chem. Geol.* **451**, 17-24.
- Fowle, D., Fein, J.B. (2000). Experimental measurements of the reversibility of metal-bacteria adsorption reactions. *Chemical Geology*, **168**, 27-36.

- Fournier, G.P., Moore, K.R., Rangel, L.T., Payette, J.G., Momper, L., Bosak, T. (2021). The Archean origin of oxygenic photosynthesis and extant cyanobacterial lineages. *Proceedings of the Royal Society B* **288**, 20210675. <https://doi.org/10.1098/rspb.2021.0675>
- Fry, B., Hopkinson Jr, C. S., Nolin, A., Wainwright, S. C. (1998).  $^{13}\text{C}/^{12}\text{C}$  composition of marine dissolved organic carbon. *Chemical Geology* **152**, 113-118.
- Gantt, E. (1980). Structure and function of phycobilisomes: light harvesting pigment complexes in red and blue-green algae. *International Review of Cytology* **66**, 45-80.
- Garcia-Pichel, F., Lombard, J., Soule, T., Dunaj, S., Wu, S.H., Wojciechowski, M.F. (2019). Timing the evolutionary advent of cyanobacteria and the later Great Oxidation Event using gene phylogenies of a sunscreen. *mBio* **10**, e00561-19.
- Glass, J.B., Dupont, C.L. (2017). *Chapter 2: Oceanic nickel biogeochemistry and the evolution of nickel use*. In: Zamlbe, D., Rowinska-Zyrek, M., Kozlowski, H. The biological chemistry of nickel. *Royal Society of Chemistry*. pp. 12-27.
- Green, N. W., Perdue, E. M., Aiken, G. R., Butler, K. D., Chen, H., Dittmar, T. (2014). An intercomparison of three methods for large-scale isolating of oceanic dissolved organic matter. *Marine Chemistry* **161**, 14-19.
- Gu, B., Bian, Y., Miller, C. L., Dong, W., Jiang, X., Liang, L. (2011). Mercury reduction and complexation by natural organic matter in anoxic environments. *Proceedings of the National Academy of Sciences*, **108**, 1479-1483.
- Hansell, D. A., Carlson, C. A. (2001). Marine Dissolved Organic Matter and the Carbon Cycle. *Oceanography* **14**, 41-49.
- Hansell, D. A. (2013). Recalcitrant dissolved organic carbon fractions. *Annual Review of Marine Sciences* **5**, 421-445.

- Hao, W., Flynn, S. L., Alessi, D. S., Konhauser, K. O. (2018) Change of point of zero net proton charge (pHPZNPC) of clay minerals with ionic strength. *Chem. Geol.* **493**, 458-467.
- Hao, W., Flynn, S. L., Kashiwabara, T., Alam, M. S., Bandara, S., Swaren, L., Robbins, L. J., Konhauser, K. O. (2019) The impact of ionic strength on the proton reactivity of clay minerals. *Chem. Geol.* **529**, 119294.
- Hao, W., Kashiwabara, T., Jin, R., Takahashi, Y., Gingras, M. K., Alessi, D. S., Konhauser, K. O. (2020) Clay minerals as a source of cadmium to estuaries. *Sci. Rep.* **10**, 10417.
- Hao, W., Swaren, L., Baker, D., Melnyk, S., Li, Y., Liu, Y., Owttrim, G.W., Zeng, H., Gingras, M.K., Alessi, D.S., Konhauser, K.O. (in review – WR65357). The impact of aggregation between clay and planktonic cyanobacteria on trace elemental cycling in estuaries. *Water Research*.
- Hedges, J. I., Keil, R. G., Benner, R. (1997). What happens to terrestrial organic matter in the ocean? *Organic Geochemistry* **27**, 195-212.
- Hedges, J.I., Eglinton, G., Hatcher, P.G, Kirchman, D.L., Arnosti, C., Derenne, S., Evershed, R.P., Kogel-Knabner, I., de Leeuw, J.W., Littke, R., Michaelis, W., Rullkotter, J. (2000). The molecularly-uncharacterized component of nonliving organic matter in natural environments. *Organic Geochemistry* **31**, 945-958.
- Herbelin, A. L., Westall, J. C. (1999) FITEQL: a Computer Program for Determination of Equilibrium Constants from Experimental Data. Department of Chemistry, Oregon State University. Corvallis, OR. *Report 99-01*.
- Hertkorn, N., Benner, R., Frommberger, M., Schmitt-Kopplin, P., Witt, M., Kaiser, K., Kettrup, A., Hedges, J. I. (2006). Characterization of a major refractory component of marine dissolved organic matter. *Geochimica et Cosmochimica Acta* **70**, 2990-3010.

- Ho, T.-Y., Quigg, A., Finkel, Z.V., Milligan, A.J., Wyman, K., Falkowski, P.G., Morel, F.M.M. (2003). The elemental composition of some marine phytoplankton. *Journal of Phycology*, **39**, 1145-1159.
- Huizenga, D.L., Kester, D.R. (1979). Protonation equilibria of marine dissolved organic matter. *Limnology and Oceanography*, **24**, 145-150.
- Iijima, H., Nakaya, Y., Kuwahara, A., Hirai, M. Y., Osanai, T. (2015) Seawater cultivation of freshwater cyanobacterium *Synechocystis* sp. PCC 6803 drastically alters amino acid composition and glycogen metabolism. *Front.Microbiol.* **6**, 326.
- Ikeuchi, M., Tabata, S. (2001) *Synechocystis* sp. PCC 6803 – a useful tool in the study of genetics of cyanobacteria. *Photosynth. Res.* **70**, 73-83.
- Jaffe, R., Ding, Y., Niggemann, J., Vahatalo, A.V., Stubbins, A., Spencer, R.G.M., Campbell, J., Dittmar, T. (2013). Global charcoal mobilization from soils via dissolution and riverine transport to the oceans. *Science* **340**, 345-347.
- Jiang, W., Saxena, A., Song, B., Ward, B. B., Beveridge, T. J., Myneni, S. C. B. (2004) Elucidation of functional groups on gram-positive and gram-negative bacterial surfaces using infrared spectroscopy. *Langmuir* **20**, 11433-11442.
- Jiao, N., Herndl, G. J., Hansell, D. A., Benner, R., Kattner, G., Wilhelm, S. W., Kirchman, D. L., Weinbauer, M. G., Luo, T., Chen, F., Azam, F. (2010). Microbial production of recalcitrant dissolved organic matter: long-term carbon storage in the global ocean. *Nature Reviews Microbiology* **8**, 593-599.
- Jiao, N., Robinson, C., Azam, F., Thomas, H., Baltar, F., Dang, H., Hardman-Mountford, N. J., Johnson, M., Kirchman, D. L., Koch, B. P., Legendre, L., Li, C., Liu, J., Luo, T., Luo, Y. W., Mitra, A., Romanou, A., Tang, K., Wang, X., Zhang, C., Zhang, R. (2014). Mechanisms

- of microbial carbon sequestration in the ocean – future research directions. *Biogeosciences* **11**, 5285-5306.
- Jiao, N., Cai, R., Zheng, Q., Tang, K., Liu, J., Jiao, F., Wallace, D., Chen, F., Li, C., Amann, R., Benner, R., Azam, F. (2018). Unveiling the enigma of refractory carbon in the ocean. *National Science Review* **5**, 459-463.
- Jorgensen, L., Stedmon, C.A., Granskog, M.A., Middelboe, M. (2014). Tracing the long-term microbial production of recalcitrant fluorescent dissolved organic matter in seawater. *Geophysical Research Letters* **41**, 2481-2488.
- Kaneko, T., Sato, S., Kotani, H., Tanaka, A., Asamizu, E., Nakamura, Y., Miyajima, N., Hirose, M., Sugiura, M., Sasamoto, S., Kimura, T., Hosouchi, T., Matsuno, A., Muraki, A., Nakazaki, N., Naruo, K., Okumura, S., Shimpo, S., Takeuchi, C., Wada, T., Watanabe, A., Yamada, M., Tabata, S. (1996) Sequence analysis of the genome of the unicellular cyanobacterium *Synechocystis* sp. Strain PCC 6803. II. Sequence determination of the entire genome and assignment of potential protein-coding regions. *DNA Res.* **3**, 109-136.
- Kawasaki, N., Sohrin, R., Ogawa, H., Nagata, T., Benner, R. (2011). Bacterial carbon content and the living and detrital bacterial contributions to suspended particulate organic carbon in the North Pacific Ocean. *Aquatic Microbial Ecology* **62**, 165-176.
- Kenney, J.P.L., Gorzsas, A. (2019) Applications of Fourier-transform Infrared Spectroscopy in Geomicrobiology. In: Kenney, J.P.L., Veeramani, H., Alessi, D.S. (Eds.), *Analytical Geomicrobiology: A Handbook of Instrumental Techniques*, Cambridge University Press, Cambridge, United Kingdom, pp. 79-92.
- Kenrick, P., Crane, P. R. (1997). The origin and early evolution of plants on land. *Nature* **389**, 33-39.

- Kharbush, J.J., Close, H.G., Van Mooy, B.A.S., Arnosti, C., Smittenberg, R.H., Le Moigne, F.A.C., Mollenhauer, G., Scholz-Bottcher, B., Obreht, I., Koch, B.P., Becker, K.W., Iverson, M.H., Mohr, W. (2020). Particulate organic carbon deconstructed: Molecular and chemical composition of particulate organic carbon in the ocean. *Frontiers in Marine Science*, **7**, 518.
- Khattar, S. J. I. S. (2009) Optimization of Cd<sup>2+</sup> removal by the cyanobacterium *Synechocystis pevalekii* using the response surface methodology. *Process Biochem.* **44**, 118-121.
- Koch, B.P., Witt, M., Engbrodt, R., Dittmar, T., Kattner, G. (2005). Molecular formulae of marine and terrigenous dissolved organic matter detected by electrospray ionization Fourier transform ion cyclotron resonance mass spectrometry. *Geochemica et Cosmochimica Acta*, **69**, 3299-3308.
- Koch, B.P., Dittmar, T., Witt, M., Kattner, G. (2007). Fundamentals of molecular formula assignment to ultrahigh resolution mass data of natural organic matter. *Analytical Chemistry* **79**, 1758-1763.
- Koch, B.P., Kattner, G., Witt, M., Passow, U. (2014). Molecular insights into the microbial formation of marine dissolved organic matter: recalcitrant or labile? *Biogeosciences* **11**, 4173-4190.
- Konhauser, K.O., Hamade, T., Raiswell, R., Morris, R.C., Ferris, F.G., Southam, G., Canfield, D.E. (2002). Could bacteria have formed the Precambrian banded iron formations? *Geology*, **30**, 1079-1082.
- Konhauser, K. O., Pecoits, E., Lalonde, S. V., Papineau, D., Nisbet, E. G., Barley, M. E., Arndt, N. T., Zahnle, K., Kamber, B. S. (2009). Oceanic nickel depletion and a methanogen famine before the Great Oxidation Event. *Nature* **458**, 750-753.

- Konhauser, K.O., Lalonde, S.V., Planavsky, N.J., Pecoits, E., Lyons, T.W., Mojzsis, S.J., Rouxel, O. J., Barley, M.E., Rostere, C., Fralick, P.W., Kump, L.R., Bekker, A. (2011). Aerobic bacterial pyrite oxidation and acid rock drainage during the Great Oxidation Event. *Nature* **478**, 369-373.
- Konhauser, K.O., Robbins, L.J., Pecoits, E., Peacock, C., Kappler, A., Lalonde, S.V. (2015). The Archean nickel famine revisited. *Astrobiology*, **15**, 804-815.
- Konhauser, K. O., Robbins, L. J., Alessi, D. S., Flynn, S. L., Gingras, M. K., Martinez, R. E., Kappler, A., Swanner, E. D., Li, Y- L., Crowe, S. A., Planavsky, N.J., Reinhard, C. T., Lalonde, S. V. (2018) Phytoplankton contributions to the trace-element composition of Precambrian banded iron formations. *Geol. Soc. Am. Bull.* **130**, 941-951.
- Koretsky, C. (2000) The significance of surface complexation reactions in hydrologic systems: a geochemist's perspective. *Journal of Hydrology* **230**, 127-171.
- Kvenvolden, K.A., Lorenson, T.D., Reeburgh, W.S. (2001). Attention turns to naturally occurring methane seepage. *EOS* **82**, 457-458.
- Lalonde, S. V., Konhauser, K. O., Reysenbach, A. -L., and Ferris, F.G. (2005) The experimental silicification of Aquificales and their role in hot spring sinter formation. *Geobiology* **3**, 41-52.
- Lalonde, S., Amskold, L., Warren L. A., and Konhauser, K. O. (2007) Surface chemical reactivity and metal adsorptive properties of natural cyanobacterial mats from an alkaline hot spring, Yellowstone National Park. *Chem. Geol.* **243**, 36-52.
- Lane, E.S., Jang, K., Cullen, J.T., Maldonado, M.T. (2008). The interaction between inorganic iron and cadmium uptake in the marine diatom *Thalassiosira oceanica*. *Limnology and Oceanography*, **53**, 1784-1789.

- Lang, S.Q., Butterfield, D.A., Lilley, M.D., Johnson, H.P., Hedges, J.I. (2006). Dissolved organic carbon in ridge-axis and ridge-flank hydrothermal systems. *Geochimica et Cosmochimica Acta* **70**, 3830-3842.
- Laurenceau, E.C., Trull, T.W., Davies, D.M., Bray, S.G., Doran, J., Planchon, F., Carlotti, F., Jouandet, M.P., Cavagna, A.J., Waite, A.M., Blain, S. (2014). The relative importance of phytoplankton aggregates and zooplankton fecal pellets to carbon export: insights from free-drifting sediment trap deployments in naturally iron-fertilised waters near the Kerguelen plateau. *Biogeosciences*, **11**, 13623-13673.
- Lechtenfeld, O. J., Kattner, G., Flerus, R., McCallister, S. L., Schmitt-Kopplin, P., Koch, B. P. (2014). Molecular transformation and degradation of refractory dissolved organic matter in the Atlantic and Southern Ocean. *Geochimica et Cosmochimica Acta* **126**, 321-337.
- Leefman, T., Frickenhaus, S., Koch, B. P. (2019). UltraMassExplorer: a browser-based application for the evaluation of high-resolution mass spectrometric data. *Rapid Communications in Mass Spectrometry* **33**, 193-202.
- Le Moigne, F.A.C. (2019). Pathways of organic carbon downward transport by the oceanic biological carbon pump. *Frontiers in Marine Science*, **6**, 634.
- Li, Y., Harir, M., Uhl, J., Kanawati, B., Lucio, M., Smirnov, K. S., Koch, B. P., Schmitt-Kopplin, P., Hertkorn, N. (2017). How representative are dissolved organic matter (DOM) extracts? A comprehensive study of sorbent selectivity for DOM isolation. *Water Research* **116**, 316-323.
- Li, Y., Sutherland, B.R., Gingras, M.K., Owttrim, G.W., Konhauser, K.O. (2021). A novel approach to investigate the deposition of (bio) chemical sediments: The sedimentation

- velocity of cyanobacteria-ferrihydrite aggregates. *Journal of Sedimentary Research* **91**, 390-398.
- Lin, Y.-S., Koch, B.P., Feseker, T., Ziervogel, K., Goldhammer, T., Schmidt, F., Witt, M., Kellermann, M.Y., Zabel, M., Teske, A., Hinrichs, K.-U. (2017). Near-surface heating of young rift sediment causes mass production and discharge of reactive dissolved organic matter. *Scientific Reports* **7**, 44864.
- Linkhorst, L., Dittmar, T., Waska, H. (2017). Molecular fractionation of dissolved organic matter in a shallow subterranean estuary: the role of the iron curtain. *Environmental Science and Technology* **51**, 1312-1320.
- Liu, Y., Alessi, D. S., Owtrim, G. W., Petrash, D. A., Mloszewska, A. M., Lalonde, S. V., Martinez, R. E., Zhou, Q., Konhauser, K. O. (2015) Cell surface reactivity of *Synechococcus* sp. PCC 7002: Implications for metal sorption from seawater. *Geochim. Cosmochim. Acta* **169**, 30-44.
- Liu, Y., Alessi, D., Owtrim, G.W., Kenney, J.P.L., Zhou, Q.X., Lalonde, S.V., and Konhauser, K.O. (2016) Cell surface acid-base properties of the cyanobacterium *Synechococcus*: Influences of nitrogen source, growth phase and N:P ratios. *Geochim. Cosmochim. Acta* **187**, 179-194.
- Lodeiro, P., Rey-Castro, C., David, C., Achterberg, E.P., Puy, J., Gledhill, M. (2020). Acid-base properties of dissolved organic matter extracted from the marine environment. *Science of the Total Environment*, **729**, 138437.
- Lohan, M. C., Crawford, D. W., Purdie, D. A., Statham, P. J. (2005). Iron and zinc enrichments in the northeastern subarctic Pacific: Ligand production and zinc availability in response to phytoplankton growth. *Limnology and Oceanography*, **50**, 1427-1437.

- Lonborg, C., Alvarez-Salgado, X.A., Letscher, R.T., Hansell, D.A. (2018). Large stimulation of recalcitrant dissolved organic carbon degradation by increasing ocean temperatures. *Frontiers in Marine Science* **4**, 436.
- Ma, X., Coleman, M.L., Waldbauer, J.R. (2018). Distinct molecular signatures in dissolved organic matter produced by viral lysis of marine cyanobacteria. *Environmental Microbiology* **20**, 3001-3011.
- Mand, K. Lalonde, S.V., Robbins, L.J., Thoby, M., Paiste, K., Kreitsmann, T., Paiste, P., Reinhard, C.T., Romashkin, A.E., Planavsky, N.J., Kirsimae, K., Lepland, A., Konhauser, K.O. (2020). Palaeoproterozoic oxygenated oceans following the Lomagundi-Jatuli Event. *Nature Geoscience* **13**, 302-306.
- Martin, J. H., Knauer, G. A., Karl, D. M., Broenkow, W. W. (1987). VERTEX: carbon cycling in the northeast Pacific. *Deep-Sea Research* **34**, 267-285.
- Minnes, R., Nissinmann, M., Maisels, Y., Gerlitz, G., Katzir, A., Yosef, R. (2017) Using Attenuated Total Reflection – Fourier Transform Infra-Red (ATR-FTIR) spectroscopy to distinguish between melanoma cells with a different metastatic potential. *Sci. Rep.* **7**, 4381.
- Moran, M. A., Kujawinski, E. B., Stubbins, A., Fatland, R., Aluwihare, L. I., Buchan, A., Crump, B. C., Dorrestein, P. C., Dyrman, S. T., Hess, N. J., Howe, B., Longnecker, K., Medeiros, P. M., Niggemann, J., Obernosterer, I., Repeta, D. J., Waldbauer, J. R. (2016). Deciphering ocean carbon in a changing world. *Proceedings of the National Academy of Sciences*, **113**, 3143-3151.
- Morel, F.M.M., Price, N.M. (2003). The biogeochemical cycles of trace metals in the oceans. *Science* **300**, 944-947.

- Muller, F. L. L., Batchelli, S. (2013). Copper binding by terrestrial versus marine organic ligands in the coastal plume of River Thurso, North Scotland. *Estuarine, Coastal and Shelf Science*, **133**, 137-146.
- Nell, R. M., Fein, J. B. (2017). Influence of sulfhydryl sites on metal binding by bacteria. *Geochimica et Cosmochimica Acta* **199**, 210-221.
- Ngwenya, B. T., Tourney, J., Magennis, M., Kapetas, L., Olive, V. (2009) A surface complexation framework for predicting water purification through metal biosorption. *Desalination* **248**, 344-351.
- Nightingale Jr., E.R. (1959). Phenomenological theory of ion solvation. Effective radii of hydrated ions. *Journal of Physical Chemistry*, **63**, 1381-1387.
- Niu, X.-Z., Harir, M., Schmitt-Kopplin, P., Croue, J.-P. (2018). Characterisation of dissolved organic matter using Fourier-transform ion cyclotron resonance mass spectrometry: Type-specific unique signatures and implications for reactivity. *Science of the Total Environment* **644**, 68-76.
- Opsahl, S., Benner, R. (1997). Distribution and cycling of terrigenous dissolved organic matter in the ocean. *Nature* **386**, 480-482.
- Owtrim, G.W. (2012). RNA Helicases in Cyanobacteria: Biochemical and Molecular Approaches. *Methods in Enzymology* **511**, 385-403.
- Ozturk, S., Aslim, B., Turker, A. R. (2009) Removal of Cadmium Ions from Aqueous Samples by *Synechocystis* Sp. *Sep. Sci. Technol.* **44**, 1467-1483.
- Ozturk, S., Aslim, B., Suludere, Z. (2010) Cadmium(II) sequestration characteristics by two isolates of *Synechocystis* sp. In terms of exopolysaccharide (EPS) production and monomer composition. *Bioresour. Technol.* **101**, 9742-9748.

- Padan, J., Marcinek, S., Cindric, A.M., Santinelli, C., Broji, S.R., Radakovitch, O., Garnier, C., Omanovic, D. (2021). Organic copper speciation by anodic stripping voltammetry in estuarine waters with high dissolved organic matter. *Frontiers in Chemistry*, **8**, 628749.
- Paxeus, N., Wedborg, M. (1985). Acid-base properties of aquatic fulvic acid. *Analytica Chimica Acta*, **169**, 87-98.
- Pedler-Sherwood, B., Shaffer, E. A., Reyes, K., Longnecker, K., Aluwihare, L. I., Azam, F. (2015). Metabolic characterization of a model heterotrophic bacterium capable of significant chemical alteration of marine dissolved organic matter. *Marine Chemistry* **177**, 357-365.
- Petrash, D. P., Raudsepp, M., Lalonde, S. V., and Konhauser, K.O. (2011) Assessing the importance of matrix materials in biofilm chemical reactivity: Insights from proton and cadmium adsorption onto the commercially-available biopolymer alginate. *Geomicrobiol. J.* **28**, 266-273.
- Pernthaler, J. (2005). Predation on prokaryotes in the water column and its ecological implications. *Nature Reviews Microbiology*, **3**, 537-546.
- Phoenix, V. R., Martinez, R. E., Konhauser, K. O., Ferris, F. G. (2002) *Characterization and Implications of the Cell Surface Reactivity of Calothrix sp. Strain KC97*. *Appl. Environ. Microbiol.* **68**, 4827-4834.
- Planavsky, N.J., Rouxel, O.J., Bekker, A., Lalonde, S.V., Konhauser, K.O., Reinhard, C.T., Lyons, T.W. (2010). The evolution of the marine phosphate reservoir. *Nature Letters* **467**, 1088-1090.
- Playter, T., Konhauser, K.O., Owttrim, G.W., Hodgson, C., Warchola, T., Mloszewska, A.M., Sutherland, B., Bekker, A., Zonneveld, J.P., Pemberton, S.G., Gingras, M.K. (2017).

- Microbe-clay interactions as a mechanisms for the preservation of organic matter and trace metal biosignatures in black shales. *Chemical Geology*, **459**, 75-90.
- Pohlman, J.W., Bauer, J.E., Waite, W.F., Osburn, C.L., Chapman, N.R. (2010). Methane hydrate-bearing seeps as a source of aged dissolved organic carbon to the oceans. *Nature Geoscience* **4**, 37-41.
- Rakhimberdieva, M.G., Vavilin, D.V., Vermaas, W.F.J., Elanskaya, I.V., Karapetyan, N.V. (2007). Phycobilin/chlorophyll excitation equilibration upon carotenoid-induced non-photochemical fluorescence quenching in phycobilisomes of the cyanobacterium *Synechocystis* sp. PCC 6803. *Biochimica et Biophysica Acta – Bioenergetics* **1767**, 757-765.
- Raven, J.A., and Falkowski, P.G. (1999). Oceanic sinks for atmospheric CO<sub>2</sub>. *Plant, Cell & Environment*, **22**, 741–755.
- Reed, R. H., Warr, S. R. C., Richardson, D. L., Moore, D. J., Stewart, W. D. P. (1985) Multiphasic osmotic adjustment in a euryhaline cyanobacterium. *FEMS Microbiol. Letters* **28**, 225-229.
- Ridgwell, A., Arndt, S. (2015). Chapter 1: Why Dissolved Organics Matter: DOC in Ancient Oceans and Past Climate Change. In: Hansell, D. A., Carlson, C. A. *Biogeochemistry of Marine Dissolved Organic Matter*. Elsevier, Cambridge, Massachusetts, pp. 1-20.
- Rippka, R., Deruelles, J., Waterbury, J. B., Herdman, M., Stainer, R. Y. (1979) Generic assignments, strain histories and properties of pure cultures of cyanobacteria. *J. Gen. Microbiol.* **111**, 1-61.
- Ritchie, J.D., Perdue, E.M. (2008). Analytical constraints on acidic functional groups in humic substances. *Organic Geochemistry*, **39**, 783-799.
- Robbins, L.J., Lalonde, S.V., Planavsky, N.J., Partin, C.A., Reinhard, C.T., Kendall, B., Scott, C., Hardisty, D.S., Gill, B.C., Alessi, D.S., Dupont, C.L., Saito, M.A., Crowe, S.A., Poulton,

- S.W., Bekker, A., Lyons, T.W., Konhauser, K.O. (2016). Trace elements at the intersection of marine biological and geochemical evolution. *Earth-Science Reviews*, **163**, 323-348.
- Saba, G.K., Steinberg, D.K., Bronk, D.A. (2011). The relative importance of sloppy feeding, excretion, and fecal pellet leaching in the release of dissolved carbon and nitrogen by *Acartia tonsa* copepods. *Journal of Experimental Marine Biology and Ecology* **404**, 47-56.
- Saito, M.A., Sigman, D.M., Morel, F.M.M. (2003). The bioinorganic chemistry of the ancient ocean: The coevolution of cyanobacterial metal requirements and biogeochemical cycles at the Archean-Proterozoic boundary? *Inorganica Chimica Acta* **356**, 308-318.
- Saito, M.A., Goepfert, T.J., Noble, A.E., Bertrand, E.M., Sedwick, P.N. (2010). A seasonal study of dissolved cobalt in the Ross Sea, Antarctica: Micronutrient behavior, absence of scavenging, and relationships with Zn, Cd, and P. *Biogeosciences*, **7**, 4059-4082.
- Sanchez-Baracaldo, P., Bianchini, G., Wilson, J.D., Knoll, A.H. (2021 in press). Cyanobacteria and biogeochemical cycles through Earth history. *Trends in Microbiology*.  
<https://doi.org/10.1016/j.tim.2021.05.008>
- Schmidt, F., Elvert, M., Koch, B.P., Witt, M., Hinrichs, K., U. (2009). Molecular characterization of dissolved organic matter in pore water of continental shelf sediments. *Geochimica et Cosmochimica Acta* **73**, 3337-3358.
- Scott, C., Planavsky, N.J., Dupont, C.L., Kendall, B., Gill, B.C., Robbins, L.J., Husband, K.F., Arnold, G.L., Wing, B.A., Poulton, S.W., Bekker, A., Anbar, A.D., Konhauser, K.O., Lyons, T.W. (2013). Bioavailability of zinc in marine sediments through time. *Nature Geoscience*, **6**, 125-128.

- Shank, G.C., Lee, R., Vahatalo, A., Zepp, R.G., Bartels, E. (2010). Production of chromophoric dissolved organic matter from mangrove leaf litter and floating *Sargassum* colonies. *Marine Chemistry* **119**, 172-181.
- Skyllberg, U., Drott, A. (2010). Competition between disordered iron sulfide and natural organic matter associated thiols for mercury(II)- an EXAFS study. *Environmental Science and Technology* **44**, 1254-1259.
- Sleighter, R. L., Hatcher, P. G. (2008). Molecular characterization of dissolved organic matter (DOM) along a river to ocean transect of the lower Chesapeake Bay by ultrahigh resolution electrospray ionization Fourier transform ion cyclotron resonance mass spectrometry. *Marine Chemistry* **110**, 140-152.
- Stanier, R. Y., Kunisawa, R., Mandel, M., Cohen-Bazire, G. (1971) Purification and Properties of Unicellular Blue-Green Algae (Order *Chroococcales*). *Bacteriol. Rev.* **35**, 171-205.
- Stedmon, C.A., Markager, S., Bro, R. (2003). Tracing dissolved organic matter in aquatic environments using a new approach to fluorescence spectroscopy. *Marine Chemistry* **82**, 239-254.
- Stedmon, C. A., Nelson, N. B. (2015). Chapter 10: The Optical Properties of DOM in the Ocean. In: Hansell, D. A., Carlson, C. A. *Biogeochemistry of Marine Dissolved Organic Matter*. Elsevier, Cambridge, Massachusetts, pp. 481-508.
- Stevens, S., Van Baalen, C. (1973). Characteristics of nitrate reductions in a mutant of the blue-green alga *Agmenellum quadruplicatum*. *Plant Physiology*, **51**, 350-356.
- Strom, S. L., Benner, R., Ziegler, S., Dagg, M. J. (1997). Planktonic grazers are a potentially important source of marine dissolved organic carbon. *Limnology and Oceanography* **42**, 1364-1374.

- Stukel, M.R., Decima, M., Selph, K.E., Taniguchi, D.A.A., Landry, M.R. (2013). The role of *Synechococcus* in vertical flux in the Costa Rica upwelling dome. *Progress in Oceanography*, **112-113**, 49-59.
- Sunda, W.G., Huntsman, S.A. (1995). Cobalt and zinc interreplacement in marine phytoplankton: biological and geochemical implications. *Limnology and Oceanography*, **40**, 1404-1417.
- Sunda, W.G. (2012). Feedback interactions between trace metal nutrients and phytoplankton in the ocean. *Frontiers in Microbiology*, **3**, 1–22.
- Suttle, C. (2007). Marine viruses – major players in the global ecosystem. *Nature Reviews Microbiology* **5**, 801-812.
- Swaren, L., Hao, W., Melnyk, S., Baker, D., Li, Y., Owttrim, G.W., Zeng, H., Gingras, M.K., Alessi, D.S., Konhauser, K.O. (2021). Surface reactivity of the cyanobacterium *Synechocystis* sp. PCC 6803 – Implications for trace metal transport to the ocean. *Chemical Geology*, **562**, 120045.
- Swarzenski, P.W., Orem, W.H., McPherson, B.F., Baskaran, M., Wan, Y. (2006). Biogeochemical transport in the Loxahatchee River estuary, Florida: The role of submarine groundwater discharge. *Marine Chemistry* **101**, 248-265.
- Tiwari, S., Mohanty, P. (1996) Cobalt induced changes in photosystem activity in *Synechocystis* PCC 6803: Alterations in energy distribution and stoichiometry. *Photosynth. Res.* **50**, 243-256.
- Tremblay, L., Caparros, J., Leblanc, K., Obernosterer, I. (2015). Origin and fate of particulate and dissolved organic matter in a naturally iron-fertilized region of the Southern Ocean. *Biogeosciences*, **12**, 607-621.

- Twining, B.S., Baines, S.B. (2013). The trace metal composition of marine phytoplankton. *Annual Reviews in Marine Science*, **5**, 191–215.
- Van den Berg, C.M.G., Nimmo, M. (1987). Determination of interactions of nickel with dissolved organic material in seawater using cathodic stripping voltammetry. *Science of the Total Environment*, **60**, 185-195.
- Van Mooy, B.A.S., Rocap, G., Fredricks, H.F., Evans, C.T., Devol, A.H. (2006). Sulfolipids dramatically decrease phosphorus demand by picocyanobacteria in oligotrophic marine environments. *Proceedings of the National Academy of Sciences* **103**, 8607-8612.
- Volkman, J. K., Tanoue, E. (2002). Chemical and biological studies of particulate organic matter in the ocean. *Journal of Oceanography* **58**, 265-279.
- Vraspir, J. M.; Butler, A. (2009). Chemistry of marine ligands and siderophores. *Annual Review of Marine Science* **1**, 43-63.
- Walker, B. D., Primeau, F. W., Beaupre, S. R., Guilderson, T. P., Druffel, E. R. M., McCarthy, M. D. (2016). Linked changes in marine dissolved organic carbon molecular size and radiocarbon age. *Geophysical Research Letters* **43**, 385-393.
- Walsh, M.J., Ahner, B.A. (2013). Determination of stability constants of Cu(I), Cd(II), and Zn(II) complexes with thiols using fluorescent probes. *Journal of Inorganic Biochemistry* **128**, 112-123.
- Wang, K., Wommack, E., Chen, F. (2011). Abundance and distribution of *Synechococcus* spp. And cyanophages in the Chesapeake Bay. *Applied and Environmental Microbiology*, **77**, 7459-7468.

- Warke, M.R., Di Rocco, T., Zerkle, A. L., Lepland, A., Prave, A.R., Martin, A.P., Ueno, Y., Condon, D.J., Claire, M.W. (2020). The Great Oxidation Event preceded a Paleoproterozoic “snowball Earth”. *PNAS* **117**, 13314-13320.
- Waterbury, J.B., Watson, S.W., Guillard, R.R.L., Brand, L.E. (1979). Widespread occurrence of a unicellular, marine, planktonic, cyanobacterium. *Nature*, **277**, 293-294.
- Woods, G. C., Simpson, M. J., Koerner, P. J., Napoli, A., Simpson, A. J. (2011). HILIC-NMR; Toward the Identification of Individual Molecular Components in Dissolved Organic Matter. *Environmental Science and Technology* **45**, 3880-3886.
- Worden, A.Z., Nolan, J.K., Palenik, B. (2004). Assessing the dynamics and ecology of marine picoplankton: the importance of the eukaryotic component. *Limnology and Oceanography*, **49**, 168-179.
- Yee, N., Fein, J. (2001) Cd adsorption onto bacterial surfaces: A universal adsorption edge? *Geochim. Cosmochim. Acta* **65**, 2037-2042.
- Yu, Q., Szymanowski, J. Myneni, S. C. B., Fein, J. B. (2014) Characterization of sulfhydryl sites within bacterial cell envelopes using selective site-blocking and potentiometric titrations. *Chem. Geol.* **373**, 50-58.
- Yu, Q., Fein, J.B. (2016). Sulfhydryl binding sites within bacterial extracellular polymeric substances. *Environmental Science and Technology*, **50**, 5498-5505.
- Yu, Q., Fein, J. B. (2017) Enhanced Removal of Dissolved Hg(II), Cd (II), and Au (III) from Water by *Bacillus subtilis* Bacterial Biomass Containing an Elevated Concentration of Sulfhydryl Sites. *Environmental Science and Technology* **51**, 14360-14367.

- Yu, Q., Boyanov, M. I., Liu, J., Kemmer, K. M., Fein, J. B. (2018) Adsorption of Selenite onto *Bacillus subtilis*: The Overlooked Role of Cell Envelope Sulfhydryl Sites in the Microbial Conversion of Se(IV). *Environmental Science and Technology* **52**, 10400-10407.
- Zark, M., Christoffers, J., Dittmar, T. (2017). Molecular properties of deep-sea dissolved organic matter are predictable by the central limit theorem: Evidence from tandem FT-ICR-MS. *Marine Chemistry* **191**, 9-15.
- Zark, M., Dittmar, T. (2018). Universal molecular structures in natural dissolved organic matter. *Nature Communications* **9**, 3178.
- Zhang, K., Kurano, N., Miyachi, S. (1999) Outdoor culture of a cyanobacterium with a vertical flat-plate photobioreactor: effects on productivity of the reactor orientation, distance setting between the plates, and culture temperature. *Appl. Microbiol. Biotechnol.* **52**, 781-786.
- Zhang, Y., Green, N.W., Perdue, E.M. (2013). Acid-base properties of dissolved organic matter from pristine oil-impacted marshes of Barataria Bay, Louisiana. *Marine Chemistry*, **155**, 42-49.
- Zhang, J., Kattner, G., Koch, B.P. (2019). Interactions of trace elements and organic ligands in seawater and implications for quantifying biogeochemical dynamics: A review. *Earth Science Reviews*, **192**, 631-649.
- Zhao, Z., Gonsoir, M., Luek, J., Timko, S., Ianiri, H., Hertkorn, N., Schmitt-Kopplin, P., Fang, X., Zeng, Q., Jiao, N., Chen F. (2017). Picocyanobacteria and deep-ocean fluorescent dissolved organic matter share similar optical properties. *Nature Communications* **8**, 15284.
- Zhao, Z., Gonsoir, M., Schmitt-Kopplin, P., Zhan, Y., Zhang, J., Jiao, N., Chen F. (2019). Microbial transformation of virus-induced dissolved organic matter from picocyanobacteria: coupling of bacterial diversity and DOM chemodiversity. *The ISME Journal* **13**, 2551-2565.

- Zhang, D., Pan, X., Zhao, L., Mu, G. (2011). Biosorption of Antimony (Sb) by the cyanobacterium *Synechocystis* sp. *Pol. J. Environ.* **20**, 1353-1358.
- Zheng, Q., Chen, Q., Cai, R., He, C., Guo, W., Wang, Y., Shi, Q., Chen, C., Jiao, N. (2019). Molecular characteristics of microbially mediated transformation of *Synechococcus*-derived dissolved organic matter as revealed by incubation experiments. *Environmental Microbiology* **21**, 2533-2542.
- Zhou, Q., Liu, Y., Li, T., Zhao, H., Alessi, D.S., Liu, W., Konhauser, K.O. (2021). Cadmium adsorption to clay-microbe aggregates: Implications for marine heavy metals cycling. *Geochimica et Cosmochimica Acta*, **290**, 124-136.

## Appendix 1: Supplementary information for Chapter 2

**SI Table 1.1:** Summary of previously identified and/or isolated strains of *Synechocystis* and their source environment.

<b>Strain</b>	<b>Location</b>	<b>Water Type</b>	<b>Reference</b>
<i>Synechocystis</i> sp. PCC 6803	California, USA	Freshwater	Stanier et al. 1971
<i>Synechocystis</i> sp. PCC 6902	Oregon, USA	Brackish water	Rippka et al. 1979
<i>Synechocystis</i> sp.	Hong Kong, China	Sewage treatment plants and polluted streams	Chong et al. 2000
<i>Synechocystis pevalekii</i>	Satluj River, India	Industrially polluted streams	Khattar, 2009
<i>Synechocystis</i> sp.	Uncali Stream/Mogan Lake/Bafa Lake, Turkey	Freshwater lakes & stream	Ozturk et al. 2009
<i>Synechocystis aquatilis</i> VAARA 1978/CB-3	Gulf of Finland	Brackish water	Pawlik and Skowronski, 1994
<i>Synechocystis aquatilis</i> SI-2	Kagoshima, Japan	Hydrothermal pool water on Satsuma-iwojima island	Zhang et al. 1999
<i>Synechocystis</i> sp. UNIWG	Wadi Gaza Coastal Wetlands, Palestine	Brackish water	Abed et al. 2002
<i>Synechocystis</i> sp.	Lakes Bogoria, Nakuru, and Elmenteita, Kenya	Alkaline-saline lakes	Ballot et al. 2004
<i>Synechocystis</i> sp.	Kasur District and Muredkey, Pakistan	Polluted effluents	Hameed et al. 2013
<i>Synechocystis</i> sp.	NW to S Coastal, Portugal	Marine (rocky coastlines)	Martins et al. 2008
<i>Synechocystis</i> sp. E35	Kucukcekmece Lagoon, Turkey	Polluted lakewater	Demirel et al. 2009
<i>Synechocystis</i> sp.	East Kolkata Wetlands, India	Sewage recycling fish-pond	Roy et al. 2008
<i>Synechocystis</i> sp.	Lake Reeve, Australia Cochin Estuary, India	Coastal back-barrier lagoon Tropical, micro-tidal estuary	Davis et al. 1995 Abdulaziz et al. 2016
<i>Synechocystis aquatilis</i> '	Barra Lagoon, Brazil	Lagoon (salinity 3 – 12 ‰)	Nascimento and Azevedo, 1999

**SI Table 1.2:** Previous thermodynamic modeling of metals to *Synechocystis* cells.

Studied Metal	Langmuir Isotherm			Freundlich Isotherm			Reference
	$q_m$ (mg g <sup>-1</sup> )	$b$ (L mg <sup>-1</sup> )	$R^2$	$K$	$1/n$	$R^2$	
Cd	5.81	0.010	0.990	1.870	1.087 <sup>a</sup>	0.974	Ozturk et al. 2009
Fe	37.03	0.320	0.954	0.850	1.087 <sup>a</sup>	0.978	Demirel et al. 2009
Sb	4.68	0.235	0.990	1.004	0.407	0.971	Zhang et al. 2011

<sup>a</sup>value reported in terms of  $n$ , recalculated to  $1/n$ .

**SI Table 1.3:** Summary of duplicate, non-electrostatic protonation model results of *Synechocystis* titration data. Site concentration is in units of mol g<sup>-1</sup>.

0.01 M NaCl (Freshwater IS)						
pKa1	Site Concentration	pKa2	Site Concentration	pKa3	Site Concentration	V(Y)
2.86	2.57E-4	6.06	3.59E-5	10.00	6.63E-5	0.10
2.79	2.35E-4	6.24	3.22E-5	10.45	6.78E-5	0.10
2.82±0.05	2.46E-4±1.55E-5	6.15±0.12	3.41E-5±2.64E-6	10.23±0.32	6.70E-5±1.00E-6	
5.50	4.83E-5	9.93	6.86E-5			0.72
5.74	3.91E-5	10.00	7.04E-5			0.50
5.62±0.17	4.37E-5±6.55E-6	9.97±0.06	6.95E-5±1.29E-6			
9.47	9.01E-5					5.38
9.60	9.00E-5					3.43
9.54±0.09	9.01E-5±7.07E-7					
0.56 M NaCl (Marine IS)						
pKa1	Site Concentration	pKa2	Site Concentration	pKa3	Site Concentration	V(Y)
2.91	2.40E-4	6.19	2.94E-5	9.94	3.17E-5	0.12
2.72	2.85E-4	5.98	2.95E-5	10.17	5.06E-5	0.44
2.81±0.13	2.62E-4±3.17E-5	6.08±0.15	2.94E-5±4.95E-8	10.05±0.16	4.11E-5±1.34E-5	
5.37	3.99E-5	9.65	5.43E-5			0.85
5.37	4.22E-5	9.66	3.56E-5			0.76
5.37±0.00	4.10E-5±1.63E-6	9.65±0.00	4.49E-5±1.32E-5			
9.54	6.84E-5					3.20
8.71	5.49E-5					3.34
9.12±0.59	6.16E-5±9.58E-6					

**SI Table 1.4:** Attenuated total reflectance Fourier transform infrared spectroscopy peak wavenumbers ( $\text{cm}^{-1}$ ) functional group assignments for *Synechocystis* sp. PCC 6803 dry cells.

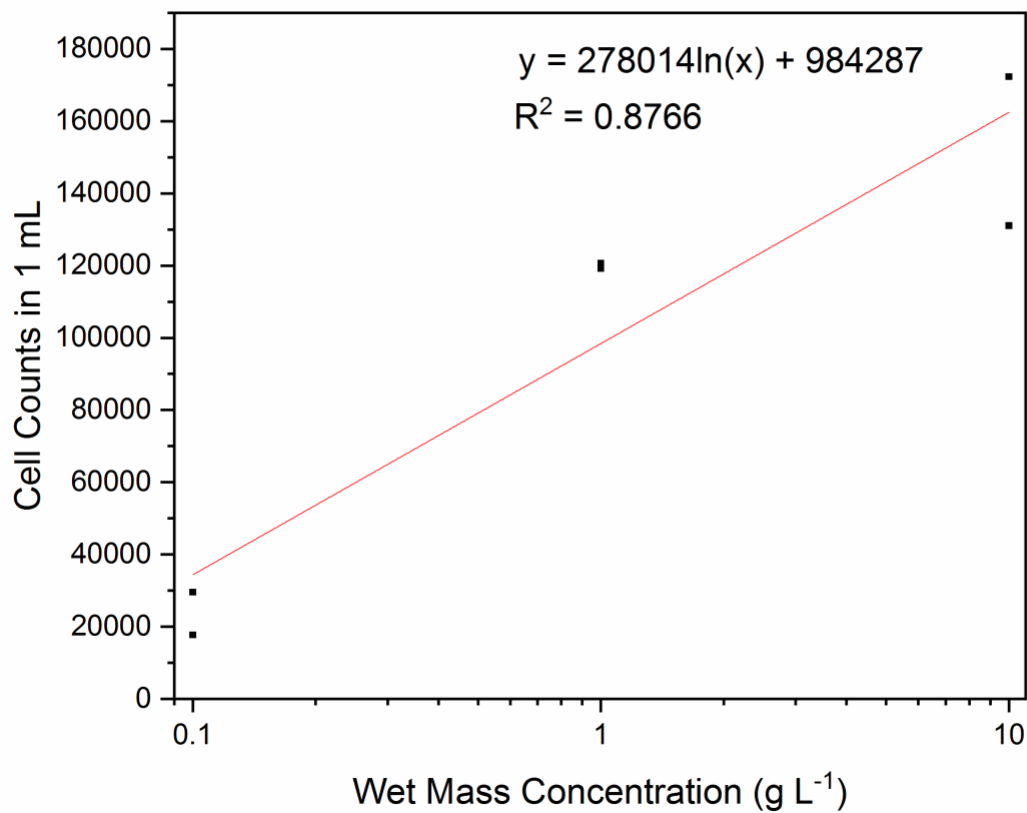
Wavenumber ( $\text{cm}^{-1}$ )	Assignment	Reference
3280	-NH	Ozturk et al. 2010
2955-2855	-CH	Jiang et al. 2004
1736	-C=O	Delille et al. 2007
1646	-NH (amide I)	Delille et al. 2007; Minnes et al. 2017
1534	-NH (amide II)	Delille et al. 2007; Minnes et al. 2017
1444	-NH (amide III)	Delille et al. 2007
1385-1342	-CO	Zhang et al. 2011
1242 (nucleic acid region)	-PO	Jiang et al. 2004; Delille et al. 2007
1200-950 (carbohydrate region)	-CO	Bouhedja et al. 1997; Delille et al. 2007
1036	-PO	Zhang et al. 2011

**SI Table 1.5:** Cd(II) hydrolysis and chloride complex reactions and thermodynamic stability constants used for creating the surface complexation model. Cd hydrolysis reactions and log K values taken from Baes and Mesmer (1976). Cd chloride complexes and logK values taken from Zirino and Yamamoto (1972) and logK values of carbonic acids and Ksp value of Cd carbonate taken from Stipp et al. (1993).

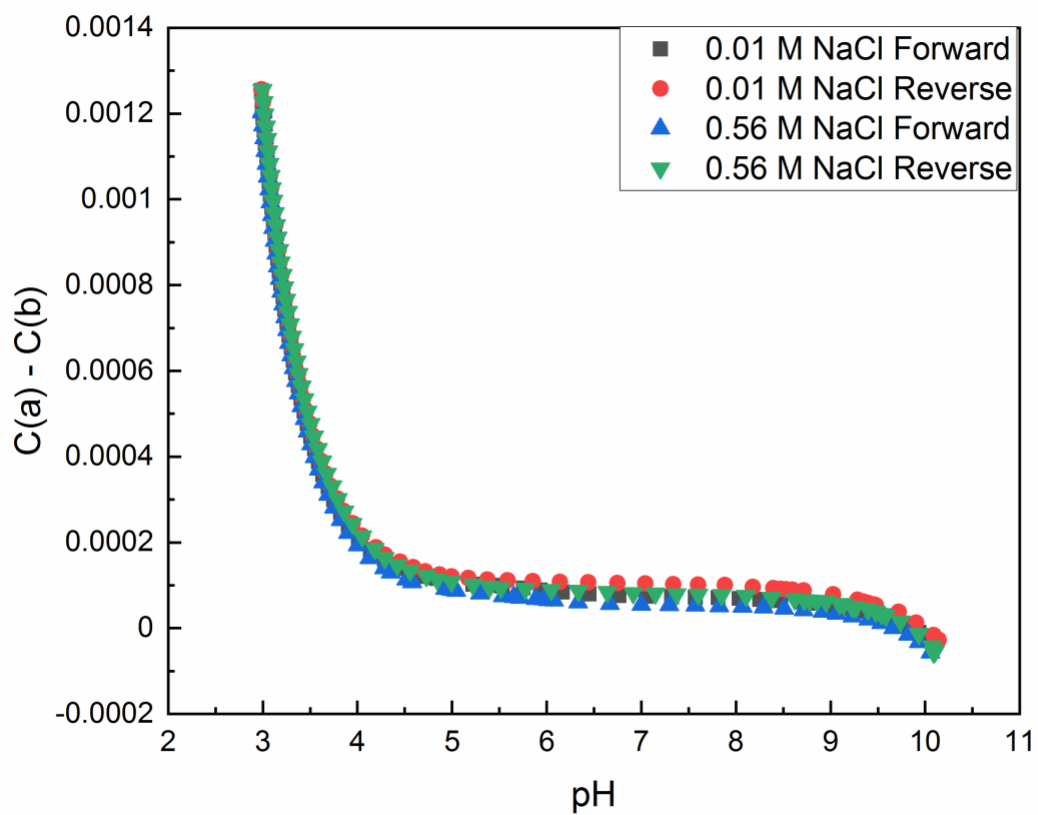
Reaction	log K
$\text{Cd}^{2+} + \text{H}_2\text{O} = \text{CdOH}^+ + \text{H}^+$	-10.1
$\text{Cd}^{2+} + 2\text{H}_2\text{O} = \text{Cd}(\text{OH})_{2(\text{aq})} + 2\text{H}^+$	-20.3
$\text{Cd}^{2+} + 3\text{H}_2\text{O} = \text{Cd}(\text{OH})^- + 3\text{H}^+$	-31.7
$\text{Cd}^{2+} + 4\text{H}_2\text{O} = \text{Cd}(\text{OH})^{2-} + 4\text{H}^+$	-47.3
$2\text{Cd}^{2+} + \text{H}_2\text{O} = \text{Cd}_2(\text{OH})^{3+} + \text{H}^+$	-9.4
$4\text{Cd}^{2+} + 4\text{H}_2\text{O} = \text{Cd}_4(\text{OH})_4^{4+} + 4\text{H}^+$	-32.8
$\text{Cd}^{2+} + \text{Cl}^- = \text{CdCl}^+$	2.0
$\text{Cd}^{2+} + 2\text{Cl}^- = \text{CdCl}_2$	2.7
$\text{Cd}^{2+} + 3\text{Cl}^- = \text{CdCl}_3^-$	2.1
$\text{CO}_2 + \text{H}_2\text{O} = \text{H}_2\text{CO}_3$	-1.46
$\text{H}_2\text{CO}_3 = \text{H}^+ + \text{HCO}_3^-$	-6.36
$\text{HCO}_3^- = \text{CO}_3^{2-} + \text{H}^+$	-10.33
$\text{Cd}^{2+} + \text{CO}_3^{2-} = \text{CdCO}_3(\text{s})$	12.10

**SI Table 1.6:** Modeling exercise results: “Blank Subtracted” indicates that the FITEQL 4.0 surface complexation model was fit using Cd adsorption data with the experimental blank Cd adsorption results subtracted from the *Synechocystis* adsorption results (see Figure S8). “Including Carbonic Acid System” indicates that the last 4 reactions from Table S5 were included in the surface complexation model. “N/C” indicates there was no convergence of the FITEQL 4.0 optimization procedure.

Model	Ionic Strength	logK <sub>Cd1</sub>	logK <sub>Cd2</sub>	logK <sub>Cd3</sub>	V(y)
Blank Subtracted (3-site)	0.01 M	2.78	4.01	N/A (-158)	2.02
	0.56 M	3.74	5.99	8.16	0.35
Blank Subtracted (2-site)	0.01 M	6.88	N/A (-155)	-	2.32
	0.56 M	5.65	7.83	-	0.31
Blank Subtracted (1-site)	0.01 M	10.74	-	-	0.72
	0.56 M	7.39	-	-	6.24
Including Carbonic Acid System (3-site)	0.01 M	N/C	-	-	-
	0.56 M	N/C	-	-	-
Including Carbonic Acid System (2-site)	0.01 M	N/C	-	-	-
	0.56 M	N/C	-	-	-
Including Carbonic Acid System (1-site)	0.01 M	23.19	-	-	19.26
	0.56 M	21.05	-	-	5.09



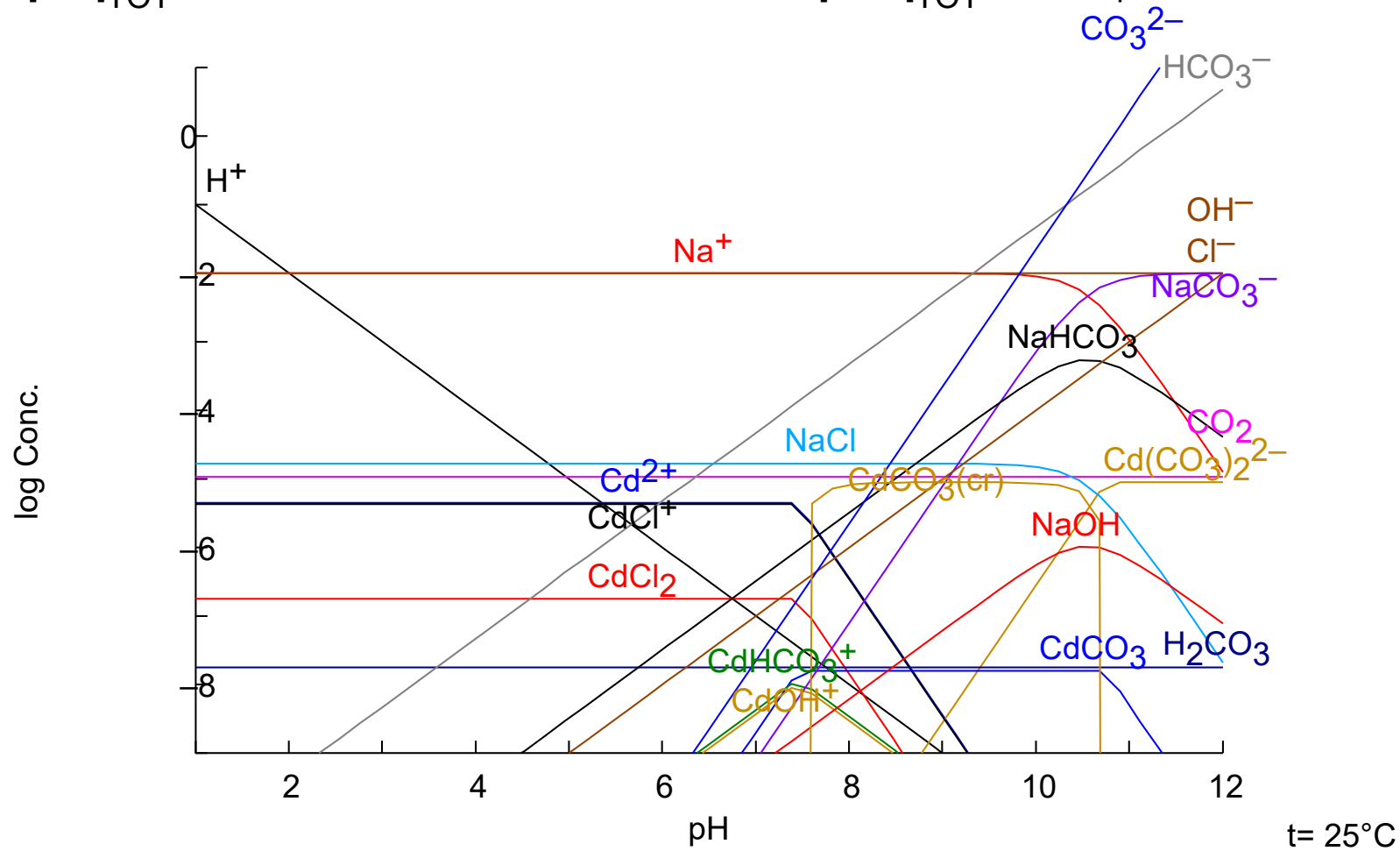
**SI Figure 1.1:** Flow cytometer (Attune NxT Flow Cytometer, ThermoFisher Scientific) data showing *Synechocystis* sp. PCC cell counts following cell washing at wet mass concentrations of 0.1 g L<sup>-1</sup>, 1 g L<sup>-1</sup> and 10 g L<sup>-1</sup>.

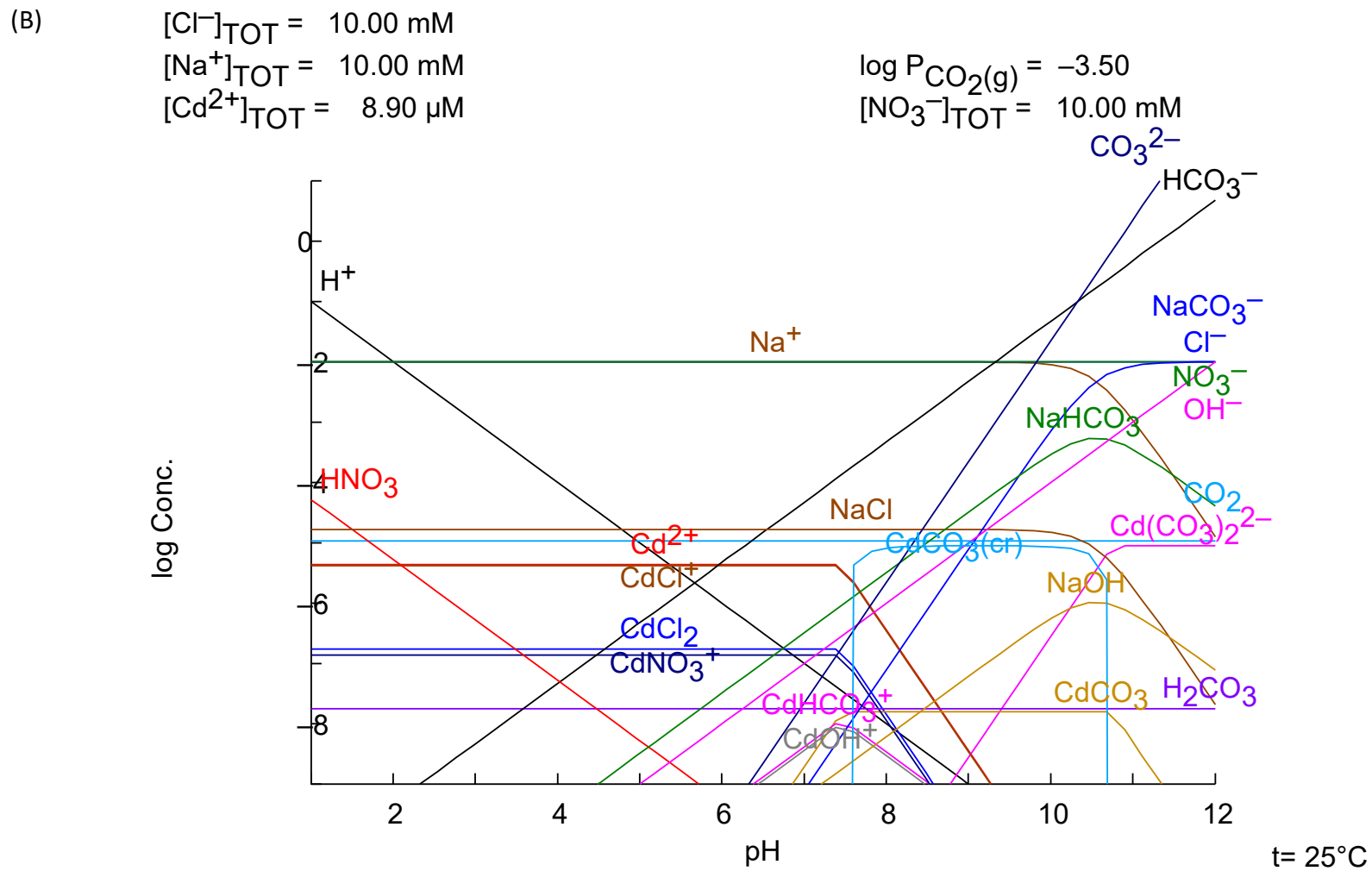


**SI Figure 1.2:** Forward and reverse titration plots for  $1 \text{ g L}^{-1}$  *Synechocystis* sp. PCC 6803 in both 0.01 and 0.56 M NaCl.  $C(a) - C(b)$  indicates the proton budget between the concentration of acid (0.1 M  $\text{HNO}_3$ ) and base (0.1 M  $\text{NaOH}$ ) in the system.

(A)  $[\text{Cl}^-]_{\text{TOT}} = 10.00 \text{ mM}$   
 $[\text{Na}^+]_{\text{TOT}} = 10.00 \text{ mM}$

$\log P_{\text{CO}_2(\text{g})} = -3.50$   
 $[\text{Cd}^{2+}]_{\text{TOT}} = 8.90 \text{ } \mu\text{M}$

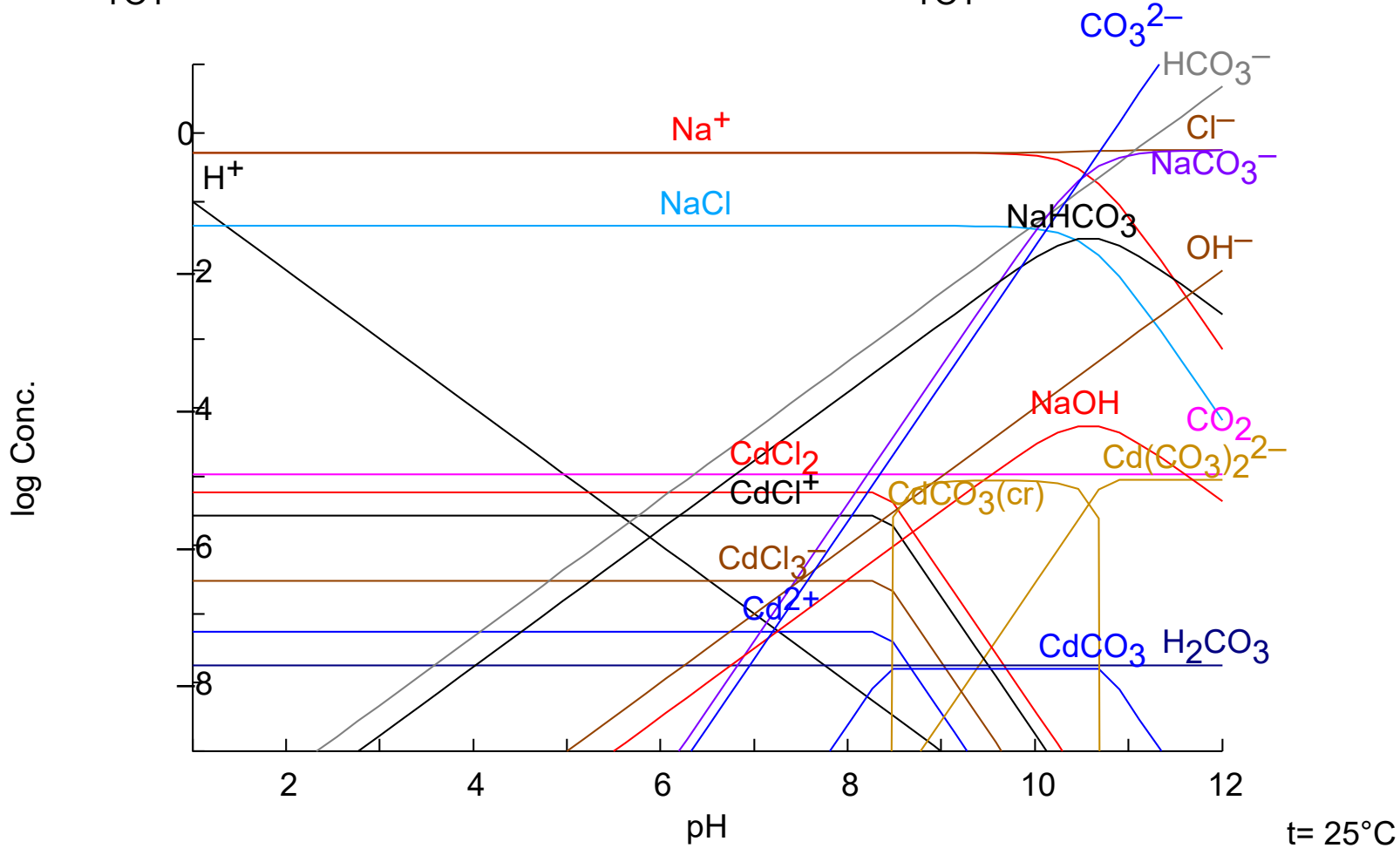




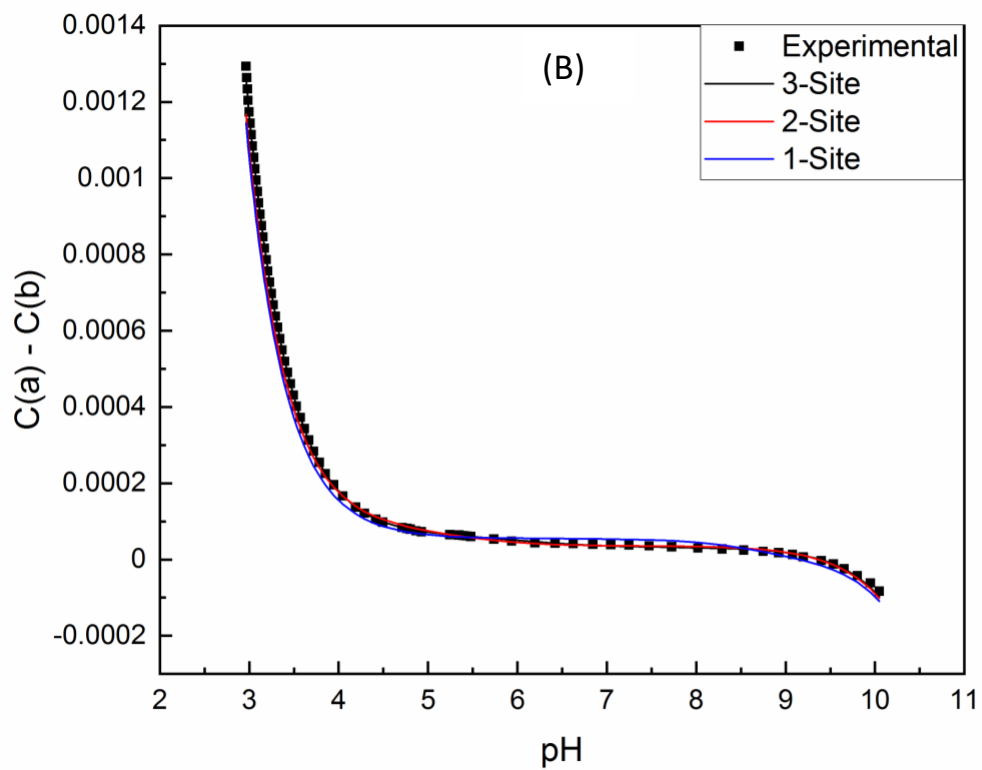
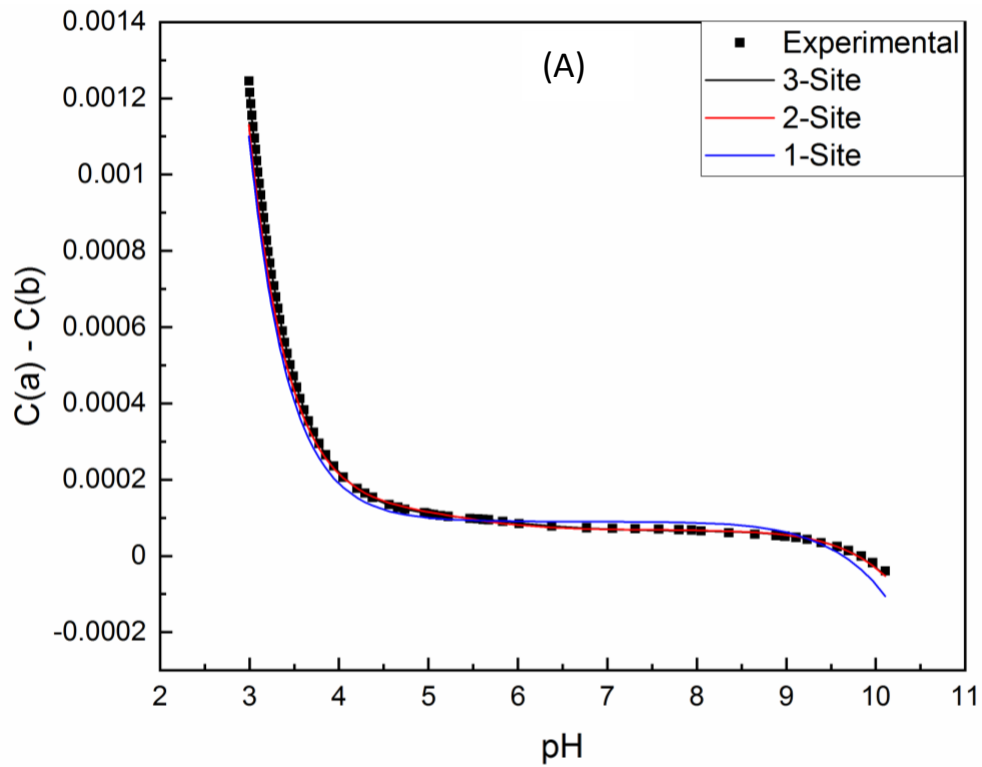
**SI Figure 1.3:** Speciation diagram of experimental conditions in (A) 0.01 M NaCl, and (B) experimental conditions including equal amounts of  $\text{NO}_3^-$  and  $\text{Cl}^-$  anions.

$[\text{Cl}^-]_{\text{TOT}} = 560.00 \text{ mM}$   
 $[\text{Na}^+]_{\text{TOT}} = 560.00 \text{ mM}$

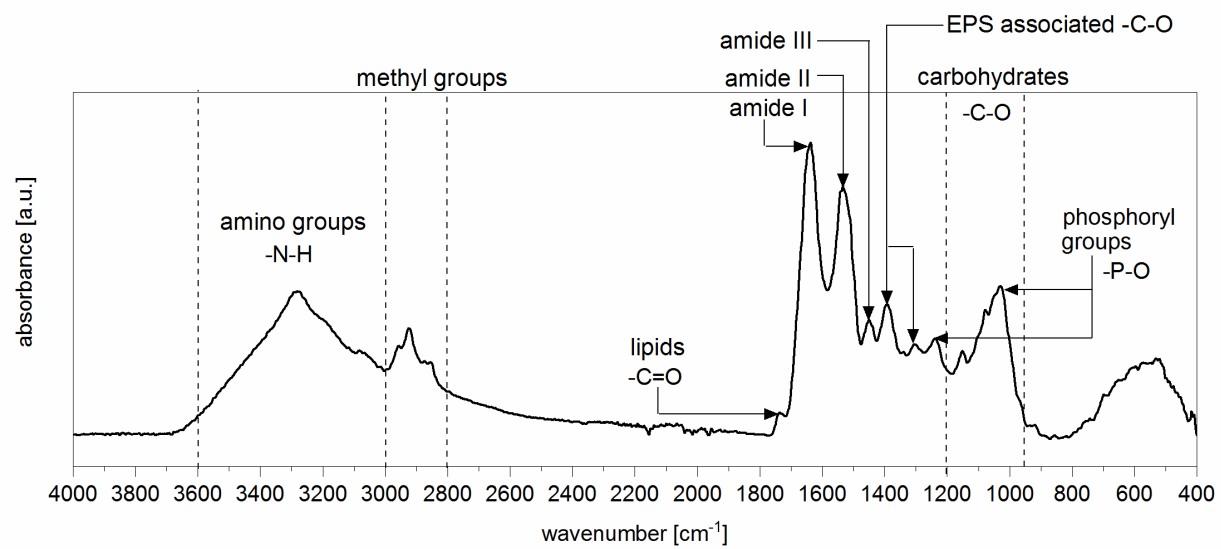
$\log P_{\text{CO}_2(\text{g})} = -3.50$   
 $[\text{Cd}^{2+}]_{\text{TOT}} = 8.90 \text{ } \mu\text{M}$



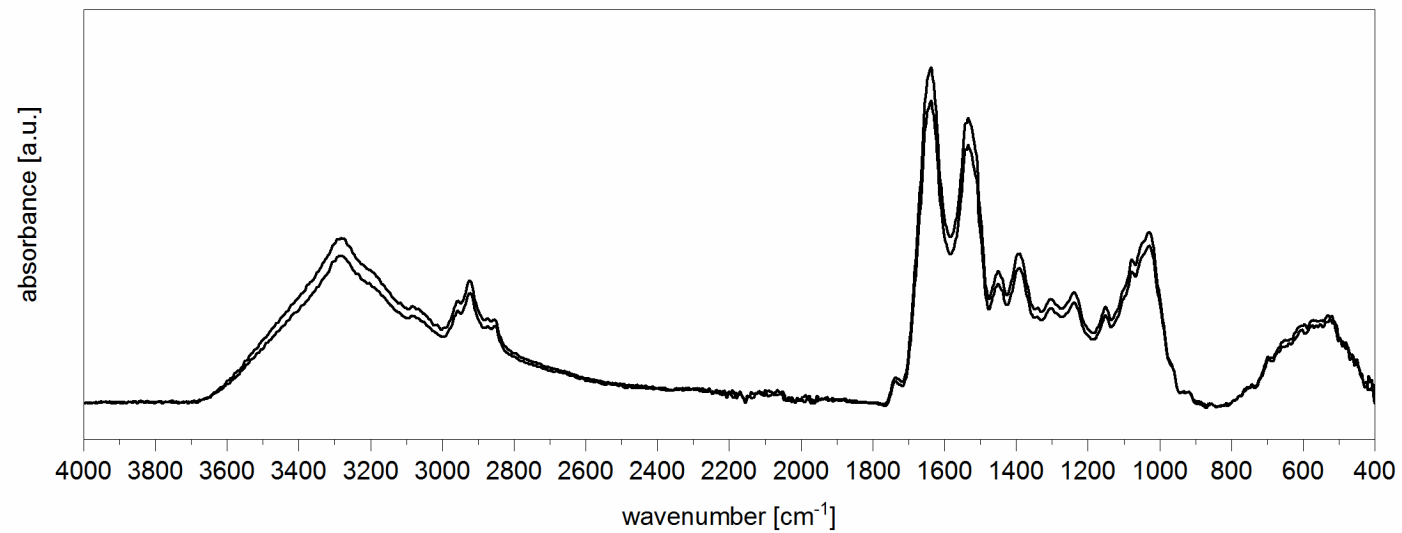
SI Figure 1.4: Speciation diagram of experimental conditions in 0.56 M NaCl.



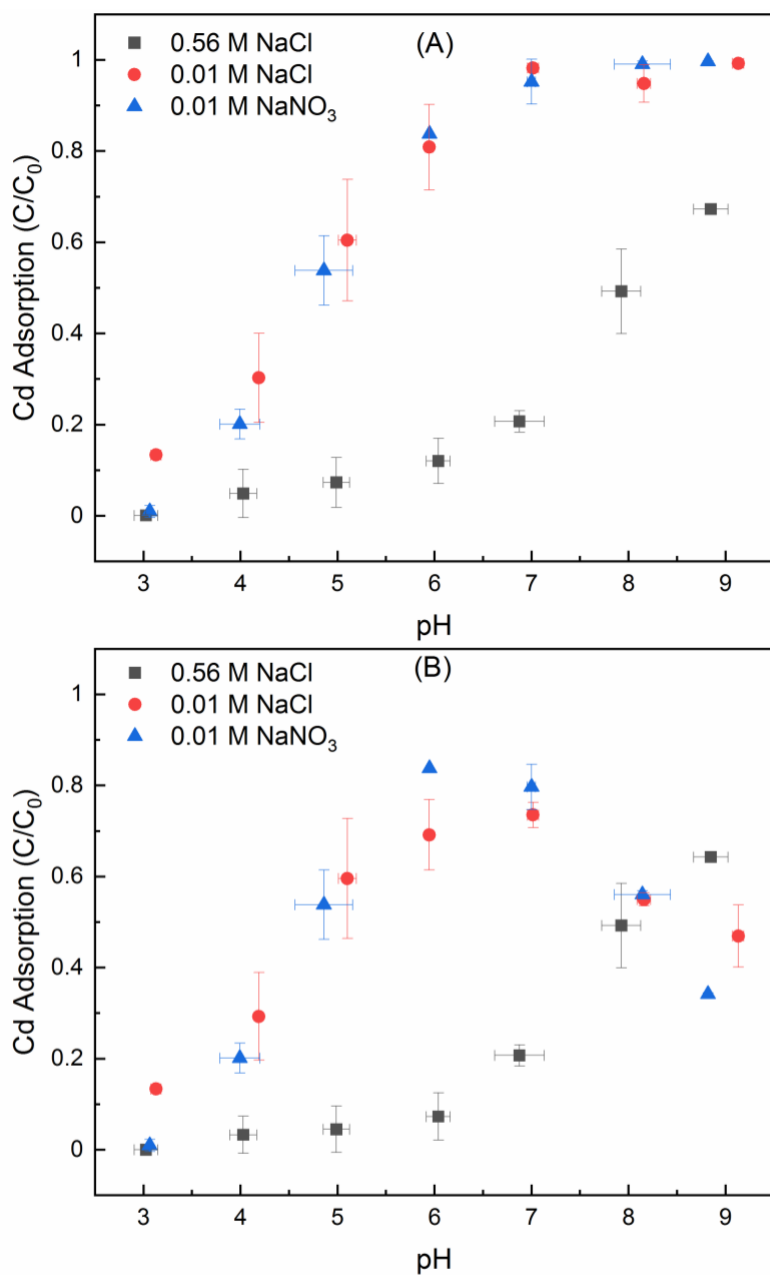
**SI Figure 1.5:** Protonation model results for titrations of  $1 \text{ g L}^{-1}$  *Synechocystis* sp. PCC 6803 in (A) 0.01 M NaCl and (B) 0.56 M NaCl.



**SI Figure 1.6:** Attenuated total reflectance fourier transform infrared (ATR-FTIR) spectra of dried and ground *Synechocystis* sp. PCC 6803 cells.



**SI Figure 1.7:** Duplicate attenuated total reflectance Fourier transform infrared (ATR-FTIR) spectra of dried and ground *Synechocystis* sp. PCC 6803 demonstrating reproducibility.



**SI Figure 1.8:** Results of Cd adsorption experiments conducted in 0.56 M, 0.01 M NaCl and 0.01 M NaNO<sub>3</sub>. (A) Displayed is the original Cd adsorption data, and (B) indicates the Cd adsorbed after subtracting the experimental blank data. As observed, the 0.56 M NaCl experiment was not influenced by possible carbonate precipitation, whereas it was more prominent at higher pH and lower ionic strength. Error bars indicate 1-sigma standard deviation.

## References

- Abdulaziz, A., Sageer, S., Chekidhenkuzhiyil, J., Vijayan, V., Pavanan, P., Athiyanathil, S., Nair, S. (2016). Unicellular cyanobacteria *Synechocystis* accommodate heterotrophic bacteria with varied enzymatic and metal resistance properties. *Journal of basic microbiology* **56**, 845-856.
- Abed, R. M. M., Safi, N. M. D., Koster, J., de Beer, D., El-Nahhal, Y., Rullkotter, J., Garcia-Pichel, F. (2002). Microbial diversity of a heavily polluted microbial mat and its community changes following degradation of petroleum compounds. *Applied and Environmental Microbiology* **68**, 1674-1683.
- Ballot, A., Krienitz, L., Kotut, K., Wiegand, C., Metcalf, J. S., Codd, G. A., Pflugmacher, S. (2004). Cyanobacteria and cyanobacterial toxins in three Alkaline Rift Valley lakes of Kenya – Lakes Bogoria, Nakuru and Elmenteita. *Journal of Plankton Research* **26**, 925-935.
- Chong, A. M. Y., Wong, Y. S., Tam, N. F. Y. (2000). Performance of different microalgal species in removing nickel and zinc from industrial wastewater. *Chemosphere* **41**, 251-257.
- Davis, R. A., Reas, C., Robbins, L. L. (1995). Calcite mud in a Holocene back-barrier lagoon: Lake Reeve, Victoria, Australia. *Journal of Sedimentary Research* **65**, 178-184.
- Demirel, S., Ustun, B., Aslim, B., Suludere, Z. (2009). Toxicity and uptake of Iron ions by *Synechocystis* sp. E35 isolated from Kucukcekmece Lagoon, Istanbul. *Journal of Hazardous Materials* **171**, 710-716.
- Hameed, A., Satoh, M., Furuhashi, Y., Oyama, Y., Hasnain, S. (2013). Induction of non protein thiols by chromium in cyanobacteria isolated from polluted areas. *African Journal of Microbiology Research* **7**, 4806-4811.

- Khattar, S. J. I. S. (2009). Optimization of Cd<sup>2+</sup> removal by the cyanobacterium *Synechocystis pevalekii* using the response surface methodology. *Process Biochemistry* **44**, 118-121.
- Martins, R. F., Ramos, M. F., Herfindal, L., Sousa, J. A., Skaerven, K., Vasconcelos, V. M. (2008). Antimicrobial and cytotoxic assessment of marine cyanobacteria – *Synechocystis* and *Synechococcus*. *Marine Drugs* **6**, 1-11.
- Nascimento, S. M., Azevedo, S. M. F. O. (1999). Changes in cellular components in a cyanobacterium (*Synechocystis aquatilis* f. *salina*) subjected to different N/P ratios – an ecophysiological study. *Environmental Toxicology* **14**, 37-44.
- Ozturk, S., Aslim, B., Turker, A. R. (2009). Removal of Cadmium Ions from Aqueous Samples by *Synechocystis* Sp. *Separation Science and Technology*, **44**, 1467-1483.
- Pawlik, B., Skowronski, T. (1994). Transport and toxicity of cadmium: its regulation in the cyanobacterium *Synechocystis aquatilis*. *Environmental and Experimental Botany* **34**, 225-233.
- Rippka, R., Deruelles, J., Waterbury, J. B., Herdman, M., Stainer, R. Y. (1979). Generic assignments, strain histories and properties of pure cultures of cyanobacteria. *Journal of General Microbiology* **111**, 1-61.
- Roy, S., Ghosh, A. N., Thakur, A. R. (2008). Uptake of Pb<sup>2+</sup> by a cyanobacterium belonging to the genus *Synechocystis*, isolated from East Kolkata Wetlands. *Biometals* **21**, 515-524.
- Stanier, R. Y., Kunisawa, R., Mandel, M., Cohen-Bazire, G. (1971). Purification and Properties of Unicellular Blue-Green Algae (Order *Chroococcales*). *Bacteriological Reviews* **35**, 171-205.
- Stipp, S. L., Parks, G. A., Nordstrom, D. K., Leckie, J. O. (1993). Solubility-product constant and thermodynamic properties for synthetic otavite, CdCO<sub>3(s)</sub>, and aqueous association

- constants for the Cd(II)-CO<sub>2</sub>-H<sub>2</sub>O system. *Geochimica et Cosmochimica Acta* **57**, 2699-2713.
- Zhang, K., Kurano, N., Miyachi, S. (1999). Outdoor culture of a cyanobacterium with a vertical flat-plate photobioreactor: effects on productivity of the reactor orientation, distance setting between the plates, and culture temperature. *Applied Microbiology and Biotechnology*, **52**, 781-786.
- Zhang, D., Pan, X., Zhao, L., Mu, G. (2011). Biosorption of Antimony (Sb) by the cyanobacterium *Synechocystis* sp. *Polish Journal of Environmental Studies* **20**, 1353-1358.
- Zirino, A., Yamamoto, S. (1972). A pH-dependent model for the chemical speciation of copper, zinc, cadmium and lead in seawater. *Limnology and Oceanography* **17**, 661-671.

## Appendix 2: Supplementary information for Chapter 3

**SI Table 2.1:** Summary of best fit, non-electrostatic protonation model results of cyPOM titration data. 3-, 2-, and 1-site model results are included for comparison. Site concentrations are in units of  $\mu\text{mol g}^{-1}$ .

pKa1	Site Concentration	pKa2	Site Concentration	pKa3	Site Concentration	Error
5.75	45.9	8.21	13.5	9.53	36.8	1.83369
5.73	42.5	8.42	21.5	10.13	18.4	2.45219
5.69	32.1	8.50	31.1	10.70	8.02	3.28612
5.73( $\pm 0.04$ )	40.2( $\pm 7.17$ )	8.38( $\pm 0.15$ )	22.0( $\pm 8.81$ )	10.12( $\pm 0.59$ )	21.0( $\pm 14.6$ )	-
5.85	48.3	9.28	47.3	-	-	1.80133
5.78	44.4	9.04	37.8	-	-	2.09281
5.71	32.7	8.70	38.5	-	-	2.81919
5.78( $\pm 0.07$ )	41.8( $\pm 8.15$ )	9.01( $\pm 0.29$ )	41.2( $\pm 5.28$ )	-	-	-
8.40	74.9	-	-	-	-	5.71117
7.83	78.3	-	-	-	-	4.27274
8.02	58.9	-	-	-	-	4.05478
8.09( $\pm 0.29$ )	68.3( $\pm 8.40$ )	-	-	-	-	-

**SI Table 2.2:** Summary of best fit, non-electrostatic protonation model results of cyDOM titration data. 2- and 1-site model results are included for comparison. Site concentrations are in units of  $\mu\text{mol g}^{-1}$ .

pKa1	Site Concentration	pKa2	Site Concentration	Error
4.82	55.6	7.02	42.9	10.4703
4.71	45.9	6.58	50.3	17.1591
5.13	26.9	6.78	18.7	0.23877
4.89( $\pm 0.22$ )	42.8( $\pm 14.6$ )	6.80( $\pm 0.22$ )	37.3( $\pm 16.5$ )	-
6.38	69.7	-	-	14.2322
6.15	74.0	-	-	17.0868
6.91	43.3	-	-	1.64414
6.48( $\pm 0.39$ )	62.3( $\pm 16.6$ )	-	-	-

**SI Table 2.3:** Hydrolysis and chloride complexation constants of  $\text{Cd}^{2+}$ ,  $\text{Co}^{2+}$ ,  $\text{Cu}^{2+}$ ,  $\text{Ni}^{2+}$ , and  $\text{Zn}^{2+}$  used in the FITEQL 4.0 surface complexation models (SCM). Hydrolysis constants taken from Baes and Mesmer (1976). Cd, Cu, and Zn chloride complexes taken from Zirino and Yamamoto (1972). Co and Ni chloride and carbonate complexes taken from Martell and Smith (1976) and logK values of carbonic acids and Ksp value of Cd carbonate taken from Stipp et al. (1993).

Species or phase	Log K
$\text{CdOH}^+$	-9.8354
$\text{Cd(OH)}_2$	-20.035
$\text{Cd(OH)}_3^-$	-31.700
$\text{Cd(OH)}_4^{2-}$	-47.830
$\text{Cd}_2(\text{OH})_3^+$	-9.665
$\text{Cd}_4(\text{OH})_4^{4+}$	-32.330
$\text{CdCl}^+$	2.0
$\text{CdCl}_2$	2.7
$\text{CdCl}_3^-$	2.1
$\text{CdCO}_3(\text{s})$	12.10
$\text{CoOH}^+$	-9.65
$\text{Co(OH)}_2$	-18.8
$\text{Co(OH)}_3^-$	-31.5
$\text{Co(OH)}_4^{2-}$	-46.3
$\text{CoCl}^+$	-0.35
$\text{CoCO}_3$	4.4
$\text{Co(CO}_3)^+$	12.289
$\text{Cu(OH)}^+$	-8.0
$\text{Cu(OH)}_2$	-17.3
$\text{Cu(OH)}_3^-$	-27.8
$\text{Cu(OH)}_4^{2-}$	-39.6
$\text{Cu(OH)}_2^{2+}$	-10.36
$\text{CuCl}_2$	-0.7
$\text{CuCl}_3^-$	-2.2
$\text{CuCl}_4^{2-}$	-4.4
$\text{Ni(OH)}_2$	-20.08
$\text{Ni(OH)}_3^-$	-29.2
$\text{Ni(OH)}_4^{2-}$	-44.0
$\text{Ni}_2(\text{OH})_3^+$	-10.6
$\text{NiCl}^+$	0.08
$\text{NiCO}_3$	4.2
$\text{ZnOH}^+$	-8.96
$\text{Zn(OH)}_2$	-16.9
$\text{Zn(OH)}_3^-$	-28.4

$\text{Zn(OH)}_4^{2-}$	-41.2
$\text{Zn}_2\text{OH}^{3+}$	-9.0
$\text{Zn}_2(\text{OH})_6^{2-}$	-57.8
$\text{ZnCl}^+$	0.4
$\text{ZnCl}_2$	0.61
$\text{ZnCl}_3^-$	0.53
$\text{ZnCl}_4^{2-}$	0.2
<hr/>	
$\text{CO}_2 + \text{H}_2\text{O} = \text{H}_2\text{CO}_3$	-1.46
$\text{H}_2\text{CO}_3 = \text{H}^+ + \text{HCO}_3^-$	-6.36
$\text{HCO}_3^- = \text{CO}_3^{2-} + \text{H}^+$	-10.33
<hr/>	

**SI Table 2.4:** FITEQL 4.0 surface complexation model (SCM) fits using trace metal adsorption data. “w/ CO<sub>2</sub>” indicates that the last 3 reactions and corresponding carbonate species associated with each trace metal from Table S1 were included in the SCM. “N/C” indicates there was no convergence of the FITEQL 4.0 optimization procedure.

	Chemical System	LogK 1	logK 2	V(y)
Cd	2-site NEM w/ CO <sub>2</sub>	N/C	-	-
	2-site NEM w/o CO <sub>2</sub>	1.55438	1.04667	0.18463
Co	2-site NEM w/ CO <sub>2</sub>	1.08485	6.09772	9.45894
	2-site NEM w/o CO <sub>2</sub>	1.24139	2.78016	5.40493
Cu	2-site NEM w/ CO <sub>2</sub>	0.72059	6.31479	1.79396
	2-site NEM w/o CO <sub>2</sub>	0.72379	2.51024	1.79743
Ni	2-site NEM w/ CO <sub>2</sub>	-0.81024	-3.72883	4.43290
	2-site NEM w/o CO <sub>2</sub>	N/C	-	-
Zn	2-site NEM w/ CO <sub>2</sub>	1.09457	2.17343	0.28256
	2-site NEM w/o CO <sub>2</sub>	N/C	-	-

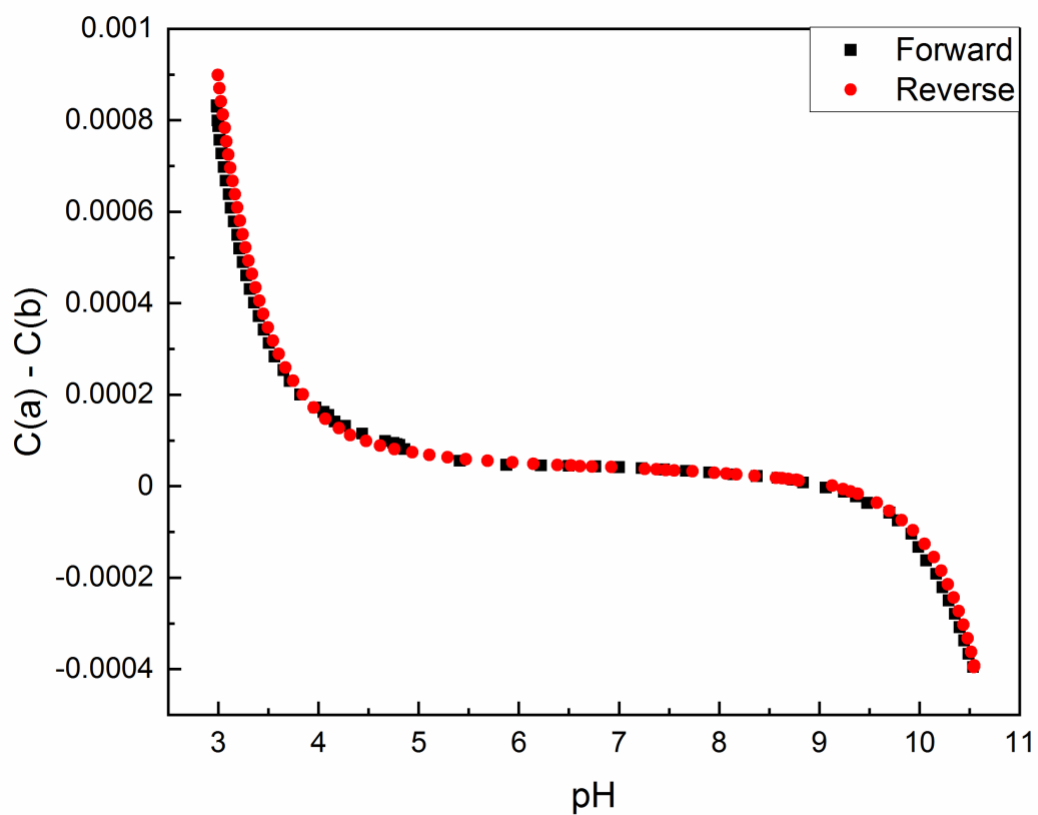
**SI Table 2.5:** Compiled metal binding ligands, ligand concentrations, and location of ligands from literature for the trace metals Cd, Co, Cu, Ni, and Zn.

<b>Location</b>	<b>Log K'<sub>CdL</sub></b>	<b>Reference</b>
<i>Open Ocean</i>		
South Pacific	9.1-9.8 (9.4)	Capodaglio et al. (1998)
North Pacific	9.9-10.7 (10.3)	Bruland, 1992
<b>Location</b>	<b>Log K'<sub>CoL</sub></b>	<b>Reference</b>
<i>Open Ocean</i>		
North Atlantic	>17.7	Baars & Croot, 2015
	15.6-16.2 (15.9)	Ellwood & van den Berg, 2001
	15.4-17.2 (16.3)	Saito & Moffett, 2001
South Atlantic	16.6-20.3 (18.4)	Bown et al. (2012)
	15.7-15.8 (15.8)	Ellwood et al. (2005)
North Pacific	≥16.8	Saito et al. (2005)
South Pacific	≥15.7	Saito et al. (2010)
	≥16.8	Saito et al. (2004)
<b>Location</b>	<b>Log K'<sub>CuL</sub></b>	<b>Reference</b>
<i>Open Ocean</i>		
North Atlantic	12.5-14.8 (13.7)	(Jacquot & Moffett 2015)
	L <sub>1</sub> = 14-15.1 (14.8)	(Oldham et al. 2014)
	L <sub>2</sub> = 12.6-14.1 (13.4)	
	L <sub>1</sub> = 13	(Kogut & Voelker 2003)
	L <sub>2</sub> = 11.5	
	L <sub>3</sub> = 10	
	13.2	Moffett, 1995
	L <sub>1</sub> = 13.2	Moffett et al. (1990)
	L <sub>2</sub> = 9.7	
	12.2-14.3 (13)	Campos & van den Berg, 1994
	L <sub>1</sub> = 12.2	van den Berg, 1984
	L <sub>2</sub> = 10.2	
	South Atlantic	L <sub>1</sub> = 13.6-16 (14.6)
L <sub>2</sub> = 12.7-13.3 (13.1)		
North Pacific	L <sub>1</sub> = 15.1-16.5 (15.6)	Whitby et al. (2018)
	L <sub>2</sub> = 11.6-13.6 (13.0)	
	12.8	Semeniuk et al. (2015)
	12.8-15.1 (14.1)	Buck et al. (2012)
	12.7-14.1 (13.7)	Moffett & Dupont, 2007
	L <sub>1</sub> = 11.6	Coale & Bruland, 1990
	L <sub>2</sub> = 8.6	
	L <sub>1</sub> = 11.5	Coale & Bruland, 1988
	L <sub>2</sub> = 8.5	
	South Pacific	12.6-14 (13.2)
L <sub>1</sub> = 12-13.6 (13.0)		Thompson et al. (2014)
L <sub>2</sub> = 11.2-11.7 (11.5)		

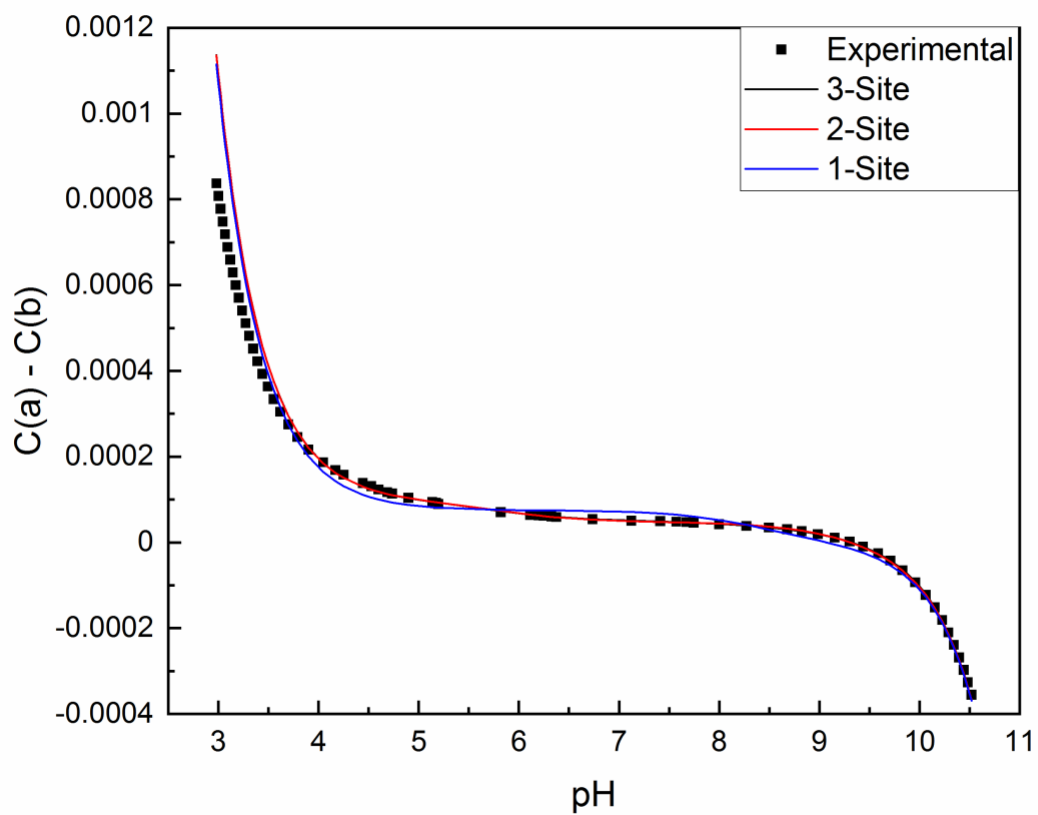
	12.6-14.0 (13.3) L <sub>1</sub> = 11-16 (13.6) L <sub>2</sub> = 7.6-9 (8.4)	Jacquot et al. (2013) Capodaglio et al. (1998)
<i>Marginal Waters</i>		
Mediterranean Sea	13-14.8 (13.8)	Campos & van den Berg, 1994
Black Sea	L <sub>1</sub> = 13.1-14.2 (13.6) L <sub>2</sub> = 9.4-11.3 (10.4)	Muller et al. (2001)
<i>Estuarine Waters</i>		
River Plume off Scotland	L <sub>1</sub> = 14.8-16.2 (15.7) L <sub>2</sub> = 11.7-12.8 (12.3)	Muller & Batchelli, 2013
San Francisco Bay, Western USA	L <sub>1</sub> = 12.9-14.3 (13.7) L <sub>2</sub> = 12-12.9 (12.4)	Buck & Bruland, 2005
Cape Fear River estuary, Eastern USA	13.5	Shank et al. (2004)
River Scheldt, Netherlands	L <sub>1</sub> = 14.7-16.1 (15.2) L <sub>2</sub> = 12.7-13.5 (13)	Laglera & van den Berg, 2003
Narragansett Bay, Eastern USA	L <sub>1</sub> = 12.8-15.6 (13.8) L <sub>2</sub> = 10.1-11.5 (10.7) L <sub>3</sub> = 9	Bruland et al. (2000)
Chesapeake Bay, Eastern USA	L <sub>1</sub> = 11 L <sub>2</sub> = 7.9	Gordon et al. (2000)
Narragansett Bay, Eastern USA	L <sub>1</sub> = >12.3 L <sub>2</sub> = 8-9.2 (8.4) L <sub>3</sub> = 7.5-7.7 (7.7)	Wells et al. (1998)
San Francisco Bay, Western USA	L <sub>1</sub> = >13.5 L <sub>2</sub> = 9-9.6 (9.3)	Donat et al. (1994)
<b>Location</b>	<b>Log K'<sub>NiL</sub></b>	<b>Reference</b>
<i>Open Ocean</i>		
South Pacific	18.5-18.7 (18.6)	Boiteau et al. (2016)
<i>Estuarine Waters</i>		
San Francisco Bay, Western USA	>17	Donat et al. (1994)
Menai Straits, Irish Sea, & English Channel	17.3-18.7 (18)	van den Berg & Nimmo, 1987
<b>Location</b>	<b>LogK'<sub>ZnL</sub></b>	<b>Reference</b>
<i>Open Ocean</i>		
Indian Ocean	10	Kim et al. (2015a)
North Atlantic	10.4	Jakuba et al. (2008)
	10.1-10.6 (10.3) L <sub>1</sub> = 8.4 L <sub>2</sub> = 7.5	Ellwood & van den Berg, 2000 van den Berg, 1985
South Atlantic	9.1-10.4 (9.8)	Baars & Croot, 2011
North Pacific	9.2-10.7 (9.8) 9.8-11 (10.2) 10.4-11.1 (10.7) 10.3-11.2 (10.8)	Kim et al. (2015b) Jakuba et al. (2012) Lohan et al. (2005) Donat & Bruland, 1990

South Pacific	10.4-10.9 (10.6)	Bruland, 1989
<i>Marginal Waters</i>	9.7-10.4 (10)	Ellwood, 2004
Black Sea	L <sub>1</sub> = 9.4-10.3 (9.9)	Muller et al. (2001)
	L <sub>2</sub> = 8.5-8.7 (8.6)	

---



**SI Figure 2.1:** Forward and reverse titration plots for  $1 \text{ g L}^{-1}$  cyPOM in  $0.56 \text{ M NaCl}$ .  $C(a) - C(b)$  indicates the proton budget between the concentration of acid ( $0.1 \text{ M HNO}_3$ ) and base ( $0.1 \text{ M NaOH}$ ) in the system.



**SI Figure 2.2:** Protonation model results for titrations of  $1 \text{ g L}^{-1}$  cyPOM in  $0.56 \text{ M NaCl}$ . Note that the 3- (black line) and 2-site (red line) models are nearly identical.

## References

- Achterberg, E. P., van den Berg, C. M. G. (1997) Chemical speciation of chromium and nickel in the western Mediterranean. *Deep-Sea Research II* 44: 693-720.
- Baars, O., Croot, P. L. (2011) The speciation of dissolved zinc in the Atlantic sector of the Southern Ocean. *Deep-Sea Research II* 58: 2720-2732.
- Baars, O., Croot, P. L. (2015) Dissolved cobalt speciation and reactivity in the eastern tropical North Atlantic. *Marine Chemistry* 173: 310-319.
- Baes, C.F., Mesmer, R.S. (1976). *The Hydrolysis of Cations*. John Wiley & Sons, New Jersey, USA.
- Boiteau, R. M., Till, C. P., Ruacho, A., Bundy, R. M., Hawco, N. J., McKenna, A. M., Barbeau, K. A., Bruland, K. W., Saito, M. A., Repeta, D. J. (2016) Structural Characterization of Natural Nickel and Copper Binding Ligands along the US GEOTRACES Eastern Pacific Zonal Transect. *Frontiers in Marine Science* 3: 1-16.
- Bown, J., Boye, M., Nelson, D. M. (2012) New insights on the role of organic speciation in the biogeochemical cycle of dissolved cobalt in the southeastern Atlantic and the Southern Ocean. *Biogeosciences* 9: 2719-2736.
- Bruland, K. W. (1989) Complexation of zinc by natural organic-ligands in the central North Pacific. *Limnology and Oceanography* 34: 269-285.
- Bruland, K. W., Rue, E. L., Donat, J. R., Skrabal, S. A., Moffett, J. W. (2000) Intercomparison of voltammetric techniques to determine the chemical speciation of dissolved copper in a coastal seawater sample. *Analytica Chimica Acta* 405: 99-113.
- Buck, K. N., Bruland, K. W. (2005) Copper speciation in San Francisco Bay: A novel approach using multiple analytical windows. *Marine Chemistry* 96: 185-198.

- Buck, K. N., Moffett, J., Barbeau, K. A., Bundy, R. M., Kondo, Y., Wu, J. (2012) The organic complexation of iron and copper: an intercomparison of competitive ligand exchange-adsorptive cathodic stripping voltammetry (CLE-ACSV) techniques. *Limnology and Oceanography: Methods* 10: 496-515.
- Bundy, R. M., Barbeau, K. A., Buck, K. N. (2013) Sources of strong copper-binding ligands in Antarctic Peninsula surface waters. *Deep-Sea Research II* 90: 134-146.
- Campos, M. L. A. M., van den Berg, C. M. G. (1994) Determination of copper complexation in sea water by cathodic stripping voltammetry and ligand competition with salicylaldehyde. *Analytica Chimica Acta* 284: 481-496.
- Capodaglio, G., Turetta, C., Toscano, G., Gambaro, A., Scarponi, G., Cesona, P. (1998) Cadmium, lead and copper complexation in Antarctic coastal seawater, Evolution during the austral summer. *International Journal of Environmental Analytical Chemistry* 71: 195-226.
- Coale, K. H., Bruland, K. W. (1988) Copper complexation in the Northeast Pacific. *Limnology and Oceanography* 33(5): 1084-1101.
- Coale, K. H., Bruland, K. W. (1990) Spatial and temporal variability in copper complexation in the North Pacific. *Deep-Sea Research* 47: 317-336.
- Donat, J. R., Bruland, K. W. (1990) A Comparison of Two Voltammetric Techniques for Determining Zinc Speciation in Northeast Pacific Ocean Waters. *Marine Chemistry* 28: 301-323.
- Donat, J. R., van den Berg, C. M. G. (1992) A new cathodic stripping voltammetric method for determining organic copper complexation in seawater. *Marine Chemistry* 38: 69-90.
- Donat, J. R., Lao, K. A., Bruland, K. W. (1994) Speciation of dissolved copper and nickel in South San Francisco Bay: a multi-method approach. *Analytica Chimica Acta* 284(3): 547-571.

- Ellwood, M. J., van den Berg, C. M. G. (2000) Zinc speciation in the Northeastern Atlantic Ocean. *Marine Chemistry* 68: 295-306.
- Ellwood, M. J., van den Berg, C. M. G. (2001) Determination of organic complexation of cobalt in seawater by cathodic stripping voltammetry. *Marine Chemistry* 75: 33-47.
- Ellwood, M. J. (2004) Zinc and cadmium speciation in subantarctic waters east of New Zealand. *Marine Chemistry* 87: 37-58.
- Ellwood, M. J., van den Berg, C. M. G., Boye, M., Veldhuis, M., de Jong, J. T. M., de Baar, H. J. W., Croot, P. L., Kattner, G. (2005) Organic complexation of cobalt across the Antarctic Polar Front in the Southern Ocean. *Marine and Freshwater Research* 56: 1069-1075.
- Gordon, A. S., Donat, J. R., Kango, R. A., Dyer, B. J., Stuart, L. M. (2000) Dissolved copper-complexing ligands in cultures of marine bacteria and estuarine water. *Marine Chemistry* 70: 149-160.
- Jacquot, J. E., Kondo, Y., Knapp, A. N., Moffett, J. W. (2013) The speciation of copper across active gradients in nitrogen-cycle processes in the eastern tropical South Pacific. *Limnology and Oceanography* 58(4): 1387-1394.
- Jacquot, J. E., Moffett, J. W. (2015) Copper distribution and speciation across the International GEOTRACES Section GA03. *Deep-Sea Research II* 116: 187-207.
- Jakuba, R., Moffett, J. W., Saito, M. A. (2008) Use of a modified, high-sensitivity, anodic stripping voltammetry method for determination of zinc speciation in the North Atlantic Ocean. *Analytica Chimica Acta* 614: 143-152.
- Jakuba, R., Saito, M. A., Moffett, J. W., Yan, X. (2012) Dissolved zinc in the subarctic North Pacific and Bering sea: Its distribution, speciation, and importance to primary producers. *Global Biogeochemical Cycles* 26: 1-15.

- Kim, T., Obata, H., Gamo, T. (2015a) Dissolved Zn and its speciation in the northeastern Indian Ocean and the Andaman Sea. *Frontiers in Marine Science* 2(60): 1-14.
- Kim, T., Obata, H., Kondo, Y., Ogawa, H., Gamo, T. (2015b) Distribution and speciation of dissolved zinc in western North Pacific and its adjacent seas. *Marine Chemistry* 173: 330-341.
- Kogut, M. B., Volker, B. M. (2003) Kinetically inert Cu in coastal waters. *Environmental Science and Technology* 37: 509-518.
- Kozelka, P. B., Bruland, K. W. (1998) Chemical speciation of dissolved Cu, Zn, Cd, Pb in Narragansett Bay, Rhode Island. *Marine Chemistry* 60: 267-282.
- Laglera L. M., van den Berg, C. M. G. (2003) Copper complexation by thiol compounds in estuarine waters. *Marine Chemistry* 82: 71-89.
- Lohan, M. C., Crawford, D. W., Purdie, D. A., Statham, P. J. (2005) Iron and zinc enrichments in the northeastern subarctic Pacific: Ligand production and zinc availability in response to phytoplankton growth. *Limnology and Oceanography* 50(5): 1427-1437.
- Martell, A.E., Smith, R.M. (1976). *Critical Stability Constants, Volume 4: Inorganic Complexes*. Plenum Press, New York.
- Moffett, J. W., Zika, R. G., Brand, L. E. (1990) Distribution and potential sources and sinks of copper chelators in the Sargasso Sea. *Deep-Sea Research* 37(1): 27-36.
- Moffett, J. W. (1995) Temporal and spatial variability of copper complexation by strong chelators in the Sargasso Sea. *Deep Sea Research Part I: Oceanographic Research Papers* 42(8): 1273-1295.

- Moffett, J. W., Dupont, C. (2007) Cu complexation by organic ligands in the sub-arctic NW Pacific and Bering Sea. *Deep Sea Research Part I: Oceanographic Research Papers* 54(4): 586-595.
- Muller, F. L. L., Kester, D. R. (1991) Voltammetric determination of the complexation parameters of zinc in marine and estuarine waters. *Marine Chemistry* 33: 71-90.
- Muller, F. L. L., Gulin, S. B., Kalvoy, A. (2001) Chemical speciation of copper and zinc in surface waters of the western Black Sea. *Marine Chemistry* 76: 233-251.
- Muller, F. L. L., Batchelli, S. (2013) Copper binding by terrestrial versus marine organic ligands in the coastal plume of River Thurso, North Scotland. *Estuarine, Coastal and Shelf Science* 133: 137-146.
- Noble, A. E., Saito, M. A., Maiti, K., Benitez-Nelson, C. R. (2008) Cobalt, manganese, and iron near the Hawaiian Islands: A potential concentrating mechanisms for cobalt within a cyclonic eddy and implications for the hybrid-type trace metals. *Deep-Sea Research II* 55: 1473-1490.
- Noble, A. E., Ohnemus, D. C., Hawco, N. J., Lam, P. J., Saito, M. A. (2017) Coastal sources, sinks and strong organic complexation of dissolved cobalt within the US North Atlantic GEOTRACES transect GA03. *Biogeosciences* 14: 2715-2739.
- Oldham, V. E., Swenson, M. M., Buck, K. N. (2014) Spatial variability of total dissolved copper and copper speciation in the inshore waters of Bermuda. *Marine Pollution Bulletin* 79: 314-320.
- Pearson, H. B. C., Comber, S. D. W., Braungardt, C., Worsfold, P. J. (2017) Predicting Copper Speciation in Estuarine Waters – Is Dissolved Organic Carbon a Good Proxy for the Presence of Organic Ligands? *Environmental Science and Technology* 51(4): 2206-2216.

- Saito, M. A., Moffett, J. W. (2001) Complexation of cobalt by natural organic ligands in the Sargasso Sea as determined by a new high-sensitivity electrochemical cobalt speciation method suitable for open ocean work. *Marine Chemistry* 75: 49-68.
- Saito, M. A., Moffett, J. W. (2002) Temporal and spatial variability of cobalt in the Atlantic Ocean. *Geochimica et Cosmochimica Acta* 66: 1943-1953.
- Saito, M. A., Moffett, J. W., DiTullio, G. R. (2004) Cobalt and nickel in the Peru upwelling region: a major flux of labile cobalt utilized as a micronutrient. *Global Biogeochemical Cycles* 18:GB4030.
- Saito, M. A., Rocap, G., Moffett, J. W. (2005) Production of cobalt binding ligands in a *Synechococcus* feature at the Costa Rica upwelling dome. *Limnology and Oceanography* 50: 279-290.
- Saito, M. A., Goepfert, T. J., Noble, A. E., Bertrand, E. M., Sedwick, P. N., DiTullio, G. R. (2010) A Seasonal Study of Dissolved Cobalt in the Ross Sea, Antarctica: Micronutrient Behavior, Absence of Scavenging, and Relationships with Zn, Cd, and P. *Biogeosciences* 7: 4059-4082.
- Semeniuk, D. M., Bundy, R. M., Payne, C. D., Barbeau, K. A., Maldonado, M. T. (2015) Acquisition of organically complexed copper by marine phytoplankton and bacteria in the northeast subarctic Pacific Ocean. *Marine Chemistry* 173: 222-233.
- Shank, G. C., Skrabal, S. A., Whitehead, R. F., Avery, G. B., Kieber, R. J. (2004) River discharge of strong Cu-complexing ligands to South Atlantic Bight waters. *Marine Chemistry* 88: 41-51.

- Skrabal, S. A., Lieseke, K. L., Kieber, R. J. (2006) Dissolved zinc and zinc-complexing ligands in an organic-rich estuary: Benthic fluxes and comparison with copper speciation. *Marine Chemistry* 100: 108-123.
- Tang, D., Warnken, K. W., Santschi, P. H. (2001) Organic complexation of copper in surface waters of Galveston Bay. *Limnology and Oceanography* 46(2): 321-330.
- Thompson, C. M., Ellwood, M. J., Sander, S. G. (2014) Dissolved copper speciation in the Tasman Sea, SW Pacific Ocean. *Marine Chemistry* 164: 84-94.
- Van den Berg, C. M. G. (1984) Determination of the complexing capacity and conditional stability constants of complexes of copper (II) with natural organic ligands in seawater by cathodic stripping voltammetry of copper-catechol complex ions. *Marine Chemistry* 15: 1-18.
- Van den Berg, C. M. G. (1985) Determination of the zinc complexing capacity in seawater by cathodic stripping voltammetry of zinc-APDC complex ions. *Marine Chemistry* 16: 121-130.
- Van den Berg, C. M. G., Nimmo, M. (1987) Determination of interactions of nickel with dissolved organic material in seawater using cathodic stripping voltammetry. *Science of the Total Environment* 60: 185-195.
- Van den Berg, C. M. G., Merks, A. G. A., Duursma, E. K. (1987) Organic Complexation and its Control of the Dissolved Concentrations of Copper and Zinc in the Scheldt Estuary. *Estuarine, Coastal and Shelf Science* 24: 785-797.
- Vega, M., van den Berg, C. M. G. (1997) Determination of Cobalt in Seawater by Catalytic Adsorptive Cathodic Stripping Voltammetry. *Analytical Chemistry* 69(5): 874-881.

- Wells, M. L., Kozelka, P. B., Bruland, K. W. (1998) The complexation of 'dissolved' Cu, Zn, Cd and Pb by soluble and colloidal organic matter in Narragansett Bay, RI. *Marine Chemistry* 62: 203-217.
- Whitby, H., van den Berg, C. M. G. (2015) Evidence for copper-binding humic substances in seawater. *Marine Chemistry* 173: 282-290.
- Whitby, H., Posacka, A. M., Maldonado, M. T., van den Berg, C. M. G. (2018) Copper-binding ligands in the NE Pacific. *Marine Chemistry* 204: 36-48.
- Zhang, H., van den Berg, C. M. G., Wollast, R. (1990) The determination of interactions of cobalt (II) with organic compounds in seawater using cathodic stripping voltammetry. *Marine Chemistry* 28(4): 285-300.
- Zirino, A., Yamamoto, S. (1972). A pH-dependent model for the chemical speciation of copper, zinc, cadmium, and lead in seawater. *Limnology and Oceanography*, **17**, 661-671.

### Appendix 3: Supplementary information for Chapter 4

**SI Table 1:** Input parameters for the UltraMassExplorer (Leefman et al. 2019) interface while using csv mode.

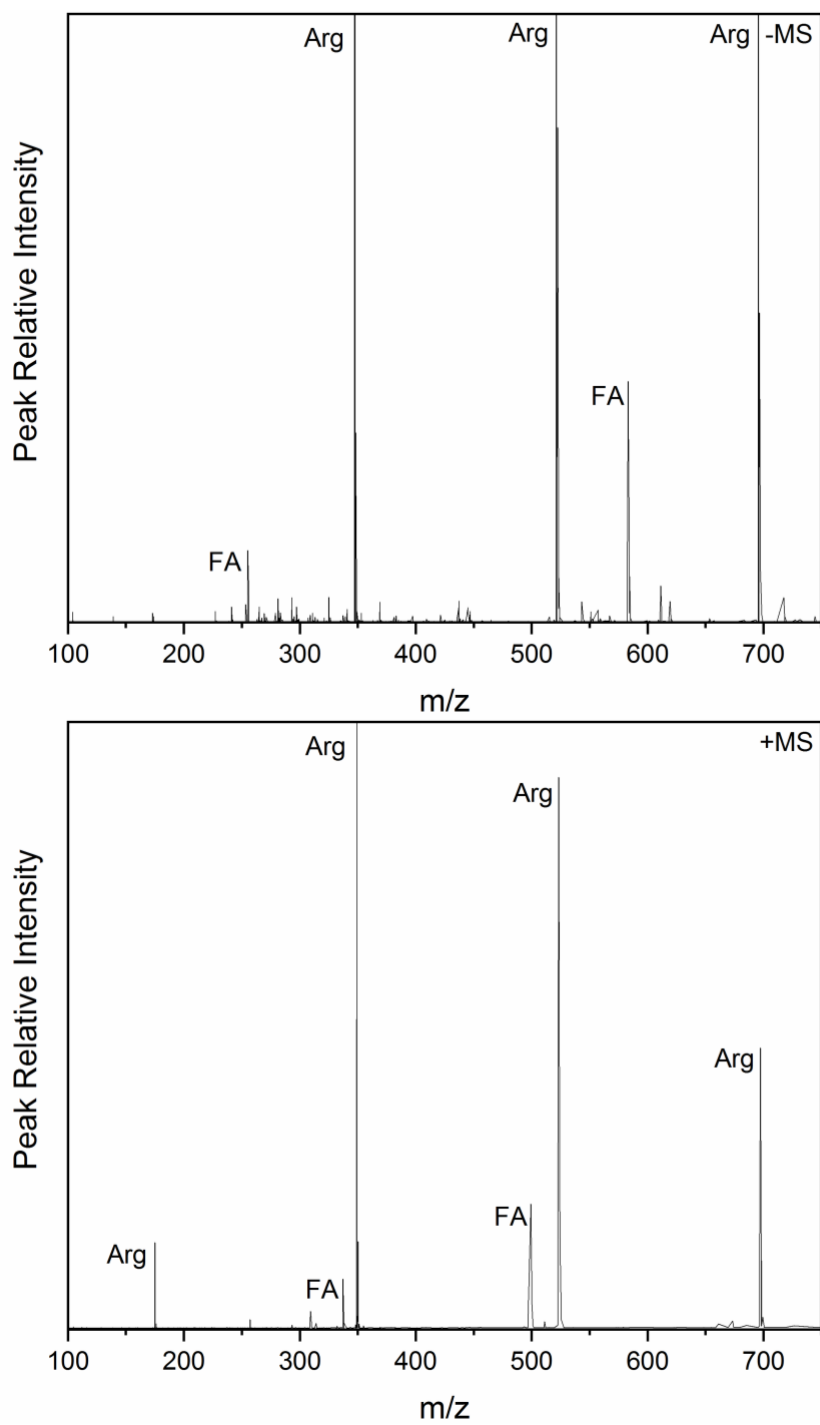
UltraMassExplorer Input Parameter	
Maximum mass error (ppm)	0.5
Lower m/z limit	93
Upper m/z limit	700
Molecular formula library filter	All CHONSP

**SI Table 2:** Hydrolysis and chloride complexation constants of  $\text{Cd}^{2+}$  used in the FITEQL 4.0 surface complexation models (SCM). Hydrolysis constants taken from Baes and Mesmer (1976). Cd chloride complexes taken from Zirino and Yamamoto (1972). Organic ligand complex constants taken from Yu and Fein, 2015; Liu et al. (2015).

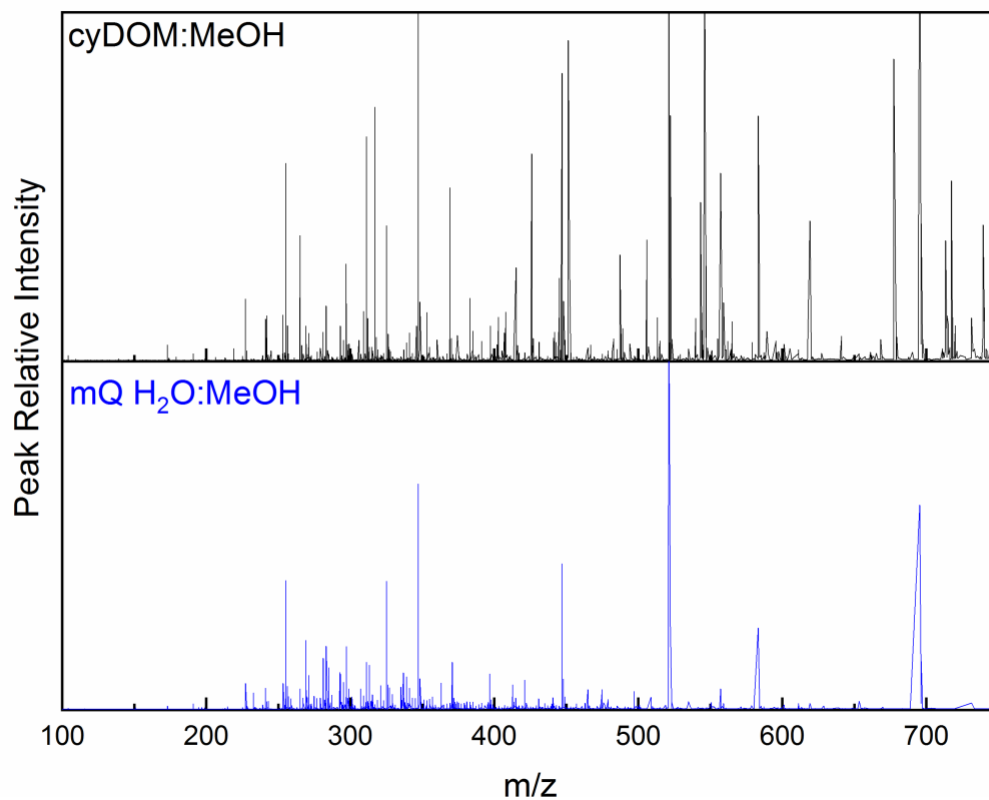
Species or phase	Log K
$\text{CdOH}^+$	-9.8354
$\text{Cd}(\text{OH})_2$	-20.035
$\text{Cd}(\text{OH})_3^-$	-31.700
$\text{Cd}(\text{OH})_4^{2-}$	-47.830
$\text{Cd}_2(\text{OH})_3^+$	-9.665
$\text{Cd}_4(\text{OH})_4^{4+}$	-32.330
$\text{CdCl}^+$	2.0
$\text{CdCl}_2$	2.7
$\text{CdCl}_3^-$	2.1
$\text{CdCO}_3(\text{s})$	12.10
Cd-Ligand(sulf)	8.3
Cd-Ligand(phos)	2.7
Cd-Ligand(amino)	1.8
Cd-Ligand(carb)	1.1

**SI Table 3:** Predictive model results at pH 7.

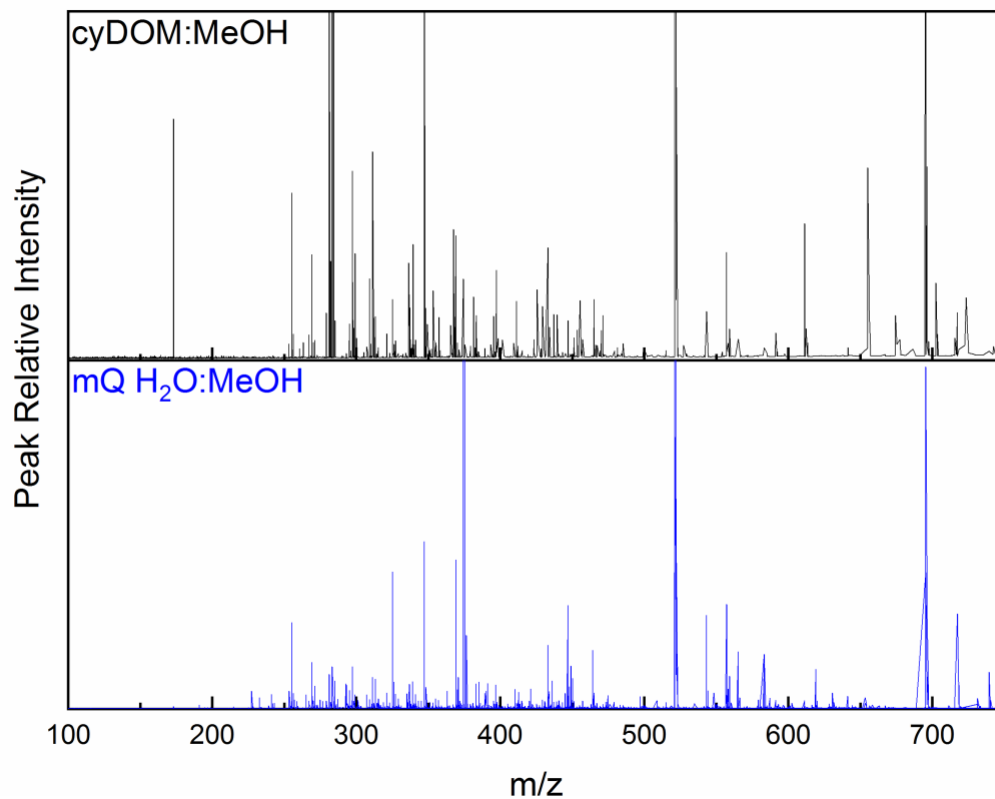
System	Adsorbed to competing ligand (%)
sulf:carb (1:1000)	99.35
phos:carb (1:1)	77.02
amino:carb (1:1)	53.03



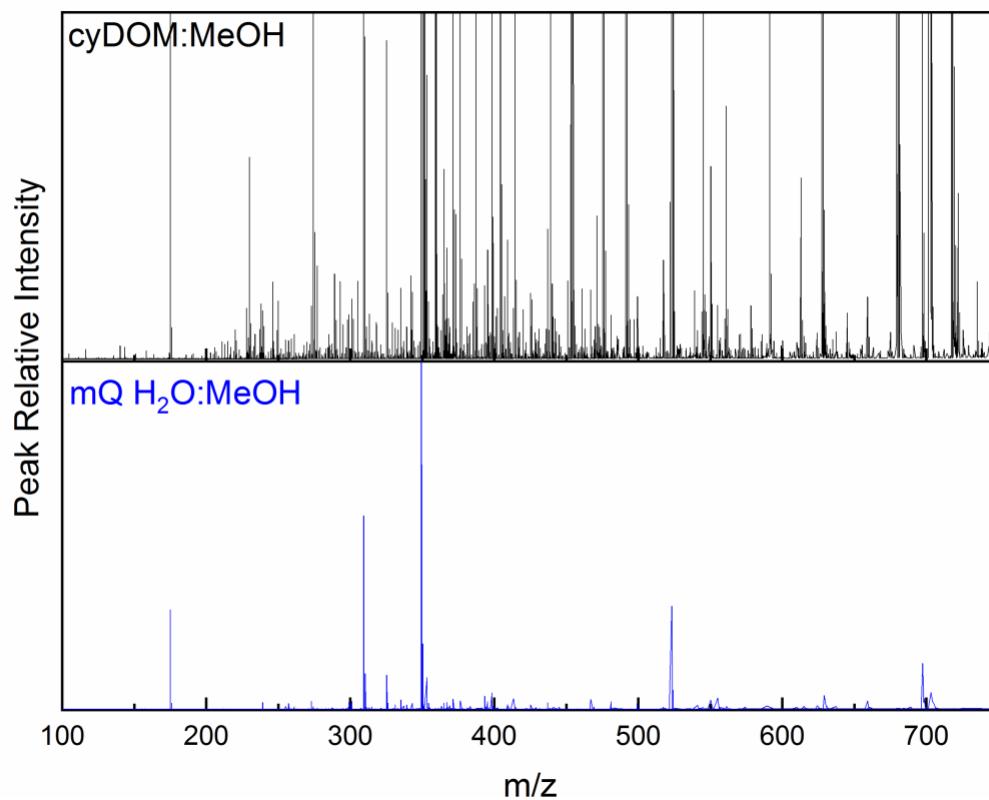
**SI Figure 1:** Arginine internal standard added to analyzed samples in negative ESI (Top) and positive ESI (Bottom). FA; fatty acid contaminants commonly found in mass spectrometry.



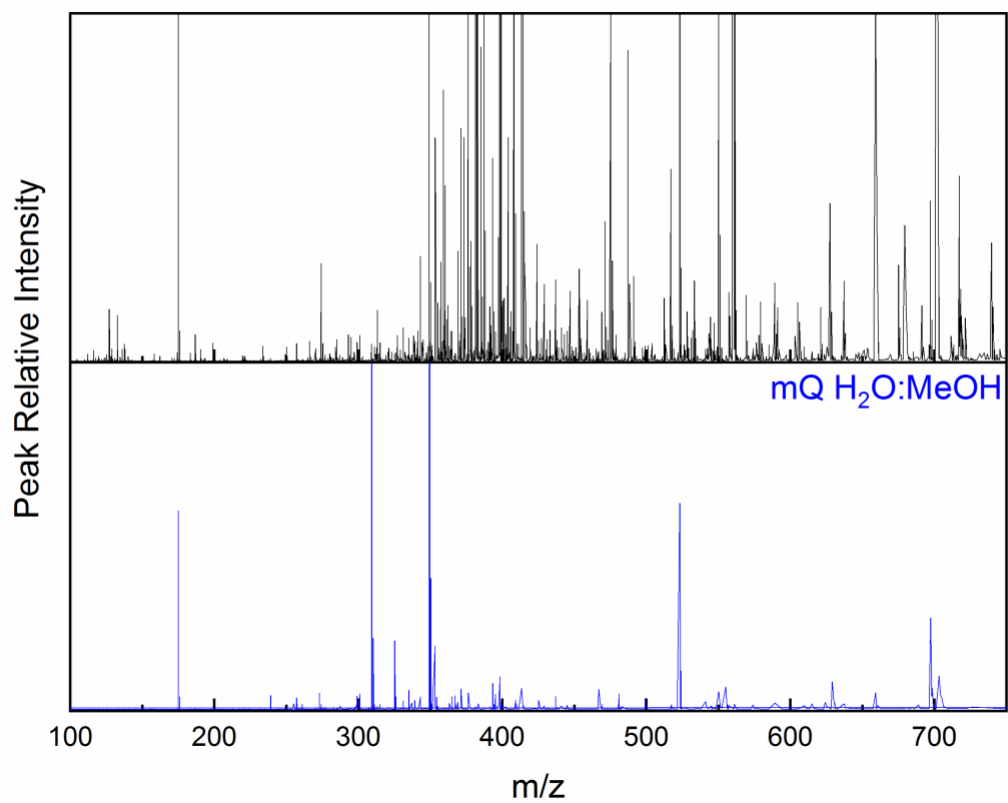
**SI Figure 2:** Negative Electrospray Ionization (ESI) Fourier Transform Ion Cyclotron Resonance (FTICR) Mass Spectra (MS) of intracellular *Synechocystis* sp. PCC 6803 dissolved organic matter (cyDOM) and ultrapure water (mQ H<sub>2</sub>O) mixed 1:1 (v:v) with methanol (MeOH).



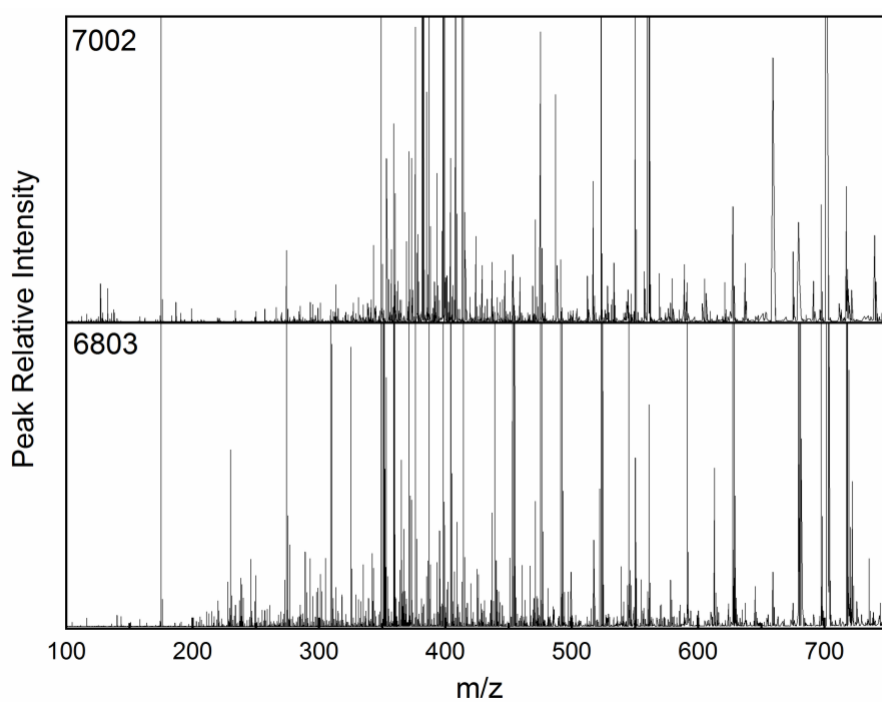
**SI Figure 3:** Negative Electrospray Ionization (ESI) Fourier Transform Ion Cyclotron Resonance (FTICR) Mass Spectra (MS) of intracellular *Synechococcus* sp. PCC 7002 dissolved organic matter (cyDOM) and ultrapure water (mQ H<sub>2</sub>O) mixed 1:1 (v:v) with methanol (MeOH).



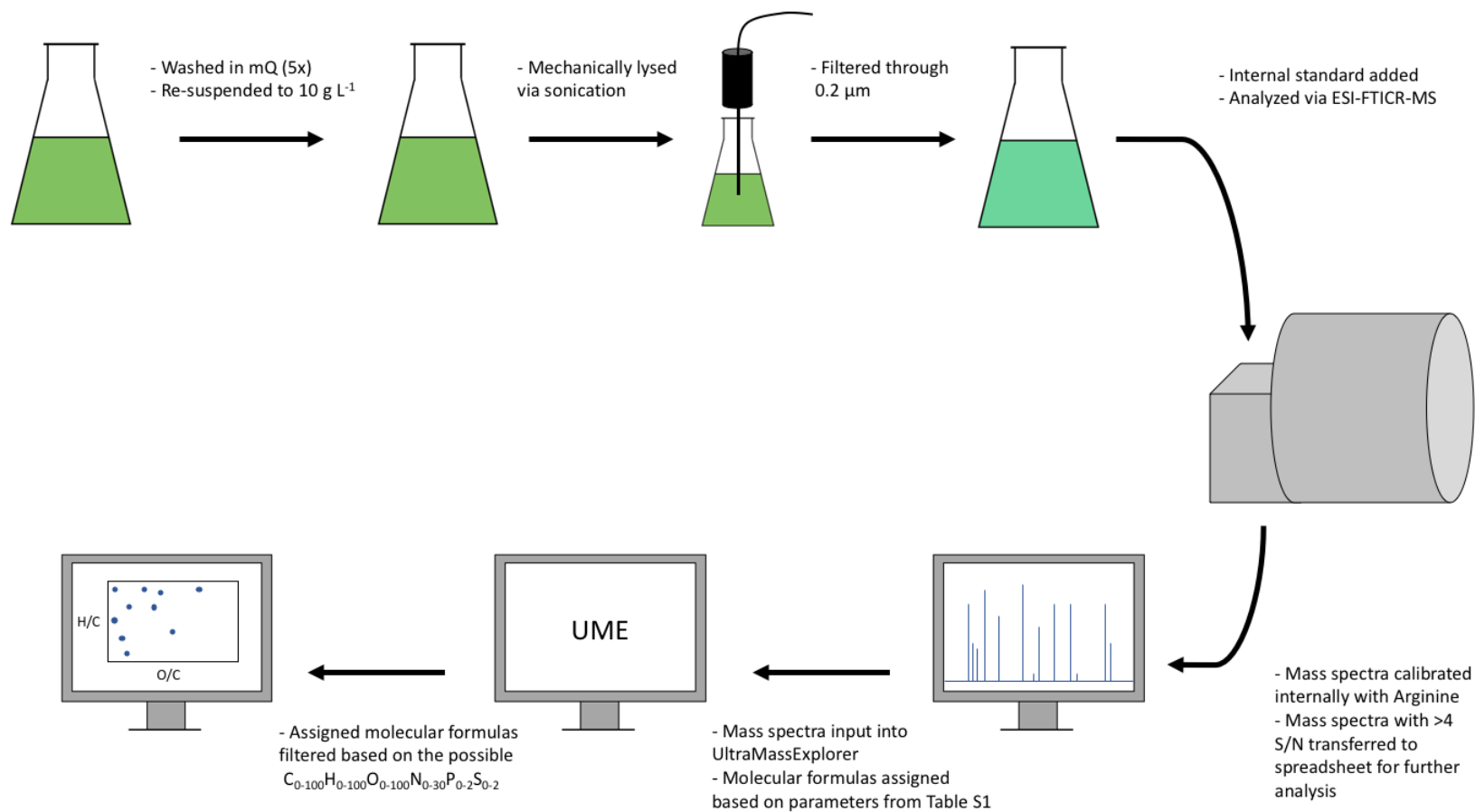
**SI Figure 4:** Positive Electrospray Ionization (ESI) Fourier Transform Ion Cyclotron Resonance (FTICR) Mass Spectra (MS) of intracellular *Synechocystis* sp. PCC 6803 dissolved organic matter (cyDOM) and ultrapure water (mQ H<sub>2</sub>O) mixed 1:1 (v:v) with methanol (MeOH).



**SI Figure 5:** Positive Electrospray Ionization (ESI) Fourier Transform Ion Cyclotron Resonance (FTICR) Mass Spectra (MS) of intracellular *Synechococcus* sp. PCC 7002 dissolved organic matter (cyDOM) and ultrapure water (mQ H<sub>2</sub>O) mixed 1:1 (v:v) with methanol (MeOH).



**SI Figure 6:** Positive ESI Fourier Transform Ion Cyclotron Resonance (FTICR) Mass Spectra (MS) of intracellular *Synechococcus* sp. PCC 7002 dissolved organic matter (7002) and intracellular *Synechocystis* sp, PCC 6803 dissolved organic matter (6803) mixed 1:1 (v:v) with methanol (MeOH).



**SI Figure 7:** Generalized schematic of the pipeline from cyanobacteria growth to cyDOM production, FTICR-MS analysis, and data interpretation.

## References

- Baes, C.F., Mesmer, R.S. (1976). The Hydrolysis of Cations. *John Wiley & Sons*, New Jersey, USA.
- Liu, Y., Alessi, D.S., Owtrim, G.W., Petrash, D.A., Mloszewska, A.M., Lalonde, S.V., Martinez, R.E., Zhou, Q., Konhauser, K.O. (2015). Cell surface reactivity of *Synechococcus* sp. PCC 7002: Implications for metal sorption from seawater. *Geochimica et Cosmochimica Acta*, **169**, 30-44.
- Yu, Q., Fein, J.B. (2015). The effect of metal loading on Cd adsorption onto *Shewanella oneidensis* bacterial cell envelopes: The role of sulfhydryl sites. *Geochimica et Cosmochimica Acta* **167**, 1-10.
- Zirino, A., Yamamoto, S. (1972). A pH-dependent model for the chemical speciation of copper, zinc, cadmium, and lead in seawater. *Limnology and Oceanography*, **17**, 661-671.

## Appendix 4: Supplementary information for Chapter 5

SI Table 5.1: Non-siderophore marine ligand concentrations and stability constants

Nickel	Metal concentration			Ligand concentration			Log K <sup>o</sup> <sub>(Metal)-L</sub>			Method, competing ligand*	Reference
	High (nM)	Low (nM)	Mean (nM)	High (nM)	Low (nM)	Mean (nM)	High	Low	Mean		
GEOTRACES Eastern Pacific Zonal Transect (Ecuador to Tahiti)	3.70	2.03	2.77 (n = 40)	-	-	-	18.68	18.45	18.565 (n = 2)	CLE-ACSV, DMG	Boiteau et al. 2016
Mediterranean Sea	5.02	1.5	-	-	-	-	-	-	-	CSV, DMG	Achterberg & van den Berg 1997
San Francisco Bay	58	50	-	28	17	22.5 (n = 2)	-	-	>17	CLE-CSV, DMG	Donat et al. 1994
Menai Straits, Irish Sea, and English Channel	12	3.2	6.94 (n = 8)	5.9	1.9	3.9 (n = 8)	18.7	17.28	18.03 (K <sup>o</sup> <sub>NIL</sub> ; n = 8)	CSV, DMG	van den Berg & Nimmo 1987
Copper	Metal concentration			Ligand concentration			Log K <sup>o</sup> <sub>(Metal)-L</sub>			Method, competing ligand*	Reference
	High (nM)	Low (nM)	Mean (nM)	High (nM)	Low (nM)	Mean (nM)	High	Low	Mean		
GEOTRACES NE Pacific (Line P Transect)	3.3 (1400m)	1.2 (75m)	2.34 (n = 23)	L <sub>1</sub> = 4.0 (1400m) L <sub>2</sub> = 20.1 (75m)	L <sub>1</sub> = 1.2 (75m) L <sub>2</sub> = 1.1 (600m)	L <sub>1</sub> = 2.61 (n = 22) L <sub>2</sub> = 7.00 (n = 21)	L <sub>1</sub> = 16.5 L <sub>2</sub> = 13.6	L <sub>1</sub> = 15.1 L <sub>2</sub> = 11.6	L <sub>1</sub> = 15.57 (n = 22) L <sub>2</sub> = 13.02 (n = 21)	CLE-CSV, SA	Whitby et al. 2018
Tamar Estuary, U.K.	189	7.7	51.87451 (n = 51)	372.2	4	71.23196 (n = 51)	13.73	10.11	11.63261 (n = 46)	CLE-AdCSV, SA	Pearson et al. 2017
GEOTRACES Eastern Pacific Zonal Transect (Ecuador to Tahiti)	2.32	0.38	0.75 (n = 40)	8.77	1.39	3.29 (n = 11)	13.95	12.55	13.21 (n = 11)	CLE-ACSV, SA	Boiteau et al. 2016
North Atlantic (Lisbon, Portugal to Cape Verde to Woods Hole, US)	3.07	0.43	~1.5	5.26	1.29	~3.275 (n = 2)	14.8	12.5	13.6584 (n = 267)	CLE-ACSV, SA	Jacquot & Moffett 2015
Seafloor from Bermuda to Cape Verde	-	-	-	5.22	2.25	3.2888 (n = 8)	13.9	12.1	13.125 (n = 8)		
NE Subarctic Pacific (Line P)	-	-	-	-	-	-	-	-	12.82±0.22 (n = 10; from unpublished data along the	CLE-CSV, SA	Semeniuk et al. 2015

									same sample line)		
Mersey Estuary & Liverpool Bay (Irish Sea)	-	-	-	-	-	-	-	-	12.08 (Log K <sup>+</sup> CuHA)	DPCSV, SA	Whitby & van den Berg 2015
Inshore Bermuda, North Atlantic	19.2	1.4	6.173 (n = 15)	L <sub>1</sub> = 13.1 L <sub>2</sub> = 31.9	L <sub>1</sub> = 1.6 L <sub>2</sub> = 2.1	L <sub>1</sub> = 5.438 (n = 8) L <sub>2</sub> = 10.83 (n = 12)	L <sub>1</sub> = 15.1 L <sub>2</sub> = 14.1	L <sub>1</sub> = 14 L <sub>2</sub> = 12.6	L <sub>1</sub> = 14.838 (n = 8) L <sub>2</sub> = 13.442 (n = 12)	CLE-ACSV, SA	Oldham et al. 2014
Tasman Sea, SW Pacific Ocean	3.41	0.32	1.1835 (n = 31)	L <sub>1</sub> = 5.22 L <sub>2</sub> = 7.76	L <sub>1</sub> = 1.08 L <sub>2</sub> = 7.44	L <sub>1</sub> = 1.78 (n = 31) L <sub>2</sub> = 7.6 (n = 2)	L <sub>1</sub> = 13.64 L <sub>2</sub> = 11.72	L <sub>1</sub> = 12.0 L <sub>2</sub> = 11.20	L <sub>1</sub> = 12.99 (n = 31) L <sub>2</sub> = 11.46 (n = 2; only found in surface samples)	CLE-ACSV, SA	Thompson et al. 2014
Antarctic Peninsula	2.39	1.56	1.9475 (n = 4)	L <sub>1</sub> = 8.04 L <sub>2</sub> = 8.32	L <sub>1</sub> = 2.26 L <sub>2</sub> = 2.54	L <sub>1</sub> = 3.752 (n = 12) L <sub>2</sub> = 6.039 (n = 10)	L <sub>1</sub> = 16.0 L <sub>2</sub> = 13.33	L <sub>1</sub> = 13.57 L <sub>2</sub> = 12.68	L <sub>1</sub> = 14.631 (n = 12) L <sub>2</sub> = 13.055 (n = 10)	CLE-ACSV, SA	Bundy et al. 2013
South Pacific	~1.75	~0.25	-	6.46	1.02	3.0536 (n = 42)	14.0	12.6	13.3405 (n = 42)	CLE-ACSV, SA	Jacquot et al. 2013
River Plume off Scotland (North Atlantic)	26.1	0.17	5.552 (n = 24) Values decrease with increasing salinity	L <sub>1</sub> = 3.63 L <sub>2</sub> = 173	L <sub>1</sub> = 0.14 L <sub>2</sub> = 53	L <sub>1</sub> = 1.139 (n = 23) L <sub>2</sub> = 102.636 (n = 22)	L <sub>1</sub> = 16.2 L <sub>2</sub> = 12.80	L <sub>1</sub> = 14.8 L <sub>2</sub> = 11.74	L <sub>1</sub> = 15.7 (n = 23) L <sub>2</sub> = 12.255 (n = 22)	ACSV, SA	Muller & Batchelli 2013
North Pacific (GEOTRACES II)	3.7 (3000m)	0.62 (125m)	2.14 (n = 3)	6.1 (3000m)	1.54 (125m)	3.3877 (n = 13)	15.11	12.84	14.0677 (n = 13)	CLE-ACSV, SA	Buck et al. 2012
NW Pacific & Bering Sea	-	-	-	4	3	3.5 (n = 2)	14.1	12.7	13.4 (n = 2)	CLE-CSV, SA & BZAC	Moffett & Dupont 2007
Station in Bering Sea (2500m & 1500m)	3.3 (2500m)	2.5 (1500m)	2.9 (n = 2)	5 (2500m)	3.7 (1500m)	4.35 (n = 2)	14.1 (1500m)	13.8 (2500m)	13.95 (n = 2)		
San Francisco Bay	49.6	17.9	26.7917 (n = 12)	L <sub>1</sub> = 265 L <sub>2</sub> = 135	L <sub>1</sub> = 22 L <sub>2</sub> = 48	L <sub>1</sub> = 75.583 (n = 12) L <sub>2</sub> = 81.091 (n = 11)	L <sub>1</sub> = 14.3 L <sub>2</sub> = 12.9	L <sub>1</sub> = 12.9 L <sub>2</sub> = 12.0	L <sub>1</sub> = 13.7 (n = 12) L <sub>2</sub> = 12.427 (n = 11)	CLE-ACSV, SA	Buck & Bruland 2005
Cape Fear River estuary, North Carolina	8.7	2.1	4.232 (n = 28)	126	4	30.571 (n = 28)	-	-	13.5	CSV	Shank et al. 2004
Coastal New England (North Atlantic)	-	-	-	-	-	L <sub>1</sub> = 1.36 L <sub>2</sub> = 15.5 L <sub>3</sub> = 238	-	-	L <sub>1</sub> = 13.0 L <sub>2</sub> = 11.5 L <sub>3</sub> = 10.0	CLE-ACSV, SA	Kogut & Voelker 2003

Estuary waters (River Scheldt, Netherlands)	23.6	9.4	18.4 (n = 13)	L <sub>1</sub> = 32.5 L <sub>2</sub> = 299	L <sub>1</sub> = 10.9 L <sub>2</sub> = 14.3	L <sub>1</sub> = 22.45 (n = 13) L <sub>2</sub> = 164.79 (n = 13)	L <sub>1</sub> = 16.14 L <sub>2</sub> = 13.46	L <sub>1</sub> = 14.71 L <sub>2</sub> = 12.70	L <sub>1</sub> = 15.20 (n = 13) L <sub>2</sub> = 12.98 (n = 13)	CSV, SA	Laglera & van den Berg 2003
Black Sea	21	4	9.4125 (n = 16)	L <sub>1</sub> = 12.6 L <sub>2</sub> = 82	L <sub>1</sub> = 2.8 L <sub>2</sub> = 23	L <sub>1</sub> = 6.694 (n = 16) L <sub>2</sub> = 44.688 (n = 16)	L <sub>1</sub> = 14.18 L <sub>2</sub> = 11.26	L <sub>1</sub> = 13.14 L <sub>2</sub> = 9.4	L <sub>1</sub> = 13.597 (n = 16) L <sub>2</sub> = 10.409 (n = 16)	DPASV	Muller et al. 2001
Galveston Bay, Texas (Top: <0.45µm filtered; Bottom: ultra-filtered, <1 kDa)	12.89	2.27	9.44 (n = 16)	83	20.5	49.6 (n = 15)	12.7	11.3	12.3 (n = 15)	CLE-CSV, catechol	Tang et al. 2001
	6.02	2.25	4.97 (n = 14)	43.6	7.4	27.8 (n = 13)	11.8	10.2	11.1 (n = 13)		
Narragansett Bay, Rhode Island	-	-	-	L <sub>1</sub> = 23.2 L <sub>2</sub> = 17.6	L <sub>1</sub> = 5.6 L <sub>2</sub> = 9	L <sub>1</sub> = 15.282 (n = 11) L <sub>2</sub> = 13.2 (n = 3) L <sub>3</sub> = 46	L <sub>1</sub> = 15.6 L <sub>2</sub> = 11.5	L <sub>1</sub> = 12.8 L <sub>2</sub> = 10.1	L <sub>1</sub> = 13.809 (n = 11) L <sub>2</sub> = 10.73 (n = 3) L <sub>3</sub> = 9	- CLE-ACSV, SA - CLE-ACSV, Ox - CLE-ACSV, BZAC - ASV	Bruland et al. 2000
Chesapeake Bay	-	-	-	L <sub>1</sub> = 40 L <sub>2</sub> = 150	L <sub>1</sub> = 1 L <sub>2</sub> = 6	L <sub>1</sub> = 31 L <sub>2</sub> = 65	-	-	L <sub>1</sub> = 11.0 L <sub>2</sub> = 7.9	DPASV	Gordon et al. 2000
Terra Nova Bay, Ross Sea, Antarctica	3.8	1.6	2.7259 (n = 27)	L <sub>1</sub> = 19.3 L <sub>2</sub> = 71	L <sub>1</sub> = 0.4 L <sub>2</sub> = 16	L <sub>1</sub> = 4.71 (n = 11) L <sub>2</sub> = 47.4 (n = 27)	L <sub>1</sub> = 16 L <sub>2</sub> = 9	L <sub>1</sub> = 11 L <sub>2</sub> = 7.62	L <sub>1</sub> = 13.573 (n = 11) L <sub>2</sub> = 8.416 (n = 27)	DPASV	Capodaglio et al. 1998
Narragansett Bay, Rhode Island	27.9	12.7	18.9 (n = 3)	L <sub>1</sub> = 38 L <sub>2</sub> = 40 L <sub>3</sub> = 100	L <sub>1</sub> = 16 L <sub>2</sub> = 15 L <sub>3</sub> = 54	L <sub>1</sub> = 23.3 (n = 3) L <sub>2</sub> = 25 (n = 3) L <sub>3</sub> = 70.33 (n = 3)	L <sub>2</sub> = 9.2 L <sub>3</sub> = 7.7	L <sub>2</sub> = 8.8 L <sub>3</sub> = 7.5	L <sub>2</sub> = 8.93 (n = 3) L <sub>3</sub> = 7.63 (n = 3)	DPASV	Kozelka & Bruland 1998
Narragansett Bay, Rhode Island	27.9	7.4	15 (n = 9)	L <sub>1</sub> = 38 L <sub>2</sub> = 110 L <sub>3</sub> = 100	L <sub>1</sub> = 16 L <sub>2</sub> = 15 L <sub>3</sub> = 40	L <sub>1</sub> = 19.625 (n = 8) L <sub>2</sub> = 49.875 (n = 8) L <sub>3</sub> = 62.75 (n = 4)	L <sub>2</sub> = 9.2 L <sub>3</sub> = 7.7	L <sub>2</sub> = 8 L <sub>3</sub> = 7.5	L <sub>1</sub> = ≥12.3 L <sub>2</sub> = 8.438 (n = 8) L <sub>3</sub> = 7.65 (n = 4)	DPASV	Wells et al. 1998
Sargasso Sea	-	-	-	2	0.9	1.418 (n = 11)	-	-	13.2 (n = 9)	ACSV, BZAC	Moffett 1995
North Sea	-	-	-	13.79	6.05	10.69 (n = 6)	14.29	12.79	13.375 (n = 6)	CSV, SA	

NE Atlantic	-	-	-	12.8	4.9	8.6 (n = 3)	13.1	12.2	12.67 (n = 3)		Campos & van den Berg 1994
NW Mediterranean Sea	-	-	-	14.4	3.2	8.167 (n = 6)	14.8	13.03	13.8283 (n = 6)		
San Francisco Bay	48	45	-	L <sub>2</sub> = 80	L <sub>2</sub> = 60	L <sub>1</sub> = 13 L <sub>2</sub> = 70	L <sub>2</sub> = 9.6	L <sub>2</sub> = 9	L <sub>1</sub> = >13.5 L <sub>2</sub> = 9.3 (n = 2)	CLE-CSV, 8-HQ	Donat et al. 1994
Indian Ocean	-	-	1.96	-	-	4.13	-	-	12.6	DPCSV, tropolone	Donat & van den Berg 1992
North Sea	-	-	3.24	17.8	14.6	16.2	12.5	12.1	12.4		
North Pacific	1.3 (Southern most station)	0.5 (Northern most station)	-	L <sub>1</sub> = 3 L <sub>2</sub> = 10	L <sub>1</sub> = 1.5 L <sub>2</sub> = 5	L <sub>1</sub> = 2 L <sub>2</sub> = 6	-	-	L <sub>1</sub> = 11.6 L <sub>2</sub> = 8.6	DPASV	Coale & Bruland 1990
Sargasso Sea	1.7	1.2	-	-	-	L <sub>1</sub> = 2 L <sub>2</sub> = 80	-	-	L <sub>1</sub> = 13.2 L <sub>2</sub> = 9.7	LE-LLP, ACAC	Moffett et al. 1990
Northeast Pacific	1.8	0.6	-	-	-	L <sub>1</sub> = 1.8 L <sub>2</sub> = 8-10	-	-	L <sub>1</sub> = 11.5 L <sub>2</sub> = 8.5	DPASV	Coale & Bruland 1988
Scheldt Estuary, Netherlands (Top: 1-site model; Bottom: 2-site model)	152	10.7	45.991 (n = 11)	206	26	119.67 (n = 12)	14	11.7	12.6475 (n = 12)	CSV, APDC	Van den Berg 1987
				L <sub>1</sub> = 121 L <sub>2</sub> = 131	L <sub>1</sub> = 23 L <sub>2</sub> = 44	L <sub>1</sub> = 63.2 (n = 9) L <sub>2</sub> = 76.167 (n = 6)	L <sub>1</sub> = 14.9	L <sub>1</sub> = 13.04	L <sub>1</sub> = 13.827 (n = 9)		
North Atlantic	-	-	-	-	-	L <sub>1</sub> = 11 L <sub>2</sub> = 33	-	-	L <sub>1</sub> = 12.2 L <sub>2</sub> = 10.2	CSV, catechol	Van den Berg 1984

\* Abbreviations: ACAC, acetylacetone; ACSV, adsorptive cathodic stripping voltammetry; APDC, ammonium pyrrolidinedithiocarbamate; ASV, anodic stripping voltammetry; BZAC, benzoylacetone; CLE, competitive ligand exchange; CSV, cathodic stripping voltammetry; DMG, dimethylglyoxime; DPASV, differential pulse anodic stripping voltammetry; DPCSV, differential pulse cathodic stripping voltammetry; FF, fresh film (Hg); LE-LLP, ligand exchange/liquid/liquid partition; PDC, pyrrolidinedithiocarbamate; SA, salicylaldehyde; 8-HQ, 8-hydroxyquinoline.

## References

- Achterberg, E. P., van den Berg, C. M. G. (1997). Chemical speciation of chromium and nickel in the western Mediterranean. *Deep-Sea Research II* 44, 693-720.
- Boiteau, R. M., Till, C. P., Ruacho, A., Bundy, R. M., Hawco, N. J., McKenna, A. M., Barbeau, K. A., Bruland, K. W., Saito, M. A., Repeta, D. J. (2016) Structural Characterization of Natural Nickel and Copper Binding Ligands along the US GEOTRACES Eastern Pacific Zonal Transect. *Frontiers in Marine Science* 3, 1-16.
- Bruland, K. W., Rue, E. L., Donat, J. R., Skrabal, S. A., Moffett, J. W. (2000). Intercomparison of voltammetric techniques to determine the chemical speciation of dissolved copper in a coastal seawater sample. *Analytica Chimica Acta* 405, 99-113.
- Buck, K. N., Bruland, K. W. (2005). Copper speciation in San Francisco Bay: A novel approach using multiple analytical windows. *Marine Chemistry* 96, 185-198.
- Buck, K. N., Moffett, J., Barbeau, K. A., Bundy, R. M., Kondo, Y., Wu, J. (2012). The organic complexation of iron and copper: an intercomparison of competitive ligand exchange-adsorptive cathodic stripping voltammetry (CLE-ACSV) techniques. *Limnology and Oceanography: Methods* 10, 496-515.
- Bundy, R. M., Barbeau, K. A., Buck, K. N. (2013). Sources of strong copper-binding ligands in Antarctic Peninsula surface waters. *Deep-Sea Research II* 90, 134-146.
- Campos, M. L. A. M., van den Berg, C. M. G. (1994). Determination of copper complexation in sea water by cathodic stripping voltammetry and ligand competition with salicylaldehyde. *Analytica Chimica Acta* 284, 481-496.

- Capodaglio, G., Turetta, C., Toscano, G., Gambaro, A., Scarponi, G., Cesona, P. (1998). Cadmium, lead and copper complexation in Antarctic coastal seawater, Evolution during the austral summer. *International Journal of Environmental Analytical Chemistry* 71, 195-226.
- Coale, K. H., Bruland, K. W. (1988). Copper complexation in the Northeast Pacific. *Limnology and Oceanography* 33, 1084-1101.
- Coale, K. H., Bruland, K. W. (1990). Spatial and temporal variability in copper complexation in the North Pacific. *Deep-Sea Research* 47, 317-336.
- Donat, J. R., van den Berg, C. M. G. (1992). A new cathodic stripping voltammetric method for determining organic copper complexation in seawater. *Marine Chemistry* 38, 69-90.
- Donat, J. R., Lao, K. A., Bruland, K. W. (1994). Speciation of dissolved copper and nickel in South San Francisco Bay: a multi-method approach. *Analytica Chimica Acta* 284, 547-571.
- Gordon, A. S., Donat, J. R., Kango, R. A., Dyer, B. J., Stuart, L. M. (2000). Dissolved copper-complexing ligands in cultures of marine bacteria and estuarine water. *Marine Chemistry* 70, 149-160.
- Jacquot, J. E., Kondo, Y., Knapp, A. N., Moffett, J. W. (2013). The speciation of copper across active gradients in nitrogen-cycle processes in the eastern tropical South Pacific. *Limnology and Oceanography* 58, 1387-1394.
- Jacquot, J. E., Moffett, J. W. (2015). Copper distribution and speciation across the International GEOTRACES Section GA03. *Deep-Sea Research II* 116, 187-207.
- Kogut, M. B., Volker, B. M. (2003). Kinetically inert Cu in coastal waters. *Environmental Science and Technology* 37, 509-518.
- Kozelka, P. B., Bruland, K. W. (1998). Chemical speciation of dissolved Cu, Zn, Cd, Pb in Narragansett Bay, Rhode Island. *Marine Chemistry* 60, 267-282.

- Laglera L. M., van den Berg, C. M. G. (2003). Copper complexation by thiol compounds in estuarine waters. *Marine Chemistry* 82, 71-89.
- Moffett, J. W., Zika, R. G., Brand, L. E. (1990). Distribution and potential sources and sinks of copper chelators in the Sargasso Sea. *Deep-Sea Research* 37, 27-36.
- Moffett, J. W. (1995). Temporal and spatial variability of copper complexation by strong chelators in the Sargasso Sea. *Deep Sea Research Part I: Oceanographic Research Papers* 42, 1273-1295.
- Moffett, J. W., Dupont, C. (2007). Cu complexation by organic ligands in the sub-arctic NW Pacific and Bering Sea. *Deep Sea Research Part I: Oceanographic Research Papers* 54, 586-595.
- Muller, F. L. L., Gulin, S. B., Kalvoy, A. (2001). Chemical speciation of copper and zinc in surface waters of the western Black Sea. *Marine Chemistry* 76, 233-251.
- Muller, F. L. L., Batchelli, S. (2013). Copper binding by terrestrial versus marine organic ligands in the coastal plume of River Thurso, North Scotland. *Estuarine, Coastal and Shelf Science* 133, 137-146.
- Oldham, V. E., Swenson, M. M., Buck, K. N. (2014). Spatial variability of total dissolved copper and copper speciation in the inshore waters of Bermuda. *Marine Pollution Bulletin* 79, 314-320.
- Pearson, H. B. C., Comber, S. D. W., Braungardt, C., Worsfold, P. J. (2017). Predicting Copper Speciation in Estuarine Waters – Is Dissolved Organic Carbon a Good Proxy for the Presence of Organic Ligands? *Environmental Science and Technology* 51, 2206-2216.
- Semeniuk, D. M., Bundy, R. M., Payne, C. D., Barbeau, K. A., Maldonado, M. T. (2015). Acquisition of organically complexed copper by marine phytoplankton and bacteria in the northeast subarctic Pacific Ocean. *Marine Chemistry* 173, 222-233.

- Shank, G. C., Skrabal, S. A., Whitehead, R. F., Avery, G. B., Kieber, R. J. (2004). River discharge of strong Cu-complexing ligands to South Atlantic Bight waters. *Marine Chemistry* **88**, 41-51.
- Tang, D., Warnken, K. W., Santschi, P. H. (2001). Organic complexation of copper in surface waters of Galveston Bay. *Limnology and Oceanography* **46**, 321-330.
- Thompson, C. M., Ellwood, M. J., Sander, S. G. (2014). Dissolved copper speciation in the Tasman Sea, SW Pacific Ocean. *Marine Chemistry* **164**, 84-94.
- Van den Berg, C. M. G. (1984). Determination of the complexing capacity and conditional stability constants of complexes of copper (II) with natural organic ligands in seawater by cathodic stripping voltammetry of copper-catechol complex ions. *Marine Chemistry* **15**, 1-18.
- Van den Berg, C. M. G., Nimmo, M. (1987). Determination of interactions of nickel with dissolved organic material in seawater using cathodic stripping voltammetry. *Science of the Total Environment* **60**, 185-195.
- Van den Berg, C. M. G., Merks, A. G. A., Duursma, E. K. (1987). Organic Complexation and its Control of the Dissolved Concentrations of Copper and Zinc in the Scheldt Estuary. *Estuarine, Coastal and Shelf Science* **24**, 785-797.
- Wells, M. L., Kozelka, P. B., Bruland, K. W. (1998). The complexation of 'dissolved' Cu, Zn, Cd and Pb by soluble and colloidal organic matter in Narragansett Bay, RI. *Marine Chemistry* **62**, 203-217.
- Whitby, H., van den Berg, C. M. G. (2015). Evidence for copper-binding humic substances in seawater. *Marine Chemistry* **173**, 282-290.
- Whitby, H., Posacka, A. M., Maldonado, M. T., van den Berg, C. M. G. (2018) Copper-binding ligands in the NE Pacific. *Marine Chemistry* **204**, 36-48.